Solution of Spectral Problem in Planar Supersymmetric Gauge Theories

Sizov, Grigory Alekseevich

Awarding institution:
King's College London

KING'S College LONDON

Solution of Spectral Problem in Planar Supersymmetric Gauge Theories

Grigory Sizov

Department of Mathematics, King's College London,
Strand, London WC2R 2LS, U.K.

Thesis supervisor Dr. Nikolay Gromov

Thesis submitted in partial fulfilment of the requirements
of the Degree of Doctor of Philosophy

August 2015

Abstract

Supersymmetric gauge theories are among the most important objects of study in modern theoretical physics. They are considered as more symmetric versions of gauge theories describing the real world and are often dual to string theories in curved backgrounds. In planar limit some supersymmetric gauge theories — $\mathcal{N} = 4$ SYM and ABJM theory among them — manifest integrability, a property which might allow to solve them exactly. In this thesis we discuss application of integrability methods to spectral problems in supersymmetric gauge theories. Our main topic is the Quantum Spectral Curve (QSC) method, the ultimate simplification of integrability tools developed over the last decade. We describe the objects of our study, $\mathcal{N} = 4$ SYM and ABJM theories and their dual string theories. Then we review the integrable structures appearing in these theories in the planar limit. A chapter is dedicated to description of QSC in $\mathcal{N} = 4$ SYM and then we solve the QSC equations in various limits, including near-BPS limits of twist operators and of a cusped Wilson line. For the last observable we explore the quasiclassical limit in more detail, finding the matrix model reformulation and the corresponding algebraic curve. We also apply QSC method to BFKL physics, a regime which establishes a more direct connection between $\mathcal{N} = 4$ SYM and QCD. In particular, we find a new, NNLO, coefficient in the weak-coupling expansion of BFKL eigenvalue. We describe an efficient algorithm of numerical solution of QSC equations and use it to explore the relation between the spin and the conformal dimension for wide range of conformal dimension, including complex values. In ABJM we also consider the near-BPS limit of twist operators, calculating the slope function, and extracted from this calculation a conjecture for so-called interpolating function $h(\lambda)$ — the long-sought-for missing ingredient for the integrability construction in ABJM.

Acknowledgements

First of all I would like to thank my supervisor Nikolay Gromov for the immense amount of time and effort he spent teaching me integrability. His brilliant supervision style made these three years of learning and research enjoyable.

I'm also very thankful to the professors, fellows and my classmates at Perimeter Institute and at Landau Institute for Theoretical Physics. I would especially like to thank Freddy Cachazo for inspiring me to start doing high energy theoretical physics. I would like to thank my fellow students at King's and especially my collaborators F. Levkovich-Maslyuk and S. Valatka. We did a lot of work together and it was great. I'm also very thankful to Fedor for carefully proofreading this thesis. I would like to thank M. Alfimov, V. Kazakov, I. Kostov, D. Serban, A. Petrovski, D. Volin, S. Caron-Huot, B. Basso, P. Vieira, J. Caetano and O. Isaeva for numerous fruitful discussions.

I'm also very grateful to my family, friends and especially my flatmates for their constant support during these years!

Contents

List of Figures

List of Tables

Part I

Objects and methods of study

1 Introduction

1.1 Integrability and supersymmetric QFTs

Quantum field theories seem to be the most suitable framework to describe Nature. We see them both on the fundamental level, describing all interactions except gravity, and as emergent theories in condensed matter systems. However, this approach meets with at least two difficulties. One, which is relevant when using QFTs as fundamental theories, is the unification with gravity. The other is that most QFTs, except the most trivial ones, are extremely hard to solve. Chronologically the first successful and still very common computational method is perturbation theory, often performed in QFTs with the use of Feynman diagrams. Many crucial results in QED, QCD and other theories were obtained in this way. However, the complexity of perturbative computations grows rapidly with number of loops and makes it almost impossible to go beyond several loops in most cases. Thus much of the recent progress in understanding of QFTs, especially gauge theories is connected with development of non-perturbative methods. Integrability, which is the main topic of this thesis, is one of the most powerful of such methods.

A major breakthrough in understanding gauge theories came in 1997, when Juan Maldacena discovered the famous AdS/CFT duality [1] which relates $\mathcal{N} = 4$ SYM , a supersymmetric modification of QCD living in four dimensions, with string theory in ten dimensions or its low-energy limit, SUGRA. The discovery is especially valuable, because it addresses the two major problems in studying gauge theories at once. First, it relates quantum field theory to gravity, thus hinting at long-awaited possibility of quantization of gravity. Second, being a weak/strong coupling duality, it allows to explore previously unaccessible regions of strong coupling in the gauge theory. In the same way the weak coupling regime of the gauge theory gives access to highly quantum regime of string theory.

In this thesis we will be working in one particular limit of AdS/CFT correspondence, called the planar limit: on the gauge theory side it means taking rank of the gauge group to infinity; on the string theory side taking the string coupling to zero, which is equivalent to considering only worldsheets with the topology of a sphere. In this limit

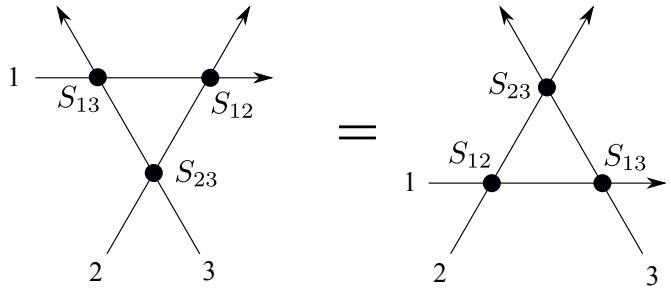

Figure 1: **Yang-Baxter equation for the scattering matrix.** In integrable systems multiparticle scattering factorizes into pairwise scatterings and the two-particle S-matrix satisfies the Yang-Baxter equation graphically represented on the picture.

both sides of the duality acquire one more unexpected additional feature — they become integrable. Although no rigorous universally accepted definition of integrability exists, one usually says that a system is integrable, if possesses additional integrals of motion, enough to allow an exact solution. In case of a system with an infinite number of degrees of freedom, like QFT, we need an infinite family of integrals of motion. Examples of integrable QFTs were known before the discovery of AdS/CFT duality, but they were mostly two-dimensional. Integrability of four-dimensional $\mathcal{N} = 4$ SYM is the first example when a non-trivial four-dimensional theory has a chance be solved exactly. A distinguishing feature of integrable systems, sometimes almost taken as their definition, is a particular form of scattering of excitations. First, n-particle scattering should factorize into pairwise scatterings and second, the scattering matrix should satisfy the Yang-Baxter equation schematically represented on Fig. 1. Such factorization is natural in two dimensions, but not in higher dimensions, that is why we often encounter integrability in two-dimensional systems [2, 3, 4, 5, 6].

In complete agreement with this logic, the easiest way to see integrability in $\mathcal{N} = 4$ SYM is in a "two-dimensional" context. An example of such a context arises when one considers the spectral problem for single-trace operators at weak coupling. It happens that such operators can be mapped to spin chains with integrable Hamiltonians. Solving the spectral problem in these spin chains by well known techniques based on their integrability, such as Bethe Ansatz, one indeed correctly reproduces the anomalous dimensions of the original $\mathcal{N} = 4$ SYM operators. Another two-dimensional system in which we can look for integrability is the worldsheet of strings describing the system at strong coupling. Indeed, the string theory on $\mathrm{AdS}_5/\mathrm{CFT}_4$ can be described as a coset sigma-model, for which a very elegant description of integrability through the monodromy construction has been

developed.

Miraculously, integrability extends beyond these limits into the full four-dimensional theory at finite coupling. We still do not have a complete understanding of why and how this happens. However, we now possess integrability-based methods describing $\mathcal{N} = 4$ SYM at finite coupling. These methods have a long history of development which we sketch in section 3. The focus of this thesis is *the spectral problem* in AdS/CFT, and so we will mainly describe the methods aimed at calculation of the anomalous dimensions of operators. Until very recently the most advanced of them was the Thermodynamical Bethe Ansatz — a system of equations describing anomalous dimensions of operators at finite length and finite coupling. This was a great achievement, however not very practical for analytical computations, because it involved solving a system of infinite number of non-linear integral equations, which is usually possible only in some very special cases, like the near-BPS limit or weak coupling. Numerical solution of TBA also was a tedious and not very efficient procedure. The situation changed when TBA was simplified to a much more compact and elegant system of equations [7, 8], which was known first as a $\mathbf{P}\mu$-system and later and in a more general formulation as the Quantum Spectral Curve (QSC). It described the spectrum of $\mathcal{N} = 4$ SYM in terms of equations for the monodromy of several functions with fixed analytic properties. QSC can be derived from TBA, but is much more accessible for analytical solution. Furthermore, as we demonstrate further in this thesis, there exists an efficient algorithm for numerical solution of QSC. In this thesis we describe the QSC and apply it in a variety of scenarios for $\mathrm{AdS}_5/\mathrm{CFT}_4$ and $\mathrm{AdS}_4/\mathrm{CFT}_3$ dualities. We hope that this ultimate simplification of the spectral problem in the form of QSC will be an important step to the future exact solution of $\mathcal{N} = 4$ SYM

.

1.2 Thesis structure

This thesis contains three parts: part I contains introductory chapters 1-4, part II mainly presents the results of the author with collaborators in chapters 5-10, and part III consists of conclusions in chapter 11 and appendices A, B, and C.
Here is a more detailed plan of the thesis:

- **Part I**
  - The current chapter contains the motivational preface 1.1 and this section.

- After this chapter we move to chapter 2 where one can find a short introduction to the AdS/CFT duality. In particular, we briefly describe its both sides and present Maldacena's argument for the duality. We elaborate on some points which will be important further in the thesis: the planar limit and most important for us classes of operators in $\mathcal{N} = 4$ SYM .
- In chapter 3 we describe the development of integrability tools in AdS_5/CFT_4 starting from perturbative methods at weak and strong coupling, through the Thermodynamic Bethe Ansatz and finally to the Quantum Spectral Curve — most recent approach to integrability in $\mathcal{N} = 4$ SYM .
- Since QSC will be our main tool in this thesis, in chapter 4 we describe it in more detail. As an example of how QSC reproduces earlier know integrability results, we discuss the large volume limit in which QSC reduces to Beisert-Eden-Staudacher Asymptotic Bethe Ansatz.

- **Part II**

  In this part we apply the integrability tools described, mostly QSC, to solving problems in AdS_5/CFT_4 and AdS_4/CFT_3 .

  - In chapter 5 we explore the near-BPS limit of twist operators in $\mathfrak{sl}(2)$ sector. It is based on the paper [9] where we calculate the quadratic in spin term in the anomalous dimension of twist operator when spin is small and obtain from this result predictions at weak and strong coupling.
  - In chapter 6 we find anomalous dimension of a family of observables generalizing cusp Wilson line. This is done in two ways: first by solving TBA and then by solving the much simpler QSC equations. This chapter is based on our paper [10].
  - In chapter 7 we describe quasiclassical limit of AdS/CFT: the traditional approach through sigma-model and its relation to the quasiclassical limit of QSC. In section 7.4, based on our paper [11], we construct a classical algebraic curve for the observable discussed in the previous chapter, cusped Wilson line with insertion of scalar operator at the cusp.
  - In chapter 8, based on our paper [12], we develop an numerical algorithm for solution of QSC equations and demonstrate its efficiency on several examples.
  - In chapter 9 we consider QSC in so-called BFKL regime. We give a brief introduction to BFKL physics, describe previous results in this area and in

section 9.3 present the result of our paper [13] — calculation of the new, NNLO coefficient in the weak coupling expansion of the BFKL eigenvalue.

– Chapter 10, unlike the rest of the thesis, deals with AdS_4/CFT_3 . After a short review of ABJM theory and the integrability methods in it we present the result of our paper [14], where calculate the slope function in ABJM and find a conjecture for the interpolating function $h(\lambda)$.

- **Part III**

  – Chapter 11 contains the conclusions and directions for further work.

  – Appendix A contains details of computation of curvature function in section 5.3 and some especially lengthy results. We also discuss generalization of the solution to higher mode numbers.

  – Appendix B contains some technical details of the derivation and some perturbative data omitted in chapter 6.

  – Appendix C contains some identities for elliptic function used in section 7.4.

1.3 Personal contribution

List of all publication of the author

Below is the list of all my publications; the papers (1)-(6) constitute the basis for this thesis:

(1) N. Gromov, F. Levkovich-Maslyuk and G. Sizov, "NNLO BFKL Pomeron eigenvalue in N=4 SYM,"

[arXiv:1507.04010 [hep-th]].

(2) N. Gromov, F. Levkovich-Maslyuk and G. Sizov, "Quantum Spectral Curve and the Numerical Solution of the Spectral Problem in AdS5/CFT4,"

[arXiv:1504.06640 [hep-th]].

(3) N. Gromov and G. Sizov, "Exact Slope and Interpolating Functions in N=6 Supersymmetric Chern-Simons Theory,"

Phys. Rev. Lett. **113**, no. 12, 121601 (2014).[arXiv:1403.1894 [hep-th]].

(4) N. Gromov, F. Levkovich-Maslyuk, G. Sizov and S. Valatka, "Quantum spectral curve at work: from small spin to strong coupling in $\mathcal{N} = 4$ SYM,"

JHEP **1407**, 156 (2014). [arXiv:1402.0871 [hep-th]].

(5) G. Sizov and S. Valatka, "Algebraic Curve for a Cusped Wilson Line,"

JHEP **1405**, 149 (2014). [arXiv:1306.2527 [hep-th]].

(6) N. Gromov, F. Levkovich-Maslyuk and G. Sizov, "Analytic Solution of Bremsstrahlung TBA II: Turning on the Sphere Angle,"

JHEP **1310**, 036 (2013). [arXiv:1305.1944 [hep-th]].

(7) B. Penante, S. Rajabi and G. Sizov, "CSW-like Expansion for Einstein Gravity,"

JHEP **1305**, 004 (2013). [arXiv:1212.6257 [hep-th]].

(8) B. Penante, S. Rajabi and G. Sizov, "Parity Symmetry and Soft Limit for the Cachazo-Geyer Gravity Amplitude,"

JHEP **1211**, 143 (2012). [arXiv:1207.4289 [hep-th]].

(9) G.A. Sizov, "Dynamics of inertial particles in a random flow with strong permanent shear,"

Phys.Rev.E 85, 016311(2012), [arXiv:1108.2691]

(10) I.V. Kolokolov, V.V. Lebedev, G.A. Sizov, "Magnetic field correlations in a random flow with strong steady shear,"

ZhETF, 140(2), 387-400 (2011) [JETP 113(2), 339-351 (2011)], [arXiv:1010.5904v1]

Below is the list of sections and chapters of this thesis based on my papers (1)-(6), in the chronological order.

- The first problem my collaborators and I worked during my PhD was solving Y-system with boundaries for generalized cusped Wilson line. In paper [10] we have solved the Y-system in the near BPS regime of the Wilson line with insertion of L scalars at the cusp. The result was a function of L, the cusp angle θ, and coupling and had a form of an expectation value in a matrix model (which was exploited in the next paper). Importantly, we presented a much shorted derivation of our result by means of QSC. This paper formed the basis for chapter 6 of this thesis.

- The second paper I published in collaboration with Saulius Valatka [11] and it was based on considering quasi-classical limit of the result of the previous paper. This result has a form of a matrix integral, which in the quasi-classical limit produces an algebraic curve. The results of this work are presented in section 7.4.

- During this time the formalism of QSC appeared and my next goal was to apply it to a computation which would give a new result and at the same time clarify and verify the QSC itself. In [9] my collaborators and I focused on the limit of small spin in twist operators. The linear contribution was known before and called the slope function. We have found the quadratic contribution for several first twists. From our result we were able to extract a new coefficient in the strong coupling expansion of Konishi anomalous dimension and also several coefficients in the expansion of the intercept at strong coupling. This work is contained in chapter 8.2 and in particular in section 5.3. The calculation of strong coupling expansion of BFKL intercept is contained in section 9.4.

- Given that QSC was also formulated for ABJM theory, it was natural to explore the regime of small spin in that theory as well.In this theory even the slope function was not known before. Performing the calculations which were technically quite similar to our previous work, in [14] we have found the slope function in ABJM for arbitrary coupling and twist. What is probably more important, by comparing the analytical structure of our result with a result for a different observable — BPS Wilson loop, we where able to extract from our computation a conjecture for so-called interpolating function $h(\lambda)$ — a missing ingredient in the integrability computations in $\mathrm{AdS}_4/\mathrm{CFT}_3$. This work is presented in sections 10.3-10.5 of chapter 10.

- In paper [12] my collaborators and I formulate a efficient method for numerical solution of QSC. We apply it to a number of scenarios, exploring $\mathfrak{sl}(2)$ sector of $\mathcal{N} = 4$ SYM , in particular dependence of spin on conformal dimension for arbitrary complex values of the latter. This work is presented in chapter 8.

- Our last result [13] included in this thesis is devoted to application of QSC to BFKL physics — an intriguing regime of high energy scattering which relates $\mathcal{N} = 4$ SYM to QCD in a non-trivial way. We find the previously unknown NNLO coefficient of weak coupling expansion of the BFKL eigenvalue and this work is contained in section 9.3 of chapter 9.

Section 7.5 contains a minor original calculation not published elsewhere.

Finally, two projects which I've been working on during my PhD are still in progress and hence are not included in this thesis.

The first, in collaboration with Ivan Kostov and Saulius Valatka, is work on application of topological recursion methods to the matrix model described in section 7.4 with a goal

of obtaining a systematic expansion of angle-dependent cusp anomalous dimension with insertion of a scalar operator at the cusp at strong coupling.

The second is work with my supervisor Nikolay Gromov on a version of Asymptotic Bethe Ansatz for BFKL regime [15].

1.4 Frequently used notation

Here we collected some notation which is most frequently used throughout the thesis.

- The coupling constant of planar $\mathcal{N}=4$ SYM is defined as

$$g = \frac{\sqrt{\lambda}}{4\pi}, \tag{1.1}$$

  where λ is the 't Hooft coupling.

- For a function $f(u)$ of spectral parameter u

$$f^{\pm} = f\left(u \pm \frac{i}{2}\right) \quad f^{[n]} = f\left(u + \frac{in}{2}\right) \tag{1.2}$$

  Branch points of most functions are situated at $\pm 2g + in$, with integer or half-integer n. Each pair of branch points can be connected by a cut either as $[-2g+in; 2g+in]$, in which case the cut is called short, or through infinity, as $(-\infty; -2g+in] \cup [2g+in; \infty)$, in which case it is called long. Choosing all cuts short is called physical kinematics, all cuts long — mirror kinematics.

  We denote the analytical continuation of f under the cut on the real axis as $\tilde{f}$.

- Spectral parameter u is related to Zhukovsky variable $x(u)$ by

$$x + 1/x = u/g \tag{1.3}$$

- Indices of Q-functions run from one to four and in the left-right symmetric case are raised with the matrix

$$\chi = \begin{pmatrix} 0 & 0 & 0 & -1 \\ 0 & 0 & 1 & 0 \\ 0 & -1 & 0 & 0 \\ 1 & 0 & 0 & 0 \end{pmatrix}. \tag{1.4}$$

- UHP stands for upper half-plane and LHP for lower half-plane

2 Overview of $\mathbf{AdS_5/CFT_4}$

In this chapter we will briefly review gauge/gravity dualities and in particular the one most relevant for this thesis, $\mathrm{AdS}_5/\mathrm{CFT}_4$ duality. This subject has been covered in many good reviews [16, 17, 18, 19, 20, 21, 22, 23], some of which we partially follow below. First in this section we draw some intuitive picture of how string-like objects might emerge in a gauge theory. Then in the next section 2.1 we describe the gauge side $\mathrm{AdS}_5/\mathrm{CFT}_4$ duality, $\mathcal{N} = 4$ SYM theory. In section 2.2 we review the string side, IIB string theory on $AdS_5 \times S^5$ background, and the statement of the duality, using Maldacena's argument for the equivalence of these two theories.

Maldacena's 1997 discovery was not the first time physicists considered a possibility that gauge theory can be related to gravity. First of all, string-like objects most naturally appeared in gauge theory as flux tubes in QCD: as is widely known, string theory was initially developed for description of strong interactions. Possibly the most fundamental property of AdS/CFT dualities, so-called holographic principle, stating that gravity can be described by gauge theory living in a space of codimension one was worked out in [24, 25]. Ideas that the fifth missing dimension might be related to the energy scale were also in the air. However, thinking about a duality between a four-dimensional gauge theory and a string theory or gravity in higher dimensions, one encounters an apparent paradox of degrees of freedom mismatch: intuitively the former should have much less states than the latter. The resolution of the paradox is that the missing degrees of freedom can come from the gauge group structure of the gauge group if one makes the rank of the gauge group N large.

Furthermore, in the limit of large N the "string worldsheet" can be seen emerging in the usual perturbative expansion of $\mathcal{N} = 4$ SYM from the summation of Feynman diagrams [26, 27]. Indeed, because of the gauge group structure of $\mathcal{N} = 4$ SYM operators, every Feynman diagram has some dependence on N and scales as a power of N in the large N limit. Thus in the large N limit perturbative expansion of an expectation value of certain observable can be organized as expansion over $1/N$. Interestingly, the behavior of a particular diagram in the expansion at large N has a nice geometric interpretation. To see this notice that graphs which can be drawn on a plane without self-intersections make the leading contribution at large N, and the rest of them are suppressed by powers of N. One can classify the graphs by the minimum number of "handles" of surface on which they can be drawn without self-intersections. Thus expansion in $1/N$ becomes expansions

over topological genus of surfaces. Even more graphically, one can turn Feynman graphs into "fat" graphs, and then different Feynman diagrams will produce "worldsheets" of different genus determined by their scaling at large N. This, of course, strongly reminds of expansion of string amplitudes in string coupling g_{str}: leading contribution comes from worldsheets of a topology of a sphere, and adding g handles to it suppresses the contribution by a power of g_{str}^{-2g}. So from this point of view Feynman diagrams appear as discretizations of string worldsheet and $1/N$ on gauge theory side should be related to string coupling constant. Later we will see this correspondence between the parameters confirmed by a more rigorous analysis.

2.1 Gauge side of the duality: $\mathcal{N} = 4$ SYM

The gauge theory side of the $\mathrm{AdS}_5/\mathrm{CFT}_4$ duality is $\mathcal{N} = 4$ super Yang-Mills theory (SYM). It is a supersymmetric non-abelian gauge theory with gauge group $SU(N)$ which has a coupling parameter g_{YM}. The theory possesses $\mathcal{N} = 4$ supercharges, which is the maximum amount of supersymmetry in four dimensions for theories with particles of spin smaller than 2. This amount of supersymmetry makes the theory in a certain sense "unique" among the four-dimensional theories: supersymmetry leaves no free parameters in the Lagrangian, except for one, which can be represented as an overall factor — the coupling constant. Its uniqueness is also reflected in the fact that it enjoys several other remarkable and apparently interconnected properties: conformal symmetry, existence of a dual string theory, and integrability. A convenient way to describe this theory is to view it as the dimensional reduction of $D = 10$ $\mathcal{N} = 1$ SYM theory defined by the following action [22]

$$S = \frac{1}{g_{SYM}^2} \int d^{10}x \ \mathrm{tr} \ \left(-\frac{1}{2} F_{MN} F^{MN} + i\bar{\chi}\gamma^M D_M \chi \right), \tag{2.1}$$

where $M = 0 \ldots 9$. Here F_{MN} is the field strength constructed from vector potential A^M and χ is a Majorana-Weyl spinor with 16 real components.

To perform the dimensional reduction, ignore the dependence of all fields of coordinates x_M for $M > 3$. After that the first four components of the vector potential will form the gauge field A_μ, $\mu = 0 \ldots 3$ and the rest will be the six massless real scalars Φ_i. The spinor χ splits into four four-dimensional Weyl spinors ϕ_a. All the fields will transform in the adjoint representation of the gauge group $SU(N)$. In terms of these fields the reduced

Lagrangian looks like

$$\mathcal{L} = \frac{1}{g_{YM}^2}\mathrm{tr}\ \left(\frac{1}{4}F_{\mu\nu}F^{\mu\nu} + \frac{1}{2}D_\mu\Phi_i D^\mu\Phi^i + \bar{\psi}^a\sigma^\mu D_\mu\psi_a \right.$$
$$\left. -\frac{1}{4}\left[\Phi_i,\Phi_j\right]\left[\Phi^i,\Phi^j\right] - \frac{i}{2}\sigma_i^{ab}\psi_a\left[\Phi^i,\psi_b\right] - \frac{i}{2}\sigma_{ab}^i\bar{\psi}^a\left[\Phi_i,\bar{\psi}^b\right]\right) \tag{2.2}$$

The theory which we have obtained has $\mathcal{N} = 4$ supersymmetries. Different supercharges are also related to each other by R-symmetry $SU(4)$, double cover of $SO(6)$, under which the scalars transform in the fundamental and fermions in spinor representations.

Conformal symmetry The theory defined by (2.2) is conformal, and this being an important property, we will elaborate on this point a bit.

Conformal transformations are "local" scaling transformations, or rigorously, those coordinate transformations, which preserve the metric up to a factor

$$ds^2 = g_{\mu\nu}(x)dx^\mu dx^\nu \to \Omega(x)g_{\mu\nu}(x)dx^\mu dx^\nu \tag{2.3}$$

Field theories which are invariant under these transformations are called Conformal Field Theories (CFT). Curiously, under very general assumptions, in QFTs just scale invariance itself implies conformal invariance [28, 29, 30]. CFTs appear as fixed points of RG flows and can be either free (most common and trivial case) or interacting. The object of our study, $\mathcal{N} = 4$ SYM belongs to the latter case. The most straightforward way to check if the theory is conformal or not is to compute its β-function. One-loop β-function for $SU(N)$ gauge theories is determined by the matter content and is given by [32, 33]

$$\beta = -\frac{g^3}{16\pi^2}\left(\frac{11}{3}N - \frac{1}{6}\sum_s C_s - \frac{1}{3}\sum_f \bar{C}_f\right), \tag{2.4}$$

where g is the coupling, the first sum goes over real scalars, the second one is over Weyl fermions, and C_s, $\bar{C}_f$ are the corresponding quadratic Casimirs. In $\mathcal{N} = 4$ SYM all the fields are in adjoint and so all Casimirs are equal to N. One can plug into this formula the six real scalar and eight Weyl fermions and check that at one loop $\mathcal{N} = 4$ SYM is indeed conformal. A much more non-trivial argument shows that β-function is actually zero to all loops; the cancellations of Feynman diagrams causing this are deeply related to the supersymmetry of the theory [34, 35, 36].

The implications of conformal symmetry are very different in two dimensional systems and in higher dimensional ones. In two dimensions the conformal algebra turns out to be infinite-dimensional, the so-called Virasoro algebra, and this fact gives rise to the rich world of two-dimensional CFTs; in higher dimensions the conformal algebra is finite. In

four dimensions, where $\mathcal{N} = 4$ SYM lives, the conformal algebra consists of fifteen generators. Ten of them constitute the Poincare algebra: they are translations P_μ and Lorentz transformations $M_{\mu\nu}$. The remaining five are specific to conformal transformations: special conformal transformation K_μ and dilatation D. Dilatation is just a uniform scaling of all coordinates

$$x'_\mu = \lambda x_\mu \tag{2.5}$$

Special conformal transformation can be represented as a superposition of inversion $x'_\mu = x'_\mu/x^2$, translation by some vector b_μ, and inversion again, thus it is easy to see that the finite form of the transformation looks like

$$x'_\mu = \frac{x_\mu - b_\mu x^2}{1 - 2b \cdot x + b^2 x^2} \tag{2.6}$$

The operators of conformal algebra can be represented as differential operators acting on functions on Minkowski space:

$$P_\mu = -i\partial_\mu \tag{2.7}$$

$$K_\mu = -i\left(2x_\mu x^\nu \partial_\nu - x^2 \partial_\mu\right) \tag{2.8}$$

$$M_{\mu\nu} = i(x_\mu \partial_\nu - x_\nu \partial_\mu) \tag{2.9}$$

$$D = -ix_\mu \partial^\mu \tag{2.10}$$

From this representation one easily derives the commutation relations

$$[D, P_\mu] = -iP_\mu, \quad [D, M_{\mu\nu}] = 0 \quad [D, K_\mu] = iK_\mu \tag{2.11}$$

$$[M_{\mu\nu}, P_\lambda] = -i\left(\eta_{\mu\lambda} P_\nu - \eta_{\lambda\nu} P_\mu\right) \quad [M_{\mu\nu}, K_\lambda] = -i\left(\eta_{\mu\lambda} K_\nu - \eta_{\lambda\nu} K_\mu\right) \tag{2.12}$$

$$[P_\mu, K_\nu] = 2i\left(M_{\mu\nu} - \eta_{\mu\nu} D\right) \tag{2.13}$$

The eigenvalue of Δ is called the conformal dimension and it will be important to us throughout the thesis, since, as we will see later, duality maps it to the energy of a string state. From the commutation relations it is obvious that K_μ lowers the conformal dimension of an operator by one. However, in a unitary theory conformal dimensions can not be negative. Thus acting with K_μ on an arbitrary operator sufficiently many times we will obtain an operator annihilated by K_μ. Such an operator is called *primary*. Inverting the logic, we can now construct the whole space of operators in this way: certain operators are taken as primaries; each of them upon the repeated action of P_μ produces a family of operators which are called descendants of this primary.

We have described the four-dimensional conformal group, which is isomorphic to the group of isometries of AdS_5. This isomorphism has significant implications for the

AdS/CFT duality. It can be made more graphic by combining the generators of the conformal algebra into the matrix representing an element of $\mathfrak{so}(4,2)$ in the following way

$$\Lambda = \begin{pmatrix} 0 & -D & -\frac{K_\mu - P_\mu}{2} \\ D & 0 & -\frac{K_\mu + P_\mu}{2} \\ \frac{K_\mu - P_\mu}{2} & \frac{K_\mu + P_\mu}{2} & M_{\mu\nu} \end{pmatrix} \tag{2.14}$$

Since $\mathcal{N}=4$ SYM is not only conformal, but also supersymmetric theory, the conformal symmetry group is enhanced to superconformal $PSU(2,2|4)$. The four-dimensional conformal group $SO(4,2)$ and the R-symmetry $SO(6)$ form its bosonic subgroup. To generate the whole superconformal group, one also have to add fermionic generators, also called supercharges, which form a graded Lie algebra. For $\mathcal{N}=4$ there are 16 supercharges $Q_{\alpha a}$ and $\tilde{Q}^a_{\dot\alpha}$, $\alpha, \dot\alpha = 1,2$ and $a = 1,\dots,4$. Commutation relation of two supercharges is proportional to the translation operator; commutation relations of supercharges with $M_{\mu\nu}$ are determined by the fact that they transform under spinor representation of Lorentz group:

$$\{Q_{\alpha a}, \tilde{Q}^b_{\dot\alpha}\} = \gamma^\mu_{\alpha\dot\alpha}\delta_a{}^b P_\mu, \quad \{Q_{\alpha a}, Q_{\alpha b}\} = \{\tilde{Q}^a_{\dot\alpha}, \tilde{Q}^b_{\dot\alpha}\} = 0 \tag{2.15}$$

$$[M^{\mu\nu}, Q_{\alpha a}] = i\gamma^{\mu\nu}_{\alpha\beta}\epsilon^{\beta\gamma}Q_{\gamma a}, \quad [M^{\mu\nu}, \tilde{Q}^a_{\dot\alpha}] = i\gamma^{\mu\nu}_{\dot\alpha\dot\beta}\epsilon^{\dot\beta\dot\gamma}\tilde{Q}^a_{\dot\gamma}, \tag{2.16}$$

where $\gamma^{\mu\nu}_{\alpha\beta} = \gamma^{[\mu}_{\alpha\dot\alpha}\gamma^{\nu]}_{\beta\dot\beta}\epsilon^{\dot\alpha\dot\beta}$.

Operators $Q_{\alpha a}$ and $\tilde{Q}^b_{\dot\alpha}$ have conformal dimension $1/2$:

$$[D, Q_{\alpha a}] = -\frac{i}{2}Q_{\alpha a}\ , \ [D, \tilde{Q}^a_{\dot\alpha}] = -\frac{i}{2}\tilde{Q}^a_{\dot\alpha} \tag{2.17}$$

To complete the algebra we have to consider the commutation relations of supercharges with bosonic generators. This produces a new class of generators called special conformal supercharges:

$$[K^\mu, Q_{\alpha a}] = \gamma^\mu_{\alpha\dot\alpha}\epsilon^{\dot\alpha\dot\beta}\tilde{S}_{\dot\beta a}\ , \ [K^\mu, Q^a_{\dot\alpha}] = \gamma^\mu_{\alpha\dot\alpha}\epsilon^{\alpha\beta}S^a_\beta \tag{2.18}$$

Their (anti)commutation relations are given by

$$\{S_{\alpha a}, \tilde{S}^b_{\dot\alpha}\} = \gamma^\mu_{\alpha\dot\alpha}\delta_a{}^b K_\mu, \quad \{S^a_\alpha, S^b_\alpha\} = \{\tilde{S}^a_{\dot\alpha a}, \tilde{S}^b_{\dot\alpha b}\} = 0 \tag{2.19}$$

$$[K_\mu, S^a_\alpha] = [K_\mu, \tilde{S}_{\dot\alpha a}] = 0 \tag{2.20}$$

Finally the algebra is closed by anticommutation relations between supercharges and special conformal supercharges

$$\{Q_{\alpha a}, S^b_\beta\} = -i\epsilon_{\alpha\beta}\sigma^{IJ}{}_a{}^b R_{IJ} + \gamma^{\mu\nu}_{\alpha\beta}\delta_a{}^b M_{\mu\nu} - \frac{1}{2}\epsilon_{\alpha\beta}\delta_a{}^b D \tag{2.21}$$

$$\{Q_{\alpha a}, \tilde{S}^b_{\dot\beta}\} = i\epsilon_{\dot\alpha\dot\beta}\sigma^{IJ}{}_b{}^a R_{IJ} + \gamma^{\mu\nu}_{\dot\alpha\dot\beta}\delta_a{}^b M_{\mu\nu} - \frac{1}{2}\epsilon_{\dot\alpha\dot\beta}\delta^a{}_b D \tag{2.22}$$

$$\{Q_{\alpha a}, \tilde{S}_{\dot\beta b}\} = \{\tilde{Q}^a_\alpha, S^b_\beta\} = 0 \tag{2.23}$$

As we mentioned before, representations of conformal group can be constructed by taking a primary operator $\mathcal{O}$ and considering all its descendants $P_{\mu_{n_1}}\dots P_{\mu_{n_k}}\mathcal{O}$. Representations of superconformal group are obviously larger. However, in a special case when the primary is annihilated by certain combinations of supercharges one can construct special, "short representations" of superconformal group. In this case the operator is called chiral primary, or BPS operator. Such operators are dual to Kaluza-Klein supergravity modes in AdS_5; they are also notable by the fact that their conformal dimensions do not receive quantum corrections. This property makes them important points in the space of operators of $\mathcal{N}=4$ SYM . In particular, it is sometimes a fruitful strategy to explore the neighbourhood around BPS point in the parameter space. We exploit this near-BPS perturbation technique in chapters 5, 6, 10.

Perhaps the most remarkable property of CFTs is that, at least in principle, all information about the theory is encoded in its two- and three-point correlators, because higher-point correlators can be reduced to them using so-called Operator Product Expansion. Moreover, these lower-point correlators have their coordinate dependence completely fixed by the conformal symmetry. Thus the whole theory is controlled by a rather small and well-understood set of parameters. Let us elaborate on these parameters. Consider a correlator of two scalar operators $\langle\mathcal{O}_1(x_1)\mathcal{O}_2(x_2)\rangle$ with conformal dimensions Δ_1 and Δ_2. We know that it can only be a function of the distance between the two points and that an operator of dimension Δ transforms under the rescaling as $\mathcal{O}(\lambda x)\to\lambda^{-\Delta}\mathcal{O}(x)$. This fixes the correlation function up to a constant, which can be absorbed into the normalization of the operators. Thus we arrive to the following expression for the two point function

$$\langle\mathcal{O}_1(x_1)\mathcal{O}_2(x_2)\rangle=\frac{\delta_{\Delta_1,\Delta_2}}{(x_1-x_2)^{2\Delta_1}} \tag{2.24}$$

Similarly, the three-point function's coordinate dependence can be fixed by the rescaling argument as before, however we do not have any freedom left to fix the constant

$$\langle\mathcal{O}_1(x_1)\mathcal{O}_2(x_2)\mathcal{O}_3(x_3)\rangle=\frac{C_{123}}{(x_1-x_2)^{\Delta_1+\Delta_2-\Delta_3}(x_1-x_3)^{\Delta_1+\Delta_3-\Delta_3}(x_2-x_3)^{\Delta_2+\Delta_3-\Delta_1}} \tag{2.25}$$

The constants C_{123} appearing in the right hand side are called structure constants. Same constants enter in the OPE of two operators, thus determining all higher-order correlators.

We can now see the importance of finding conformal dimensions and structure constants of $\mathcal{N}=4$ SYM : this information is enough to determine the rest of correlators in the theory. In this thesis we will focus on the spectral problem, i.e. finding the dimensions. However, the Quantum Spectral Curve method which is our main tool in solving this prob-

lem could in principle be applicable to calculation of three-point functions via Sklaynin's of separation of variables procedure. We speculate on this a little in the conclusions.

2.2 String side of the duality and Maldacena's argument

The AdS/CFT correspondence states that $\mathcal{N} = 4$ SYM theory described above is equivalent to a completely different theory — type IIB string theory on $AdS_5 \times S^5$ background. More precisely, $\mathrm{AdS}_5/\mathrm{CFT}_4$ correspondence states the equivalence of partition functions with sources in these two theories: the left hand side of the duality is partition function of $\mathcal{N} = 4$ SYM with sources J for local operators, and the right hand side is partition function of the worldsheet model with sources for vertex operators fixed to value J at the boundary of AdS. This means that there is a map between the string observables on the boundary of AdS and states of SYM; in particular, the expectation values of these observables are equal.

The string side of the duality is reviewed in [37]. Another useful for us formulation is given in terms of a coset sigma-model [38] (see also [39] and section 7.1 of this thesis).

The easiest way to describe $(n+1)$-dimensional Anti-de Sitter (AdS) space is to embed it into $(n+2)$-dimensional flat space with the metric $ds^2 = dX_0^2 + dX_{n+2}^2 - \sum_{k=1}^{n+1} dX_k^2$ as a surface

$$X_0^2 + X_{n+2}^2 - \sum_{k=1}^{n+1} X_k^2 = -R^2. \tag{2.26}$$

One can introduce a coordinate system $(x^1, ..x^n, z)$ which covers part of AdS space $(z > 0)$ and in which the metric looks like

$$ds^2 = \frac{dx_\mu dx^\mu + dz^2}{z^2} \tag{2.27}$$

where x_μ are coordinates of n-dimensional Minkowski space.

From this coordinate parametrization it is easy to see that the boundary of AdS_{n+1} space $(z \to 0)$ is conformally equivalent to n-dimensional Minkowski space. This fact makes possible the holographic nature of AdS/CFT correspondence: we place the gauge theory on the boundary of AdS_5 space, which is precisely four-dimensional Minkowski space. The first remarkable thing to notice is the matching of symmetry groups: indeed, the isometries of AdS_5 form $SO(2,4)$ group and this is same as conformal group in four dimensions. There remain as well isometries of S^5, which form $SU(4) \cong SO(6)$. It turns out that they have their precise counterpart in $\mathcal{N} = 4$ SYM — the R-symmetry, rotating, for example, six real scalars in the fundamental.

The correspondence was proposed in 1997 when Maldacena [40] suggested that planar limit of certain CFTs contains supergravity as their subsector. Some manifestations of a two-dimensional gauge/gravity duality were known before [41, 42, 43], but this was the first duality of this kind involving a four-dimensional theory.

In order to see how Maldacena's argument works we have to introduce solitonic objects called Dirichlet-branes or D-branes — flat objects extended into $p+1$ space-time dimensions. In string perturbation theory they enter as boundary conditions for open strings: open strings end on a D-brane and satisfy Dirichlet boundary conditions on it.

One then considers type IIB string theory in the presence of a stack of N_c such branes. There are two types of excitations in this system: closed strings in the bulk and open strings which end on the branes. In the low energy limit the closed strings decouple and open strings on the branes produce $SU(N_c)$ gauge theory. For type IIB string theory this is $\mathcal{N} = 4$ SYM .

Let us sketch an argument supporting the duality. One starts by considering a stack of N_c D3 branes in 9+1 Minkowski space. There are two types of excitations in this system: closed strings in the bulk and opens strings which end on the branes. Each brane couples to gravity with coupling g_s, so the total effect on the metric is proportional to $g_s N_c$. We are going to consider the low-energy limit of this system. This can be done in two different regimes.

When $g_s N_c \ll 1$ the space is almost flat, so the theory in the bulk decouples and gives just ten-dimensional supergravity. The lower energy limit of the open strings ending on the branes is four-dimensional gauge theory, $\mathcal{N} = 4$ SYM .

On the other hand, in the limit $g_s N_c \gg 1$ the stack is described by an extremal black 3-brane (a generalization of a black hole to an extended object). The energy seen by an observer depends on the distance to the brane, in particular near the horizon all string modes effectively become massless. Thus the near-horizon limit again decouples from the bulk. The near-horizon limit of the black brane supergravity solution can be written as

$$ds^2 \approx R^2 \left(\frac{-dt^2 + dx^2 + dy^2 + dz^2 + du^2}{u^2} + d\Omega_5^2 \right), \tag{2.28}$$

which is nothing but the AdS_5 metric (2.27) times a sphere.

Hence we see that in the low-energy limit the physics near the branes decouples from the rest, both at large and small $g_s N_c$. In the bulk we get supergravity in both cases. And on the branes interesting things happen: in one regime we get string theory on the $AdS_5 \times S^5$ background and in the other a gauge theory. The most natural assumption is that these two theories: $\mathcal{N} = 4$ SYM and type IIB string theory on $AdS_5 \times S^5$ are two

regimes of the same theory.

Parameters on the two sides of the duality should be matched. On the gauge theory side we have the coupling g_{YM} and the number of colours N_c, which are combined into the 't Hooft coupling $\lambda = g_{YM}^2 N_c$. The string theory side is parametrized by the inverse string tension α', the string coupling g_{str}, and the radius R of AdS and of the sphere; one also introduces effective string tension $T = \frac{R^2}{2\pi\alpha'}$. These parameters are related through

$$\lambda = 4\pi^2 T^2, \; g_{YM}^2 = g_{str} \tag{2.29}$$

The duality has been proposed by Maldacena as a conjecture and since then it has received a lot of confirmations. In particular, in [44, 45] an exact correspondence was established between some states of $\mathcal{N} = 4$ SYM and supergravity modes. Another confirmation came from studying the so-called BMN operators [46, 47, 48]. On gauge theory side these are operators with large R-charge, which can be represented as long traces made of the same fields with finite number of "impurities" inserted. R-charge of gauge theory operator is translated into angular momentum of rotation on a sphere. Thus BMN operators correspond to short strings rotating fast on the sphere.

Duality implies that all fields and parameters on one side have their correspondences on the other. One of the most important observables for us, the dimension of an operator in the gauge theory, equals to the mass of the corresponding string state. The supergravity fields can be mapped to states of CFT: for example, the graviton corresponds to energy-momentum tensor, dilaton to gauge kinetic term $F_{\mu\nu}^2$ and the gauge field in the bulk maps to conserved currents in CFT.

Once again revisiting the picture of gauge theory defined on the boundary of the AdS space, in the bulk of which lives a string theory, one can see that correlators of local operators are dual to string states with corresponding boundary conditions. This means, in particular, that their expectation values can be calculated as the corresponding string amplitudes. But the duality is not restricted to local operators: it turns out that expectation values of Wilson lines can be calculated as regularized areas of minimal surfaces with boundary conditions defined by the corresponding Wilson line.

AdS_5/CFT_4 was the first and the most well studied of AdS/CFT dualities. After it was discovered it was natural to look for similar dualities in different number of dimensions and, indeed, it turned out that a three-dimensional supersymmetric gauge theory, ABJM, is dual to string theory in $AdS_4 \times \mathbb{C}P^3$ background [49, 50]. This system will be the object of our studies in chapter 10. Later even lower-dimensional examples of AdS/CFT correspondences were discovered: string theory on $AdS_3 \times S^3 \times T^4$ or $AdS_3 \times S^3 \times S^3 \times S^1$

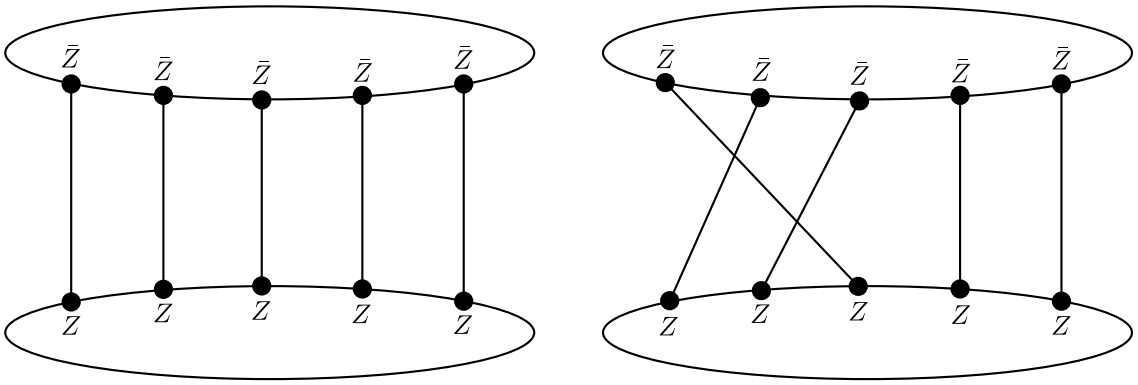

Figure 2: Planar and non-planar contributions to $\langle \text{tr } Z^L \text{tr } \bar{Z}^L \rangle$

is dual to a two-dimensional CFT [51, 52, 53].

2.3 Planar limit

In this thesis we will always be dealing with a particular limit of AdS/CFT system, the so-called planar limit [54]. On the gauge side of the duality one should take the number of colours N_c to infinity and the coupling constant g_{YM} to zero, keeping their combination $g^2_{YM}N_c$ constant:

$$\lambda = g^2_{YM}N_c = \text{fixed},\ g_{YM} \to 0,\ N_c \to \infty \tag{2.30}$$

The planar limit is remarkable for many reasons: first of all, many calculations simplify significantly in this limit. The main reason is that of all Feynman diagrams only those which can be drawn on a plane without self-intersection will survive, and the rest are suppressed by powers of N_c.

Taking the planar limit affects the class of operators we should take into account. Indeed, consider a simple example: the correlator of two BPS operators tr Z^L and tr $\bar{Z}^L$ shown on Fig 2. Different Feynman diagrams contributing to the result correspond to different ways of pairing Z operators with different $\bar{Z}$s. All N_c Feynman diagrams pairing the scalars in non-intersecting ways scale like N_c^L, and all the intersecting ones are suppressed as powers of N_c. Moreover, consider splitting one of the traces into two: the resulting correlator will again be suppressed. One can show that this is a general rule: contributions from multi-trace operators are suppressed compared to single trace ones. The planar limit has a very nice geometric meaning on the string theory side: (2.30) is equivalent to $g_{str} \to 0$, in other words taking into account only worldsheets with topology of a sphere.

2.4 Classes of operators in $\mathcal{N} = 4$ SYM

The duality implies, in particular, that each operator of $\mathcal{N} = 4$ SYM corresponds to a string state. Here we will review the most common classes of operators and their corresponding classical string solutions.

Local operators In a gauge theory the fields transform under the action of the gauge group, but all physically relevant information about the theory should be contained in gauge-invariant quantities. Consider first local operators: products of covariantly transforming fields and covariant derivatives taken at the same point in space-time. A natural way of making such an object gauge-invariant is taking the trace. One can construct an operator consisting of just one trace, or a product of several traces. However, in the planar limit the latter are reduced to the former inside the correlators: correlation between fields belonging to different traces is suppressed by powers of N. So we arrive to a class of operators of the form

$$\mathcal{O}(x) = \text{tr } (Q_1(x) \dots Q_L(x)) \tag{2.31}$$

where each letter Q_i is one of the fields ϕ_I, $\bar{\psi}^a_{\dot{\alpha}}, \psi_{a\alpha}$, $F_{\alpha\beta}$ or their covariant derivatives.

Among all possible operators a special role is played by the chiral primary operators, which, as we have mentioned before, are annihilated by certain combinations of supercharges. R-symmetry fixes the conformal dimensions of such operators to (half)integer values, and thus it can not vary continuously with coupling, i.e. it does not receive quantum corrections; because of this such operators are also called "protected". Simplest examples of local BPS operators can be constructed as traces of products of scalar operators: any combination of the kind $\chi^{i_1 \dots i_k} \phi_{i_1} \dots \phi_{i_k}$ with traceless symmetric tensor χ is protected. In particular, we will often refer to its highest weight representative tr Z^L, where we introduced the notation

$$X = \phi_5 + i\phi_6, \quad \bar{X} = \phi_5 - i\phi_6, \tag{2.32}$$

$$Y = \phi_3 + i\phi_4, \quad \bar{Z} = \phi_3 - i\phi_4, \tag{2.33}$$

$$Z = \phi_1 + i\phi_2, \quad \bar{Z} = \phi_1 - i\phi_2. \tag{2.34}$$

Such an operator has one non-zero charge on the sphere $J_1 = L$ and one in AdS $\Delta = L$. On the string side in the quasiclassical limit this corresponds to a BMN solutions — point-like string sitting at the centre of AdS_5 and rotating with angular momentum L around a big circle of S^5 [46].

Consider now a single trace operator made out of scalars of two types, for example X and Y. Linear combinations of such operators form a closed subsector in the whole algebra of operators, in the sense that they do not mix with other operators under the action the dilatation operator. Scalars X and Y transform under the action of the $\mathfrak{su}(2)$ subalgebra of $\mathfrak{psu}(2,2|4)$, so this subsector is called $\mathfrak{su}(2)$ subsector. The corresponding string solution has one non-zero global charge in AdS and two on the sphere, which makes it sit in the center of AdS and spin on $S^3 \subset S^5$ [55].

Another subsector which is very relevant for us is called the $\mathfrak{sl}(2)$ subsector: it is spanned by single-trace operators consisting of one scalar, i.e. Z and light-cone derivatives $D = D_0 - D_1$. Denoting the number of scalars by L and the number of derivatives by S we can write an operator of this subsector schematically as

$$\text{tr } \left(D^S Z^L\right) + \ldots, \tag{2.35}$$

where dots denote permutations of derivatives acting on different scalars. Since the number of derivatives acting on a particular scalar can be arbitrarily large, $\mathfrak{sl}(2)$ subsector is called non-compact. Many of problems studied in this thesis deal with operators from this subsector: the slope and curvature functions in chapter 5, the BFKL regime in chapter 9 and the slope function in ABJM in section 10.2. We often refer to L as the twist or the length of an operator and to S as its spin.

In the limit of large spin and length the AdS/CFT duality matches the operator (2.35) with a classical solution called folded string, which is spinning in AdS as well as on the sphere [47, 56]. If, on the other hand, one keeps the length finite while taking the spin to infinity the anomalous dimension scales logarithmically with spin

$$\Delta = S + f(g) \ln S \tag{2.36}$$

The function $f(g)$ is called the cusp anomalous dimension, because it also determines the anomalous dimension of light-like cusped Wilson line [57, 58]. It is often convenient to describe the classical string solution in terms of the so-called classical spectral curve, on which we elaborate in section 7.3.

Finally, we will refer to the subsector of single-trace operators made of just scalars as to $\mathfrak{so}(6)$ subsector. The corresponding string will sit at the origin of AdS_5 and rotate on the sphere with all three angular momenta non-zero. A particular class of such solutions was studied in [59, 60].

Wilson Lines Besides the local operators described above one can also study non-local operators, of which the most often considered examples are Wilson lines. In gauge

theories Wilson lines are usually defined by integrating a gauge field around some contour and depend on the path of integration $x_\mu(t)$ in spacetime.

$$W_L = \text{tr } \mathcal{P} \exp \left(i \oint_C dx^\mu A_\mu \right) \tag{2.37}$$

where $\mathcal{P}\exp$ is path-ordered exponent. Such a Wilson line operator is gauge invariant if the integration contour is closed.

A supersymmetric version of the Wilson line we consider in SYM is constructed as

$$W_L = \text{tr } \mathcal{P} \exp \oint_C dt \left(i A_\mu \dot{x}^\mu + \vec{\Phi} \cdot \vec{n} |\dot{x}| \right), \tag{2.38}$$

The second term, required by supersymmetry, includes a six-dimensional path in the "internal space" $\vec{n}(t)$, such that $\vec{n}^2 = 1$. This can be understood as a remainder of the compactification from ten-dimensional theory: together 4 components of A_μ and six components of $\vec{n}(t)$ form a "path" in a ten-dimensional space. Wilson lines have a physical meaning: in QCD, for example, they describe a string connecting a quark and antiquark. Governed by this logic in chapter 6 we extract the quark-antiquark potential from the expectation value of cusped Wilson line.

The AdS/CFT duality maps Wilson lines to string states defined by their boundary conditions, i.e. whose worldsheets end on the corresponding Wilson line. Thus their expectation values are string partition functions with fixed boundary conditions, which in the supergravity limit have a nice geometrical interpretation: they become regularized areas of minimal surfaces in AdS space. Null-polygonal Wilson lines in $\mathcal{N} = 4$ SYM are also closely related to scattering amplitudes [61, 62]. Thus Wilson lines can serve as an important tool to explore AdS/CFT correspondence.

3 Integrability in $\text{AdS}_5/\text{CFT}_4$

In this short chapter we will discuss some integrability techniques and concepts existing in the context of $\text{AdS}_5/\text{CFT}_4$. In the subsequent subsections they will be presented roughly in the order of their development. The reader can see how each next tool is more powerful and has a broader scope of application. Our stating point will be weak-coupling integrability in section 3.1 and the last tool discussed here will be TBA in section 3.3. TBA can be reformulated into a much more compact and elegant form, called QSC, which we will describe in detail in the next chapter 4.

The review in this section only gives a sketch of the available techniques. Some are explained in more detail later in the text, where they are used; for a comprehensive review of others see [63].

3.1 Weak coupling: mapping to spin chains

Integrability in the context AdS/CFT was initially noticed on the gauge theory side. The first such occasion might be the appearance of Heisenberg spin chain Hamiltonian in the context of Regge limit of one-loop QCD amplitudes: in [64] the lattice model proposed in [65] to describe high energy gluon scattering was identified with integrable Heisenberg spin chain, which was further explored in [66, 67, 68]. This limit is also studied in chapter 9 of this thesis.

Later the Heisenberg spin chain appeared again in the study of four-dimensional gauge theories in a different context: the one-loop dilatation operator in $\mathcal{N} = 4$ SYM was identified with Hamiltonian of integrable spin chain in [69]. The spectral problem for long single-trace operators at one loop can be mapped onto a spectral problem for a spin chain Hamiltonian which happens to be integrable. This spectral problem is reduced to so-called Bethe ansatz equations, which are algebraic equations for the variables called roots. The problem at higher loops can also be mapped to spin chains, but with interaction range increasing with the number of loops. So one-loop Bethe ansatz was generalized to any coupling, producing so-called Asymptotic Bethe Ansatz (ABA). ABA gives answer up to exponentially small in spin chain length corrections. These corrections, called wrapping corrections, can be systematically computed.

In [71] the $\mathfrak{so}(6)$ subsector of $\mathcal{N} = 4$ SYM was proven to be integrable at one loop and evidence has been presented that this integrability could be extended to all loops. The analysis of this last paper was soon continued in [72], extending the one-loop integrability to all the subsectors. As a first solid confirmation of conjectured integrability beyond one loop, in [73] the three-loop dilatation operator was fixed from supersymmetry and other constraints and was found to be integrable.

In order to give an idea how integrable structures appear in $\mathcal{N} = 4$ SYM , let us briefly describe the mapping of single trace operators to spin chains at weak coupling and the derivation of Bethe equations. To this end, consider operators made of a trace of L scalar operators Z and $\bar{Z}$,

$$\mathcal{O} = \mathrm{tr}\ \left(Z Z \bar{Z} Z \bar{Z} \bar{Z} \ldots\right) \tag{3.1}$$

Such operators can be naturally mapped to spin chains of length L, representing on each site Z as spin up and $\bar{Z}$ as spin down, so that, for example, the operator above is mapped to $|\uparrow\uparrow\downarrow\uparrow\downarrow\downarrow\ldots\rangle$. The cyclicity of trace in the original picture induces periodic boundary conditions on the spin chain, i.e. closes it into a circle. It has been shown in [74] that in this representation the one-loop dilatation operator takes a form of Heisenberg XXX spin chain Hamiltonian, which is known to be integrable:

$$\hat{D} = L + \frac{\lambda}{16\pi^2}\sum_{l=1}^{L}(1 - P_{l,l-1}), \tag{3.2}$$

where $P_{l,l-1}$ is a permutation operator acting on sites l and $l-1$. One can now solve the spectral problem, i.e. find the eigenstates and the corresponding eigenvalues by the means of the Bethe ansatz.

In order to derive Bethe ansatz let us try to construct an eigenstate of the Hamiltonian (3.2) in terms of excitations above some vacuum. As a vacuum we can take, for example, as state with all spins up $\Omega = |\uparrow\uparrow\ldots\uparrow\rangle$. Then the simplest excited states will be those with one spin flipped down. One can check that the following linear combinations of them will be eigenstates of the Hamiltonian

$$|p\rangle = \frac{1}{\sqrt{L}}\sum_{l=1}^{L} e^{ipl}|\uparrow\uparrow\ldots\underset{l}{\downarrow}\ldots\uparrow\uparrow\rangle \tag{3.3}$$

Such a state is called a single magnon propagating with momentum p and has an energy

$$\epsilon(p) = \frac{\lambda}{2\pi^2}\sin^2\frac{p}{2} \tag{3.4}$$

A state with two magnons should be constructed from spin chains with two spins flipped down. Since magnon scatter on each other, the wave function can consist of two different contributions differing by the relation between the "positions" l_1, l_2 of the magnons.

$$|p_1,p_2\rangle = \sum_{l_1<l_2} e^{ip_1l_1+ip_2l_2}|\ldots\underset{l_1}{\downarrow}\ldots\underset{l_2}{\downarrow}\ldots\rangle + e^{i\phi}\sum_{l_1>l_2} e^{ip_1l_1+ip_2l_2}|\ldots\underset{l_2}{\downarrow}\ldots\underset{l_1}{\downarrow}\ldots\rangle \tag{3.5}$$

The two terms can be seen as asymptotic states at right and left infinities in time (if $p_1 > p_2$ then $l_1 > l_2$ at $t = \infty$ and the other ways round). Thus the relative phase of the second term is the two-magnon scattering phase. Requiring that a state of the form (3.5) should be an eigenstate of the Hamiltonian, one fixes the value of the scattering phase to

$$e^{i\phi} = S_{jk} = \frac{u_j - u_k - i}{u_j - u_k + i}, \tag{3.6}$$

where we introduced a rapidity variable u

$$e^{ip} = \frac{u + i/2}{u - i/2}. \tag{3.7}$$

The corresponding eigenvalue, i.e. the energy, is the sum of the energies (3.4) of two magnons. Similarly, for states with M magnons, i.e. M spins down, the eigenstates are

$$|p_1,\dots,p_M\rangle = \sum_{l_1<\dots<l_m} e^{ip_1l_1+\dots+ip_Ml_M}|\dots\underset{l_1}{\downarrow}\dots\underset{l_2}{\downarrow}\dots\underset{l_m}{\downarrow}\dots\rangle+\dots \tag{3.8}$$

where the dots stand for terms with all possible permutations of magnons, each multiplied by a corresponding factor of S-matrix. Since the system is integrable, scattering of many magnons factorizes into the product of individual scatterings, in other words the S-matrix of an M-magnon system is a product of S-matrices corresponding to pairwise permutations.

Consider a transformation under which the wave function has to be invariant: moving one magnon around the circle to its original place. The wave function acquires factors from the translation operator e^{iLp} and also a factor of $S(p,p_j)$ from scattering with every other magnon.

From (3.7) and (3.6) we then rewrite the condition of invariance of the wave-function as

$$\left(\frac{u_j+i/2}{u_j-i/2}\right)^L = \prod_{k\neq j}^{M}\frac{u_j-u_k+i}{u_j-u_k-i}, \tag{3.9}$$

where the left hand side is the phase coming from the translation operator and right hand side is the scattering. This equation was first derived by Hans Bethe in 1931 [75].

Periodicity of the spin chain imposes one more constraint on the set of Bethe roots: the total momentum $\sum_{k=1}^{M} p_k$ should vanish, which in terms of rapidity variables is

$$\prod_{j=1}^{M}\frac{u_j+i/2}{u_j-i/2}=1 \tag{3.10}$$

Suppose we know a solution of this system, a set of Bethe roots u_j satisfying (3.9) and (3.10). Then the energy of the corresponding eigenstate, i.e. the anomalous dimension of the corresponding operator, can be found by summing the energies of individual magnons given by (3.4)

$$\gamma = \frac{\lambda}{8\pi^2}\sum_{j=1}^{M}\frac{1}{u_j^2+1/4} \tag{3.11}$$

Another elegant way to obtain Bethe equations, which comes from the Algebraic Bethe Ansatz [76], is to construct so-called transfer matrix. Introduce first the monodromy operator defined as

$$\hat{M}(u) = \left(u+\frac{i}{2}\sigma_L\otimes\sigma\right)\left(u+\frac{i}{2}\sigma_{L-1}\otimes\sigma\right)\dots\left(u+\frac{i}{2}\sigma_1\otimes\sigma\right) = \begin{pmatrix} A(u) & B(u)\\ C(u) & D(u)\end{pmatrix} \tag{3.12}$$

Here σ_k is a Pauli matrices acting on k^{th} site and σ a Pauli matrix acting in the auxiliary space. Transfer matrix is the trace of the monodromy operator over the auxiliary space so it is an operator in the Hilbert space of the spin chain:

$$\hat{T}(u) = \mathrm{tr}_a M(u) = A(u) + D(u) \tag{3.13}$$

Transfer-matrices at different values of spectral parameter u commute with each other, and thus encode an infinite family of conserved charges. A state corresponding to a set of Bethe roots $u_1 \dots u_k$ is created by operators $B(u_i)$ acting on vacuum:

$$|\Psi\rangle = B(u_1) \dots B(u_k)|\Omega\rangle, \tag{3.14}$$

Acting on this state with the transfer matrix and using the commutation relation of $A(u)$ and $D(u)$ with $B(u)$ one can show that the eigenvalues of $\hat{T}(u)$ are given by

$$T(u) = (u + i/2)^L \prod_{k=1}^{J} \frac{u - u_k - i}{u - u_k} + (u - i/2)^L \prod_{k=1}^{J} \frac{u - u_k + i}{u - u_k} \tag{3.15}$$

On the other hand, $\hat{T}(u)$ is polynomial in u by construction. Thus there are no poles $u = u_k$ in (3.15), which immediately leads to (3.9).

3.2 Asymptotic Bethe Ansatz

The one-loop Bethe ansatz demonstrated above can be generalized to all loops in the limit of infinite spin chain length [77]. At finite coupling the elementary excitations — magnons are characterized by the following dispersion relation

$$e^{ip} = \frac{x^+}{x^-}, \quad E = ig\left(x^- - \frac{1}{x^-} - x^+ + \frac{1}{x^+}\right) \tag{3.16}$$

where Zhukovsky variable x is defined by

$$g(x + 1/x) = u \tag{3.17}$$

and $x^\pm = x(u \pm i/2)$ as everywhere in the text. As a function of the spectral parameter $x(u)$ has two branch points in the complex plane at $u = \pm 2g$. These can be connected by the so-called Zhukovsky cut, which will appear many times in the rest of this thesis. More precisely, out of two solutions of (3.17) we pick the one with a short cut and satisfies $|x| > 1$, i.e.

$$x(u) = \frac{1}{2}\left(\frac{u}{g} + \sqrt{\frac{u}{g} - 2}\,\sqrt{\frac{u}{g} + 2}\right) \quad . \tag{3.18}$$

S-matrix (3.6) has to be replaced by a more complicated all-loop matrix expression. Up to an overall factor it can be fixed from $\mathfrak{psu}(2,2|4)$ symmetry constraints [78]:

$$\hat{S} = \hat{S}_0 \sigma^{-2} \tag{3.19}$$

The overall factor, the so-called dressing phase was not known when a conjecture for all-loop Bethe ansatz equations for all subsectors of $\mathfrak{psu}(2,2|4)$ was proposed in [79]. Later the dressing phase σ was found in [80] by implementing crossing relations for the S-matrix. In a general situation ABA equations include 7 types of Bethe roots interacting with each other. The roots of type four determine the energy and the momentum and are called momentum-carrying or middle-node roots. For operators belonging to one of $\mathfrak{su}(2)$, $\mathfrak{sl}(2)$ or $\mathfrak{su}(1|1)$ sectors, only momentum-carrying roots survive. In this case Bethe equations look like

$$\left(\frac{x_k^+}{x_k^-}\right)^L = \prod_{j=1, j\neq k}^{K} \left(\frac{x_k^+ - x_j^-}{x_k^- - x_j^+}\right)^\eta \frac{1 - \frac{g^2}{2x_k^+ x_j^-}}{1 - \frac{g^2}{2x_k^- x_j^+}} \sigma^2(x_k, x_j). \tag{3.20}$$

Momentum-carrying roots and are constrained by zero momentum condition analogous to (3.10)

$$1 = \prod_{j=1}^{K_4} \frac{x_{4,j}^+}{x_{4,j}^-} \tag{3.21}$$

The energy is found from the momentum-carrying roots as a sum of energies of individual magnons

$$\gamma = \frac{i}{g^2} \sum_{j=1}^{K_4} \left(\frac{1}{x_{4,j}^+} - \frac{1}{x_{4,j}^-}\right) \tag{3.22}$$

We will give more details on ABA in section 4.5, where it is derived from the Quantum Spectral Curve. As we have said before, Asymptotic Bethe Ansatz is limited to infinite spin length: perturbatively at weak coupling it is valid to the order g^{2L-4}. At the next order a new type of Feynman diagrams appears and wrapping corrections have to be taken into account, which originates from virtual magnons going around the worldsheet. This was demonstrated in [81] by pointing out the discrepancy between ABA results and predictions from BFKL constraints. Going beyond infinite volume limit was first achieved through Lüscher corrections: for a general two-dimensional QFT Lüscher calculated leading order shifts to energy levels when the system is put on a cylinder [82]. His formulas can be applied to the wrapping interactions in $\mathcal{N} = 4$ SYM and give explicit formulas for corrections to the anomalous dimensions at weak [83, 84] and strong coupling [85, 86] (see also the review [87]).

A more universal, but at the same time more complex approach is given by Thermodynamical Bethe Ansatz described in the next section.

3.3 Thermodynamical Bethe Ansatz

The infinite volume limitation of ABA can be overcome by the so-called Matsubara trick, which leads to the Thermodynamical Bethe Ansatz [88, 89, 90] .

The idea is that by considering thermodynamics of a system of Bethe roots at finite temperature (but in an infinite spin-chain) and then performing a trick of exchanging length and inverse temperature one obtains a description of the operators of finite length. Indeed, consider a QFT on a torus with circumferences R and L. Notice that its partition function $Z(R, L)$ can be written in two ways:

$$Z(R, L) = \sum_k e^{-LE_k(R)} = \sum_j e^{-R\tilde{E}_j(L)}, \tag{3.23}$$

where $E_k(R)$ are the energy levels of the theory on the circle of circumference R at the temperature $1/L$ and $\tilde{E}_k(L)$ are the energy levels of the theory on the circle of circumference L at the temperature $1/R$. If we now take a limit $R \to \infty$, the first sum can be interpreted as a partition function of a QFT at temperature $1/L$ in the infinite volume and in the second one only the term corresponding to the ground state energy survives: it will give a partition function of a QFT at zero temperature, but finite volume. Hence this procedure allows to calculate the spectrum in the finite volume:

$$E_0(L) = \lim_{R\to\infty} \frac{1}{R} \sum_j e^{-R\tilde{E}_j(L)} \tag{3.24}$$

In order to calculate the right hand side we need to consider behavior of Bethe roots at finite temperature, i.e. in the thermodynamical limit. We assume that all states in this limit are bound states with densities ρ_A, where A labels different types of magnons. One then has to consider a thermodynamical limit of ABA equations of the type (3.20) which gives

$$\bar{\rho}_A(u) + \rho_A(u) = \frac{i}{2\pi} \frac{d\epsilon_A^*(u)}{du} - K_{BA}(v, u) * \rho_B(v) \tag{3.25}$$

Here ρ_A and $\bar{\rho}_A$ are densities of excitations and holes, ϵ is the dispersion relation and the kernel K_{AB}, describing the interaction between different types of excitations, is just proportional to the logarithm of the S-matrix element. One then has to minimize the free energy of the system on the class of densities satisfying the equation (3.25). This results in an infinite system of non-linear integral equations for Y-functions, related to the densities above, which depend on a complex spectral parameter u. These function are indexed by nodes on a T-shaped lattice and information about the state described by the system is encoded in their asymptotic behavior. The resulting equations are quite complicated and

can be schematically represented as

$$\log Y_A = K_{AB} * \log(1 + 1/Y_B) + \text{driving terms}, \tag{3.26}$$

where K_{AB} is a linear integral operator and the driving terms are source terms depending on specific operator under consideration.

Later analysis of analytical properties of Y-functions allowed to reduce the infinite system of TBA equations to a finite set, called FiNLE (Finite System of Non-Linear Integral Equations) [91]. First of all, TBA integral equation can be reformulated as purely functional equations

$$Y^+_{1,m} Y^-_{1,m} = (1 + Y_{1,m-1})\,(1 + Y_{1,m+1}) \tag{3.27}$$

and some analyticity constraints for Y-functions. Another important observation which made this reduction possible is the existence of an ansatz for Y-function in terms of new set of functions $T_{a,s}$

$$Y_{a,s} = \frac{T_{a,s+1} T_{a,s-1}}{T_{a+1,s} T_{a-1,s}} \tag{3.28}$$

in terms of which the original equations are equivalent to Hirota dynamics

$$T^+_{a,s} T^-_{a,s} = T_{a+1,s} T_{a-1,s} + T_{a,s+1} T_{a,s-1} \tag{3.29}$$

A general solution for Hirota equation can be written explicitly [92, 93, 94].

TBA allows to reduce the problem of calculating the anomalous dimension of an operator in $\mathcal{N} = 4$ SYM to a system of algebraic equations, which then can be solved numerically. In rare cases TBA can be solved exactly, one of the examples being the near-BPS limit of a cusped Wilson line, which was solved in [95, 91] and generalized in our paper [10] (see section 6). One should also mention that TBA equations were derived and tested for a lower-dimensional example of the AdS/CFT correspondence, $\mathrm{AdS}_4/\mathrm{CFT}_3$ [96, 97].

3.4 Classical spectral curve

A ground-breaking paper [98] established the relation between the perturbative integrability at weak coupling and the integrability observed in the sigma-model formulation at strong coupling (see also the review [99]). This is done through the construction of the classical spectral curve - a complex algebraic curve encoding all the information about a particular state, which, in principle, allows one to recover the corresponding classical

solution. We will discuss the classical spectral curve in chapter 7 where it is, in particular, derived from the Quantum Spectral Curve.

For closed strings there is a standard procedure for constructing the spectral curve corresponding to finite gap solutions. One first constructs a family of flat connections on the worldsheet parameterized by the spectral parameter and considers its monodromy around the worldsheet. The eigenvalues of this monodromy are invariants of motion and together they form eight sheets of the spectral curve. As we said before, the spectral curve encodes all conserved charges of the classical solution, in particular, the energy. Moreover, a procedure of one-loop quantization based on the spectral curve was developed in [39], where excitations around the classical solution correspond to adding poles connecting the sheets of the curve. For open strings a procedure of constructing a curve for an arbitrary solution is still lacking, although curves can be constructed for some special families of solutions (see, for example, [100, 101, 102, 103, 104]). In our paper [11] we proposed an algebraic curve for a classical limit of a system consisting of a cusped Wilson line and a scalar operator inserted at the cusp. Our method is a generalization of [91] and can be found in section 7.4 of this thesis.

* * *

TBA in the form of FiNLE and algebraic curve remained the most advanced tools until very recently, when TBA was simplified to an elegant system of equations for monodromies of just eight functions with well-controlled analytical properties, call Quantum Spectral Curve or $\mathbf{P}\mu$-system [7]. This system is the topic of the next section.

4 Quantum Spectral Curve of $\mathbf{AdS}_5/\mathbf{CFT}_4$

As follows from the description of the historical development of the integrability approach in $\mathcal{N} = 4$ SYM in the previous chapter, the first approach to the solution of the spectral problem which was valid at arbitrary coupling and for an arbitrary operator was Thermodynamical Bethe Ansatz (or Y-system). Unfortunately in practice using TBA was massively inconvenient. First, its analytical solution was possible only in few specific, mostly near-BPS cases. Second, since the system of TBA equations is so cumbersome, it does not give any additional insights about the mathematical structure of the theory. Last, even numerical solution of TBA equations proved to be quite difficult - existing algorithms converge slowly and do not give high precision results.

Fortunately, the spectral problem in $\mathcal{N}=4$ SYM can be reformulated as a new system of equations, which is more convenient to deal with and does not have the disadvantages listed above. This new system is called Quantum Spectral Curve (QSC) and it is equivalent to TBA, however much simpler. As opposed to infinite system of non-linear integral equations for infinite number of Y-functions, which constitutes the TBA, QSC is formulated as constraints for monodromy of a set of a total of 9 function with fixed analytical properties. The elegance of the formulation hints at some deeper structure underlying the problem and suggests that there might be a direct derivation of QSC from the first principles, avoiding the messy TBA step. Finally, as we show in chapter 8, there exists a highly efficient algorithm for numerical solution of QSC.

For a large number of quantum integrable systems, including $\mathrm{AdS}_5/\mathrm{CFT}_4$, Y-functions can be parametrized as ratios of T-functions, for which the equations take much simpler form. In fact, they look like Hirota equation on a lattice with special boundary conditions supplemented by restrictions on analytical properties of T-functions. In particular, for spin chains with su(N) algebras, one have to solve Hirota equation on a semi-infinite strip of width N. The general solution is given in terms of N functions of spectral parameter [105]. Generalizations were also obtained for superalgebras of compact su(K|M) [106] and non-compact su(K_1,K_2|M) types [107, 108, 93]. They correspond to solutions of Hirota equations on a hook where the width of horizontal and vertical bands are given by ranks of bosonic and fermionic parts of the superalgebra respectively. In this thesis we are mostly interested in the $\mathfrak{psu}(2,2|4)$ algebra, which is the symmetry algebra of both sides of $\mathrm{AdS}_5/\mathrm{CFT}_4$ duality. QSC, which we describe below in this section, gives us a convenient parametrization of a general solution of Y-system for this algebra in terms of so-called Q-functions. We give its definition and properties in sections 4.1-4.3, consider the important case of left-right symmetric states in 4.4 and in 4.5 show how the large volume limit of QSC produces ABA. For the sake of brevity we do not give the derivation of QSC from TBA. This derivation and much more complete description of QSC can be found in [8, 109].

4.1 Algebraic Q-system

As mentioned before, a general solution of Y-system for a system with $\mathfrak{psu}(2,2|4)$ symmetry algebra can be parametrized in terms of 8 independent functions of spectral parameter. It turns out, however, that in order to obtain finite, Wronskian-like formulas for the solution it is convenient to introduce 2^8 Q-functions satisfying certain functional algebraic relations.

Following this logic, the body of Q-system is constituted by Q-functions $Q_{A|I} = Q_{a_1 a_2 \ldots | i_1 i_2 \ldots}$, parametrized by indices $a_k = 1 \ldots 4$, $i_k = 1 \ldots 4$ and depending on the spectral parameter u. Indices a_k are called bosonic and i_k — fermionic, and Q-functions are antisymmetric with respect to permutation of bosonic or fermionic indices. The reader can easily calculate that this leaves maximum 2^8 non-trivial Q-functions; they can have up to four bosonic and four fermionic indices. By definition the Q-functions satisfy a number of relations:

$$Q_{Aab|I} Q_{A|I} = Q^{+}_{Aa|I} Q^{-}_{Ab|I} - Q^{-}_{Aa|I} Q^{+}_{Ab|I} \tag{4.1}$$

$$Q_{A|I} Q_{A|Iij} = Q^{+}_{A|Ii} Q^{-}_{Ab|Ij} - Q^{-}_{A|Ii} Q^{+}_{A|Ij} \tag{4.2}$$

$$Q_{Aa|I} Q_{A|Ii} = Q^{+}_{Aa|Ii} Q^{-}_{A|I} - Q^{-}_{Aa|Ii} Q^{+}_{A|I} \tag{4.3}$$

Here, again, A and I are multi-indices. The relations above can be understood better if one views the set of 2^8 Q-functions as Plukker coordinates on Grassmanians [109, 105, 107].

It is easy to see that the defining relations (4.1)-(4.3) enjoy gauge symmetry

$$Q_{A|I} \to \frac{g^{[|A|-|I|]}}{g^{[-(|A|-|I|)]}} Q_{A|I} \tag{4.4}$$

which we fix by requiring $Q_{\emptyset|\emptyset} = 1$.

Q-system satisfies another, discrete symmetry, which originates from the exchange of the right and left wings of the T-hook in TBA. Q-system can be reformulated in the language of antisymmetric forms; in this language this symmetry will correspond to Hodge duality, thus we will call the symmetry in question Hodge symmetry. We will denote the Hodge dual of $Q_{A|I}$ as $Q^{A|I}$ and define it as [1]

$$Q^{A|I} \equiv (-1)^{|A'||I|} \epsilon^{A'A} \epsilon^{I'I} Q_{A'|I'}, \tag{4.5}$$

where $\{A'\} = \{1,2,3,4\}/\{A\}$, $\{I'\} = \{1,2,3,4\}/\{I\}$, and ϵ is the four-dimensional antisymmetric tensor. In particular, one can see that Hodge transformation takes $Q_{\emptyset|\emptyset}$ to $Q_{1234|1234}$. It can be shown that $Q_{1234|1234}$ can also be normaized to 1:

$$Q_{1234|1234} = Q^{\emptyset|\emptyset} = 1, \tag{4.6}$$

the property of AdS/CFT possibly related to unimodularity of the symmetry algebra $\mathfrak{psu}(2,2|4)$.

The presence of a large number of relations between Q-functions makes us search for a minimal subset from which all the rest could be generated (which we will call a "basis",

[1] It is worth noting that only one Q-function enters the right hand side.

although it is not a linear basis, strictly speaking). One possible basis consists of all Q-functions with one index, for which we introduce the notation

$$\mathbf{Q}_i = Q_{\emptyset|i}, \quad \mathbf{P}_a \equiv Q_{a|\emptyset}. \tag{4.7}$$

To see how to obtain the rest of Q-functions from the basis, consider first a particular case of (4.3)

$$Q^+_{a|i} - Q^-_{a|i} = \mathbf{P}_a \mathbf{Q}_i \tag{4.8}$$

All Q-functions with two indices can be obtained from this equation; solution can be written as a form of formal series

$$Q_{a|i} = -\sum_{n=1}^{\infty} (\mathbf{P}_a \mathbf{Q}_i)^{[2n+1]} + \mathcal{P}, \tag{4.9}$$

where $\mathcal{P}$ is an arbitrary periodic function. Two things should be noted about this solution: first, the infinite sum might happen not to be convergent, and one has to find a way to regularize it. Particular schemes of regularization will be described in the parts of this thesis where we have to solve this equation in practice. Second, $\mathcal{P}$ is not constrained by the equation above and has to be fixed from the asymptotics of $Q_{a|i}$, which we will discuss in section 4.3. After we have Q-function with one and two indices, the relations (4.1)-(4.3) can be used to restore the rest of the Q-system.

Q-functions with two indices can be used to relate Q-function with one bosonic and Q-functions with one fermionic index:

$$\mathbf{Q}_i \equiv Q_{\emptyset|i} = -Q^{a|\emptyset} Q^{\pm}_{a|i}, \quad \mathbf{Q}^i \equiv Q^{\emptyset|i} = Q_{a|\emptyset} \left(Q^{a|i}\right)^{\pm} \tag{4.10}$$

$$\mathbf{P}_a \equiv Q_{a|\emptyset} = -Q^{\emptyset|i} Q^{\pm}_{a|i}, \quad \mathbf{P}^a \equiv Q^{a|\emptyset} = Q_{\emptyset|i} \left(Q^{a|i}\right)^{\pm} \tag{4.11}$$

They also satisfy the following orthogonality relations

$$Q^{a|i} Q_{a|j} = -\delta^i{}_j, \qquad Q^{a|i} Q_{b|i} = -\delta^a{}_b \tag{4.12}$$

$$Q^{a|\emptyset} Q_{a|\emptyset} = 0, \qquad Q^{\emptyset|i} Q_{\emptyset|i} = 0 \tag{4.13}$$

These relation follow from the definition of Hodge dual and from the normalization (4.6).

After gauge and Hodge symmetries are taken into account, there still remains a residual symmetry of Q-system called H-transformation. Since, as we have seen before, all the Q-functions can be reconstructed from those with one no more than one index, it is enough to define the symmetry action on them:

$$Q_{a|\emptyset} \to \left(H^{\pm}_b\right)_a{}^c Q_{c|\emptyset}, \quad Q_{\emptyset|i} \to \left(H^{\pm}_f\right)_i{}^j Q_{\emptyset|j} \tag{4.14}$$

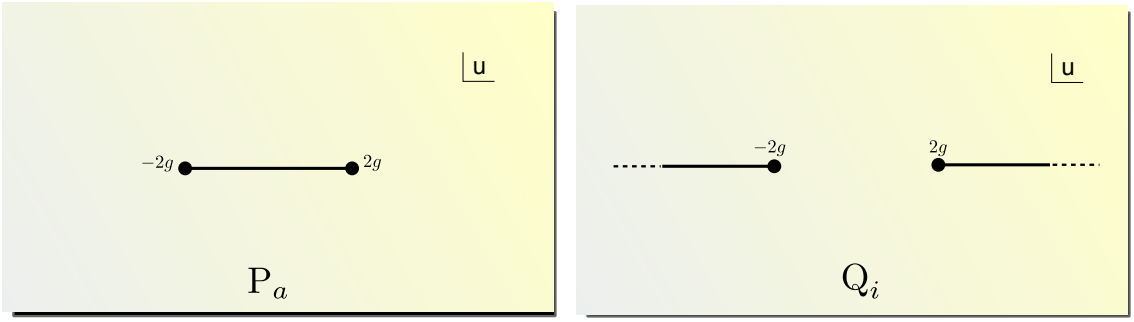

Figure 3: $\mathbf{P}_a$ and $\mathbf{Q}_i$ have one cut on the real axis as functions with short and long cuts respectively.

An important special case of H-symmetry is rescaling realized by diagonal H-matrices

$$Q_{a|\emptyset} \to \alpha_a Q_{a|\emptyset} \; Q_{\emptyset|i} \to \beta_i Q_{\emptyset|i} \tag{4.15}$$

$$Q^{a|\emptyset} \to \frac{1}{\alpha_a} Q^{a|\emptyset} \; Q^{\emptyset|i} \to \frac{1}{\beta_i} Q^{\emptyset|i} \tag{4.16}$$

The "unimodularity" constraint (4.6) requires $\alpha_1\alpha_2\alpha_3\alpha_4\beta_1\beta_2\beta_3\beta_4 = 1$.

4.2 Analytic structure

In the previous section we described the set of Q-functions and algebraic relations between them constituting the Q-system. So far we have not said anything about the analytical properties of Q-functions as functions of the spectral parameter u. We will describe them in this section. For the sake of clarity our presentation will be axiomatic: we will declare certain properties for particular Q-functions, namely $\mathbf{P}_a$, and see what it implies for the rest of Q-system. The rigorous way would be to present the derivation of Q-system from TBA, but for this technical and rather tedious derivation we refer the reader to [8]. Moreover, we hope that at some point a direct derivation of Q-system will appear, without the necessity to pass through TBA.

Q-functions are analytic functions of complex spectral parameter u in the UHP, and can have quadratic branch points on the real axis and below. Let us start by formulating the analytic properties of basic Q-function $\mathbf{Q}_i$ and $\mathbf{P}_a$, from which the rest can be constructed. On the main sheet $\mathbf{P}_a$ have one short cut on the real axis from $-2g$ to $2g$ as shown on Fig. 3. Monodromy of $\mathbf{P}_a$ around these branch points is described by an antisymmetric matrix $\mu_{ab}(u)$ which also depends on a spectral parameter, in the following way

$$\tilde{\mathbf{P}}_a = \mu_{ab}\mathbf{P}^b, \;\; \tilde{\mathbf{P}}^a = \mu^{ab}\mathbf{P}_b, \tag{4.17}$$

where μ^{bc} is the inverse of μ_{ab}. Monodromy of μ_{ab} is in its turn described by $\mathbf{P}_a$:

$$\tilde{\mu}_{ab} - \mu_{ab} = \mathbf{P}_a\tilde{\mathbf{P}}_b - \mathbf{P}_b\tilde{\mathbf{P}}_a. \tag{4.18}$$

When taken with long cut, μ_{ab} should be i-periodic: $\mu_{ab}(u) = \mu_{ab}(u+i)$, see Fig. 4. One can see that in the picture with short cuts this condition is equivalent to

$$\tilde{\mu}_{ab}(u) = \mu_{ab}(u+i) \tag{4.19}$$

In addition to this μ_{ab} is constrained by $\mathrm{Pf}(\mu) = 1$. Notice also that $\mathbf{P}_a\mathbf{P}^a = 0$ as we

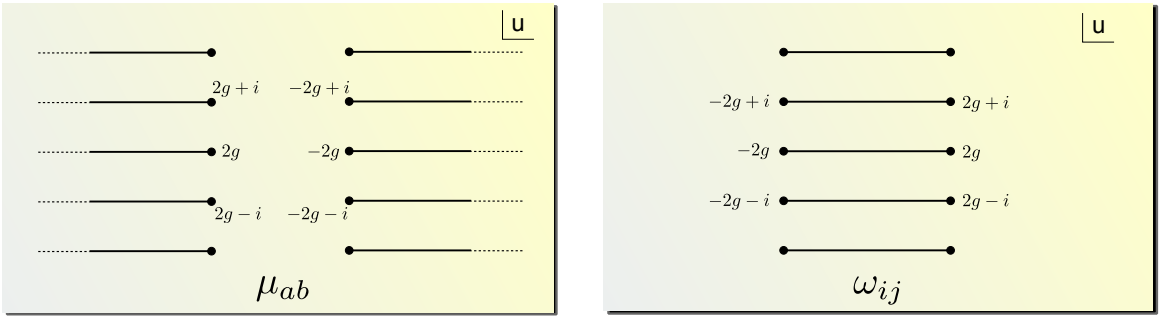

Figure 4: μ_{ab} and ω_{ij} are periodic as functions with long and short cuts respectively.

derived in the previous section. The set of the algebraic and analytic properties satisfied by $\mathbf{P}_a$, $\mathbf{P}^a$, and μ_{ab} forms a closed system, called $\mathbf{P}\mu$-system

$$\tilde{\mathbf{P}}_a = \mu_{ab}\mathbf{P}^b, \quad \tilde{\mathbf{P}}^a = \mu^{ab}\mathbf{P}_b \tag{4.20}$$

$$\tilde{\mu}_{ab} - \mu_{ab} = \mathbf{P}_a\tilde{\mathbf{P}}_b - \mathbf{P}_b\tilde{\mathbf{P}}_a \tag{4.21}$$

$$\mathrm{Pf}(\mu) = 1, \quad \mathbf{P}_a\mathbf{P}^a = 0 \tag{4.22}$$

Analytical properties of $\mathbf{Q}$ parallel that of $\mathbf{P}$ with systematic differences. We see that $\mathbf{Q}_i$ can be obtained from $\mathbf{P}_a$ using "rotation" by a Q-function with two indices (4.10). Let us also perform the corresponding "rotation" on μ_{ab}, i.e. define ω_{ij} such that

$$\mu_{ab} = Q^-_{a|i}Q^-_{b|j}\omega_{ij} \tag{4.23}$$

Then equations (4.20)-(4.22) and the analytical properties of $Q_{a|i}$ imply the following relations for the monodromy of $\mathbf{Q}_i$

$$\tilde{\mathbf{Q}}_i = \omega_{ij}\mathbf{Q}^j, \quad \tilde{\mathbf{Q}}^i = \omega^{ij}\mathbf{Q}_j, \tag{4.24}$$

where ω^{ij} the inverse of ω_{ij}, and for the monodromy of ω:

$$\tilde{\omega}_{ij} - \omega_{ij} = \mathbf{Q}_i \tilde{\mathbf{Q}}_j - \mathbf{Q}_j \tilde{\mathbf{Q}}_i \tag{4.25}$$

As opposed to μ_{ab}, which is i-periodic with long cuts, ω_{ij} is i-periodic with short cuts (Fig. 4). Correspondingly in the picture with long cuts $\mathbf{Q}_i$ have only one cut on the real axis, see Fig. 3.

The system of equations for $\mathbf{Q}$'s and ω_{ij} is called $\mathbf{Q}\omega$-system

$$\tilde{\mathbf{Q}}_i = \omega_{ij}\mathbf{Q}^j, \quad \tilde{\mathbf{Q}}_i = \omega_{ij}\mathbf{Q}^j \tag{4.26}$$

$$\tilde{\omega}_{ij} - \omega_{ij} = \mathbf{Q}_i \tilde{\mathbf{Q}}_j - \mathbf{Q}_j \tilde{\mathbf{Q}}_i \tag{4.27}$$

$$\mathrm{Pf}(\omega) = 1 \quad \mathbf{Q}_i \mathbf{Q}^i = 0 \tag{4.28}$$

Now that the analytical properties of the basic Q-function are defined, we can see what it implies for the whole Q-system. Q-function with two indices is generated from $\mathbf{P}_a$ and $\mathbf{Q}_i$ by solving the equation (4.8). We can always choose a solution regular in the UHP, for example the one given by (4.9). Then it is easy to see that the cut of the right hand side on the real axis generates an infinite ladder of cuts $[-2g - in, 2g - in]$, $n \in \mathbb{N}$ in the LHP. Same ladder of cuts will propagate to the rest of Q-functions.

Equation for Q Sometimes it is convenient to eliminate μ and ω from the description and work with $\mathbf{Q}$ and $\mathbf{P}$. It is actually possible to obtain a fourth-order finite-difference equation for $\mathbf{Q}_i$ with coefficients formed of $\mathbf{P}_a$ [110], namely

$$\mathbf{Q}^{[+4]} D_0 - \mathbf{Q}^{[+2]} \left[D_1 - \mathbf{P}_a^{[+2]} \mathbf{P}^{a[+4]} D_0 \right] + \frac{1}{2} \mathbf{Q} \left[D_2 - \mathbf{P}_a \mathbf{P}^{a[+2]} D_1 + \mathbf{P}_a \mathbf{P}^{a[+4]} D_0 \right] + c.c. = 0 \tag{4.29}$$

where

$$D_0 = \det \begin{pmatrix} \mathbf{P}^{1[+2]} & \mathbf{P}^{2[+2]} & \mathbf{P}^{3[+2]} & \mathbf{P}^{4[+2]} \\ \mathbf{P}^{1} & \mathbf{P}^{2} & \mathbf{P}^{3} & \mathbf{P}^{4} \\ \mathbf{P}^{1[-2]} & \mathbf{P}^{2[-2]} & \mathbf{P}^{3[-2]} & \mathbf{P}^{4[-2]} \\ \mathbf{P}^{1[-4]} & \mathbf{P}^{2[-4]} & \mathbf{P}^{3[-4]} & \mathbf{P}^{4[-4]} \end{pmatrix}, \tag{4.30}$$

$$D_1 = \det \begin{pmatrix} \mathbf{P}^{1[+4]} & \mathbf{P}^{2[+4]} & \mathbf{P}^{3[+4]} & \mathbf{P}^{4[+4]} \\ \mathbf{P}^{1} & \mathbf{P}^{2} & \mathbf{P}^{3} & \mathbf{P}^{4} \\ \mathbf{P}^{1[-2]} & \mathbf{P}^{2[-2]} & \mathbf{P}^{3[-2]} & \mathbf{P}^{4[-2]} \\ \mathbf{P}^{1[-4]} & \mathbf{P}^{2[-4]} & \mathbf{P}^{3[-4]} & \mathbf{P}^{4[-4]} \end{pmatrix} \tag{4.31}$$

$$D_2 = \det \begin{pmatrix} \mathbf{P}^{1[+4]} & \mathbf{P}^{2[+4]} & \mathbf{P}^{3[+4]} & \mathbf{P}^{4[+4]} \\ \mathbf{P}^{1[+2]} & \mathbf{P}^{2[+2]} & \mathbf{P}^{3[+2]} & \mathbf{P}^{4[+2]} \\ \mathbf{P}^{1[-2]} & \mathbf{P}^{2[-2]} & \mathbf{P}^{3[-2]} & \mathbf{P}^{4[-2]} \\ \mathbf{P}^{1[-4]} & \mathbf{P}^{2[-4]} & \mathbf{P}^{3[-4]} & \mathbf{P}^{4[-4]} \end{pmatrix} \tag{4.32}$$

In particular cases this fourth-order equation can factor into two second-order equations. Then two of four solutions satisfy a second order equation which is nothing else but Baxter equation. This will be the situation in chapter 9, where we solve QSC in the BFKL regime.

4.3 Identifying the state

Different solutions of the Q-system correspond to different states of $\mathcal{N} = 4$ SYM . The relation between the two is established via the asymptotics of Q-functions, which are determined by global charges of the corresponding state. It is enough to specify the asymptotics of the basis Q-functions. Let us recall that $\mathbf{P}_a$ with short cuts and $\mathbf{Q}_i$ with long have one cut on the main sheet and hence power-like behaviour at infinity. The powers are

$$\mathbf{P}_a \sim A_a u^{-\tilde{M}_a}, \quad \mathbf{Q}_i \sim B_i u^{\hat{M}_i - 1}, \; \mathbf{P}^a \sim A^a u^{\tilde{M}_a - 1}, \; \mathbf{Q}^i \sim B^i u^{-\hat{M}_i} \tag{4.33}$$

where

$$\tilde{M}_a = \left\{ \frac{J_1 + J_2 - J_3 + 2}{2}, \frac{J_1 - J_2 + J_3}{2}, \frac{-J_1 + J_2 + J_3 + 2}{2}, \frac{-J_1 - J_2 - J_3}{2} \right\} , \tag{4.34}$$

$$\hat{M}_i = \left\{ \frac{\Delta - S_1 - S_2 + 2}{2}, \frac{\Delta + S_1 + S_2}{2}, \frac{-\Delta - S_1 + S_2 + 2}{2}, \frac{-\Delta + S_1 - S_2}{2} \right\} . \tag{4.35}$$

The powers can be deduced by comparison of the quasiclassical limit of the spectral curve with the classical algebraic curve. The leading coefficients A_a, B_i are also constrained in

terms of the global charges:

$$A^{a_0}A_{a_0} = i\frac{\prod_j \left(\tilde{M}_{a_0} - \hat{M}_j\right)}{\prod_{b\neq a_0}\left(\tilde{M}_{a_0} - \tilde{M}_b\right)},\ B^{j_0}B_{j_0} = i\frac{\prod_j \left(\hat{M}_{j_0} - \tilde{M}_a\right)}{\prod_{k\neq j_0}(\hat{M}_{j_0} - \hat{M}_k)},\ a_0, j_0 = 1,2,3,4 \tag{4.36}$$

where no summation over a_0, j_0 is assumed in the left hand side.

Having constrained the asymptotics of Q-functions with one index, it is easy to find the asymptotics of the rest. For example, from (4.8) we immediately conclude that

$$Q_{a|i} \approx -iA_aB_i\frac{u^{-\tilde{M}_a+\hat{M}_i}}{-\tilde{M}_a+\hat{M}_i},\ \ u\to\infty \tag{4.37}$$

It remains to fix the asymptotics of μ_{ab} and ω_{ij}; we assume them to be power-like. Since ω_{ij} with short cuts is also periodic we conclude that it is constant at infinity. Now the relation (4.23) can be employed to determine the asymptotics of μ_{ab}, since $Q_{ab|ij}$ and its asymptotics can easily be expressed through Q-functions with known asymptotics, e.g. $Q_{a|i}$. The asymptotics of μ_{ab} which we find in this way are

$$\mu_{12} = -\mu^{34} \propto u^{\Delta-J_1},\ \ \mu^{12} = -\mu_{34} \propto u^{\Delta+J_1} \tag{4.38}$$

$$\mu_{13} = \mu^{24} \propto u^{\Delta-J_2-1},\ \ \mu^{13} = \mu_{24} \propto u^{\Delta+J_2+1} \tag{4.39}$$

$$\mu_{14} = -\mu^{23} \propto u^{\Delta+J_3},\ \ \mu^{14} = -\mu_{23} \propto u^{\Delta-J_3} \tag{4.40}$$

All the aforesaid holds for physical operators, which require, in particular integer quantum number. However, sometimes it seems useful to explore analytical continuation of operators into the unphysical domain, to real or even complex quantum numbers. In this case asymptotics of μ_{ab} and ω_{ij} have to be modified. This is discussed in the parts of this thesis in which we work with non-integer quantum numbers, such as chapters 5,8,9.

4.4 Left-right symmetric states

A particularly important for us class of solutions are those invariant under the left-right (LR) symmetry, exchange of left and right $\mathfrak{su}(2|2)$ subalgebras of $\mathfrak{psu}(2,2|4)$. In terms of the global charges this is equivalent to $S_2 = 0, J_3 = 0$, i.e. two non-trivial charges left in AdS and two on the sphere.

For LR-symmetric solutions Q-functions with upper and lower indices are related by

$$\chi^{ij} = \begin{pmatrix} 0 & 0 & 0 & -1 \\ 0 & 0 & 1 & 0 \\ 0 & -1 & 0 & 0 \\ 1 & 0 & 0 & 0 \end{pmatrix}, \tag{4.41}$$

for example,

$$\mathbf{Q}^i = \chi^{ij}\mathbf{Q}_j,\ \mathbf{P}^a = \chi^{ab}\mathbf{P}_b. \tag{4.42}$$

Hence equation (4.17) in the symmetric case takes the form

$$\tilde{\mathbf{P}}_1 = -\mathbf{P}_3\mu_{12} + \mathbf{P}_2\mu_{13} - \mathbf{P}_1\mu_{14} \tag{4.43}$$

$$\tilde{\mathbf{P}}_2 = -\mathbf{P}_4\mu_{12} + \mathbf{P}_2\mu_{14} - \mathbf{P}_1\mu_{24} \tag{4.44}$$

$$\tilde{\mathbf{P}}_3 = -\mathbf{P}_4\mu_{13} + \mathbf{P}_3\mu_{14} - \mathbf{P}_1\mu_{34} \tag{4.45}$$

$$\tilde{\mathbf{P}}_4 = -\mathbf{P}_4\mu_{14} + \mathbf{P}_3\mu_{24} - \mathbf{P}_2\mu_{34}\ . \tag{4.46}$$

It is also easy to show that in this sector matrices μ_{ab} and ω_{ij} satisfy

$$\mu_{14} = \mu_{23},\ \ \omega_{14} = \omega_{23} \tag{4.47}$$

in addition to antisymmetry.

Such LR-symmetric solutions correspond, in particular, to twist-L operators tr $(D^S Z^L)$ discussed in section 2.4. [2]

For such operators only two quantum numbers $S_1 \equiv S$ and $J_1 \equiv L$ are non-zero and the formulas for asymptotics of the Q-function from section 4.3 simplify. In particular, the asymptotics of $\mathbf{P}_a$ and $\mathbf{Q}_i$ are now

$$\mathbf{P}_a \sim (A_1 u^{-L/2}, A_2 u^{-L/2-1}, A_3 u^{L/2}, A_4 u^{L/2-1}) \tag{4.48}$$

$$\mathbf{Q}_a \sim (B_1 u^{\frac{\Delta-S}{2}}, B_2 u^{\frac{\Delta+S-2}{2}}, B_3 u^{-\frac{\Delta+S}{2}}, B_4 u^{\frac{-\Delta+S-2}{2}}), \tag{4.49}$$

where the leading coefficients A_a, B_i are related to global charges as

$$A_1 A_4 = \frac{\left((L+S-2)^2-\Delta^2\right)\left((L-S)^2-\Delta^2\right)}{16iL(L-1)} \tag{4.50}$$

$$A_2 A_3 = \frac{\left((L-S+2)^2-\Delta^2\right)\left((L+S)^2-\Delta^2\right)}{16iL(L+1)}\ . \tag{4.51}$$

and

$$B_1 B_4 = i\frac{\left((\Delta-S+2)^2-L^2\right)\left((\Delta-S)^2-L^2\right)}{16\Delta(S-1)(\Delta-S+1)} \tag{4.52}$$

$$B_2 B_3 = i\frac{\left((\Delta+S-2)^2-L^2\right)\left((\Delta+S)^2-L^2\right)}{16\Delta(S-1)(\Delta+S-1)}\ . \tag{4.53}$$

The general case (4.38) of the asymptotics of μ_{ab} reduces to

$$(\mu_{12},\ \mu_{13},\ \mu_{14},\ \mu_{24},\ \mu_{34}) \sim \left(u^{\Delta-L},\ u^{\Delta+1},\ u^{\Delta},\ u^{\Delta-1},\ u^{\Delta+L}\right) \tag{4.54}$$

[2] Sometimes in the thesis we will use J instead of L to denote the twist.

H-transformation in $\mathfrak{sl}(2)$ sector It will be useful to work out the particular form H-transformations (4.14) take in the $\mathfrak{sl}(2)$ sector. In addition to preserving the equations of Q-system we will require that the asymptotics (4.48), (4.49), (4.54) stay invariant. Consider a transformation of the type (4.14) which leaves $\mathbf{Q}_i$ invariant and transforms $\mathbf{P}_a$ as $\mathbf{P}'_a = R_a{}^b \mathbf{P}_b$ with a non-degenerate constant matrix R. In order to preserve the system (4.20), μ_{ab} should at the same time be transformed as

$$\mu' = -R\mu\chi R^{-1}\chi. \tag{4.55}$$

Such a transformation also preserves the form of (4.18) if

$$R^T\chi R\chi = -1\ , \tag{4.56}$$

which also automatically ensures antisymmetry of μ_{ab}, Pf $\mu = 1$, and (4.47). However, a general transformation of this form will spoil the asymptotics of $\mathbf{P}_a$. These asymptotics are ordered as $|\mathbf{P}_2| < |\mathbf{P}_1| < |\mathbf{P}_4| < |\mathbf{P}_3|$, which implies that the matrix R must have the following structure[3]

$$R = \begin{pmatrix} * & * & 0 & 0 \\ 0 & * & 0 & 0 \\ * & * & * & * \\ * & * & 0 & * \end{pmatrix}. \tag{4.57}$$

The general form of R which satisfies (4.56) and does not spoil the asymptotics generates a 6-parametric transformation, which we will call a γ-transformation. The simplest γ-transformation is the following rescaling:

$$\mathbf{P}_1 \to \alpha\mathbf{P}_1\ ,\ \ \mathbf{P}_2 \to \beta\mathbf{P}_2\ ,\ \ \mathbf{P}_3 \to 1/\beta\mathbf{P}_3\ ,\ \ \mathbf{P}_4 \to 1/\alpha\mathbf{P}_4\ , \tag{4.58}$$

$$\mu_{12} \to \alpha\beta\mu_{12}\ ,\ \ \mu_{13} \to \frac{\alpha}{\beta}\mu_{13}\ ,\ \ \mu_{14} \to \mu_{14}\ ,\ \ \mu_{24} \to \frac{\beta}{\alpha}\mu_{24}\ ,\ \ \mu_{34} \to \frac{1}{\alpha\beta}\mu_{34}\ , \tag{4.59}$$

with α, β being constants.

In left-right symmetric situation it is possible to use H-transformations to bring $\mathbf{P}_a$ and μ_{ab} to definite parity (even or odd depending on the asymptotics). After that we are left with parity-preserving transformations, which can be described as following: $\mathbf{P}_1$ and $\mathbf{P}_2$ always have opposite parity (as one can see from (4.48)) and thus should not mix under such transformations; the same is true about $\mathbf{P}_3$ and $\mathbf{P}_4$. Thus, depending on parity of J the parity-preserving γ-transformations are either

$$\mathbf{P}_3 \to \mathbf{P}_3 + \gamma_3\mathbf{P}_2,\ \mathbf{P}_4 \to \mathbf{P}_4 + \gamma_2\mathbf{P}_1, \tag{4.60}$$

$$\mu_{13} \to \mu_{13} + \gamma_3\mu_{12},\ \mu_{24} \to \mu_{24} - \gamma_2\mu_{12},\ \mu_{34} \to \mu_{34} + \gamma_3\mu_{24} - \gamma_2\mu_{13} - \gamma_2\gamma_3\mu_{12}$$

[3]This matrix would of course be lower triangular if we ordered $\mathbf{P}_a$ by their asymptotics.

for odd J or

$$\mathbf{P}_3 \to \mathbf{P}_3 + \gamma_1 \mathbf{P}_1,\ \mathbf{P}_4 \to \mathbf{P}_4 - \gamma_1 \mathbf{P}_2, \tag{4.61}$$
$$\mu_{14} \to \mu_{14} - \gamma_1 \mu_{12},\ \mu_{34} \to \mu_{34} + 2\gamma_1 \mu_{14} - \gamma_1^2 \mu_{12}\ ,$$

for even J.

4.5 Large volume limit

One of the simplest non-trivial limits of QSC is the limit of large operator length. As we know, in this limit the spectrum is described by Beisert-Eden-Staudacher Asymptotic Bethe Ansatz with exponential precision. Here we will give an idea how the QSC presented above gives rise to the ABA equations. In brief, in this limit it is possible to write a closed system of equations for a certain subset of Q-functions. The Q-functions in this subset are parametrized in terms of finite number of roots. We will end up with a system of equations for these roots, which will be exactly BES ABA equations. Since our goal here is to present the result rather than derivation, we will follow [8], sometimes modifying the order of its logical flow for the sake of brevity.

To begin with, one needs to understand the scaling of different Q-functions as $L \to \infty$. We assume that this can be deduced from their large u asymptotics (4.33), which contain L. The behavoir of a Q-function in such a limit depends on how many of its indices are 1 or 2 and how many are 3 or 4. Thus it is convenient to introduce undotted indices α, β, which can take values $1, 2$ and dotted indices $\dot{\alpha}, \dot{\beta}$, which take values $3, 4$. We also introduce a small parameter $\epsilon \sim u^{-L/2}$. Then from (4.33) we deduce that

$$\mathbf{P}_\alpha \sim \mathbf{Q}^\alpha \sim \mathbf{P}^{\dot{\alpha}} \sim \mathbf{Q}_{\dot{\alpha}} \sim \epsilon \tag{4.62}$$
$$\mathbf{P}^\alpha \sim \mathbf{Q}_\alpha \sim \mathbf{P}_{\dot{\alpha}} \sim \mathbf{Q}^{\dot{\alpha}} \sim 1/\epsilon \tag{4.63}$$

Similar analysis for μ_{ab} and ω_{ij} gives

$$\mu_{\alpha\beta} \sim 1,\ \ \mu_{\alpha\dot{\beta}} \sim \epsilon^{-2},\ \ \mu_{\dot{\alpha}\dot{\beta}} \sim \epsilon^{-4} \tag{4.64}$$
$$\omega_{ij} \sim \omega^{ij} \sim 1 \tag{4.65}$$

The Bethe ansatz equations describing the spectrum are not unique, and different forms are related to each other through dualities [111, 112, 113]. The precise form we will obtain is determined by choosing a path on the Hasse diagram. The path starts with $Q_{\emptyset|\emptyset} = 1$ and, adding one bosonic or fermionic index at each step, ends up in the

$Q_{1234|1234} = Q^{\emptyset|\emptyset} = 1$; of course, one should not forget that adding one lower index is equivalent to eliminating one upper index and vice versa. We will be able to write down a closed system of equations for the Q-functions on the path if they all will be large as $L \to \infty$. Guided by the rule (4.62) about dotted and undotted indices we make the following (non-unique) choice:

$$Q_{\emptyset|1}, Q_{1|1}, Q_{12|1}, Q_{12|12} = Q^{34|34}, Q^{34|4}, Q^{4|4}, Q^{4|\emptyset} \tag{4.66}$$

To parameterize these seven Q-functions we introduce seven types of roots

$$u_{1,k},\ k = 1, \dots, K_1$$
$$u_{2,k},\ k = 1, \dots, K_2$$
$$\dots$$
$$u_{7,k},\ k = 1, \dots, K_7$$

For each type we define a polynomial $\mathbb{Q}_{A|I}$ encoding all the roots of this type

$$\mathbb{Q}_{\emptyset|1} = \prod_{i=1}^{K_1}(u - u_{1,i}) \tag{4.67}$$
$$\mathbb{Q}_{1|1} = \prod_{i=1}^{K_2}(u - u_{2,i}) \tag{4.68}$$
$$\dots \tag{4.69}$$
$$\mathbb{Q}^{4|\emptyset} = \prod_{i=1}^{K_7}(u - u_{7,i}) \tag{4.70}$$

It is also useful to introduce "Hilbert transform" $B_{A|I}$ for each $\mathbb{Q}_{A|I}$, for example,

$$B_{\emptyset|1} = \prod_{i=1}^{K_1}\sqrt{\frac{g}{x_{1,k}}}\left(\frac{1}{x} - x_{1,k}\right), \tag{4.71}$$

and its analytical continuation under the cut $R_{A|I} = \tilde{B}_{A|I}$. It is easy to check that the two satisfy $R_{A|I}B_{A|I} = (-1)^{\deg \mathbb{Q}_{A|I}}\mathbb{Q}_{A|I}$. Roots of type four are also zeros of μ_{12}^{+}; for them and the corresponding polynomial we will omit the index "4" and additionally define

$$B_{(\pm)} = \prod_{i=1}^{K_4}\sqrt{\frac{g}{x_k^{\mp}}}\left(\frac{1}{x} - x_k^{\mp}\right), x_k^{\pm} = x(u_k \pm i/2) \tag{4.72}$$

As it is shown in [8] the QQ-relations and analyticity constraints result in the following ansatz for the Q-functions with lower undotted indices

$$\mathbf{P}_\alpha \equiv Q_{\alpha|\emptyset} \propto x^{-L/2}R_{\alpha|\emptyset}B_{\alpha|12}\sigma \qquad Q_{\alpha|12} \propto x^{L/2}B_{\alpha|\emptyset}R_{\alpha|12}\sigma^{-1}ff^{[2]} \tag{4.73}$$
$$\mathbf{Q}_\alpha \equiv Q_{\emptyset|\alpha} \propto x^{L/2}R_{\emptyset|\alpha}B_{12|\alpha}\sigma^{-1}\frac{f^{[2]}}{B_{(-)}} \qquad Q_{12|\alpha} \propto x^{-L/2}B_{\emptyset|\alpha}R_{12|\alpha}\sigma ff^{[2]}B_{(+)} \tag{4.74}$$
$$Q_{\alpha|\beta} \propto \mathbb{Q}_{\alpha|\beta}f^{+}, \qquad Q_{12|12} \propto \mathbb{Q}(f^{+})^2 \tag{4.75}$$
$$\mu_{12} \propto -\frac{B_{(+)}}{B_{(-)}}\bar{f}^{[-2]}f^{[+2]}\mathbb{Q}^{-}, \qquad \omega^{12} \propto \frac{B_{(-)}}{B_{(+)}}\frac{\bar{f}^{[-2]}}{f^{[+2]}} \tag{4.76}$$

Here

$$f \propto \prod_{n=0}^{\infty} \frac{B_{(+)}^{[2n]}}{B_{(-)}^{[2n]}} \tag{4.77}$$

and σ is a function with one Zhukovsky cut on the main sheet which satisfies

$$\sigma\tilde{\sigma} \propto \bar{f}^{[-2]} f^{[2]}, \;\; \sigma(\infty) = 1. \tag{4.78}$$

An analogous ansatz representation holds for the Q-functions with upper dotted indices.

The ansatz above plus the QQ-relations can be further used to produce Bethe equations constraining the roots $u_{1,k}, \ldots, u_{7,k}$. These equations for the "lower indices" wing look like

$$\frac{\mathbb{Q}_{1|1}\left(u_{1,k}+\frac{i}{2}\right) B_{(-)}\left(u_{1,k}\right)}{\mathbb{Q}_{1|1}\left(u_{1,k}-\frac{i}{2}\right) B_{(+)}\left(u_{1,k}\right)} = 1 \tag{4.79}$$

$$\frac{\mathbb{Q}_{1|1}\left(u_{3,k}+\frac{i}{2}\right) R_{(-)}\left(u_{3,k}\right)}{\mathbb{Q}_{1|1}\left(u_{1,k}-\frac{i}{2}\right) R_{(+)}\left(u_{3,k}\right)} = 1 \tag{4.80}$$

$$-\frac{\mathbb{Q}_{1|\emptyset}\left(u_{2,k}-\frac{i}{2}\right) \mathbb{Q}_{12|1}\left(u_{2,k}-\frac{i}{2}\right)}{\mathbb{Q}_{1|\emptyset}\left(u_{2,k}+\frac{i}{2}\right) \mathbb{Q}_{12|1}\left(u_{2,k}+\frac{i}{2}\right)} = \frac{\mathbb{Q}_{1|1}\left(u_{2,k}-i\right)}{\mathbb{Q}_{1|1}\left(u_{2,k}+i\right)} \tag{4.81}$$

and the opposite wing is obtained from this one in an obvious way. The Bethe equation for the middle-node roots takes the form

$$\frac{\mathbb{Q}^{[2]}}{\mathbb{Q}^{[-2]}} \left(\frac{B_{(-)}^{-}}{B_{(+)}^{+}}\right)^2 \prod_{k=1}^{K_4} \sigma_{\mathrm{BES}}^{-2}(u,u_k) \times \frac{B_{|1}^{-} R_{12|1}^{-} B^{\emptyset|4-} B^{34|4-}}{B_{|1}^{+} R_{12|1}^{+} B^{\emptyset|4+} B^{34|4+}} = \left(\frac{x^-}{x^+}\right)^L, \quad u = u_j, j = 1, \ldots K_4, \tag{4.82}$$

where σ_{BES} is the BES dressing phase [111, 114]. The conformal dimension of the operator, or the energy of the corresponding spin-chain state enters, for example, the asymptotic of μ_{ab} (4.38). By calculating this asymptotic from the ansatz (4.73) one finds that it is completely determined by the middle-node roots

$$\Delta = J_1 + \sum_{k=1}^{N} \left(1 + \frac{2gi}{x_k^+} - \frac{2gi}{x_k^-}\right) \tag{4.83}$$

The ansatz (4.73) describes the state in terms of numbers of roots of each kind. These numbers are obviously related to the global charges through the asymptotics of the Q-

function. Namely,

$$2K_1 = \Delta - L - S_1 - S_2 \tag{4.84}$$

$$2K_2 = \Delta - L - J_2 + J_3 - S_1 - S_2 \tag{4.85}$$

$$2K_3 = \Delta - L - S_1 - S_2 \tag{4.86}$$

$$2K_4 = \Delta - L \tag{4.87}$$

$$2K_5 = \Delta - L - S_1 + S_2 \tag{4.88}$$

$$2K_6 = \Delta - L - J_2 - J_3 - S_1 + S_2 \tag{4.89}$$

$$2K_7 = \Delta - L - S_1 + S_2 \tag{4.90}$$

The set of equations (4.79), (4.82) and the relation to the global charges (4.84) reproduces exactly the BES ABA. This is a highly non-trivial verification of QSC equations, especially taking into account emergence of the BES dressing phase, which was non a priori present in the formulation of QSC. A similar set of equations corresponding to a different path on the Hasse diagram can be derived in BFKL regime [15].

Part II

Applications and results

5 Small spin limit

In this chapter, based on our paper [9], we will apply the QSC to the calculation of the twist operator in the $\mathfrak{sl}(2)$ sector of $\mathcal{N} = 4$ SYM . For this we will only use the part of QSC called the $\mathbf{P}\mu$-system, i.e. we will operate only with $\mathbf{P}_a$ and μ_{ab} and use the names QSC and $\mathbf{P}\mu$-system interchangeably.

As described in section 4.4, twist operators of $\mathfrak{sl}(2)$ sector can be written as [4]

$$\mathcal{O} = \mathrm{Tr}\left(Z^{J-1}\,\mathcal{D}^S Z\right) + \dots \tag{5.1}$$

Scaling dimension of such operator has the form

$$\Delta = J + S + \gamma(g), \tag{5.2}$$

where $\gamma(g)$ is the anomalous dimension. Small spin limit is a near-BPS regime in which we expect QSC to simplify considerably. The anomalous dimension $\gamma(g)$ vanishes at $S = 0$;

[4] We will consider a two-cut configuration with a symmetric distribution of Bethe roots, thus for physical states S is even.

at small S it has an expansion

$$\gamma(g) = \gamma^{(1)}(g)S + \gamma^{(2)}(g)S^2 + \mathcal{O}(S^3). \tag{5.3}$$

The first term, $\gamma^{(1)}(g)$, is called the *slope function*. In the brilliant paper [115] it was found exactly at any coupling

$$\gamma^{(1)}(g) = \frac{4\pi g I_{J+1}(4\pi g)}{J I_J(4\pi g)} \ . \tag{5.4}$$

The reason for the simplicity of this expression is that this quantity is protected from finite-size wrapping corrections and thus the ABA prediction is exact. It is also not sensitive to the dressing phase of the ABA, which contributes only starting from order S^2. The formula above was derived from ABA equations in two different ways [116, 117] and further studied and generalized in [118, 119, 120, 121, 122].

Our key observation is that near $S = 0$ the QSC can be solved iteratively order by order in the spin. In the next section we first solve the QSC in the leading order and reproduce the slope function (5.4). Then in section 5.2 we explain the subtleties of working with non-integer values of spin and in 5.3 compute the coefficient of the S^2 term in the expansion, i.e. the function $\gamma^{(2)}(g)$ which we call the *curvature function*. For values of twist $J = 2, 3, 4$ we obtain closed exact expressions for it in the form of a double integral. Unlike the slope function, $\gamma^{(2)}(g)$ is affected by the dressing phase in the ABA and by wrapping corrections, all of which are incorporated in QSC-system. We have checked our results against available results in literature at weak and strong coupling, and found full agreement. We also made new predictions from these expansions: in section 5.4 we perform weak-coupling expansion of our result and in section 5.5 we use its strong coupling expansion to find the value of a new term in the Konishi operator (i.e. $\mathrm{Tr}\left(\mathcal{D}^2 Z^2\right)$) anomalous dimension at strong coupling.

5.1 Leading order in S: Slope function

The description of QSC in the previous chapter was done for physical operators. Our goal is to take a rather special limit when the number of covariant derivatives S goes to zero. As we will see this requires some extension of the asymptotic requirement for μ functions. In this section we will be guided by principles of naturalness and simplicity to deduce these modifications which we will summarize in section 5.2. There we also give a concrete prescription for analytical continuation in S, which we then use to derive the curvature

function. [5]

Consider first μ_{ab}. Since $\Delta = J + \mathcal{O}(S)$, from (4.50), (4.51) it is easy to see that $A_1 A_4$ and $A_2 A_3$ are of order S as $S \to 0$, so we can assume that the functions $\mathbf{P}_a$ are of order $\sqrt{S}$. This is a key simplification, because now (4.18) indicates that the discontinuities of μ_{ab} on the cut are small when S goes to zero. Thus at leading order in S all μ_{ab} are just periodic entire functions without cuts. On the other hand, the asymptotics of μ_{ab} at large u are power-like, as we know from (4.54). Thus the only possibility is that all μ_{ab} are just constants! However, we found that in this case there is only a trivial solution, i.e. $\mathbf{P}_a \equiv 0$. Obviously, this can be interpreted as QSC telling us that for physical states S must be integer and thus cannot be arbitrarily small. Nevertheless, a sensible question would be to define an analytical continuation of QSC from integer values of S.[6]

Thus we have to relax the requirement of power-like behavior at infinity. The first possibility is to allow for $e^{2\pi u}$ asymptotics at $u \to +\infty$. We should, however, remember about the constraints Pf $\mu = 1$ and (4.47) which restrict our choice and the fact that we can also use γ-symmetry.

What follows depends on the parity of J. Since solving QSC for even J is slightly simpler, we will start with this case. [7]

Let us show that by allowing μ_{24} to have exponential behavior and setting it to $\mu_{24} = C \sinh(2\pi u)$, with other μ_{ab} being constant, we obtain the correct result. This choice is dictated by our assumptions concerning the analytic continuation of μ_{ab} to non-integer values of S, and this point is discussed in detail in section 5.2. We will also see in that section that by using the γ-transformation (described in at the end of section 4.4) and the constraint

$$\text{Pf } \mu = 1 \tag{5.5}$$

we can set the constant C to 1 and also $\mu_{12} = 1,\ \mu_{13} = 0,\ \mu_{14} = -1,\ \mu_{34} = 0$ (see (5.48)).

[5] Another discussion of analytical continuation to non-integer quantum numbers happens in section 8.3 of this thesis, however there we focus more of $\mathbf{Q}_i$ and ω_{ij} rather than on $\mathbf{P}_a$ and μ_{ab}.

[6] Restricting the large positive S behavior one can achieve uniqueness of the continuation.

[7] For odd J extra branch points at infinity will appear in $\mathbf{P}_a$ due to the asymptotics (4.48)

Having fixed all μ's at leading order we get the following system of equations[8] for $\mathbf{P}_a$:

$$\tilde{\mathbf{P}}_1 = -\mathbf{P}_3 + \mathbf{P}_1, \tag{5.6}$$

$$\tilde{\mathbf{P}}_2 = -\mathbf{P}_4 - \mathbf{P}_2 - \mathbf{P}_1 \sinh(2\pi u), \tag{5.7}$$

$$\tilde{\mathbf{P}}_3 = \quad -\mathbf{P}_3, \tag{5.8}$$

$$\tilde{\mathbf{P}}_4 = \quad +\mathbf{P}_4 + \mathbf{P}_3 \sinh(2\pi u). \tag{5.9}$$

It follows from here that $\tilde{\mathbf{P}}_a$ have the same analytic structure as $\mathbf{P}_a$, i.e. only single short cut on the main sheet! Hence all $\mathbf{P}_a$ can be represented as infinite Laurent series of the type (8.1) in the Zhukovsky variable $x(u)$, which rationalizes the Riemann surface with two sheets and one cut. Equations (5.7) and (5.8) with the asymptotics (4.48) have a unique solution $\mathbf{P}_1 = \epsilon x^{-J/2}$ and $\mathbf{P}_3 = \epsilon \left(x^{-J/2} - x^{+J/2}\right)$, where ϵ is a constant yet to be fixed; we expect it to be proportional to $\sqrt{S}$. Thus the equations (5.7) and (5.9) become

$$\tilde{\mathbf{P}}_2 + \mathbf{P}_2 \;=\; -\mathbf{P}_4 - \epsilon x^{-J/2} \sinh(2\pi u)\,, \tag{5.10}$$

$$\tilde{\mathbf{P}}_4 - \mathbf{P}_4 \;=\; \epsilon (x^{-J/2} - x^{+J/2}) \sinh(2\pi u)\,. \tag{5.11}$$

We will first solve the second equation. It is useful to introduce operations $[f(x)]_+$ and $[f(x)]_-$, which take parts of Laurent series with positive and negative powers of x respectively. Taking into account that

$$\sinh(2\pi u) = \sum_{n=-\infty}^{\infty} I_{2n+1} x^{2n+1}, \tag{5.12}$$

where $I_k \equiv I_k(4\pi g)$ is the modified Bessel function of the first kind, we can write $\sinh(2\pi u)$ as

$$\sinh(2\pi u) = \sinh_+ + \sinh_-, \tag{5.13}$$

where explicitly

$$\sinh_+ = [\sinh(2\pi u)]_+ = \sum_{n=1}^{\infty} I_{2n-1} x^{2n-1} \tag{5.14}$$

$$\sinh_- = [\sinh(2\pi u)]_- = \sum_{n=1}^{\infty} I_{2n-1} x^{-2n+1}\,. \tag{5.15}$$

In this notation the general solution of equation (5.11) with asymptotics at infinity $\mathbf{P}_4 \sim u^{J/2-1}$ can be written as

$$\mathbf{P}_4 = \epsilon (x^{J/2} - x^{-J/2}) \sinh_- + Q_{J/2-1}(u), \tag{5.16}$$

[8] In this section we only consider the leading order of $\mathbf{P}$'s at small S, so the equations involving them are understood to hold at leading order in S. In section 5.3 we will study the next-to-leading order and elaborate the notation for contributions of different orders.

where $Q_{J/2-1}$ is a polynomial of degree $J/2-1$ in u. The polynomial $Q_{J/2-1}$ can be fixed from the equation (5.10) for $\mathbf{P}_2$. Indeed, from the asymptotics of $\mathbf{P}_2$ we see that the left hand side of (5.10) does not have powers of x from $-J/2+1$ to $J/2-1$. This fixes

$$Q_{J/2-1}(x) = -\epsilon \sum_{k=1}^{J/2} I_{2k-1} \left(x^{\frac{J}{2}-2k+1} + x^{-\frac{J}{2}+2k-1} \right). \tag{5.17}$$

Once $Q_{J/2-1}$ is found, we set $\mathbf{P}_2$ to be the part of the right hand side of (5.10) with powers of x less than $-J/2$, which gives

$$\mathbf{P}_2 = -\epsilon x^{+J/2} \sum_{n=\frac{J}{2}+1}^{\infty} I_{2n-1} x^{1-2n}. \tag{5.18}$$

Thus (for even J) we have uniquely fixed all $\mathbf{P}_a$ with the only unknown parameter being ϵ. The solution is summarized below:

$$\mu_{12} = 1,\ \mu_{13} = 0,\ \mu_{14} = -1,\ \mu_{24} = \sinh(2\pi u),\ \mu_{34} = 0, \tag{5.19}$$

$$\mathbf{P}_1 = \epsilon x^{-J/2} \tag{5.20}$$

$$\mathbf{P}_2 = -\epsilon x^{+J/2} \sum_{n=J/2+1}^{\infty} I_{2n-1} x^{1-2n} \tag{5.21}$$

$$\mathbf{P}_3 = \epsilon \left(x^{-J/2} - x^{+J/2} \right) \tag{5.22}$$

$$\mathbf{P}_4 = \epsilon \left(x^{J/2} - x^{-J/2} \right) \sinh_- - \epsilon \sum_{n=1}^{J/2} I_{2n-1} \left(x^{\frac{J}{2}-2n+1} + x^{-\frac{J}{2}+2n-1} \right). \tag{5.23}$$

In the next section we fix the remaining parameter ϵ of the solution in terms of S and find the energy, but before that let us briefly discuss the solution for odd J. As we mentioned abov,e the main difference is that in this case the functions $\mathbf{P}_a$ have a branch point at $u = \infty$, which is dictated by the asymptotics (4.48). In addition, the parity of μ_{ab} is different according to the asymptotics of these functions (4.54). The solution is still very similar to the even J case, and we discuss it in detail in Appendix A.2. Let us present the result here:

$$\mu_{12} = 1,\ \mu_{13} = 0,\ \mu_{14} = 0,\ \mu_{24} = \cosh(2\pi u),\ \mu_{34} = 1 \tag{5.24}$$

$$\mathbf{P}_1 = \epsilon x^{-J/2}, \tag{5.25}$$

$$\mathbf{P}_2 = -\epsilon x^{J/2} \sum_{k=-\infty}^{-\frac{J+1}{2}} I_{2k} x^{2k}, \tag{5.26}$$

$$\mathbf{P}_3 = -\epsilon x^{J/2}, \tag{5.27}$$

$$\mathbf{P}_4 = \epsilon x^{-J/2} \cosh_- - \epsilon x^{-J/2} \sum_{k=1}^{\frac{J-1}{2}} I_{2k} x^{2k} - \epsilon I_0 x^{-J/2}. \tag{5.28}$$

Note that now $\mathbf{P}_a$ include half-integer powers of x.

Fixing the global charges of the solution. Finally, to fix our solution completely we have to find the value of ϵ in terms of global charges and express the energy through spin using (4.50) and (4.51). To this end we first extract the coefficients A_a of the leading terms for all $\mathbf{P}_a$ (see the asymptotics (4.48)). From (5.20)-(5.23) or (5.25)-(5.28) we get

$$A_1 = g^{J/2}\epsilon, \tag{5.29}$$

$$A_2 = -g^{J/2+1}\epsilon I_{J+1}, \tag{5.30}$$

$$A_3 = -g^{-J/2}\epsilon, \tag{5.31}$$

$$A_4 = -g^{-J/2+1}\epsilon I_{J-1}. \tag{5.32}$$

Expanding (4.50), (4.51) at small S with $\Delta = J + S + \gamma$, where $\gamma = \mathcal{O}(S)$, we find at linear order

$$\gamma = i(A_1A_4 - A_2A_3) \tag{5.33}$$

$$S = i(A_1A_4 + A_2A_3)\,. \tag{5.34}$$

Plugging in the coefficients (5.29)-(5.32) we find that

$$\epsilon = \sqrt{\frac{2\pi i S}{J I_J(\sqrt{\lambda})}} \tag{5.35}$$

and hence the anomalous dimension at leading order is

$$\gamma = \frac{\sqrt{\lambda} I_{J+1}(\sqrt{\lambda})}{J I_J(\sqrt{\lambda})} S + \mathcal{O}(S^2), \tag{5.36}$$

which precisely coincides with the slope function of Basso [115].

While the above discussion concerned the ground state, i.e. the $\mathfrak{sl}(2)$ sector operator with the lowest anomalous dimension at given twist J, it can be generalized for higher mode numbers. In the asymptotic Bethe ansatz for such operators we have two symmetric cuts formed by Bethe roots, with corresponding mode numbers being $\pm n$ (for the ground state $n = 1$). We found that in order to describe these operators within QSC one should take $\mu_{24} = C\sinh(2\pi n u)$ instead of $\mu_{24} = C\sinh(2\pi u)$ (and for odd J we similarly use $\mu_{24} = C\cosh(2\pi n u)$ instead of $\mu_{24} = C\cosh(2\pi u)$). Then the solution is very similar to the one above, and we find

$$\gamma = \frac{n\sqrt{\lambda} I_{J+1}(n\sqrt{\lambda})}{J I_J(n\sqrt{\lambda})} S\,, \tag{5.37}$$

which reproduced the result of [115] for non-trivial mode number n. In Appendix A.5 we also show how using QSC one can reproduce the slope function for a configuration of Bethe roots with arbitrary mode numbers and filling fractions.

In summary, we have shown how QSC correctly computes the energy at the linear order in S. In section 5.3 we will compute the next, S^2 term in the anomalous dimension.

5.2 Prescription for analytical continuation

The LO solution of QSC for small S which we found in the previous section contains μ_{ab} with exponential asymptotics. In order to proceed to the next order we need to deduce the general prescription for the asymptotics of μ_{ab} for non-integer S. To this end we first study the possible asymptotics of μ_{ab} for given $\mathbf{P}_a$ in more detail. One can combine (4.18) with (4.17) and take into account that

$$\mu^{+}_{ab} = \tilde{\mu}_{ab} \tag{5.38}$$

to write a finite difference equation on μ_{ab}:

$$\mu_{ab}(u+i) = \mu_{ab}(u) - \mu_{bc}(u)\chi^{cd}\mathbf{P}_d\mathbf{P}_a + \mu_{ac}(u)\chi^{cd}\mathbf{P}_d\mathbf{P}_b. \tag{5.39}$$

The matrix μ_{ab} has 5 linear independent components. Thus the system above can be recast as a 5th order finite-difference equation with 5 independent solutions which we denote $\mu_{ab,A},\ A = 1,\dots,5$. Given the asymptotics of $\mathbf{P}_a$ (4.48) and (4.50), (4.51) there are exactly 5 different asymptotics a solution of (5.39) could have as discussed in [7, 8]. We denote these 5 independent solutions of (5.39) as $\mu_{12,A}$ where $A = 1,\dots,5$ and summarize their leading asymptotics at large $u > 0$ in the table below

$A=$	1	2	3	4	5
$\mu_{12,A}\sim$	$u^{\Delta-J}$	$C_{1,2}u^{-S+1-J}$	$C_{1,3}u^{-J}$	$C_{1,4}u^{S-1-J}$	$C_{1,5}u^{-\Delta-J}$
$\mu_{13,A}\sim$	$C_{2,1}u^{\Delta+1}$	$C_{2,2}u^{-S+2}$	$C_{2,3}u^{+1}$	u^{S}	$C_{2,5}u^{-\Delta+1}$
$\mu_{14,A}\sim$	$C_{3,1}u^{\Delta}$	$C_{3,2}u^{-S+1}$	1	$C_{3,4}u^{S-1}$	$C_{3,5}u^{-\Delta}$
$\mu_{24,A}\sim$	$C_{4,1}u^{\Delta-1}$	u^{-S}	$C_{4,3}u^{-1}$	$C_{4,4}u^{S-2}$	$C_{4,5}u^{-\Delta-1}$
$\mu_{34,A}\sim$	$C_{5,1}u^{\Delta+J}$	$C_{5,2}u^{-S+1+J}$	$C_{5,3}u^{+J}$	$C_{5,4}u^{S-1+J}$	$u^{-\Delta+J}$

(5.40)

where we fix the normalization of our solutions so that some coefficients are set to 1[9]. As it was pointed out in [7] the asymptotics for different $A's$ are obtained by replacing Δ in (4.54) by $\pm\Delta, \pm(S-1)$ and 0. We label these solutions so that in the small S regime these asymptotics are ordered $\Delta > 1-S > 0 > S-1 > -\Delta$.

Obviously, any combination of solutions of (5.39) with i-periodic coefficients still remains a solution. The actual solution μ_{ab} is thus a linear combination of the partial solutions $\mu_{ab,A}$ with some constant or periodic coefficients. The precise combination is additionally constrained by the analyticity condition (5.38) which is satisfied by a general solution of (5.39).

[9]The coefficients $C_{a,A}$ are some rational functions of S, Δ, J and A_1, A_2. In the small S limit all $C_{a,A} \to 0$ in our normalization.

The prescription for analytical continuation in S which we propose here is based on the large u asymptotics of these periodic coefficients. As we discussed in the previous section the assumption that all these coefficients are asymptotically constant is too constraining already at the leading order in S, and we must assume that at least some of these coefficients grow exponentially as $e^{2\pi u}$. To get some extra insight into the asymptotic behavior of these coefficients it is very instructive to go to the weak coupling regime.

It is known that at one loop the equation (5.39) is reduced to a second order equation. When written as a finite difference equation for μ_{12} it coincides exactly with the Baxter equation for the non-compact $\mathfrak{sl}(2)$ spin chain. For $J = 2$ it reads

$$\left(2u^2 - S^2 - S - \frac{1}{2}\right) Q(u) = (u + \tfrac{i}{2})^2 Q(u + i) + (u - \tfrac{i}{2})^2 Q(u - i) \tag{5.41}$$

where $Q(u) = \mu_{12}(u + i/2)$. This equation is already very well studied and all its solutions are known explicitly [123]. Th reader can easily see that the asymptotics of two solutions at infinity are u^S and $1/u^{S+1}$. It is also known that at one loop and for any integer S (5.41) has a polynomial solution which gives the energy as $\Delta = J + S + 2ig^2 \partial_u \log \frac{Q(u-i/2)}{Q(u-i/2)}\Big|_{u=0} = S + J + 8g^2 H_S$. At the same time, for non-integer S there are of course no polynomial solutions, and according to [124] and [125] the solution which produces the energy $S + J + 8g^2 H_S$ cannot even have power-like asymptotics. Instead the correct large u behavior must be:

$$Q(u) \sim \left(u^S + \ldots\right) + (A + Be^{2\pi u}) \left(\frac{1}{u^{S+1}} + \ldots\right) \quad , \quad u \to +\infty \, . \tag{5.42}$$

Furthermore, there is a unique entire Q-function with the above asymptotics. For $S > -1/2$ we can reformulate the prescription by saying that the correct solution consists of a part with power-like asymptotics, which is linear combination of possible solutions, plus the smallest (at infinity) solution reinforced with an exponent.

In this form we can try to apply this prescription to our case. Notice that for $g \to 0$ we have $\mu_{12,1} \sim u^S$ and $\mu_{12,2} \sim u^{-S-1}$, which tells us that at least the second solution must be allowed to have a non-constant periodic coefficient in the asymptotics. We also assume that the coefficient in front of $\mu_{ab,3}$ tends to a constant[10]. This extra condition does not follow from the one-loop analysis we deduced from our solution. We will show how this prescription produces the correct known result for the leading order in S. From our analysis it is hard to make a definite statement about the behavior of the periodic coefficients in front of $\mu_{12,4}$ and $\mu_{12,5}$, but due to the expected $\Delta \to -\Delta$ symmetry, which

[10]It could be hard or even impossible to separate $\mu_{ab,3}$ from $\mu_{ab,2}$ in a well defined way. In these cases $\mu_{ab,2}$ is defined modulo $\mu_{ab,3}$ and other subleading solutions. Our prescription then means that the exponential part of the coefficient in front of $\mu_{ab,3}$ is proportional to that of in front of $\mu_{ab,2}$.

interchanges $\mu_{12,5}$ and $\mu_{12,1}$, one may expect that the coefficient of $\mu_{12,5}$ should also go to a constant. All said above can be summarized by the formula

$$\mu_{ab}(u) = \sum_{A=1}^{5} c_A \mu_{ab,A}(u) + \sum_{A=2,4,5} p_A(u) \mu_{ab,A}(u) \tag{5.43}$$

where c_A are constants and $p_A(u)$ are some linear combinations of $e^{\pm 2\pi u}$.[11]

Prescription at small S. In the small S limit the functions $\mathbf{P}_a$ are also small and the equation (5.39) simply tells us that $\mu_{ab}(u+i) = \mu_{ab}(u)$ which implies that in the leading order in S the five independent solutions are just constants. The only solution giving a contribution to μ_{12} in the leading order in this limit is $\mu_{12,1}$ as all the other solutions could only produce negative powers. So we start from $\mu_{ab} = C_{ab} + D_{ab}\sinh(2\pi u) + E_{ab}\cosh(2\pi u)$ for some constants C_{ab}, D_{ab}, E_{ab} such that $D_{12} = E_{12} = 0$. Thus we have five different C's, 4 different D's and 4 different E's. We notice that this general form of μ_{ab} can be significantly simplified. First, using the Pfaffian constraint (5.5) and the γ-transformation (4.55) it is possible to show that any generic μ_{ab} of this form can be reduced to one belonging to the following two-parametric family inside the original 13-parametric space:

$$\mu_{12} = 1,\ \mu_{14} = a^2 \sinh 2\pi u + \frac{a}{2}\cosh 2\pi u\ , \tag{5.44}$$

$$\mu_{24} = b\sinh 2\pi u + \sinh 2\pi u\ ,\ \mu_{34} = \frac{a^2}{4}\frac{(1-2ab)^2}{b^2-1} + 1\ , \tag{5.45}$$

where μ_{13} is found from the Pfaffian constraint. Second, recall that according to our prescription the 1st and 3rd solutions (columns in the table (5.40)) cannot contain exponential terms. Consider μ_{14} and μ_{24}, we again see that the 4th and 5th solutions could only contain negative powers of u and thus only the 2nd solution can contribute to the parts of μ_{14} and μ_{24} that are non-decaying at infinity. This means that these components can be represented in the following form

$$\mu_{14} = (a_1 \sinh 2\pi u + a_2 \cosh 2\pi u)\mu_{14,2}(u) + \mathcal{O}\left(e^{2\pi u}/u\right)\ , \tag{5.46}$$

$$\mu_{24} = (a_1 \sinh 2\pi u + a_2 \cosh 2\pi u)\mu_{24,2}(u) + \mathcal{O}\left(e^{2\pi u}/u\right)\ , \tag{5.47}$$

for $u \to +\infty$. The $\mathcal{O}\left(e^{2\pi u}/u\right)$ terms contain contributions from all of the solutions except for the 2nd. One can see that (5.45) can be of this form only in two cases: if $a = 0$ or if $a = \frac{1}{2b}$. Both of these cases can be brought to the form

$$\mu_{12} = 1,\ \mu_{13} = 0,\ \mu_{14} = 0,\ \mu_{24} = d_1 \sinh 2\pi u + d_2 \cosh 2\pi u,\ \mu_{34} = 1 \tag{5.48}$$

[11] Some of the coefficients of p_A should be zero which can be seen from the constraint (5.5).

by a suitable γ-transformation (5.45). However, we found that there is an additional constraint which follows from compatibility of μ_{ab} with the decaying asymptotics of $\mathbf{P}_2$. As we show in appendix A.5 for even J one must set $d_2 = 0$. For odd J we must set $d_1 = 0$ as a compatibility requirement. This justifies the choice of μ_{ab} used in the previous section. In the next section we will show how the same prescription can be applied at the next order in S and leads to nontrivial results which we subjected to intensive tests later in the text.

5.3 Next order in S

In this section we use QSC to compute the S^2 correction to the anomalous dimension in the expansion (5.3), which we call the curvature function $\gamma^{(2)}(g)$. We thoroughly discuss the case $J = 2$ and then describe the modifications of the solution for the cases $J = 3$ and $J = 4$, more details on which can be found in appendix A.3.

5.3.1 Iterative procedure for the small S expansion

For convenience let us reproduce here the leading order solution of QSC for $J = 2$ (see (5.19)-(5.23)):

$$\mathbf{P}_1^{(0)} = \epsilon\frac{1}{x} \quad , \quad \mathbf{P}_2^{(0)} = +\epsilon I_1 - \epsilon x[\sinh(2\pi u)]_- \ , \tag{5.49}$$

$$\mathbf{P}_3^{(0)} = \epsilon\left(\frac{1}{x} - x\right) \quad , \quad \mathbf{P}_4^{(0)} = -2\epsilon I_1 - \epsilon\left(\frac{1}{x} - x\right)[\sinh(2\pi u)]_-. \tag{5.50}$$

Here ϵ is a small parameter, proportional to $\sqrt{S}$ (see (5.35)), and by $\mathbf{P}_a^{(0)}$ we denote the $\mathbf{P}_a$ functions at leading order in ϵ.

The key observation is that QSC can be solved iteratively order by order in ϵ. Indeed, let us write $\mathbf{P}_a$ and μ_{ab} as expansions in this small parameter:

$$\mathbf{P}_a = \mathbf{P}_a^{(0)} + \mathbf{P}_a^{(1)} + \mathbf{P}_a^{(2)} + \dots \tag{5.51}$$

$$\mu_{ab} = \mu_{ab}^{(0)} + \mu_{ab}^{(1)} + \mu_{ab}^{(2)} + \dots \ . \tag{5.52}$$

where $\mathbf{P}_a^{(0)} = \mathcal{O}(\epsilon)$, $\mathbf{P}_a^{(1)} = \mathcal{O}(\epsilon^3)$, $\mathbf{P}_a^{(2)} = \mathcal{O}(\epsilon^5)$, $\dots$, and $\mu_{ab}^{(0)} = \mathcal{O}(\epsilon^0)$, $\mu_{ab}^{(1)} = \mathcal{O}(\epsilon^2)$, $\mu_{ab}^{(2)} = \mathcal{O}(\epsilon^4)$, etc. [12] The procedure goes like this: since the leading order $\mathbf{P}_a$ are of order ϵ, equation (4.18) implies that the discontinuity of μ_{ab} on the cut is of order ϵ^2; thus to find μ_{ab} in the next to leading order (NLO) we only need the functions $\mathbf{P}_a$ at

[12] This structure of the expansion is dictated by the equations (4.17) and (4.18), as we will soon see.

leading order. After that we can find the NLO correction to $\mathbf{P}_a$ from equations (4.17). This will be done below, and having thus the full solution of the $\mathbf{P}\mu$-system at NLO we will find the energy at order S^2.

Correcting μ_{ab}... In this subsection we find the NLO corrections $\mu_{ab}^{(1)}$ to μ_{ab}. As follows from (4.18) and (5.38), they should satisfy the equation

$$\mu_{ab}^{(1)}(u+i) - \mu_{ab}^{(1)}(u) = \mathbf{P}_a^{(0)}\tilde{\mathbf{P}}_b^{(0)} - \mathbf{P}_b^{(0)}\tilde{\mathbf{P}}_a^{(0)}, \tag{5.53}$$

in which the right hand is known explicitly. In this thesis we will often encounter these kinds of equations, so it is convenient to define an operator for solving them. More precisely, suppose

$$f(u+i) - f(u) = h(u). \tag{5.54}$$

and functions $f(u)$ and $h(u)$ have one cut in u between $-2g$ and $2g$ and no poles. Such functions can be represented as infinite Laurent series (8.1) in the Zhukovsky variable $x(u)$, and we additionally restrict ourselves to the case where for $h(u)$ this expansion does not have a constant term[13].

As always with inhomogeneous equations, the general solution of (5.54) has a form of a particular solution plus an arbitrary i-periodic function — a zero mode of the equation above. First we will describe the construction of the particular solution and later deal with zero modes. The linear operator which gives the particular solution of (5.54) described below will be denoted as Σ.

Notice that given the explicit form (5.50) of $\mathbf{P}_a^{(0)}$, the right hand side of (5.53) can be represented in a form

$$\alpha(x)\sinh(2\pi u) + \beta(x), \tag{5.55}$$

where $\alpha(x), \beta(x)$ are power series in x growing at infinity not faster than polynomially. We first define action of Σ on expressions of this form:

$$\Sigma \cdot [\alpha(x)\sinh(2\pi u) + \beta(x)] \equiv \sinh(2\pi u)\Sigma \cdot \alpha(x) + \Sigma \cdot \beta(x). \tag{5.56}$$

We also define $\Sigma \cdot x^{-n} = \Gamma' \cdot x^{-n}$ for $n > 0$, where the integral operator Γ' defined as

$$\left(\Gamma' \cdot h\right)(u) \equiv \oint_{-2g}^{2g} \frac{dv}{4\pi i} \partial_u \log \frac{\Gamma[i(u-v)+1]}{\Gamma[-i(u-v)]} h(v). \tag{5.57}$$

[13]It is easy to see that there is indeed no constant term in the right hand side of (5.53), as it would cancel in any expression of the form $F(u) - \tilde{F}(u)$.

This requirement is consistent because of the following relation [14]

$$\left(\Gamma' \cdot h\right)(u+i) - \left(\Gamma' \cdot h\right)(u) = -\frac{1}{2\pi i}\oint_{-2g}^{2g} \frac{h(v)}{u-v} dv = h_-(u) - \widetilde{h_+}(u). \tag{5.58}$$

What is left is to define Σ on positive powers of x. We do it by requiring

$$\Sigma \cdot [x^a + 1/x^a] \equiv p'_a(u) \tag{5.59}$$

where $p'_a(u)$ is a polynomial in u of degree $a+1$, which is a solution of

$$p'_a(u+i) - p'_a(u) = \frac{1}{2}\left(x^a + 1/x^a\right) \tag{5.60}$$

and satisfies the following additional properties: $p'_a(0) = 0$ for odd a and $p'_a(i/2) = 0$ for even a. One can check that this definition is consistent and defines of $p'_a(u)$ uniquely. The explicit form of the first few $p'_a(u)$, which we call periodized Chebyshev polynomials, can be found in appendix A.1.

From the aforesaid one can see that the class of functions (5.55) is closed under the action of Σ — what is important for us is that no exponential functions other than $\sinh(2\pi u)$ appear in the result.

A good illustration of how the definitions above work would be the following two simple examples. Suppose one wants to calculate $\Sigma \cdot \left(x - \frac{1}{x}\right)$, then it is convenient to split the argument of Σ in the following way:

$$\Sigma \cdot \left(x - \frac{1}{x}\right) = \Sigma \cdot \left(x + \frac{1}{x}\right) - 2\Sigma \cdot \frac{1}{x}. \tag{5.61}$$

In the first term we recognize $p'_1(u) = \frac{iu(u-i)}{2g}$, whereas in the second the argument of Σ is decaying at infinity, thus Σ is equivalent to Γ' in this context. Notice also that $\Gamma' \cdot \frac{1}{x} = -\Gamma' \cdot x$. All together, we get

$$\Sigma \cdot \left(x - \frac{1}{x}\right) = \Sigma \cdot \left(x + \frac{1}{x}\right) - 2\Sigma \cdot \frac{1}{x} = 2p'_1(u) + 2\Gamma' \cdot x \tag{5.62}$$

In a similar way, in order to calculate $\Sigma \cdot \frac{\sinh_- - \sinh_+}{2}$, one can write $\frac{\sinh_- - \sinh_+}{2} = \sinh_- - \frac{1}{2}\sinh(2\pi u)$. Notice that since $\sinh_-$ decays at infinity,

$$\Sigma \cdot \sinh_- = \Gamma' \cdot \sinh_- . \tag{5.63}$$

Also, since i-periodic functions can be factored out of Σ,

$$\Sigma \cdot \sinh(2\pi u) = \sinh(2\pi u)\Sigma \cdot 1 = \sinh(2\pi u)p'_0(u)/2. \tag{5.64}$$

[14] We remind that f_+ and f_- stand for the part of the Laurent expansion with, respectively, positive and negative powers of x, while $\tilde{f}$ is the analytic continuation around the branch point at $u = 2g$ (which amounts to replacing $x \to \frac{1}{x}$)

Finally,

$$\Sigma \cdot \frac{\sinh_- - \sinh_+}{2} = \Gamma' \cdot (\sinh_-) - \frac{1}{2}\sinh(2\pi u) p_0'(u). \tag{5.65}$$

As an example we present the particular solution for two components of μ_{ab} (below we will argue that π_{12} and π_{13} can be chosen to be zero, see (5.75))

$$\mu^{(1)}_{13} - \pi_{13} = \Sigma \cdot \left(\mathbf{P}_1\tilde{\mathbf{P}}_3 - \mathbf{P}_3\tilde{\mathbf{P}}_1\right) = \epsilon^2\Sigma \cdot \left(x^2 - \frac{1}{x^2}\right) = \epsilon^2\left(\Gamma' \cdot x^2 + p_2'(u)\right), \tag{5.66}$$

$$\mu^{(1)}_{12} - \pi_{12} = \Sigma \cdot \left(\mathbf{P}_1\tilde{\mathbf{P}}_2 - \mathbf{P}_2\tilde{\mathbf{P}}_1\right) =$$

$$= -\epsilon^2\left[2I_1\Gamma' \cdot x - \sinh(2\pi u)\ \Gamma' \cdot x^2 - \Gamma' \cdot \left(\sinh_-\left(x^2 + \frac{1}{x^2}\right)\right)\right]. \tag{5.67}$$

Now let us apply Σ defined above to (5.53), writing that its general solution is

$$\mu^{(1)}_{ab} = \Sigma \cdot (\mathbf{P}^{(0)}_a\tilde{\mathbf{P}}^{(0)}_b - \mathbf{P}^{(0)}_b\tilde{\mathbf{P}}^{(0)}_a) + \pi_{ab}, \tag{5.68}$$

where the zero mode π_{ab} is an arbitrary i-periodic entire function, which can be written similarly to the leading order as $c_{1,ab}\cosh 2\pi u + c_{2,ab}\sinh 2\pi u + c_{3,ab}$. Again, many of the coefficients $c_{i,ab}$ can be set to zero. First, the prescription from section 5.2 implies that the non-vanishing at infinity part of coefficients of $\sinh(2\pi u)$ and $\cosh(2\pi u)$ in μ_{12} is zero. As one can see from the explicit form (5.67) of the particular solution which we choose for μ_{12}, it does not contain $\cosh(2\pi u)$ and the coefficient of $\sinh(2\pi u)$ is decaying at infinity. So in order to satisfy the prescription, we have to set $c_{1,12}$ and $c_{2,12}$ to zero. Second, since the coefficients $c_{n,ab}$ are of order S, we can remove some of them by making an infinitesimal γ-transformation, i.e. with $R = 1 + \mathcal{O}(S)$ (see equation (4.55)). Further, the Pfaffian constraint (5.5) imposes 5 equations on the remaining coefficients, which leaves the following 2-parametric family of zero modes

$$\pi_{12} = 0,\ \pi_{13} = 0,\ \pi_{14} = \frac{1}{2}c_{1,34}\cosh 2\pi u, \tag{5.69}$$

$$\pi_{24} = c_{1,24}\cosh 2\pi u,\ \pi_{34} = c_{1,34}\cosh 2\pi u. \tag{5.70}$$

Let us now look closer at the exponential part of μ_{14} and μ_{24}. Combining the leading order (5.19) and the perturbation (5.68) and taking into account the fact that operator Σ does not produce terms proportional to $\cosh 2\pi u$, we obtain

$$\mu_{14} = \frac{1}{2}c_{1,34}\cosh 2\pi u + \mathcal{O}(\epsilon)\sinh 2\pi u + \mathcal{O}(\epsilon^2) + \ldots, \tag{5.71}$$

$$\mu_{24} = \frac{1}{2}c_{1,24}\cosh 2\pi u + (1 + \mathcal{O}(\epsilon))\sinh 2\pi u + \mathcal{O}(\epsilon^2) + \ldots, \tag{5.72}$$

where dots stand for powers-like terms or exponential terms suppressed by powers of u.

As we remember from section 5.2, only the 2nd solution of the 5th order Baxter equation (5.39) can contribute to the exponential part of μ_{14} and μ_{24}, which means that

μ_{14} and μ_{24} are proportional to the same linear combination of $\sinh 2\pi u$ and $\cosh 2\pi u$. From the second equation one can see that this linear combination can be normalized to be $\frac{1}{2}c_{1,24}\cosh 2\pi u + (1+\mathcal{O}(\epsilon))\sinh 2\pi u$. Then

$$\mu_{14} = C\left(\frac{1}{2}c_{1,24}\cosh 2\pi u + (1+\mathcal{O}(\epsilon))\sinh 2\pi u\right), \tag{5.73}$$

where C is some constant, which is of order $\mathcal{O}(\epsilon)$, because the coefficient of $\sinh 2\pi u$ in the first equation is $\mathcal{O}(\epsilon)$. Taking into account that $c_{1,24}$ is $\mathcal{O}(\epsilon)$ itself, we find that $c_{1,34} = \mathcal{O}(\epsilon^2)$, i.e. it does not contribute at the order which we are considering. So the final form of the zero mode in (5.68) is

$$\pi_{12} = 0,\ \pi_{13} = 0,\ \pi_{14} = 0, \tag{5.74}$$

$$\pi_{24} = c_{1,24}\cosh 2\pi u,\ \pi_{34} = 0. \tag{5.75}$$

In this way, using the particular solution given by Σ and the form of zero modes (5.75) we have computed all the functions $\mu^{(1)}_{ab}$. The details and the results of the calculation can be found in appendix A.3.

Correcting $\mathbf{P}_a$... In the previous section we found the NLO part of μ_{ab}. Now, according to the iterative procedure described in section 5.3.1, we can use it to write a closed system of equations for $\mathbf{P}^{(1)}_a$. Indeed, expanding the system (4.46) to NLO we get

$$\tilde{\mathbf{P}}^{(1)}_1 - \mathbf{P}^{(1)}_1 = -\mathbf{P}^{(1)}_3 + r_1, \tag{5.76}$$

$$\tilde{\mathbf{P}}^{(1)}_2 + \mathbf{P}^{(1)}_2 = -\mathbf{P}^{(1)}_4 - \mathbf{P}^{(1)}_1\sinh(2\pi u) + r_2, \tag{5.77}$$

$$\tilde{\mathbf{P}}^{(1)}_3 + \mathbf{P}^{(1)}_3 = r_3, \tag{5.78}$$

$$\tilde{\mathbf{P}}^{(1)}_4 - \mathbf{P}^{(1)}_4 = \mathbf{P}^{(1)}_3\sinh(2\pi u) + r_4, \tag{5.79}$$

where the free terms are given by

$$r_a = -\mu^{(1)}_{ab}\chi^{bc}\mathbf{P}^{(0)}_c. \tag{5.80}$$

Notice that r_a does not change if we add a matrix proportional to $\mathbf{P}^{(0)}_a\tilde{\mathbf{P}}^{(0)}_b - \mathbf{P}^{(0)}_b\tilde{\mathbf{P}}^{(0)}_a$ to $\mu^{(1)}_{ab}$, due to the relations

$$\mathbf{P}_a\chi^{ab}\mathbf{P}_b = 0,\ \mathbf{P}_a\chi^{ab}\tilde{\mathbf{P}}_b = 0, \tag{5.81}$$

which follow from the $\mathbf{P}\mu$-system equations. In particular we can use this property to replace $\mu^{(1)}_{ab}$ in (5.80) by $\mu^{(1)}_{ab} + \frac{1}{2}\left(\mathbf{P}^{(0)}_a\tilde{\mathbf{P}}^{(0)}_b - \mathbf{P}^{(0)}_b\tilde{\mathbf{P}}^{(0)}_a\right)$. This will be convenient for us, since in expressions for $\mu^{(1)}_{ab}$ in terms of p_a and Γ (see (5.66), (5.67) and appendix A.3) this change amounts to simply replacing Γ' by a convolution with a more symmetric kernel:

$$\Gamma' \to \Gamma, \tag{5.82}$$

$$(\Gamma \cdot h)(u) \equiv \oint_{-2g}^{2g} \frac{dv}{4\pi i} \partial_u \log \frac{\Gamma[i(u-v)+1]}{\Gamma[-i(u-v)+1]} h(v), \tag{5.83}$$

while at the same time replacing

$$p'_a(u) \to p_a(u), \tag{5.84}$$

$$p_a(u) = p'_a(u) + \frac{1}{2}\left(x^a(u) + x^{-a}(u)\right). \tag{5.85}$$

Having made this comment, we will now develop tools for solving the equations (5.76) - (5.79). Notice first that if we solve them in the order (5.78), (5.76), (5.79), (5.77), substituting into each subsequent equation the solution of all the previous, then at each step the problem we have to solve has a form

$$\tilde{f} + f = h \ \text{ or } \ \tilde{f} - f = h \ , \tag{5.86}$$

where h is known, f is unknown and both the right hand side and the left hand side are power series in x. It is obvious that equations (5.86) have solutions only for h such that $h = \tilde{h}$ and $h = -\tilde{h}$ respectively. On the class of such h a particular solution for f can be written as

$$f = [h]_- + [h]_0/2 \equiv H \cdot h \ \ \Rightarrow \ \ \tilde{f} + f = h \tag{5.87}$$

and

$$f = [h]_- \equiv K \cdot h \ \ \Rightarrow \ \ \tilde{f} - f = h, \tag{5.88}$$

where $[h]_0$ is the constant part of Laurent expansion of h (it does not appear in the second equation, because h such that $h = -\tilde{h}$ does not have a constant part). The operators K and H introduced here can be also defined by their integral kernels

$$H(u,v) = -\frac{1}{4\pi i} \frac{\sqrt{u-2g}\sqrt{u+2g}}{\sqrt{v-2g}\sqrt{v+2g}} \frac{1}{u-v} dv, \tag{5.89}$$

$$K(u,v) = +\frac{1}{4\pi i} \frac{1}{u-v} dv. \tag{5.90}$$

which are equivalent to (5.87),(5.88) of the classes of h such that $h = \tilde{h}$ and $h = -\tilde{h}$ respectively[15]. The particular solution $f = K \cdot h$ of the equation $\tilde{f} + f = h$ is unique in the class of functions f decaying at infinity, and the solution $f = H \cdot h$ of $\tilde{f} - f = h$ is unique for non-growing f. In all other cases the general solution will include zero modes, which, in our case are fixed by asymptotics of $\mathbf{P}_a$.

[15] We denote e.g. $K \cdot h = \oint_{-2g}^{2g} K(u,v)h(v)dv$ where the integral is around the branch cut between $-2g$ and $2g$.

Now it is easy to write the explicit solution of the equations (5.76)-(5.79):

$$\begin{aligned}
\mathbf{P}_3^{(1)} &= H \cdot r_3, && (5.91)\\
\mathbf{P}_1^{(1)} &= \frac{1}{2}\mathbf{P}_3^{(1)} + K \cdot \left(r_1 - \frac{1}{2} r_3\right), && (5.92)\\
\mathbf{P}_4^{(1)} &= K \cdot \left(-\frac{1}{2}\left(\tilde{\mathbf{P}}_3^{(1)} - \mathbf{P}_3^{(1)}\right)\sinh(2\pi u) + \frac{2r_4 + r_3\sinh(2\pi u)}{2}\right) - 2\delta, && (5.93)\\
\mathbf{P}_2^{(1)} &= H \cdot \left(-\frac{1}{2}\left(\mathbf{P}_4^{(1)} + \sinh(2\pi u)\mathbf{P}_1^{(1)} + \tilde{\mathbf{P}}_4^{(1)} + \sinh(2\pi u)\tilde{\mathbf{P}}_1^{(1)}\right) + \right. && (5.94)\\
&\quad \left. + \frac{r_4 + \sinh(2\pi u) r_1 + 2r_2}{2}\right) + \delta,
\end{aligned}$$

where δ is a constant fixed uniquely by requiring $\mathcal{O}(1/u^2)$ asymptotics for $\mathbf{P}_2$. This asymptotic also sets the last coefficient $c_{1,24}$ left in π_{12} to zero. Thus in the class of functions with asymptotics (4.48) the solution for μ_{ab} and $\mathbf{P}_a$ is unique up to a γ-transformation.

5.3.2 Result for $J = 2$

In order to obtain the result for the anomalous dimension, we again use the formulas (4.50), (4.51) which connect the leading coefficients of $\mathbf{P}_a$ with Δ, J and S. After plugging in A_i which we find from our solution, we obtain the result for the S^2 correction to the anomalous dimension:

$$\begin{aligned}
\gamma^{(2)}_{J=2} &= \frac{\pi}{g^2(I_1 - I_3)^3}\oint\frac{du_x}{2\pi i}\oint\frac{du_y}{2\pi i}\left[\frac{8I_1^2(I_1+I_3)\left(x^3 - \left(x^2+1\right)y\right)}{(x^3-x)\,y^2}\right.\\
&\quad + \frac{8\mathrm{sh}^x_-\mathrm{sh}^y_-\left(x^2y^2-1\right)\left(I_1(x^4y^2+1) - I_3x^2(y^2+1)\right)}{x^2\left(x^2-1\right)y^2}\\
&\quad - \frac{4(\mathrm{sh}^y_-)^2x^2\left(y^4-1\right)\left(I_1(2x^2-1) - I_3\right)}{\left(x^2-1\right)y^2}\\
&\quad + \frac{8I_1^2\mathrm{sh}^y_-x\left(2\left(x^3-x\right)\left(y^3+y\right) - 2x^2\left(y^4+y^2+1\right) + y^4 + 4y^2 + 1\right)}{\left(x^2-1\right)y^2}\\
&\quad - \frac{8(I_1-I_3)I_1\mathrm{sh}^y_-x(x-y)(xy-1)}{\left(x^2-1\right)y}\\
&\quad \left. - \frac{4(I_1-I_3)(\mathrm{sh}^x_-)^2\left(x^2+1\right)y^2}{\left(x^2-1\right)}\right]\frac{1}{4\pi i}\partial_u\log\frac{\Gamma(iu_x - iu_y + 1)}{\Gamma(1 - iu_x + iu_y)}\,. \qquad (5.95)
\end{aligned}$$

Here the integration contour goes around the branch cut at $(-2g, 2g)$. We also denote $\mathrm{sh}^x_- = \sinh_-(x)$, $\mathrm{sh}^y_- = \sinh_-(y)$ (recall that $\sinh_-$ was defined in (5.15)). This is our final result for the curvature function at any coupling.

It is interesting to note that our result contains the combination $\log\frac{\Gamma(iu_x - iu_y+1)}{\Gamma(1-iu_x+iu_y)}$ which plays an essential role in the construction of the BES dressing phase. We will use this identification in section 5.5.3 to compute the integral in (5.95) numerically with high precision.

In the next subsections we will describe generalizations of the $J = 2$ result to operators with $J = 3$ and $J = 4$.

5.3.3 Results for higher J

Solving the $\mathbf{P}\mu$-system for $J = 3$ is similar to the $J = 2$ case described above, except for several technical complications, which we will describe here, leaving the details for appendix A.3. As in the previous section, the starting point is the LO solution of the $\mathbf{P}\mu$ system, which for $J = 3$ reads

$$\mathbf{P}_1 = \epsilon x^{-3/2},\ \mathbf{P}_3 = -\epsilon x^{3/2}, \tag{5.96}$$

$$\mathbf{P}_2 = -\epsilon x^{3/2}\cosh_- + \epsilon x^{-1/2} I_2, \tag{5.97}$$

$$\mathbf{P}_4 = -\epsilon x^{1/2} I_2 - \epsilon x^{-3/2} I_0 - \epsilon x^{-3/2}\cosh_-, \tag{5.98}$$

$$\mu_{12} = 1,\ \mu_{13} = 0,\ \mu_{14} = 0,\ \mu_{24} = \cosh(2\pi u),\ \mu_{34} = 1\ . \tag{5.99}$$

The first step is to construct $\mu^{(1)}_{ab}$ from its discontinuity given by the equation (5.53). The full solution consists of a particular solution and a general solution of the corresponding homogeneous equation, i.e. zero mode π_{ab}. In our case the zero mode can be an i-periodic function, i.e. a linear combination of $\sinh(2\pi u)$, $\cosh(2\pi u)$ and constants. As in the case of $J = 2$, we use a combination of the Pfaffian constraint, prescription from section 5.2 and a γ-transformation to reduce all the parameters of the zero mode to just one, sitting in μ_{24}:

$$\pi_{12} = 0,\ \pi_{13} = 0,\ \pi_{14} = 0,\ \pi_{24} = c_{24,2}\sinh(2\pi u)\,,\ \pi_{34} = 0. \tag{5.100}$$

As in the previous section, the next step is to find $\mathbf{P}^{(1)}_a$ from the $P\mu$ system expanded to the first order, namely from

$$\tilde{\mathbf{P}}^{(1)}_1 + \mathbf{P}^{(1)}_3 = r_1, \tag{5.101}$$

$$\tilde{\mathbf{P}}^{(1)}_2 + \mathbf{P}^{(1)}_4 + \mathbf{P}^{(1)}_1\cosh(2\pi u) = r_2, \tag{5.102}$$

$$\tilde{\mathbf{P}}^{(1)}_3 + \mathbf{P}^{(1)}_1 = r_3, \tag{5.103}$$

$$\tilde{\mathbf{P}}^{(1)}_4 + \mathbf{P}^{(1)}_2 - \mathbf{P}^{(1)}_3\cosh(2\pi u) = r_4, \tag{5.104}$$

where r_a are defined by (5.80) and for $J = 3$ are given explicitly in appendix A.3. In attempting to solve this system, however, we encounter another technical complication. As one can see from (5.96)-(5.98), the LO solution contains half-integer powers of J, meaning that the $\mathbf{P}_a$ now have an extra branch point at infinity. However, the operations H and K defined by (5.90) work only for functions which have Laurent expansion in integer

powers of x. In order to solve equations of the type (5.53) on the class of functions which allow Laurent-like expansion in x with only half-integer powers x, we introduce operations H^*, K^*:

$$H^* \cdot f \equiv \frac{x+1}{\sqrt{x}} H \cdot \frac{\sqrt{x}}{x+1} f, \tag{5.105}$$

$$K^* \cdot f \equiv \frac{x+1}{\sqrt{x}} K \cdot \frac{\sqrt{x}}{x+1} f. \tag{5.106}$$

In terms of these operations the solution of the system (5.101)-(5.104) is

$$\mathbf{P}_1^{(1)} = \frac{1}{2}\left(H^*(r_1+r_3) + K^*(r_1-r_3)\right) + \mathbf{P}_1^{\rm zm}, \tag{5.107}$$

$$\mathbf{P}_3^{(1)} = \frac{1}{2}\left(H^*(r_1+r_3) - K^*(r_1-r_3)\right) + \mathbf{P}_2^{\rm zm}, \tag{5.108}$$

$$\begin{aligned}\mathbf{P}_2^{(1)} = \frac{1}{2}&\left(H^*(r_2+r_4) + K^*(r_2-r_4) - \right.\\ &\left. - H^*\left(\cosh(2\pi u) K^*(r_1-r_3)\right) - K^*\left(\cosh(2\pi u) H^*(r_1+r_3)\right)\right) + \mathbf{P}_3^{\rm zm},\end{aligned} \tag{5.109}$$

$$\begin{aligned}\mathbf{P}_4^{(1)} = \frac{1}{2}&\left(H^*(r_2+r_4) - K^*(r_2-r_4) - \right.\\ &\left. - H^*\left(\cosh(2\pi u) K^*(r_1-r_3)\right) + K^*\left(\cosh(2\pi u) H^*(r_1+r_3)\right)\right) + \mathbf{P}_4^{\rm zm},\end{aligned} \tag{5.110}$$

where $\mathbf{P}_a^{\rm zm}$ is a solution of the system (5.101)-(5.104) with right hand side set to zero, whose explicit form $\mathbf{P}_a^{\rm zm}$ is given in Appendix A.3 (see (A.49)-(A.50)) and which is parametrized by four constants L_1, L_2, L_3, L_4, e.g.

$$\mathbf{P}_1^{\rm zm} = L_1 x^{-1/2} + L_3 x^{1/2}. \tag{5.111}$$

These constants are fixed by requiring correct asymptotics of $\mathbf{P}_a$, which also fixes the parameter $c_{24,2}$ in the zero mode (5.100) of μ_{ab} [16]. Indeed, a priori $\mathbf{P}_2$ and $\mathbf{P}_1$ have wrong asymptotics. Imposing a constraint that $\mathbf{P}_2$ decays as $u^{-5/2}$ and $\mathbf{P}_1$ decays as $u^{-3/2}$ produces five equations, which fix all the parameters uniquely.

Skipping the details of the intermediate calculations, we present the final result for the

[16] Actually in this way $c_{24,2}$ is fixed to be zero.

anomalous dimension:

$$\gamma^{(2)}_{J=3} = \oint \frac{du_x}{2\pi i} \oint \frac{du_y}{2\pi i} i \frac{1}{g^2(I_2-I_4)^3} \left[\frac{2\left(x^6-1\right) y(\mathrm{ch}^y_-)^2(I_2-I_4)}{x^3\left(y^2-1\right)} \right.$$
$$- \frac{4\mathrm{ch}^x_-\mathrm{ch}^y_-\left(x^3y^3-1\right)\left(I_2x^5y^3+I_2-I_4x^2\left(xy^3+1\right)\right)}{x^3\left(x^2-1\right)y^3}$$
$$+ \frac{(y^2-1)(\mathrm{ch}^y_-)^2 I_2\left(\left(x^8+1\right)\left(2y^4+3y^2+2\right)-\left(x^6+x^2\right)\left(y^2+1\right)^2\right)}{x^3\left(x^2-1\right)y^3}$$
$$- \frac{(y^2-1)(\mathrm{ch}^y_-)^2 I_4\left(\left(x^8+1\right)y^2+\left(x^6+x^2\right)\left(y^4+1\right)\right)}{x^3\left(x^2-1\right)y^3}$$
$$- \frac{4I_2\mathrm{ch}^y_-(x-y)(xy-1)\left(I_2\left(\left(x^6+1\right)\left(y^3+y\right)+\left(x^5+x\right)\left(y^4+y^2+1\right)-x^3\left(y^4+1\right)\right)+I_4x^3y^2\right)}{x^3\left(x^2-1\right)y^3}$$
$$\left. - \frac{I_2^2(y^2-1)(x-y)(xy-1)\left(I_2\left(\left(x^6+x^4+x^2+1\right)y+2x^3\left(y^2+1\right)\right)+I_4\left(x^5+x\right)\left(y^2+1\right)\right)}{x^3\left(x^2-1\right)y^3} \right]$$
$$\times \frac{1}{4\pi i}\partial_u \log\frac{\Gamma(iu_x-iu_y+1)}{\Gamma(1-iu_x+iu_y)}. \tag{5.112}$$

We defined $\mathrm{ch}^x_- = \mathrm{cosh}_-(x)$ and $\mathrm{ch}^y_- = \mathrm{cosh}_-(y)$, where $\mathrm{cosh}_-(x)$ is the part of the Laurent expansion of $\cosh\left(g(x+1/x)\right)$ vanishing at infinity, i.e.

$$\mathrm{cosh}_-(x) = \sum_{k=1}^{\infty} I_{2k} x^{-2k}. \tag{5.113}$$

The result for $J=4$ is given in appendix A.3.

5.4 Weak coupling tests and predictions

Our results for the curvature function $\gamma^{(2)}(g)$ at $J=2,3,4$ (equations (5.95), (5.112), (A.66)) are straightforward to expand at weak coupling. Let us start with the $J=2$ case, for which we found

$$\begin{aligned}\gamma^{(2)}_{J=2} &= -8g^2\zeta_3 + g^4\left(140\zeta_5 - \frac{32\pi^2\zeta_3}{3}\right) + g^6\left(200\pi^2\zeta_5 - 2016\zeta_7\right) \\ &+ g^8\left(-\frac{16\pi^6\zeta_3}{45} - \frac{88\pi^4\zeta_5}{9} - \frac{9296\pi^2\zeta_7}{3} + 27720\zeta_9\right) \\ &+ g^{10}\left(\frac{208\pi^8\zeta_3}{405} + \frac{160\pi^6\zeta_5}{27} + 144\pi^4\zeta_7 + 45440\pi^2\zeta_9 - 377520\zeta_{11}\right) + \ldots\end{aligned} \tag{5.114}$$

Notice that the result can be written in terms of simple ζ-functions and that the transcendentality is uniform at each order. Same holds for the $J=3$ and $J=4$ cases.

Expansions up to 10 loops are given in appendix A.4.

We can check our expansions against known results, as the anomalous dimensions of twist-two operators have been computed up to five loops for arbitrary spin [126, 127, 128, 129, 130, 81, 84, 131] (see also [132] and the review [133]). Up to three loops they can be found by using solely the ABA equations, while at four and five loops wrapping corrections

need to be taken into account which was done in [84, 131] by utilizing generalized Lüscher formulas. All these results are given by linear combinations of harmonic sums[17]

$$S_a(N) = \sum_{n=1}^{N} \frac{(\text{sign}(a))^n}{n^{|a|}}, \quad S_{a_1,a_2,a_3,\ldots}(N) = \sum_{n=1}^{N} \frac{(\text{sign}(a_1))^n}{n^{|a_1|}} S_{a_2,a_3,\ldots}(n) \tag{5.115}$$

with argument equal to the spin S. To make a comparison with our results we expanded these predictions in the $S \to 0$ limit. For this lengthy computation, as well as to simplify the final expressions, we used the `Mathematica` packages HPL [134], the package [135] provided with the paper [136], and the HarmonicSums package [137].

In this way we have confirmed the coefficients in (5.114) to four loops. Let us note that expansion of harmonic sums leads to multiple zeta values $\zeta_{k_1,\ldots,k_n}$, defined as

$$\zeta_{k_1,\ldots,k_n} = \sum_{i_1>i_2>\cdots>i_n>0} \frac{1}{i_1^{k_1} \ldots i_n^{k_n}} \tag{5.116}$$

However, these transcendental constants miraculously cancel in the final result leaving only single zeta values, i.e. ζ_k.

Importantly, the part of the four-loop coefficient which comes from the wrapping correction is essential for matching with our result, which confirms the validity of QSC beyond the ABA level. Additional evidence that our result incorporates all finite-size effects is found at strong coupling (see section 5.5).

For operators with $J = 3$, our prediction at weak coupling is

$$\begin{aligned} \gamma^{(2)}_{J=3} &= -2g^2\zeta_3 + g^4\left(12\zeta_5 - \frac{4\pi^2\zeta_3}{3}\right) + g^6\left(\frac{2\pi^4\zeta_3}{45} + 8\pi^2\zeta_5 - 28\zeta_7\right) \\ &+ g^8\left(-\frac{4\pi^6\zeta_3}{45} - \frac{4\pi^4\zeta_5}{15} - 528\zeta_9\right) + \ldots \end{aligned} \tag{5.117}$$

The known results for any spin in this case are available at up to six loops, including the wrapping correction which first appears at five loops [138, 139, 140]. Expanding them at $S \to 0$ we have verified our calculation to four loops.[18]

For future reference, in appendix A.4 we present an expansion of known results for $J = 2, 3$ up to order S^3 at first several loop orders. In particular, we found that multiple zeta values appear in this expansion, which did not happen at lower orders in S.

[17] Notice that a similar basis of harmonic sums plays a crucial role in section 9.3, where we study weak coupling expansion of BFKL eigenvalue

[18] As a further check it would be interesting to expand to order S^2 the known results for twist-two operators at five loops, and for twist-three operators at five and six loops – all of which are given by huge expressions.

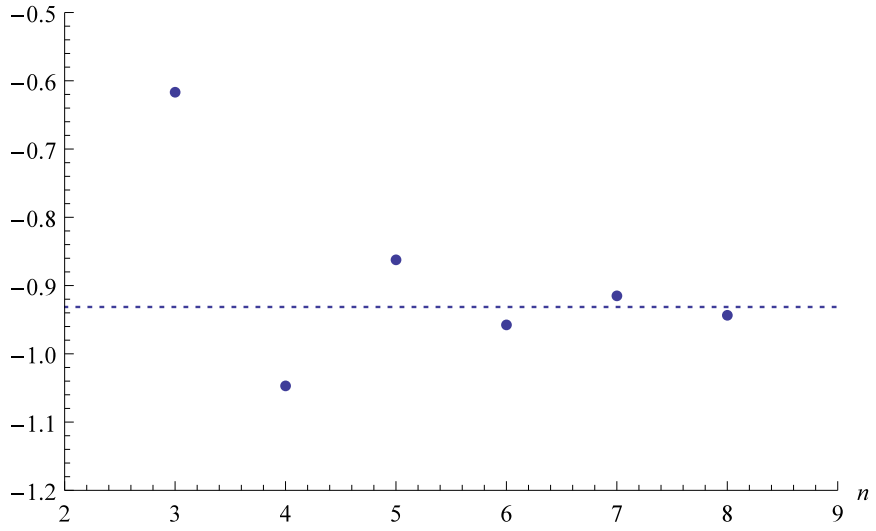

Figure 5: **One-loop energy at $J = 4$ from the Bethe ansatz.** The dashed line shows the result from QSC for the coefficient of S^2 in the 1-loop energy at $J = 4$, i.e. $-\frac{14\zeta_3}{5} + \frac{48\zeta_5}{\pi^2} - \frac{252\zeta_7}{\pi^4} \approx -0.931$ (see (5.118)). The dots show the Bethe ansatz prediction (5.119) expanded to orders $1/J^3, 1/J^4, \ldots, 1/J^8$ (the order of expansion n corresponds to the horizontal axis), and it appears to converge to QSC result.

Let us now discuss the $J = 4$ case. The expansion of our result reads:

$$\begin{aligned}\gamma^{(2)}_{J=4} &= g^2\left(-\frac{14\zeta_3}{5} + \frac{48\zeta_5}{\pi^2} - \frac{252\zeta_7}{\pi^4}\right) \\ &+ g^4\left(-\frac{22\pi^2\zeta_3}{25} + \frac{474\zeta_5}{5} - \frac{8568\zeta_7}{5\pi^2} + \frac{8316\zeta_9}{\pi^4}\right) \\ &+ g^6\left(\frac{32\pi^4\zeta_3}{875} + \frac{3656\pi^2\zeta_5}{175} - \frac{56568\zeta_7}{25} + \frac{196128\zeta_9}{5\pi^2} - \frac{185328\zeta_{11}}{\pi^4}\right) \\ &+ g^8\left(-\frac{4\pi^6\zeta_3}{175} - \frac{68\pi^4\zeta_5}{75} - \frac{55312\pi^2\zeta_7}{125} + \frac{1113396\zeta_9}{25} - \frac{3763188\zeta_{11}}{5\pi^2}\right. \\ &\qquad \left. + \frac{3513510\zeta_{13}}{\pi^4}\right) + \ldots\end{aligned} \tag{5.118}$$

Unlike for the $J = 2$ and $J = 3$ cases, we could not find a closed expression for the energy at any spin S in literature even at one loop, however there is another way to check our result. One can expand the asymptotic Bethe ansatz equations at large J for fixed values of $S = 2, 4, 6, \ldots$ and then extract the coefficients in the expansion which are polynomial in S. This was done in [118] (see appendix C there) where at one loop the expansion was found up to order $1/J^6$:

$$\gamma(S,J) = g^2\left(\frac{S}{2\,J^2} - \left(\frac{S^2}{4} + \frac{S}{2}\right)\frac{1}{J^3} + \left[\frac{3S^3}{16} + \left(\frac{1}{8} - \frac{\pi^2}{12}\right)S^2 + \frac{S}{2}\right]\frac{1}{J^4} + \ldots\right) + \mathcal{O}(g^4) \tag{5.119}$$

Now taking the part proportional to S^2 and substituting $J = 4$ one may expect to get a numerical approximation to the 1-loop coefficient in our result (5.118), i.e. $-\frac{14\zeta_3}{5} + \frac{48\zeta_5}{\pi^2} - \frac{252\zeta_7}{\pi^4}$. To increase the precision we extended the expansion in (5.119) to order $1/J^8$. Remarkably, in this way we confirmed the 1-loop part of the QSC prediction (5.118) with about 1% accuracy! In Fig. 5 one can also see that the ABA result converges to our prediction when the order of expansion in $1/J$ is being increased.

Also, in contrast to $J = 2$ and $J = 3$ cases we see that negative powers of π appear in (5.118) (although still all the contributions at a given loop order have the same transcendentality). It would be interesting to understand why this happens from the gauge theory perspective, especially since the expansion of the leading S term (5.4) has the same structure for all J,

$$\gamma_J^{(1)} = \frac{8\pi^2 g^2}{J(J+1)} - \frac{32\pi^4 g^4}{J(J+1)^2(J+2)} + \frac{256\pi^6 g^6}{J(J+1)^3(J+2)(J+3)} + \dots \tag{5.120}$$

The change of structure at $J = 4$ might be related to the fact that for $J \geq 4$ the ground state anomalous dimension even at one loop is expected to be an irrational number for integer $S > 0$ (see [141], [142]), and thus cannot be written as a linear combination of harmonic sums with integer coefficients.

In the next section we will discuss tests and applications of our results at strong coupling.

5.5 Strong coupling tests and predictions

In this section we will present the strong coupling expansion of our results for the curvature function and reëxpand these results to obtain anomalous dimensions of short operators at strong coupling.

5.5.1 Expansion of the curvature function for $J = 2, 3, 4$

The integral representation of the result (5.95), (5.112), (A.66) makes it surprisingly difficult to obtain its strong coupling expansion analytically. Thus we chose another way: we evaluated the result numerically with high precision for a range of values of g and then made a fit to find the expansion coefficients. It would be of course interesting to carry out the expansion analytically, and we leave this for the future.

For numerical study it is convenient to write our exact expressions (5.95), (5.112),

(A.66) for $\gamma^{(2)}(g)$, which all have the form

$$\gamma^{(2)}(g) = \oint du_x \oint du_y f(x,y)\partial_{u_x} \log \frac{\Gamma(iu_x - iu_y + 1)}{\Gamma(1 - iu_x + iu_y)} \tag{5.121}$$

where the integration goes around the branch cut between $-2g$ and $2g$, in a slightly different way (we remind that we use notation $x + \frac{1}{x} = \frac{u_x}{g}$ and $y + \frac{1}{y} = \frac{u_y}{g}$). Namely, by changing the variables of integration to x, y and integrating by parts one can write the result as

$$\gamma^{(2)}(g) = \oint dx \oint dy F(x,y) \log \frac{\Gamma(iu_x - iu_y + 1)}{\Gamma(iu_y - iu_x + 1)} \tag{5.122}$$

where $F(x,y)$ is some polynomial in the following variables: x, $1/x$, y, $1/y$, sh_-^x and sh_-^y (for $J = 3$ it includes ch_-^x, ch_-^y instead of the sh_- functions). The integral in (5.122) is over the unit circle. The advantage of this representation is that plugging in sh_-^x, sh_-^y as series expansions (truncated to some large order), we see that it only remains to compute integrals of the kind

$$C_{r,s} = \frac{1}{i} \oint \frac{dx}{2\pi} \oint \frac{dy}{2\pi} x^r y^s \log \frac{\Gamma(iu_x - iu_y + 1)}{\Gamma(iu_y - iu_x + 1)} \tag{5.123}$$

These are nothing but the coefficients of the BES dressing phase [111, 143, 114, 144]. Luckily the strong coupling expansion for them is known [111]:

$$C_{r,s} = \sum_{n=0}^{\infty} \left[-\frac{2^{-n-1}(-\pi)^{-n} g^{1-n} \zeta_n \left(1 - (-1)^{r+s+4}\right) \Gamma\left(\frac{1}{2}(n-r+s-1)\right) \Gamma\left(\frac{1}{2}(n+r+s+1)\right)}{\Gamma(n-1)\Gamma\left(\frac{1}{2}(-n-r+s+3)\right) \Gamma\left(\frac{1}{2}(-n+r+s+5)\right)} \right] \tag{5.124}$$

However this expansion is only asymptotic and does not converge. For fixed g the terms will start growing with n when n is greater than some value N, and so we only sum the terms up to $n = N$ which gives the value of $C_{r,s}$ with very good precision for large enough g.

Using this approach we computed the curvature function for a range of values of g (typically we took $7 \le g \le 30$) and then fitted the result as an expansion in $1/g$. This gave us only numerical values of the expansion coefficients, but in fact we found that with very high precision the coefficients are as follows. For $J = 2$

$$\begin{aligned} \gamma^{(2)}_{J=2} &= -\pi^2 g^2 + \frac{\pi g}{4} + \frac{1}{8} - \frac{1}{\pi g}\left(\frac{3\zeta_3}{16} + \frac{3}{512}\right) - \frac{1}{\pi^2 g^2}\left(\frac{9\zeta_3}{128} + \frac{21}{512}\right) \\ &+ \frac{1}{\pi^3 g^3}\left(\frac{3\zeta_3}{2048} + \frac{15\zeta_5}{512} - \frac{3957}{131072}\right) + \dots , \end{aligned} \tag{5.125}$$

then for $J = 3$

$$\begin{aligned} \gamma^{(2)}_{J=3} &= -\frac{8\pi^2 g^2}{27} + \frac{2\pi g}{27} + \frac{1}{12} - \frac{1}{\pi g}\left(\frac{1}{216} + \frac{\zeta_3}{8}\right) - \frac{1}{\pi^2 g^2}\left(\frac{3\zeta_3}{64} + \frac{743}{13824}\right) \\ &+ \frac{1}{\pi^3 g^3}\left(\frac{41\zeta_3}{1024} + \frac{35\zeta_5}{512} - \frac{5519}{147456}\right) + \dots , \end{aligned} \tag{5.126}$$

and finally for $J = 4$

$$\begin{aligned}\gamma^{(2)}_{J=4} &= -\frac{\pi^2 g^2}{8} + \frac{\pi g}{32} + \frac{1}{16} - \frac{1}{\pi g}\left(\frac{3\zeta_3}{32} + \frac{15}{4096}\right) - \frac{0.01114622551913}{g^2} \\ &+ \frac{0.004697583899}{g^3} + \dots\,.\end{aligned} \tag{5.127}$$

To fix coefficients for the first four terms in the expansion we were guided by known analytic predictions which will be discussed below, and found that our numerical result matches these predictions with high precision. Then for $J = 2$ and $J = 3$ we extracted the numerical values obtained from the fit for the coefficients of $1/g^2$ and $1/g^3$, and plugging them into the online calculator EZFace [145] we obtained a prediction for their exact values as combinations of ζ_3 and ζ_5. Fitting again our numerical results with these exact values fixed, we found that the precision of the fit at the previous orders in $1/g$ increased. This is a highly nontrivial test for the proposed exact values of $1/g^2$ and $1/g^3$ terms. For $J = 2$ we confirmed the coefficients of these terms with absolute precision 10^{-17} and 10^{-15} at $1/g^2$ and $1/g^3$ respectively (at previous orders of the expansion the precision is even higher). For $J = 3$ the precision was correspondingly 10^{-15} and 10^{-13}.

For $J = 4$ we were not able to get a stable fit for the $1/g^2$ and $1/g^3$ coefficients from EZFace, so above we gave their numerical values (with uncertainty in the last digit). However below we will see that based on $J = 2$ and $J = 3$ results one can make a prediction for these coefficients, which we again confirmed by checking that precision of the fit at the previous orders in $1/g$ increases. The precision of the final fit at orders $1/g^2$ and $1/g^3$ is 10^{-16} and 10^{-14} respectively.

5.5.2 Generalization to any J

The reader might be surprised, but based on the strong coupling expansions for several finite J presented in the previous section we were able to recover the strong coupling expansion of the curvature function for any J. To see how this is possible consider the structure of classical expansions of the scaling dimension. Let us introduce the "inverse" function $S(\Delta)$, frequently encountered in the context of BFKL. It has a few simple properties: e.g. the curve $S(\Delta)$ goes through the points $(\pm J, 0)$ at any coupling, because at $S = 0$ the operator is BPS. At the same time for non-BPS states one should have $\Delta(\lambda) \propto \lambda^{1/4} \to \infty$ [45] which indicates that if Δ is fixed, S should go to zero. Combining this with the knowledge of fixed points $(\pm J, 0)$ we conclude that at infinite coupling $S(\Delta)$ is simply the line $S = 0$. As the coupling becomes finite $S(\Delta)$ starts bending from the $S = 0$ line and starts looking like a parabola going through the points $\pm J$, see fig. 15.

Based on this qualitative picture and the scaling $\Delta(\lambda) \propto \lambda^{1/4}$ at $\lambda \to \infty$ and fixed J and S, one can write down the following ansatz,

$$S(\Delta) = \left(\Delta^2 - J^2\right)\left(\alpha_1 \frac{1}{\lambda^{1/2}} + \alpha_2 \frac{1}{\lambda} + (\alpha_3 + \beta_3 \Delta^2)\frac{1}{\lambda^{3/2}}\right. \tag{5.128}$$

$$\left. + (\alpha_4 + \beta_4 \Delta^2)\frac{1}{\lambda^2} + (\alpha_5 + \beta_5 \Delta^2 + \gamma_5 \Delta^4)\frac{1}{\lambda^{5/2}} + (\alpha_6 + \beta_6 \Delta^2 + \gamma_6 \Delta^4)\frac{1}{\lambda^3} + \dots\right).$$

We omitted the odd powers of the scaling dimension from the ansatz taking into account the fact that only the square of Δ enters into (4.50) and (4.51). We can now invert the relation and express Δ in terms of S at strong coupling, which gives

$$\Delta^2 = J^2 + S\left(A_1\sqrt{\lambda} + A_2 + \dots\right) + S^2\left(B_1 + \frac{B_2}{\sqrt{\lambda}} + \dots\right) + S^3\left(\frac{C_1}{\lambda^{1/2}} + \frac{C_2}{\lambda} + \dots\right) + \mathcal{O}(S^4)\,, \tag{5.129}$$

where the coefficients $A_i,\ B_i,\ C_i$ are some functions of J. There exists a one-to-one mapping between the coefficients α_i, β_i, etc. and A_i, B_i etc, which is rather complicated but easy to find. We note that this structure of Δ^2 coincides with Basso's conjecture in [115] for mode number $n = 1$ [19]. The pattern in (5.129) continues to higher orders in S with further coefficients D_i, E_i, etc. and powers of λ suppressed incrementally. This structure is a nontrivial constraint on Δ itself as one easily finds from (5.129) that

$$\Delta = J + \frac{S}{2J}\left(A_1\sqrt{\lambda} + A_2 + \frac{A_3}{\sqrt{\lambda}} + \dots\right) + S^2\left(-\frac{A_1^2}{8J^3}\lambda - \frac{A_1 A_2}{4J^3}\sqrt{\lambda}\right.$$

$$\left. + \left[\frac{B_1}{2J} - \frac{A_2^2 + 2A_1A_3}{8J^3}\right] + \left[\frac{B_2}{2J} - \frac{A_2A_3 + A_1A_4}{4J^3}\right]\frac{1}{\sqrt{\lambda}} + \dots\right). \tag{5.130}$$

By definition the coefficients of S and S^2 are the slope and curvature functions respectively, so now we have their expansions at strong coupling in terms of $A_i,\ B_i,\ C_i$, etc. Since the S coefficient only contains the constants A_i, we can find all of their values by simply expanding the slope function (5.36) at strong coupling. We get

$$A_1 = 2\ \ ,\ \ A_2 = -1\ \ ,\ \ A_3 = J^2 - \frac{1}{4}\ \ ,\ \ A_4 = J^2 - \frac{1}{4}\dots\ . \tag{5.131}$$

Note that in this series the power of J increases by two at every other member, which is a direct consequence of omitting odd powers of Δ from (5.128). We also expect the same pattern to hold for the coefficients B_i, C_i, etc.

The curvature function written in terms of A_i, B_i, etc. is given by

$$\gamma_J^{(2)}(g) = -\frac{2\pi^2 g^2 A_1^2}{J^3} - \frac{\pi g A_1 A_2}{J^3} - \frac{A_2^2 + 2A_1A_3 - 4B_1J^2}{8J^3} \tag{5.132}$$

$$-\frac{A_2A_3 + A_1A_4 - 2B_2J^2}{16\pi g J^3} - \frac{A_3^2 + 2A_2A_4 + 2A_1A_5 - 4B_3J^2}{128\pi^2 g^2 J^3} \tag{5.133}$$

$$-\frac{A_3A_4 + A_2A_5 + A_1A_6 - 2B_4J^2}{256\pi^3 g^3 J^3} + \mathcal{O}\left(\frac{1}{g^4}\right).$$

[19] The generalization of (5.129) for $n > 1$ is not fully clear, as noted in [147], and this case will be discussed in appendix A.5.

The remaining unknowns here (up to order $1/g^4$) are B_1, B_2, which we expect to be constant due to the power pattern noticed above and B_3, B_4, which we expect to have the form aJ^2+b with a and b constant. These unknowns are immediately fixed by comparing the general curvature expansion (5.132) to the two explicit cases that we know for $J=2$ and $J=3$. We find

$$B_1 = 3/2 \ , \ \ B_2 = -3\,\zeta_3 + \frac{3}{8}, \tag{5.134}$$

and

$$B_3 = -\frac{J^2}{2} - \frac{9\,\zeta_3}{2} + \frac{5}{16} \ , \ \ B_4 = \frac{3}{16}J^2(16\,\zeta_3 + 20\,\zeta_5 - 9) - \frac{15\,\zeta_5}{2} - \frac{93\,\zeta_3}{8} - \frac{3}{16}. \tag{5.135}$$

Having fixed all the unknowns we can write the strong coupling expansion of the curvature function for arbitrary values of J as

$$\begin{aligned}\gamma_J^{(2)}(g) = &-\frac{8\pi^2 g^2}{J^3} + \frac{2\pi g}{J^3} + \frac{1}{4J} + \frac{1 - J^2(24\,\zeta_3+1)}{64\pi g J^3} - \frac{8J^4 + J^2(72\,\zeta_3+11) - 4}{512 g^2\,(\pi^2 J^3)} \\ &+\frac{3\left(8J^4(16\,\zeta_3+20\,\zeta_5-7) - 16J^2(31\,\zeta_3+20\,\zeta_5+7)+25\right)}{16384\pi^3 g^3 J^3} + \mathcal{O}\left(\frac{1}{g^4}\right).\end{aligned} \tag{5.136}$$

Expanding $\gamma^{(2)}_{J=4}$ defined in (A.66) at strong coupling numerically we were able to confirm the above result with high precision.

5.5.3 Anomalous dimension of short operators

In this section we will use the knowledge of slope and curvature functions $\gamma_J^{(n)}$ at strong coupling to find the strong coupling expansions of scaling dimensions of operators with finite S and J. As an important example we will find the three-loop coefficient of the Konishi operator by utilizing the techniques of [115, 147]. Below we briefly review the main ideas in these papers.

We are interested in the coefficients of the strong coupling expansion of Δ, namely

$$\Delta = \Delta^{(0)}\lambda^{\frac{1}{4}} + \Delta^{(1)}\lambda^{-\frac{1}{4}} + \Delta^{(2)}\lambda^{-\frac{3}{4}} + \Delta^{(3)}\lambda^{-\frac{5}{4}} + \dots \tag{5.137}$$

First, we use Basso's conjecture (5.129) and by fixing S and J we re-expand the square root of Δ^2 at strong coupling to find

$$\Delta = \sqrt{A_1 S}\,\sqrt[4]{\lambda} + \frac{\sqrt{A_1}\left(J^2 + A_2 S + B_1 S^2\right)}{2A_1\sqrt{S}}\,\frac{1}{\sqrt[4]{\lambda}} + \mathcal{O}\left(\frac{1}{\lambda^{\frac{3}{4}}}\right). \tag{5.138}$$

Thus we reformulate the problem entirely in terms of the coefficients A_i, B_i, C_i, etc. For example, the next coefficient in the series, namely the two-loop term is given by

$$\Delta^{(2)} = -\frac{\left(2A_2 + 4B_1 + J^2\right)^2 - 16A_1(A_3 + 2B_2 + 4C_1)}{16\sqrt{2}A_2^{3/2}}. \tag{5.139}$$

Further coefficients become more and more complicated, however a very clear pattern can be noticed after looking at these expressions: we see that the term $\Delta^{(n)}$ only contains coefficients with indices up to $n+1$, e.g. the tree level term $\Delta^{(0)}$ only depends on A_1, the one-loop term depends on A_1, A_2, B_1, etc. Thus we can associate the index of these coefficients with the loop level. Conversely, from the last section we learned that the letter of A_i, B_i, etc. can be associated with the order in S, i.e. the slope function fixed all A_i coefficients and the curvature function in principle fixes all B_i coefficients.

Matching with classical and semiclassical results Looking at (5.138) we see that knowing A_i and B_i only takes us to one loop, in order to proceed we need to know some coefficients in the C_i and D_i series. This is where the next ingredient in this construction comes in, which is the knowledge of the classical energy and its semiclassical correction in the Frolov-Tseytlin limit, i.e. when $\mathcal{S} \equiv S/\sqrt{\lambda}$ and $\mathcal{J} \equiv J/\sqrt{\lambda}$ remain fixed, while S, J, $\lambda \to \infty$. As we will explain in more detail in section 7.3[20], in this limit the square of the classical energy of the string has expansion (7.32) as $\mathcal{S} \to 0$. We will also need the expansion (7.33) of one-loop correction in the same limit.

If the parameters $\mathcal{S}$ and $\mathcal{J}$ are fixed to some values then the sum in (7.33) can be evaluated explicitly in terms of zeta-functions. We now add up the classical and the 1-loop contributions[21], take S and J fixed at strong coupling and compare the result to (5.129). By requiring consistency we are able to extract the following coefficients,

$$\begin{aligned}
A_1 &= 2, & A_2 &= -1 \\
B_1 &= 3/2, & B_2 &= -3\,\zeta_3 + \tfrac{3}{8} \\
C_1 &= -3/8, & C_2 &= \tfrac{1}{16}\,(60\,\zeta_3 + 60\,\zeta_5 - 17) \\
D_1 &= 31/64, & D_2 &= \tfrac{1}{512}(-5520\,\zeta_3 - 5120\,\zeta_5 - 3640\,\zeta_7 + 901)
\end{aligned}$$

As discussed in the previous section, we can in principle extract all coefficients with indices 1 and 2. In order to find e.g. B_3 we would need to extend the quantization of the classical solution to the next order. Note that the coefficients A_1, A_2 and B_1, B_2 have the same exact values that we extracted from the slope and curvature functions.

Result for the anomalous dimensions at strong coupling The key observation in [147] was that once written in terms of the coefficients A_i, B_i, C_i, the two-loop term $\Delta^{(2)}$ only depends on $A_{1,2,3}$, $B_{1,2}$, C_1 as can be seen in (5.139). As discussed in the last

[20] We apologize for referring to the result which will appear only later in the thesis, but there seems to be no linear way to organize the material

[21] Note that they mix various orders of the coupling.

(S,J)	$\lambda^{-5/4}$ prediction	$\lambda^{-5/4}$ fit	error	fit order
$(2,2)$	$\frac{15\,\zeta_5}{2}+6\,\zeta_3-\frac{1}{2}=14.48929958$	14.12099034	2.61%	6
$(2,3)$	$\frac{15\,\zeta_5}{2}+\frac{63\,\zeta_3}{8}-\frac{1131}{512}=15.03417190$	14.88260078	1.02%	5
$(2,4)$	$\frac{21\,\zeta_3}{2}+\frac{15\,\zeta_5}{2}-\frac{25}{8}=17.27355565$	16.46106336	4.94%	7

Table 1: Comparisons of strong coupling expansion coefficients for $\lambda^{-5/4}$ obtained from fits to TBA data versus our predictions for various operators. The fit order is the order of polynomials used for the rational fit function (see [147] for details).

section, the one-loop result fixes all of these constants except A_3, which in principle is a contribution from a true two-loop calculation. However we already fixed it from the slope function and thus we are able to find

$$\Delta^{(2)}=\frac{-21\,S^4+(24-96\,\zeta_3)S^3+4\left(5J^2-3\right)S^2+8J^2S-4J^4}{64\sqrt{2}\,S^{3/2}}. \tag{5.140}$$

Now that we know the strong coupling expansion of the curvature function and thus all the coefficients B_i, we can do the same trick and find the three loop strong coupling scaling dimension coefficient $\Delta^{(3)}$, which now depends on $A_{1;2;3;4}$, $B_{1,2,3}$, $C_{1,2}$, D_1. We find it to be

$$\begin{aligned}\Delta^{(3)} &= \frac{187\,S^6+2\left(624\,\zeta_3+480\,\zeta_5-193\right)S^5+\left(-146\,J^2-4\left(336\,\zeta_3-41\right)\right)S^4}{512\sqrt{2}\,S^{5/2}}\\ &+ \frac{\left(32\left(6\,\zeta_3+7\right)J^2-88\right)S^3+\left(-28\,J^4+40\,J^2\right)S^2-24\,J^4S+8\,J^6}{512\sqrt{2}\,S^{5/2}},\end{aligned} \tag{5.141}$$

for $S=2$ it simplifies to

$$\Delta^{(3)}_{S=2}=\frac{1}{512}\left(J^6-20J^4+48J^2(4\zeta_3-1)+192(12\,\zeta_3+20\,\zeta_5+1)\right) \tag{5.142}$$

and finally for the Konishi operator, which has $S=2$ and $J=2$ we get[22]

$$\Delta^{(3)}_{S=2,J=2}=\frac{15\,\zeta_5}{2}+6\,\zeta_3-\frac{1}{2}. \tag{5.143}$$

In order to compare our predictions with data available from TBA calculations [149], we employed Padé type fits as explained in [147]. The fit results are shown in Tab. 1, we see that our predictions are within 5% error bounds, which is a rather good agreement. However we must be honest that for the $J=3$ and especially $J=4$ states we did not have as many data points as for the $J=2$ state and the fit is somewhat shaky.

[22]The ζ_3 and ζ_5 terms are coming from semi-classics and were already known before [119] and match our result.

6 Bremsstrahlung function

6.1 Cusped Wilson line

In this chapter, based on [10], we will study an observable called Bremsstrahlung function. It arises as a limit of the quark-antiquark potential on the three-sphere, or equivalently the generalized cusp anomalous dimension Γ_{cusp}. Cusp anomalous dimension describes the divergence in the expectation value of a Wilson loop made of two lines forming a cusp,

$$\langle W \rangle \sim \left(\frac{\Lambda_{IR}}{\Lambda_{UV}} \right)^{\Gamma_{\text{cusp}}}, \tag{6.1}$$

with Λ_{UV} and Λ_{IR} being the UV and IR cutoffs [150]. The quantity Γ_{cusp} is also related to a number of other physical quantities, such as IR divergence in amplitudes and radiation power from a moving quark, see e.g. [151, 152, 153, 122]. The cusp anomalous dimension is a function of two angles, ϕ and θ, which describe the geometry of the Wilson line setup shown in Fig. 6 [154]. The first angle, ϕ, is the angle between the quark and antiquark lines at the cusp. The second angle, θ, arises because the locally supersymmetric Wilson lines considered here include a coupling to the scalar fields, as described in the end of section 2.4. As there are six real scalars in $\mathcal{N} = 4$ SYM the coupling can be defined by a unit vector $\vec{n}$ which gives a point on S^5. At each arm of the cusp the coupling is constant but different, given by vectors $\vec{n}$ and $\vec{n}_\theta$ respectively. Obviously they only enter the answer through an angle θ between them. We can write the cusped Wilson line explicitly as

$$W_0 = \mathrm{P} \exp \int_{-\infty}^{0} dt \left[iA \cdot \dot{x}_q + \vec{\Phi} \cdot \vec{n} \, |\dot{x}_q| \right] \times \mathrm{P} \exp \int_{0}^{\infty} dt \left[iA \cdot \dot{x}_{\bar{q}} + \vec{\Phi} \cdot \vec{n}_\theta \, |\dot{x}_{\bar{q}}| \right], \tag{6.2}$$

where $\vec{\Phi}$ is a vector consisting of the six real scalars of $\mathcal{N} = 4$ SYM , while $x_q(t)$ and $x_{\bar{q}}(t)$ are the quark and antiquark trajectories (straight lines through the origin) which make up an angle ϕ at the cusp (see Fig.6).

A fully nonperturbative description for the value of Γ_{cusp} was obtained in a remarkable development by Drukker [155] and by Correa, Maldacena & Sever [95]. They proposed an infinite system of TBA integral equations which compute this quantity at arbitrary 't Hooft coupling λ and for arbitrary angles. In order to implement the TBA approach, the cusp anomalous dimension was generalized for the case when a local operator with R-charge L is inserted at the cusp (cf. Fig. 6):

$$W_L = \mathrm{P} \exp \int_{-\infty}^{0} dt \left(iA \cdot \dot{x}_q + \vec{\Phi} \cdot \vec{n} \, |\dot{x}_q| \right) \times Z^L \times \mathrm{P} \exp \int_{0}^{\infty} dt \left(iA \cdot \dot{x}_{\bar{q}} + \vec{\Phi} \cdot \vec{n}_\theta \, |\dot{x}_{\bar{q}}| \right). \tag{6.3}$$

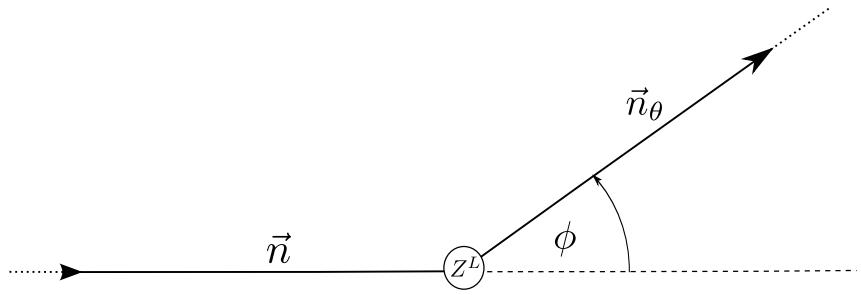

Figure 6: The setup: a Wilson line with a cusp angle ϕ and L scalar fields $Z = \Phi_1 + i\Phi_2$ inserted at the cusp. Coupling of the scalar fields to the two half lines is defined by directions $\vec{n}$ and $\vec{n}_\theta$ in the internal space, with the angle θ between them. We consider the near-BPS limit corresponding to $\phi \approx \theta$.

As defined before, $Z = \Phi_1 + i\Phi_2$, with Φ_1 and Φ_2 being two scalars independent from $(\vec{\Phi} \cdot \vec{n})$ and $(\vec{\Phi} \cdot \vec{n}_\theta)$. The anomalous dimension $\Gamma_L(\phi, \theta, \lambda)$ corresponding to such Wilson line is captured by the TBA equations exactly at any value of L. For $L = 0$ the usual quark-antiquark potential is recovered. The number of field insertions plays the role of the system's volume in the TBA description, and $\Gamma_L(\phi, \theta, \lambda)$ is obtained as the vacuum state energy.

While the infinite system of these TBA equations is rather complicated, having the two angles as continuous parameters opens the possibility to look for simplifications in some limits where an exact analytical solution may be expected[23]. There are at least two interesting near-BPS limits. For example, when both angles are zero, the set-up degenerates into a straight line, which is obviously BPS. Expansion around this configuration in parameter space, more precisely the regime when one of the angle is zero and the other is small, was studied in [91]. Another BPS configuration, around which we expand in this chapter, is $\phi = \theta$ [159, 160][24]. Non-renormalization of anomalous dimension in this limit can be understood from the classical string theory perspective. In a general situation the S^5 part of the curve is determined by parameters θ and L, whereas the parameters of the AdS_5 part are ϕ and Δ. The two parts governed by the same (up to analytical continuation) equations and are related through the Virasoro condition. When $\phi = \theta$, Δ becomes equal to L, which is, of course, quantized.

The small deviations from this supersymmetric case are known to be partially under control: the cusp dimension at $L = 0$ was computed for $\phi \approx \theta$ analytically at any coupling

[23] On the other hand, non-perturbative predictions from the spectral TBA have been mostly restricted to numerics [156, 149, 148, 157]; see also [158].

[24] Strictly speaking the BPS condition allows $\phi = -\theta$ in addition to $\phi = \theta$ but these two cases are trivially related.

in [151, 152] using results from localization methods [161, 162]. The answer in the planar limit reads

$$\Gamma_{\text{cusp}}(\phi,\theta,\lambda) = -\frac{1}{4\pi^2}(\phi^2-\theta^2)\frac{1}{1-\frac{\theta^2}{\pi^2}}\frac{\sqrt{\tilde{\lambda}}\, I_2\left(\sqrt{\tilde{\lambda}}\right)}{I_1\left(\sqrt{\tilde{\lambda}}\right)} + \mathcal{O}\left((\phi^2-\theta^2)^2\right), \quad \tilde{\lambda} = \lambda\left(1-\frac{\theta^2}{\pi^2}\right) \tag{6.4}$$

where I_n are the modified Bessel functions of the first kind. The existence of such an explicit result suggests that the cusp TBA system should simplify dramatically when $\phi \approx \theta$. Even though the full set of TBA equations was simplified a bit in this limit as described in [95], the result is still an enormously complicated infinite set of integral equations. Remarkably, it turned out that these equations admit an exact *analytical* solution. For the near-BPS configuration where $\theta = 0$ and ϕ is small it was obtained in [91]. The result of [91] covers all values of L and λ and for $L = 0$ reproduces the localization result (6.4) in which θ should be set to zero.

In this chapter we extend the results of [91] to the generic near-BPS limit. Thus, we consider the case when $\phi \approx \theta$, but θ is arbitrary and is an extra parameter in the result. We obtain an explicit expression valid for all values of θ, L and λ. Our final result for arbitrary θ takes a particularly elegant form

$$\Gamma_L(g) = \frac{\phi-\theta}{4}\partial_\theta \log\frac{\det \mathcal{M}_{2L+1}}{\det \mathcal{M}_{2L-1}}, \tag{6.5}$$

where we define an $N+1 \times N+1$ matrix

$$\mathcal{M}_N = \begin{pmatrix} I_1^\theta & I_0^\theta & \cdots & I_{2-N}^\theta & I_{1-N}^\theta \\ I_2^\theta & I_1^\theta & \cdots & I_{3-N}^\theta & I_{2-N}^\theta \\ \vdots & \vdots & \ddots & \vdots & \vdots \\ I_N^\theta & I_{N-1}^\theta & \cdots & I_1^\theta & I_0^\theta \\ I_{N+1}^\theta & I_N^\theta & \cdots & I_2^\theta & I_1^\theta \end{pmatrix} \tag{6.6}$$

and I_n^θ are

$$I_n^\theta = \frac{1}{2} I_n\left(\sqrt{\tilde{\lambda}}\right)\left[\left(\sqrt{\frac{\pi+\theta}{\pi-\theta}}\right)^n - (-1)^n\left(\sqrt{\frac{\pi-\theta}{\pi+\theta}}\right)^n\right]. \tag{6.7}$$

At $L = 0$ this result just reduces to the localization result (6.4). For $L > 0$ our result complements and generalizes the calculation of [91] as another integrability-based prediction for localization techniques. As in [91], the determinant expressions we got suggest a possible link to matrix models. Apart from being interesting from purely mathematical point of view, this comes in very handy when one considers a quasiclassical expansion of our result in order to compare with the corresponding string solution (think about the large L limit of (6.5)). We will explore this topic in section 7.4.

The main result of this chapter (6.5) is obtained in two ways. First, we use the old approach of solving the Bremsstrahlung TBA analytically, following the strategy developed in [91]. In section 6.2.1 we describe the initial simplification of the TBA system in the near-BPS limit, resulting in an infinite set of the Bremsstrahlung TBA equations. Then in section 6.2.2 we apply the powerful methods developed for the spectral problem to reduce this system to a finite set of equations, known as FiNLIE [94, 163][25]. In section 6.2.3 we make an analytic ansatz for the unknowns in the FiNLIE and construct its explicit solution, obtaining our result for the energy. As in [91] a key structure we encounter in the process is a Baxter equation for a set of auxiliary Bethe roots. Second, in section 6.3 we demonstrate how the same result can be obtained in a much simpler way using the QSC method. The QSC we work with here differs from the one described in chapter 4 by taking into account twisted boundary conditions. It is relevant for studying Wilson lines or observables in twisted SYM [166, 109]. We also describe checks of our result at both strong and weak coupling in section 6.4. Appendix B contains various technical details.

6.2 Pre-QSC solution

6.2.1 TBA equations in the near-BPS limit

In this section we discuss the first simplification of the cusp TBA system in the near-BPS regime, when the two angles ϕ and θ are close to each other. Following [95] we will thus obtain a somewhat simpler, but still infinite, set of integral equations – the Bremsstrahlung TBA.[26]

Let us remind that the cusp TBA equations are analogous to those describing the spectrum of single trace operator anomalous dimensions. The two infinite sets of equations for the Y-functions $Y_{a,s}(u)$ can be brought to similar form by subtracting the asymptotic large L solution. The integer indices (a, s) of the Y-functions take values in the infinite T-shaped domain familiar from the spectral TBA (see Fig. 7). The only difference is in an extra symmetry requirement for the Y-functions, and in the large L asymptotic solution[27].

The asymptotic solution encodes, in particular, the boundary scattering phase which has a double pole at zero mirror momentum. Due to this, the momentum-carrying func-

[25] See also [164, 165] for an alternative approach.

[26] The authors of [95] obtained the Bremsstrahlung TBA equations for the generic case $\phi \approx \theta$, but the equations were given explicitly in [95] only for the small angles case so we will repeat the derivation here.

[27] The extra symmetry requirement in the cusp TBA reads $Y_{a,s}(u) = Y_{a,-s}(-u)$ but is irrelevant in our discussion as for our state all Y-functions are even.

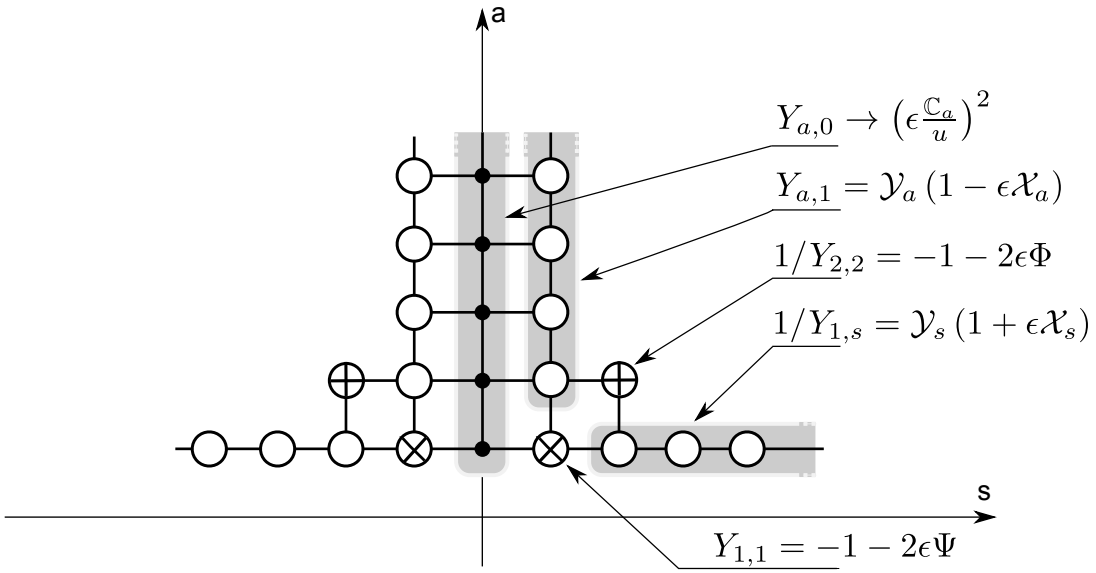

Figure 7: **The Y-hook.** The indices (a, s) of Y-functions take values on the infinite T-shaped lattice in the figure. We also show the form of expansion in small ϵ for different groups of Y-functions. Notice that the momentum carrying Y-functions $Y_{a,0}$ are small in ϵ and enter the system only through the singularity at $u = 0$.

tions $Y_{a,0}(u)$ have a double pole for $u = 0$. This greatly simplifies their dynamics in the near-BPS regime – only the residue at this pole is important and gives a non-vanishing contribution. This residue is small for $\phi \approx \theta$, and thus the structure of the expansion of the cusp TBA system in our case is very similar to what happens in the small angles regime discussed in detail in [95, 91].

We found it convenient to use a small expansion parameter

$$\epsilon \equiv (\phi - \theta) \tan \phi_0, \tag{6.8}$$

where[28] we denote $\phi_0 = (\phi + \theta)/2$. As in the small angles case, it is sufficient to keep only the leading orders in the expansion of the Y-functions, which are

$$\begin{aligned} &Y_{a,1} = \mathcal{Y}_a \left[1 + \epsilon(\Omega_a - \mathcal{X}_a)\right], \; 1/Y_{1,s} = \mathcal{Y}_s \left[1 + \epsilon(\Omega_s + \mathcal{X}_s)\right], \\ &Y_{1,1} = -1 - 2\epsilon\Psi, \; 1/Y_{2,2} = -1 - 2\epsilon\Phi, \end{aligned} \tag{6.9}$$

while the residue of $Y_{a,0}$ reads

$$\lim_{u\to 0} \left(u^2 Y_{a,0}\right) = (\epsilon\, \mathbb{C}_a)^2 . \tag{6.10}$$

This expansion (except for the Ω_a functions which will not enter our equations) is also shown in Fig. 7.

[28] To shorten notation we will sometimes use θ instead of ϕ_0 in the text, on the understanding that equations containing θ are assumed to hold to the leading order in ϵ.

It is straightforward to plug these expansions into the cusp TBA system, and then simplify the equations a bit further using the same techniques as in the small angles case. We give more technical details in appendix B.2. The resulting set of Bremsstrahlung TBA equations reads:

$$\Phi - \Psi = \pi \mathbb{C}_a \hat{K}_a(u), \tag{6.11}$$

$$\Phi + \Psi = \mathbf{s} * \left[-2\frac{\mathcal{X}_2}{1+\mathcal{Y}_2} + \pi(\hat{K}_a^+ - \hat{K}_a^-)\mathbb{C}_a - \pi\delta(u)\mathbb{C}_1 \right], \tag{6.12}$$

$$\log Y_{1,m} = \mathbf{s} * I_{m,n} \log(1+Y_{1,n}) - \delta_{m,2}\mathbf{s}\hat{*}\left(\log\frac{\Phi}{\Psi} + \epsilon(\Phi-\Psi)\right) - \epsilon\pi\mathbf{s}\mathbb{C}_m, \tag{6.13}$$

$$\Delta_a = [\mathcal{R}^{(10)}_{ab} + \mathcal{B}^{(10)}_{a,b-2}]\hat{*}\log\frac{1+\mathcal{Y}_b}{1+A_b} + \mathcal{R}^{(10)}_{a1}\hat{*}\log\left(\frac{\Psi}{1/2}\right) - \mathcal{B}^{(10)}_{a1}\hat{*}\log\left(\frac{\Phi}{1/2}\right), \tag{6.14}$$

$$\mathbb{C}_a = (-1)^{a+1} a \frac{\sin a\theta}{\tan\theta}\left(\sqrt{1+\frac{a^2}{16g^2}} - \frac{a}{4g}\right)^{2+2L} F(a,g)e^{\Delta_a}, \tag{6.15}$$

where the kernels and conventions are the same as in [91] and are defined in appendix B.1 and in 1.4. The equation (6.13) for $Y_{1,m}$ should be understood to hold at orders $\mathcal{O}(\epsilon^0)$ and $\mathcal{O}(\epsilon^1)$ only. Notice that as in the small angles case the functions Ω_a from (6.9) have dropped out of the equations.

We see that our Bremsstrahlung TBA equations are almost the same as in [91]. However, importantly, the asymptotic condition at large real u is different:

$$1/Y_{1,m} \to \frac{\sin^2\theta}{\sin(m+1)\theta\sin(m-1)\theta}, \tag{6.16}$$

which should hold up to terms of order $\mathcal{O}(\epsilon)$ inclusive. Finally, the cusp anomalous dimension is determined by the double pole of momentum-carrying Y-functions:

$$\Gamma_L(g) = \epsilon\sum_{a=1}^{\infty}\frac{\mathbb{C}_a}{\sqrt{1+16g^2/a^2}}. \tag{6.17}$$

In the next section we will reduce this TBA system to a finite set of nonlinear equations.

6.2.2 From TBA to FiNLIE

Twisted ansatz for T-functions In this section we apply the same methods as in [91] to reduce the Bremsstrahlung TBA given above to a finite set of nonlinear integral equations (FiNLIE). The FiNLIE approach of [91] is very helpful to truly reveal the power of the spectral TBA [167, 136] [29]. For us it allows to reduce drastically the number of unknown functions, opening the way to the analytic solution of the problem in section 6.2.3.

[29] One can also use the Lüscher approximation to extract the first several orders like in [84, 168, 169].

Our main task is to reduce the infinite set of equations (6.13) for the functions $Y_{1,m}$. In order to do this we use its relation to the Y-system and Hirota equations in the horizontal right wing of the T-hook. Indeed, from the integral form of (6.13) and the analyticity of the kernels it is clear that $Y_{1,m}(u)$ are analytic and regular in the strip $|\text{Im } u| < \frac{m-1}{2}$. Then for $m > 2$ the equation (6.13) can be rewritten as the Y-system functional equation using the property (B.47):

$$\log\left(Y^+_{1,m}Y^-_{1,m}\right) = \log\left(1+Y_{1,m-1}\right)\left(1+Y_{1,m+1}\right). \tag{6.18}$$

This set of functional equations can be solved by switching to the so-called T-functions according to

$$1/Y_{1,m} = \frac{T^+_{1,m}T^-_{1,m}}{T_{1,m+1}T_{1,m-1}} - 1. \tag{6.19}$$

In terms of T-functions the Y-system equation becomes the Hirota equation in the horizontal strip, for which the general solution is known [94, 93] and involves only two unknown functions which we denote Q_1 and Q_2:

$$T_{1,s} = C \begin{vmatrix} Q_1^{[s]} & \bar{Q}_1^{[-s]} \\ Q_2^{[s]} & \bar{Q}_2^{[-s]} \end{vmatrix}. \tag{6.20}$$

In this way we are able to replace the infinite set of Y_m functions ($m = 2, 3, \dots$) by two functions $Q_1(u)$ and $Q_2(u)$[30]. Now the problem is reduced to finding an ansatz for them. The main requirement for this ansatz is that the $Y_{1,m}$ generated by (6.19), (6.20) should have the correct asymptotics at large real u given by (6.16). For small angles the asymptotics is $\frac{1}{m^2-1}$ and the corresponding ansatz for the Q-functions is known [91]. Here we present an ansatz which works also in a deformed case with nontrivial twists.

The ansatz also has to ensure the correct analytical properties of the Y-functions which are dictated by the integral equations (6.13). First of all, the $Y_{1,m}$ functions should be analytic inside the strip $|\text{Im } u| < \frac{m-1}{2}$ and even as functions of u. The term with $\delta_{m,2}$ in (6.13) can be reproduced if $Y_{1,2}(u)$ has branch cuts starting at $u = i/2 \pm 2g$ and $u = -i/2 \pm 2g$.

Our proposal for Q-functions meeting these requirements is:

$$Q_1 = \bar{Q}_1 = e^{+\theta(u-i\mathcal{G}(u))}, \tag{6.21}$$

$$Q_2 = \bar{Q}_2 = e^{-\theta(u-i\mathcal{G}(u))}, \tag{6.22}$$

[30] Later we will see that these functions are related to Q-functions of QSC

where $\mathcal{G}(u)$ should be a function with a branch cut on the real axis in order to satisfy the properties of T-functions listed above. Note that the asymptotics (6.16) of Y-functions is automatically satisfied for any $\mathcal{G}(u)$ decaying at infinity. Finally, as $T_{1,s}$ are even and real functions (to ensure the same properties for Y-functions), $\mathcal{G}(u)$ should be odd and imaginary.

With this choice of Q_1 and Q_2 we can calculate $T_{1,s}$ from (6.20) where for consistency with [91] in the small angle limit we choose $C = \frac{1}{2i\sin\theta}$

$$T_{1,s} = \frac{\sin(s - \mathcal{G}^{[s]} + \mathcal{G}^{[-s]})\theta}{\sin\theta}. \tag{6.23}$$

The discontinuity of the function $\mathcal{G}$ can be found from the equation analogous to (6.18) for $m = 2$ [94]. It reads

$$\frac{T_{1,1}^{+_+}T_{1,1}^{-_-}}{T_{1,1}^{+_-}T_{1,1}^{-_+}} = r, \quad \text{where} \quad r = \frac{1 + 1/Y_{2,2}}{1 + Y_{1,1}} \tag{6.24}$$

and we denoted

$$T^{+\pm}(u) = T(u + i/2 \pm i0) \qquad \text{and} \qquad T^{-\pm}(u) = T(u - i/2 \pm i0)\,. \tag{6.25}$$

More explicitly, using the formula (6.23) for $T_{1,1}$ one can write

$$r = \frac{\sin\left(1 - \mathcal{G}^{[+2]} + \mathcal{G} - \rho/2\right)\theta \sin\left(1 + \mathcal{G}^{[-2]} - \mathcal{G} - \rho/2\right)\theta}{\sin\left(1 - \mathcal{G}^{[+2]} + \mathcal{G} + \rho/2\right)\theta \sin\left(1 + \mathcal{G}^{[-2]} - \mathcal{G} + \rho/2\right)\theta}, \tag{6.26}$$

where $\mathcal{G}(u)$ is the average of $\mathcal{G}$ on both sides of the cut if u is on the cut, and it is equal to $\mathcal{G}(u) + \rho(u)/2$ away from the cut. This allows to deduce the discontinuity of the function $\mathcal{G}$ with one real Zhukovsky cut in terms of a combination (6.24) of "fermionic" Y-functions $Y_{1,1}$ and $Y_{2,2}$.

Finally, for small θ the combinations $Q_1 \pm Q_2$ obtained from our ansatz nicely match[31] (up to overall factors) the Q-functions in the small angles case [91], where $Q_1 = 1$ and $Q_2 = -iu - \mathcal{G}(u)$.

Expansion in the near-BPS case The ansatz presented in the previous subsection is valid for a general, not necessarily near-BPS situation. Here we will apply it to the case of $\phi \approx \theta$ (i.e. small ϵ) studied in this chapter.

As we have seen above, the solution for Y-functions is completely defined by a single function $\mathcal{G}(u)$, which we will call the resolvent. For the calculation we are doing here we

[31] As $T_{1,s}$ are given by a determinant, we are free to replace $Q_{1,2}$ by their linear combinations

only need to know $\mathcal{G}$ up to the linear in ϵ terms inclusive. Our proposal for the resolvent is

$$\mathcal{G}(u) = \frac{1}{2\pi i}\int_{-2g}^{2g} dv \frac{\rho(v)}{u-v} + \epsilon \sum_{a\neq 0} \frac{b_a}{u - ia/2}\,. \tag{6.27}$$

The first term creates a short branch cut[32] in $\mathcal{G}(u)$, which translates into the branch cuts of $\mathcal{Y}_m$. The discontinuity of the resolvent across this cut is the density ρ:

$$\rho(u) = G(u - i0) - G(u + i0). \tag{6.28}$$

The second term in (6.27) produces poles at $\pm i/2$ with residues proportional to ϵ in Y-functions, which account for the term $\epsilon\pi\mathfrak{s}\mathbb{C}_m$ in (6.13).

One can see that the properties of $T_{1,m}$ being real and even imposes the following constraints on the density and poles: ρ should be even and real as a function with a long cut, while $b_a = b_{-a}$ and $b_a = -b_a^*$.

Most of the equations in this chapter are already expanded in ϵ, so it is convenient to introduce expanded to the leading order versions of the quantities above. The leading order part of the resolvent is[33]

$$G(u) = \frac{1}{2\pi i}\int_{-2g}^{2g} dv \frac{\rho(v)}{u-v}. \tag{6.29}$$

We also introduce the leading order T-functions $\mathcal{T}_m$ related to the leading order Y-functions as

$$\mathcal{Y}_m = \frac{\mathcal{T}_m^+\mathcal{T}_m^-}{\mathcal{T}_{m+1}\mathcal{T}_{m-1}} - 1. \tag{6.30}$$

Explicitly, the leading order part of (6.31) gives

$$\mathcal{T}_s = \frac{\sin\left(s - G^{[s]} + G^{[-s]}\right)\phi_0}{\sin\phi_0}. \tag{6.31}$$

Final reduction to FiNLIE We now use the ansatz discussed above and finalize the reduction of the initial Bremsstrahlung TBA system to a finite set of equations. The remaining steps in the derivation are analogous to [91] so we will be brief here (more details are given in appendix B.3).

The first two TBA equations (6.11), (6.12) contain the "fermionic" functions Φ and Ψ in the left hand side. In order to deal with them, notice that after plugging the expansion

[32] i.e. a cut from $-2g$ to $2g$.

[33] The density ρ contains both the leading order in ϵ part and the linear correction, however, in this chapter we will never need to deal with this correction. Hence, we will denote the full density and its leading order part by the same letter ρ hoping that this will not cause any confusion.

(6.9) of Y-functions into r defined by (6.24) one gets $r = \Phi/\Psi$. Thus the equation (6.24) at the leading order becomes

$$\frac{\Phi}{\Psi} = \frac{\mathcal{T}_1^{++}\mathcal{T}_1^{--}}{\mathcal{T}_1^{+-}\mathcal{T}_1^{-+}}, \tag{6.32}$$

where the notation analogous to (6.25) is used. The equation (6.32) allows us to introduce another quantity which will play an important role in the FiNLIE:

$$\eta \equiv \frac{\Psi\mathcal{T}_2}{\mathcal{T}_1^{-+}\mathcal{T}_1^{+-}} = \frac{\Phi\mathcal{T}_2}{\mathcal{T}_1^{--}\mathcal{T}_1^{++}}. \tag{6.33}$$

Using this definition and the explicit form of $\mathcal{T}_m$ (6.31) we are able to express Ψ and Φ in terms of η, ρ and G. Then we plug them into the first two TBA equations and get the first two FiNLIE equations (6.35), (6.36) which are given below.

To get the third FiNLIE equation we plug the explicit form of the $\mathcal{Y}_m$ functions expressed through $\mathcal{T}_m$ using (6.30) and (6.23) into the equation for Δ_a (equation (6.14)). This equation then greatly simplifies (for a detailed derivation see appendix B.3) and we find

$$\Delta_a = \tilde{K}_a \hat{*} \log\eta + \log\frac{\mathcal{T}_a}{\sin a\theta \cot\theta}\bigg|_{u=0}. \tag{6.34}$$

Combining this with the last equation of Bremsstrahlung TBA (6.15) we obtain (6.37).

In summary, the FiNLIE equations read:

$$\eta\frac{\sin\theta\rho}{\sin\theta} = -\sum_a \pi\mathbb{C}_a\hat{K}_a, \tag{6.35}$$

$$\eta\frac{\cos\theta\rho\cos(2-G^+ + G^-)\theta - \cos(2G - G^+ - G^-)\theta}{\sin\theta\sin(2-G^+ + G^-)\theta} =$$

$$= \mathbf{s} * \left[-2\frac{\mathcal{X}_2}{1+\mathcal{Y}_2} + \pi(\hat{K}_a^+ - \hat{K}_a^-)\mathbb{C}_a - \pi\delta(u)\mathbb{C}_1\right], \tag{6.36}$$

$$\mathbb{C}_a = (-1)^a a\mathcal{T}_a(0)\left(\sqrt{1+\frac{a^2}{16g^2}} - \frac{a}{4g}\right)^{2+2L}\exp\left[\tilde{K}_a\hat{*}\log\left(\eta\frac{\sinh 2\pi u}{2\pi u}\right)\right]. \tag{6.37}$$

Here $G(u)$ is the average of the resolvent on both sides of the cut if u is on the cut, and it is equal to $G(u) + \rho(u)/2$ away from the cut. Other notation and the kernels can be found in appendix B.1.

Our FiNLIE is a set of equations for functions $\rho(u)$, $\eta(u)$ and the coefficients $\mathbb{C}_a$ (we remind that G is obtained from ρ according to (6.29)). As written this is a closed system of equations up to one subtlety. Namely, the right hand side of the second equation, (6.36), also includes an unknown function $\mathcal{X}_2$ which should contain the linear in ϵ correction to ρ.

This correction obeys an equation which is straightforward to derive by the same methods as in [91][34]. However, in fact we will not need this equation in the following, so we do not write it. It is replaced by a certain simple analyticity condition described in the next section. This condition is a simple consequence of QSC formulation, which is, however, very hard to prove directly from TBA.

Finally, the FiNLIE should be also supplemented by a relation which determines the residues of the resolvent at $u = ia/2$, i.e. the coefficients b_a which we introduced in (6.27). To derive it we compare residues at $ia/2$ of both sides of the third equation (6.13) in the Bremsstrahlung TBA system. This gives a recursion relation of the form

$$q_a b_{a-2} - (q_a + p_a) b_a + p_a b_{a+2} = \mathbb{C}_a, \tag{6.38}$$

where q_a and p_a depend on the values of the resolvent at the points $ia/2$, $i(a \pm 2)/2$, and are defined in appendix B.3 in which the derivation of (6.38) is discussed.

In the next section we will construct an analytic solution of this FiNLIE, leading to an explicit expression for the energy.

6.2.3 Analytical ansatz for FiNLE

In the previous sections we presented the FiNLIE - a system of equations for $\mathbb{C}_a, \rho, \eta$. Following the spirit of [91], in order to solve it we will analyse the analytical properties of η and ρ as functions in the whole complex plane. We will parametrize these functions in terms of auxiliary Bethe roots, for which we will obtain a set of Bethe equations. Then we solve them using Baxter equation techniques and obtain the result for the anomalous dimension $\Gamma_L(g)$.

Analytical ansatz for η and ρ In this section we will explore the analytical properties of ρ and η. Although one would prefer to derive them starting from the FiNLIE, there seems to be no easy way to do this. Instead we make a conjecture that the key quantities entering the FiNLIE do not have infinitely many Zhukovsky cuts. In section 6.3 we will see that this conjecture follows almost trivially from the QSC formulation. Since QSC itself can be derived from TBA, this can be seen as an indirect derivation from TBA. In this way we also justify similar assumptions made in [91] without a proof.

The main assumption is that $\eta(u)$ has simple poles at $ia/2$ for $a \in \mathbb{Z} \setminus \{0\}$, and $\eta^2(u)$ is a meromorphic function in the whole complex plane. Then, taking into account that η

[34] see eq. (**F3**) in section 3.5 of [91]

is even we can write the following representation

$$\eta^2(u) = (\cos\theta)^2 \prod_{k\neq 0} \frac{u^2 - u_k^2}{u^2 + k^2/4}, \tag{6.39}$$

where the product goes from $-\infty$ to ∞. The prefactor $(\cos\theta)^2$ comes from the asymptotics

$$\eta(u) \to \cos\theta, \ u \to \infty, \tag{6.40}$$

which is easily seen from the definition (6.33).

In [91], where the case $\theta = 0$ was considered, η was a meromorphic function with poles at $ia/2$ for nonzero integer a. In our case η is not meromorphic, but η^2 is. The analyticity of η in the $\theta = 0$ limit is recovered as pairs of zeros u_k collide and produce a double zero. We enumerate these zeros u_k in such a way that the colliding pairs are u_k and $-u_{-k}$. For large k the value of the factors under the product in (6.39) should approach 1, meaning that the roots accumulate close to the half-integer points on the imaginary axis:

$$\begin{aligned} u_k &\to ik/2, \\ -u_{-k} &\to ik/2, \ k \to +\infty. \end{aligned} \tag{6.41}$$

Thus η has an infinite number of square-root cuts, each going between u_k and $-u_{-k}$, located close to $ik/2$. We will refer to these cuts as S-cuts, and they are shown in Fig. 6.2.3.

Now let us explore the properties of the density ρ. Every kernel $\hat{K}_a$ in the right hand side of the first FiNLIE equation (6.35) is proportional to $\sqrt{u^2 - 4g^2}$, so the whole expression has a cut from $-2g$ to $2g$, which we will call the Z-cut. First, let us note that ρ is defined as a discontinuity of the resolvent G and as such it simply changes its sign when passing the Z-cut and so the Z-cut is already taken care of by the $\sin\theta\rho$ multiplier.

It only remains to understand the behavior of ρ when we go through an S-cut. As the combination $\eta\sin\theta\rho$ has no S-cuts due to (6.35) and since η does have infinitely many S-cuts, it must be that $\sin\theta\rho$ changes its sign simultaneously with η when we go through any S-cut leaving the whole expression unchanged. Next, let us show that $\cos\theta\rho$ also changes sign on an S-cut. Indeed, in the second FiNLIE equation (6.36) the right hand side does not have any S-cuts and the left hand side can be expanded into a sum of terms proportional to $\eta\sin\theta\rho$ and $\eta\cos\theta\rho$. Since from the first FiNLIE equation (6.35) we know that $\eta\sin\theta\rho$ does not branch on an S-cut, the same should be true for $\eta\cos\theta\rho$. Again, since η changes its sign on S-cuts, the same should hold for $\cos\theta\rho$.

This means that on the Z-cut ρ changes its sign and on an S-cut it is shifted as

$$\rho \to \rho + \pi/\theta. \tag{6.42}$$

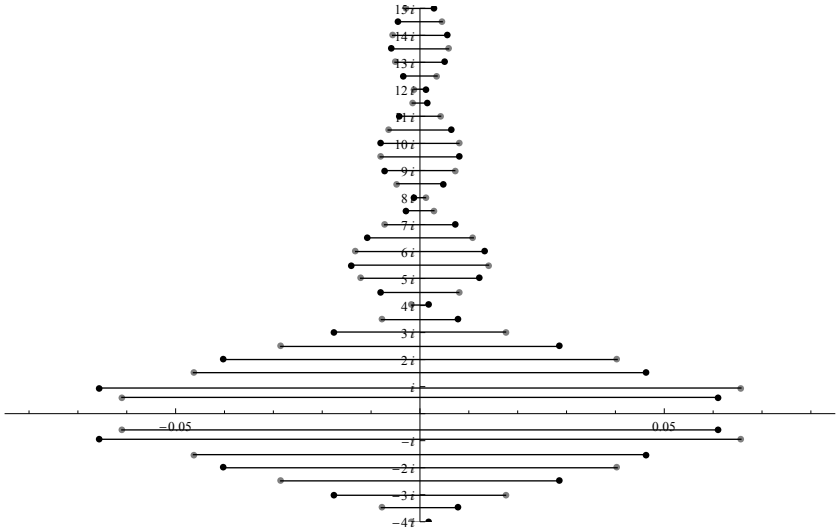

Figure 8: **The S-cuts of $\eta(u)$ and $\rho(u)$** The function $\eta(u)$ has an infinite number of square root cuts, which we call S-cuts, each connecting u_k (black dots) to $-u_{-k}$ (grey dots). For $\rho(u)$ these cuts are logarithmic. The full set of branch points consists of $\{u_k\}$ together with $\{-u_k\}$.

The transformation properties of different quantities with respect to transitions through Z- and S-cuts can be summarized into the following table:

	η	ρ	$\cos\theta\rho$	$\sin\theta\rho$
S-cut	$-\eta$	$\rho+\pi/\theta$	$-\cos\theta\rho$	$-\sin\theta\rho$
Z-cut	η	$-\rho$	$\cos\theta\rho$	$-\sin\theta\rho$

Having understood the transformation properties of ρ on both types of cuts, let us try and build out of ρ a quantity which would be meromorphic. First of all, to this end it is convenient to consider ρ as a function of Zhukovsky variable $x(u)$ defined in (3.17). It is easy to see that Zhukovsky transformation resolves the Z-cut: two sheets of the Riemann surface connected by the cut in variable u become the interior and the exterior of the unit circle in variable x. Thus as a function of x the density has only S-cuts. Moreover, since on an S-cut ρ transforms to $\rho+\pi/\theta$, the combination $e^{2i\theta\rho(x)}$ is meromorphic in $\mathbb{C}\setminus\{0\}$. Going under the Z-cut in variable u is equivalent to $x\to 1/x$ transformation in variable x, hence the property of ρ changing sign on the Z-cut now reads

$$e^{2i\theta\rho(x)} = 1/e^{2i\theta\rho(1/x)}. \tag{6.43}$$

Being meromorphic, $e^{2i\theta\rho(x)}$ is completely characterized by its zeros and poles (and asymptotics). Let us call the zeros outside the unit circle $x_{k,+}$ and the zeros inside it

$1/x_{k,-}$. Then from (6.43) one can see that the poles of $e^{2i\theta\rho(x)}$ are $1/x_{k,+}$ and $x_{k,-}$. These poles and zeros are shown in Fig. 9.

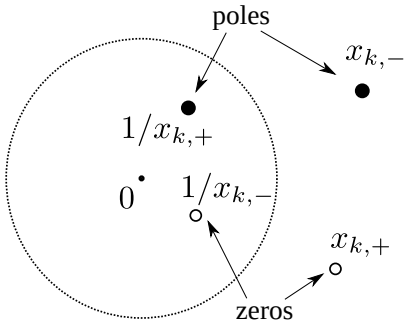

Figure 9: **The singularities of ρ.** Poles and zeros of $e^{2i\theta\rho(x)}$ inside and outside the unit circle. The density ρ has logarithmic singularities at these points, which are in fact images of $\pm u_k$ under the Zhukovsky map.

It is convenient to introduce bookkeeping functions which encode $x_{k,\pm}$

$$\mathbf{Q}_{\pm}(x) = \prod_{k\neq 0} \frac{x_{k,\pm} - x}{x_{k,\pm}} \,. \tag{6.44}$$

These functions are analogous to functions $R_{A|I}$ appearing in the derivation of ABA in section 4.5. We denote their analytical continuation under the Z-cut by adding a tilde, i.e. $\tilde{\mathbf{Q}}_{\pm}(x) = \mathbf{Q}_{\pm}(1/x)$. Knowing the zeros and the poles of $e^{2i\theta\rho(x)}$ and taking into account that $\rho \to 0$ as $x \to \infty$, we can reconstruct it uniquely as

$$e^{2i\theta\rho(x)} = \frac{\mathbf{Q}_{+}\tilde{\mathbf{Q}}_{-}}{\mathbf{Q}_{-}\tilde{\mathbf{Q}}_{+}}. \tag{6.45}$$

Using this representation for ρ we can fix η completely. Indeed, as discussed above the left hand side of the first FiNLIE equation (6.35) does not have S-cuts. On the other hand, we can use (6.45) to write it in terms of $\mathbf{Q}$ as

$$\eta \sin\theta\rho = \frac{\eta}{2i} \frac{\tilde{\mathbf{Q}}_{-}\mathbf{Q}_{+} - \tilde{\mathbf{Q}}_{+}\mathbf{Q}_{-}}{\sqrt{\mathbf{Q}_{-}\tilde{\mathbf{Q}}_{-}\mathbf{Q}_{+}\tilde{\mathbf{Q}}_{+}}}. \tag{6.46}$$

Thus the square root in the denominator of (6.46) should completely cancel the numerator of η which is equal to $\prod\limits_{k\neq 0}\sqrt{u^2-u_k^2}$. The asymptotics of the numerator should be $\sinh 2\pi u$, because $\eta(u)$ is finite at infinity. Thus the zeros of $\sqrt{\mathbf{Q}_{-}\tilde{\mathbf{Q}}_{-}\mathbf{Q}_{+}\tilde{\mathbf{Q}}_{+}}$ should approach the zeros of $\sinh 2\pi u$ and there is a way to enumerate $x_{k,+}$ so that $x_{k,+} \to ik/2$ at large k. Since ρ is odd[35], the zeros of the numerator and the denominator of (6.45) should map onto each other as sets under $x \to -x$. In particular, considering only the zeros outside

[35] as a function with a short Z-cut

the unit circle, the zeros of $\mathbf{Q}_+$ map onto zeros of $\mathbf{Q}_-$. Then it is possible to enumerate the zeros of $\mathbf{Q}_-$ (i.e. $x_{k,-}$) so that $x_{k,+} = -x_{-k,-}$. Notice that now $u(x_{k,+}),\ u(x_{-k,-}) \to ik/2$ as $k \to \infty$. Introducing v_k such that $x(v_k) = x_{k,+}$, we can write

$$\mathbf{Q}_+\mathbf{Q}_-\tilde{\mathbf{Q}}_+\tilde{\mathbf{Q}}_- = \prod_{k\neq 0} \frac{x - x_{k,+}}{x_{k,+}} \frac{x - x_{-k,-}}{x_{-k,-}} \left(1 - \frac{1}{x x_{k,+}}\right) \left(1 - \frac{1}{x x_{-k,-}}\right) = \prod_{k\neq 0} \frac{u^2 - v_k^2}{-g^2 x_{k,+}^2} \tag{6.47}$$

Comparing this product with the product in the numerator of η^2 we see that u_k and v_k coincide as sets. Up to relabelling we can set $v_k = u_k$, thus establishing the relation

$$u_k/g = x_{k,+} + 1/x_{k,+} = -x_{-k,-} - 1/x_{-k,-}. \tag{6.48}$$

Finally, we notice that the formula (6.45) allows us to find the resolvent in terms of $\mathbf{Q}_\pm$ without performing the integration which is prescribed by (6.29). Indeed, suppose we define a function $G(u)$ as $e^{i\theta G(u)} = \sqrt{\tilde{\mathbf{Q}}_+ (x(u)) / \tilde{\mathbf{Q}}_- (x(u))}$. It decays at infinity, does not have poles on the main sheet ($|x| > 1$) and has a Z-cut with the discontinuity ρ, the same as the resolvent. Hence by Liouville's theorem it coincides with the resolvent.

Let us summarize the results of this section:

$$e^{i\theta\rho} = \sqrt{\frac{\mathbf{Q}_+\tilde{\mathbf{Q}}_-}{\mathbf{Q}_-\tilde{\mathbf{Q}}_+}}, \quad \eta = \cos\theta \frac{\sqrt{\mathbf{Q}_+\mathbf{Q}_-\tilde{\mathbf{Q}}_+\tilde{\mathbf{Q}}_-}}{\tilde{C}\frac{\sinh 2\pi u}{2\pi u}}\,, \tag{6.49}$$

$$e^{i\theta G} = \sqrt{\tilde{\mathbf{Q}}_+/\tilde{\mathbf{Q}}_-}\,. \tag{6.50}$$

In order to rewrite the ansatz for η (6.39) in the form above we used the identity

$$\frac{\sinh 2\pi u}{2\pi u} = \prod_{k=1}^{\infty} \frac{u^2 + k^2/4}{k^2/4} \tag{6.51}$$

and we also introduced

$$\tilde{C} = \prod_{k=1}^{\infty} \frac{-k^2/4}{g^2 x_{k,+} x_{k,-}}. \tag{6.52}$$

We managed to write all the key quantities in terms of an infinite number of roots u_k. By plugging these expressions into the FiNLIE equations in the next two sections we will find a closed set of Bethe-like equations for these roots.

Fixing residues of η Here we will find a relation for the residues of η and as a result establish an important relation between values of ρ and G at half-integer points on the imaginary axis which will be used in the next section to derive an auxiliary Bethe-like

equation. Here we only outline the main steps, with more details given in appendix B.4 [36].

First, we will use the second FiNLIE equation (6.36), i.e.

$$\eta\frac{\cos\theta\rho\cos\left(2-G^{+}+G^{-}\right)\theta-\cos\left(2G-G^{+}-G^{-}\right)\theta}{\sin\theta\sin\left(2-G^{+}+G^{-}\right)\theta}= \tag{6.53}$$
$$=\mathbf{s}*\left[-2\frac{\mathcal{X}_2}{1+\mathcal{Y}_2}+\pi(\hat{K}_a^{+}-\hat{K}_a^{-})\mathbb{C}_a-\pi\delta(u)\mathbb{C}_1\right],$$

to compute the residue of $\eta\cos\theta\rho$ at $ia/2$. According to our assumptions about the analytical properties of η, both sides of this equation have poles at $ia/2$. Using the identity (B.47) we can get rid of the convolution with $\mathbf{s}$. Then the residues at the pole on both sides can be expressed through $\mathbb{C}_a$, $G(ia/2)$ and the residues of $\eta\cos\theta\rho$ and $\mathcal{X}_a$. Due to the presence of $\mathcal{X}_2$, the residue of the right hand side appears to depend on b_a (see the definition of G, where the poles with residues b_a appear in the first order in ϵ). However, as in [91], the dependence on b_a can be completely eliminated by taking into account the recursion relation (6.38). Thus we can regard the second FiNLIE equation (6.36) as an equation for the residues of $\eta\cos\theta\rho$ which produces as shown in appendix B.4:

$$\operatorname*{Res}_{u=ia/2}(\eta\cos\theta\rho)=\frac{1}{2i}\mathbb{C}_a\frac{\sin\theta}{\tan\left(2G(ia/2)\theta-a\theta\right)}. \tag{6.54}$$

In addition, let us make use of the first FiNLIE equation (6.35),

$$\eta\frac{\sin\theta\rho}{\sin\theta}=-\sum_a\pi\mathbb{C}_a\hat{K}_a. \tag{6.55}$$

Equating the residues of the poles at $ia/2$ on both sides gives us at once

$$\operatorname*{Res}_{u=ia/2}(\eta\sin\theta\rho)=-\frac{1}{2i}\mathbb{C}_a\sin\theta. \tag{6.56}$$

The equations (6.54) and (6.56) that we have just derived allow us to relate ρ and G at $u=ia/2$. Since we assume that ρ is regular at $ia/2$ and the pole comes from η, from these two equations it is easy to see that

$$\tan\theta\rho(ia/2)=\tan\left(a\theta-2G(ia/2)\theta\right), \tag{6.57}$$

leading to

$$\theta\rho(ia/2)=a\theta-2\theta G(ia/2)+\pi n,\quad n\in\mathbb{Z}\,. \tag{6.58}$$

We can also write this equation as[37]

$$\exp\left[i\theta\rho+2i\theta G(ia/2)-ia\theta\right]=1\,. \tag{6.59}$$

[36] the calculation is analogous to that done in sections 3.2.1 and 4.2 of [91]

[37] For odd n in (6.58) we would get minus in right hand side of (6.59), but this is incompatible with the small θ limit (see equation (103) in [91]).

This relation already constrains the set of our parameters u_k and will be very useful in the next section.

Effective Bethe equations Above we have parametrized ρ and η in terms of two families of roots $x_{k,\pm}$. Here we will show that these roots satisfy a set of Bethe-like equations, which will be solved in the subsequent sections. In [91] the effective Bethe equation was derived by substituting the ansatz for η into the FiNLIE equation for $\mathbb{C}_a$. In our case this is equation (6.37) which reads

$$\mathbb{C}_a = (-1)^a a \mathcal{T}_a(0) \left(\sqrt{1 + \frac{a^2}{16g^2}} - \frac{a}{4g} \right)^{2+2L} \exp\left[\tilde{K}_a \hat{*} \log\left(\eta \frac{\sinh 2\pi u}{2\pi u} \right) \right]. \tag{6.60}$$

Plugging into this equation our ansatz for η (6.49) and following the same steps as in [91], we get

$$1 = \left(\frac{i}{y_a} \right)^{2L+2} \sqrt{\frac{\tilde{\mathbf{Q}}_+ \tilde{\mathbf{Q}}_-}{\mathbf{Q}_+ \mathbf{Q}_-}} \quad , \quad \text{with } y_a \equiv x(ia/2). \tag{6.61}$$

In the $\theta = 0$ limit $\mathbf{Q}_+ = \mathbf{Q}_-$ and this equation coincides with the effective Bethe equation in [91]. In addition to (6.59) this equation allows to fix completely all the roots x_k, thus providing the full solution to the problem.

Indeed, expressing ρ and G in (6.59) through $\mathbf{Q}_\pm$ by means of (6.49) and (6.50) we obtain

$$1 = e^{-2u\theta} \sqrt{\frac{\mathbf{Q}_+ \tilde{\mathbf{Q}}_+}{\mathbf{Q}_- \tilde{\mathbf{Q}}_-}} \quad , \quad u = ia/2. \tag{6.62}$$

Notice that this equation contains θ (as opposed to (6.61)) and tells us how the two families of roots are separated. In the $\theta = 0$ limit it has a trivial solution $\mathbf{Q}_+ = \mathbf{Q}_-$, causing the roots $x_{k,+}$ and $-x_{-k,-}$ to collide and producing double zeros in η^2, thus making η meromorphic.

Multiplying (6.62) and (6.61) we get rid of the square root and finally obtain the following auxiliary Bethe equations:

$$\boxed{1 = e^{-ia\theta} \left(\frac{i}{y_a} \right)^{2L+2} \frac{\tilde{\mathbf{Q}}_+(y_a)}{\mathbf{Q}_-(y_a)}.} \tag{6.63}$$

We remind that y_a stands for $x(ia/2)$, $a \in \mathbb{Z}$. From this equation we can find the Baxter polynomials $\mathbf{Q}_\pm$. For that in the next section we will use the Baxter equation.

Baxter equations At this point everything we want to know about the system is parametrized in terms of two infinite series of roots $x_{k,\pm}$. These roots are governed by the effective Bethe equations (6.63), and to solve them we will apply Baxter equation techniques, similarly to [91].

Namely, let us construct the function

$$\mathbf{T}(x) = e^{+2g\theta x} x^{L+1} \mathbf{Q}_-(x) + (-1)^L \frac{e^{-2g\theta/x}}{x^{L+1}} \tilde{\mathbf{Q}}_+(x). \tag{6.64}$$

which encodes the whole set of auxiliary Bethe roots x_k. We will call $\mathbf{T}(x)$ the Baxter function. Due to the Bethe equations (6.63) we have $\mathbf{T}(y_a) = 0$. In addition, the relation $\mathbf{Q}_\pm(-x) = \mathbf{Q}_\mp(x)$ means that $\mathbf{T}$ has a symmetry

$$\mathbf{T}(-1/x) = -\mathbf{T}(x) \tag{6.65}$$

Let us now clarify the asymptotics of $\mathbf{T}(x)$. It is easy to see from the definitions (6.44) and (6.33) that $\tilde{\mathbf{Q}}_\pm \to 1$ and $\eta \to \cos\theta$ at large x. Moreover, since $\mathbf{Q}_\pm(-x) = \mathbf{Q}_\mp(x)$, the asymptotics of $\mathbf{Q}_+$ and $\mathbf{Q}_-$ at large u are the same and from (6.49) we get

$$\mathbf{Q}_\pm \sim \tilde{C} \frac{\sinh 2\pi u}{2\pi u}, \ u \to +\infty \, . \tag{6.66}$$

Therefore the second term in (6.64) is suppressed[38] compared to the first one and the asymptotics of the whole expression at large x is $\mathbf{T}(x) \sim x^L e^{2g(\pi+\theta)x}$. Then from (6.65) we can find the asymptotics of $\mathbf{T}(x)$ at $x \to 0$, and combining all these analytical properties together we can fix it uniquely to be

$$\mathbf{T}(x) = \sinh(2\pi u) e^{2g\theta(x-1/x)} P_L(x), \tag{6.67}$$

where $P_L(x)$ should be a rational function with behavior $\sim x^L$ at infinity. Since $\mathbf{T}(x)$ should not have singularities apart from $x = 0$ and $x = \infty$, the function P_L must be a polynomial in x and $1/x$. Moreover, (6.65) means that $P_L(-1/x) = -P_L(x)$ and hence we can write

$$P_L(x) = C_1 x^L + C_2 x^{L-1} \cdots + (-1)^L C_1 x^{-L}. \tag{6.68}$$

To find $\mathbf{T}(x)$ explicitly it only remains to determine the coefficients C_i. This is straightforward to do by imposing the condition that the right hand side of (6.67) does not contain powers of x from $-L$ to L in its Laurent expansion (as follows from (6.64)) which must be the case since $\mathbf{Q}_-$ is regular at the origin.

The energy Before proceeding with fixing completely the Baxter function $\mathbf{T}(x)$, let us explain how to extract from it the value of the energy. To do this we will use the first FINLIE equation (6.35). At large u each of the kernels $\hat{K}_a$ in its right hand side decays as

[38] Strictly speaking this is so for $-\pi < \theta < \pi$. Using periodicity in θ we can always restrict ourselves to this range.

$1/u$, so the whole sum is proportional to the sum in the definition of $\Gamma_L(g)$ (6.17). Hence we get

$$\Gamma_L(g) = -i(\phi - \theta)\theta \lim_{u\to\infty} u\rho(u). \tag{6.69}$$

The density is defined through $\mathbf{Q}_\pm$ in (6.49), so we can find the asymptotics of $\mathbf{Q}_\pm$ from (6.67), plug them into (6.49) and finally get

$$\Gamma_L(g) = -2(\phi - \theta)g\left[-\frac{C_2}{2C_1} + \frac{c}{2} + g\theta\right], \tag{6.70}$$

where c is the leading expansion coefficient of $\mathbf{Q}_\pm$:

$$\mathbf{Q}_\pm(x) \simeq 1 \mp cx \ \ , \ \ x \to 0. \tag{6.71}$$

Notice that the coefficients C_1, C_2 are also encoded in $\mathbf{Q}_\pm$: from (6.64), (6.67) we find

$$\mathbf{Q}_\pm(x) \simeq \sinh(2\pi u)\left[\frac{C_1}{x} \pm \frac{2g\theta C_1}{x^2} \mp \frac{C_2}{x^2} + \dots\right] \ \ , \ \ x \to \infty\,. \tag{6.72}$$

Now we have all the necessary tools to obtain the energy explicitly.

The $L = 0$ case Let us first discuss the $L = 0$ case, because it is technically simpler. The function $P_L(x)$ from (6.67) is then just a constant,

$$P_L(x) = C_1. \tag{6.73}$$

To fix it we need to know the expansion of (6.67) in powers of x. Using that the exponent of $x + 1/x$ is a generating function for the modified Bessel functions of the first kind, $e^{2\pi g(x+1/x)} = \sum_{n=-\infty}^{\infty} I_n(4\pi g)x^n$, we get the expansion

$$\sinh\left(2\pi g(x + 1/x)\right) e^{2g\theta(x-1/x)} = \sum_{n=-\infty}^{+\infty} I_n^\theta x^n, \tag{6.74}$$

where I_n^θ are the "deformed" Bessel functions

$$I_n^\theta = \frac{1}{2} I_n\left(4\pi g\sqrt{1 - \frac{\theta^2}{\pi^2}}\right)\left[\left(\sqrt{\frac{\pi+\theta}{\pi-\theta}}\right)^n - (-1)^n\left(\sqrt{\frac{\pi-\theta}{\pi+\theta}}\right)^n\right]. \tag{6.75}$$

Below we will omit the argument of I_n, always assuming it to be the same as in (6.75).

The expansion (6.74) allows us to write the Baxter function (6.67) as

$$\mathbf{T}(x) = e^{+2g\theta x} x\mathbf{Q}_-(x) + \frac{e^{-2g\theta/x}}{x}\mathbf{Q}_+(1/x) = C_1 \sum_{n=-\infty}^{+\infty} I_n^\theta x^n.$$

We can now find $\mathbf{Q}_-$ as the regular part of the Laurent expansion of $\mathbf{T}$:

$$\mathbf{Q}_-(x) = C_1 \frac{e^{-2g\theta x}}{x} \sum_{n=1}^{+\infty} I_n^\theta x^n. \tag{6.76}$$

From (6.44) we see that $\mathbf{Q}_{\pm}(0) = 1$, so setting $x = 0$ in the last equation we fix C_1 as

$$C_1 = \frac{\sqrt{\pi^2 - \theta^2}}{\pi I_1}. \tag{6.77}$$

Since $L = 0$ we have $C_2 = 0$, while the coefficient c in (6.71) is read off from (6.76):

$$c \;\; = \;\; -2g\theta + \frac{2\theta}{\sqrt{\pi^2 - \theta^2}} \frac{I_2}{I_1} \, . \tag{6.78}$$

Then from (6.70) we get the energy

$$\Gamma_L(g) = -2(\phi - \theta) \frac{\theta g}{\sqrt{\pi^2 - \theta^2}} \frac{I_2\left(\tilde{\lambda}^{1/2}\right)}{I_1\left(\tilde{\lambda}^{1/2}\right)}, \; \tilde{\lambda} = (4\pi g)^2 \left(1 - \tfrac{\theta^2}{\pi^2}\right). \tag{6.79}$$

Remarkably, this is precisely the localization result of [151]! This is the first successful check of our construction.

Non-zero L Let us now find the explicit expression for the energy at any L.

First we need to compute the coefficients C_k, using the equation (6.67). From (6.64) we see that the left hand side of (6.67) should not contain terms with powers of x from $-L$ to L, and also the coefficient of the x^{L+1} term should be 1. After we expand the right hand side according to (6.74) this condition generates $2L+1$ equations for $2L+1$ variables C_k:

$$\begin{cases} \sum\limits_{k=-L}^{L} I^{\theta}_{m-k} C_{k+L+1} = 0, \;\; m = -L+1 \ldots L, \\ \sum\limits_{k=-L}^{L} I^{\theta}_{m-k} C_{k+L+1} = 1, \;\; m = L+1. \end{cases} \tag{6.80}$$

This linear system can be formulated in matrix form:

$$(\mathcal{M}_{2L})_{ik} C_{k+L+1} = \delta_{i,L+1}, \tag{6.81}$$

where

$$\mathcal{M}_N = \begin{pmatrix} I^{\theta}_1 & I^{\theta}_0 & \cdots & I^{\theta}_{2-N} & I^{\theta}_{1-N} \\ I^{\theta}_2 & I^{\theta}_1 & \cdots & I^{\theta}_{3-N} & I^{\theta}_{2-N} \\ \vdots & \vdots & \ddots & \vdots & \vdots \\ I^{\theta}_N & I^{\theta}_{N-1} & \cdots & I^{\theta}_1 & I^{\theta}_0 \\ I^{\theta}_{N+1} & I^{\theta}_N & \cdots & I^{\theta}_2 & I^{\theta}_1 \end{pmatrix}. \tag{6.82}$$

By Cramer's rule we obtain the solution

$$C_k = \frac{\det \mathcal{M}^{(2L+1,k)}_{2L}}{\det \mathcal{M}_{2L}}, \tag{6.83}$$

where $\mathcal{M}_N^{(a,b)}$ is the matrix obtained from $\mathcal{M}_N$ by deleting a^{th} row and b^{th} column. Plugging these coefficients into $P_L(x)$ we can combine it into a determinant again:

$$P_L(x) = \frac{1}{\det \mathcal{M}_{2L}} \begin{vmatrix} I_1^\theta & I_0^\theta & \cdots & I_{2-2L}^\theta & I_{1-2L}^\theta \\ I_2^\theta & I_1^\theta & \cdots & I_{3-2L}^\theta & I_{2-2L}^\theta \\ \vdots & \vdots & \ddots & \vdots & \vdots \\ I_{2L}^\theta & I_{2L-1}^\theta & \cdots & I_1^\theta & I_0^\theta \\ x^{-L} & x^{1-L} & \cdots & x^{L-1} & x^L \end{vmatrix} . \tag{6.84}$$

Notice that now from (6.67) we have the Baxter function $\mathbf{T}(x)$ in a fully explicit form. In particular, one can easily find the functions $\mathbf{Q}_\pm$ encoding the Bethe roots. Namely, $\mathbf{Q}_-$ is the regular part of the Laurent expansion of $\mathbf{T}(x)$,

$$\mathbf{Q}_-(x) = x^{-L-1} e^{-2g\theta x} \left[\mathbf{T}(x)\right]_+ , \tag{6.85}$$

while $\mathbf{Q}_+(x) = \mathbf{Q}_-(-x)$.

It remains to find c — the coefficient of expansion of $\mathbf{Q}_\pm$ which enters the expression for $\Gamma_L(g)$. Consider expansion of (6.67) around $x = 0$, taking into account the definition of $\mathbf{T}$ (6.64):

$$(1+2g\theta x+\dots)x^{L+1}(1+cx+\dots)+\text{negative powers} = \sum_{n=-\infty}^{+\infty} I_n^\theta x^n \sum_{k=-L}^{L} C_{k+L+1} x^k \tag{6.86}$$

Equating the coefficients of x^L on both sides we get

$$2g\theta + c = \sum_{k=-L}^{L} I_{L+2-k} C_{k+L+1} . \tag{6.87}$$

Plugging the solution for C_k into the right hand side of the last equation we see that it combines nicely into a ratio of two determinants, resulting in

$$c = -2g\theta + \frac{\det \mathcal{M}_{2L+1}^{(2L+1,2L+2)}}{\det \mathcal{M}_{2L}} . \tag{6.88}$$

The determinants $\det \mathcal{M}_N^{(a,b)}$ satisfy a number of useful identities which we describe in appendix B.6. They allow us to bring the expressions for c and C_1/C_2 to the following form:

$$c = -2g\theta + \frac{\det \mathcal{M}_{2L+1}^{(1,2)}}{\det \mathcal{M}_{2L+1}^{(1,1)}}, \;\; C_1/C_2 = \frac{\det \mathcal{M}_{2L}^{(1,2)}}{\det \mathcal{M}_{2L}^{(1,1)}} . \tag{6.89}$$

Finally we can plug (6.89) into (6.70) and write our main result for $\Gamma_L(g)$

$$\Gamma_L(g) = (\phi - \theta) g \left(r_{2L-1} - r_{2L}\right) , \; r_N = \frac{\det \mathcal{M}_{N+1}^{(1,2)}}{\det \mathcal{M}_N} . \tag{6.90}$$

Using the identities given in appendix B.6, we can represent it in a compact form. The final formula reads

$$\boxed{\Gamma_L(g) = \frac{\phi-\theta}{4}\partial_\theta \log \frac{\det \mathcal{M}_{2L+1}}{\det \mathcal{M}_{2L-1}}}\,. \tag{6.91}$$

As an example, for $L = 1$ it reduces to

$$\Gamma_1(g) = (\phi-\theta)g\frac{1}{I_1^\theta}\frac{\left(I_2^\theta\right)^3 - 2I_1^\theta I_2^\theta I_3^\theta + \left(I_1^\theta\right)^2 I_4^\theta}{\left(I_1^\theta\right)^2 - I_1^\theta I_3^\theta + \left(I_2^\theta\right)^2}, \tag{6.92}$$

while for higher values of L the expression becomes quite lengthy.

A form more suitable for some calculations is

$$\Gamma_L(g) = (-1)^{L+1}(\phi-\theta)g\frac{\det \mathcal{M}_{2L+1}^{(1,2L+2)}}{\det \mathcal{M}_{2L}}. \tag{6.93}$$

Notice that here the matrix in the numerator is just $\mathcal{M}_{2L}$ with all indices of deformed Bessel functions I_n^θ increased by 1.

The explicit result for the energy (6.91) concludes our analytical solution of the cusp TBA equations. In section 6.4 we will describe several verifications of the result.

6.3 Solution from Twisted QSC

In this section we will see that the result obtained earlier in this chapter using cumbersome TBA calculations can be obtained much easier from QSC. For this the QSC construction described in chapter 4 has to be modified to take into account the effect of the "boundary"[166]. As the usual QSC is equivalent to TBA, this modified QSC is equivalent to the boundary TBA of [155] and [95]. We will not reproduce here neither the derivation nor the full description of the boundary QSC, presenting only the minimum necessary to describe the LO solution for the cusped Wilson line.

Most part of the usual QSC construction still holds for the boundary one. The only difference comes from the asymptotics of μ_{ab}, ω_{ij} and the Q-functions. Again, as in the case of non-integer S, one has to allow for exponential asymptotics. In particular, for $\mathbf{P}_a$ one finds

$$\mathbf{P}_1 \sim A_1 u^{-1/2-L} e^{\theta u}(1 + a_1/u + \dots) \tag{6.94}$$

$$\mathbf{P}_2 \sim A_2 u^{-1/2-L} e^{-\theta u}(1 - a_1/u + \dots) \tag{6.95}$$

$$\mathbf{P}_3 \sim A_3 u^{3/2+L} e^{\theta u}(1 + b_1/u + \dots) \tag{6.96}$$

$$\mathbf{P}_4 \sim A_4 u^{3/2+L} e^{-\theta u}(1 - b_1/u + \dots) \tag{6.97}$$

For the sake of brevity here we will focus on the case $L = 0$, although it is of course not difficult to obtain the solution for arbitrary L. In a general situation global charges are related to the expansion coefficients of $\mathbf{P}_a$ and $\mathbf{Q}_a$ in way analogous to (4.50), (4.52) but far more complicated. One need to expand $\mathbf{P}_a$ to the four order at large u in order to write down a closed system for asymptotic coefficients! Fortunately, in the leading order of near-BPS limit the situation simplifies. It turns out that

$$\Delta = (\theta - \phi)\sqrt{a_1^2 - a_1 b_2^{(0)} + b_3^{(0)}}, \tag{6.98}$$

where $b_n^{(0)} = \lim\limits_{\theta\to\phi}(\theta-\phi)b_n$, Thus we should solve the equations of QSC and the coefficients of expansion of $\mathbf{P}_1$ and $\mathbf{P}_3$ will yield the energy.

In the near-BPS limit of twist operators we studied in chapter 5 we found that $\mathbf{P}_a$ were small. For the near-BPS Wilson line operator we study here we make an assumption that $\mathbf{P}_a$ will be small as well, and later find that this assumption produces a consistent solution. If $\mathbf{P}_a$ are small, the $\tilde{\mathbf{P}}_a$ are small as well and so are the discontinuities of μ_{ab}. This means that in the leading order μ_{ab} are constants or periodic functions. Taking into account that Pf $\mu = 1$ and the γ-transformations (4.61) it is possible to bring the leading order solution for μ_{ab} to the following form

$$\mu_{12} = A\sinh(2\pi u),\ \ \mu_{13} = 1,\ \ \mu_{14} = 0,\ \ \mu_{24} = -1,\ \ \mu_{34} = 0. \tag{6.99}$$

Plugging this solution into the system (4.46) we obtain

$$\tilde{\mathbf{P}}_1 = A\sinh 2\pi u\ \mathbf{P}_3 - \mathbf{P}_2 \tag{6.100}$$

$$\tilde{\mathbf{P}}_2 = A\sinh 2\pi u\ \mathbf{P}_4 - \mathbf{P}_1 \tag{6.101}$$

$$\tilde{\mathbf{P}}_3 = \mathbf{P}_4 \tag{6.102}$$

$$\tilde{\mathbf{P}}_4 = \mathbf{P}_3 \tag{6.103}$$

It is easy to find the solution to this system of equations with asymptotics (6.94), starting from $\mathbf{P}_3$ and $\mathbf{P}_4$. The equations for $\mathbf{P}_1$ and $\mathbf{P}_2$ are solved by the same method as the Baxter equations (6.64). The result is

$$\mathbf{P}_1 = B\sqrt{u}e^{g\theta(x-1/x)}\sum_{n=1}^{\infty} I_n^{\theta} x^{-n} \tag{6.104}$$

$$\mathbf{P}_2 = B\sqrt{u}e^{-g\theta(x-1/x)}\sum_{n=1}^{\infty} I_n^{-\theta} x^{-n} \tag{6.105}$$

$$\mathbf{P}_3 = B\sqrt{u}e^{g\theta(x-1/x)} \tag{6.106}$$

$$\mathbf{P}_4 = B\sqrt{u}e^{-g\theta(x-1/x)} \tag{6.107}$$

From this solution one finds that

$$a_1 = g\frac{I_2^\theta}{I_1^\theta} - 2\theta g^2,\ b_2 = -\frac{4g^2\phi}{\theta-\phi},\ b_3 = \frac{4g^4\phi^2}{\theta-\phi}, \tag{6.108}$$

so the energy is

$$\Delta = (\theta-\phi)\frac{I_2^\theta}{I_1^\theta} \tag{6.109}$$

which after plugging in the definition (6.75) of I_n^θ exactly reproduces the result (6.79)

Let us now confirm the conjecture made in section 4.2 about the absence of cuts in η (we switch back to the case of arbitrary L). We know a formula (6.49) for η in terms of $\mathbf{Q}_\pm$. It is easy to see that $\mathbf{Q}_\pm$ are related to $\mathbf{P}_1$ and $\mathbf{P}_2$ from QSC. Indeed, $\mathbf{Q}_\pm$ are determined from the Baxter equation (6.64) where $T(u)$ is given by (6.67). On the other hand, the equation (6.100) for $\mathbf{P}_1$ takes a similar form after plugging in the solution for $\mathbf{P}_3$. This allow to establish the following relationship between $\mathbf{P}_1$, $\mathbf{P}_2$ and $\mathbf{Q}_\pm$.

$$\mathbf{P}_1 \propto \sqrt{u}e^{2g\theta x}\mathbf{Q}_- \tag{6.110}$$

$$\mathbf{P}_2 \propto \sqrt{u}e^{2g\theta x}\mathbf{Q}_+ \tag{6.111}$$

So we express $\mathbf{Q}_\pm$ through $\mathbf{P}_1$, $\mathbf{P}_2$ using (6.111) to obtain

$$\eta^2 \propto \frac{\mathbf{P}_1\mathbf{P}_2\tilde{\mathbf{P}}_1\tilde{\mathbf{P}}_2}{\sinh(2\pi u)^2} \propto \frac{\mathbf{P}_1\mathbf{P}_2\tilde{\mathbf{P}}_1\tilde{\mathbf{P}}_2}{\mu_{12}^2} \tag{6.112}$$

Although in general $\tilde{\mathbf{P}}_a$ can have an infinite ladder of cuts, for this particular solution μ_{ab} has no cuts in the leading order and, as a consequence, $\tilde{\mathbf{P}}_a$ has only the cut on the real axis. This cut is however cancelled in the combination appearing in the numerator. Thus we see that from the point of view of QSC the conjecture in question is a simple consequence of the analytical properties of $\mathbf{P}_a$ and μ_{ab}.

6.4 Weak and strong coupling limits

While for $L = 0$ our result matches fully the prediction from localization, at nonzero L our result is new. Here we will show that it passes several nontrivial checks.

At strong coupling our computation should reproduce the energy of the corresponding classical string solution which was computed in [91]. To do this we first expanded the energy at large g and fixed L for several first values of L. The dependence on L happened to be polynomial which allows us to easily extend the result to an arbitrary L (see (B.57)):

$$\frac{\Gamma_L}{2(\phi-\theta)\theta} = -\frac{g}{\sqrt{\pi^2-\theta^2}} + \frac{6L+3}{8\left(\pi^2-\theta^2\right)} - \frac{3\left(\left(6L^2+6L+1\right)\pi^2 - 2\theta^2(L+1)L\right)}{128g\pi^2\left(\pi^2-\theta^2\right)^{3/2}} + \dots \tag{6.113}$$

To compare with the classical string energy we re-expanded this formula in the regime when L and g are both large, but $\mathcal{L} = L/g$ is fixed. Then at leading order in g we found (more details are given in appendix B.5)

$$\begin{aligned}\frac{\Gamma_L}{2(\phi-\theta)\theta} &= \left(-\frac{g}{\pi}+\frac{3L}{4\pi^2}-\frac{9L^2}{64g\pi^3}-\frac{5L^3}{256g^2\pi^4}+\frac{45L^4}{16384g^3\pi^5}\right) \\ &+ \theta^2\left(-\frac{g}{2\pi^3}+\frac{3L}{4\pi^4}-\frac{21L^2}{128g\pi^5}-\frac{L^3}{16g^2\pi^6}-\frac{105L^4}{32768g^3\pi^7}\right) \\ &+ \theta^4\left(-\frac{3g}{8\pi^5}+\frac{3L}{4\pi^6}-\frac{99L^2}{512g\pi^7}-\frac{3L^3}{32g^2\pi^8}-\frac{2085L^4}{131072g^3\pi^9}\right) \\ &+ \theta^6\left(-\frac{5g}{16\pi^7}+\frac{3L}{4\pi^8}-\frac{225L^2}{1024g\pi^9}-\frac{L^3}{8g^2\pi^{10}}-\frac{7905L^4}{262144g^3\pi^{11}}\right) \\ &+ \theta^8\left(-\frac{35g}{128\pi^9}+\frac{3L}{4\pi^{10}}-\frac{1995L^2}{8192g\pi^{11}}-\frac{5L^3}{32g^2\pi^{12}}-\frac{97425L^4}{2097152g^3\pi^{13}}\right),\end{aligned} \tag{6.114}$$

which perfectly matches the expansion of the classical string energy from [91]! Since the classical energy was derived without appealing to integrability, this matching is a direct test of our calculation for nonzero L. Relation to the classical string solution is discussed in much more detail in section 7.4 of the next chapter.

At weak coupling we can compare our result against the leading Lüscher correction to the energy. This correction was computed, as well as shown to follow from the TBA equations, in [95] and [155] for generic ϕ and θ. When $\theta \sim \phi$ it reduces to

$$\Gamma_L = (\phi-\theta)g^{2L+2}\frac{(-1)^L(4\pi)^{1+2L}}{(1+2L)!}B_{1+2L}\left(\frac{\pi-\theta}{2\pi}\right)+\mathcal{O}(g^{2L+4}) \tag{6.115}$$

where B_{1+2L} are the Bernoulli polynomials. For $L = 0, 1, 2, 3, 4$ we have checked that this expression precisely coincides with the leading weak-coupling term of our result.

7 Quasi-classical limit of $\mathbf{AdS_5/CFT_4}$

It has been known for a long time that IIB string theory on $\mathrm{AdS}_5/\mathrm{CFT}_4$ background can be rewritten as a sigma-model on a coset space [171]. This representation is particularly useful for exploring the integrability of the theory in the quasiclassical limit: for every closed string solution of the equation of motions one can construct an algebraic curve, in which all the conserved charges will be encoded as holomorphic integrals [38, 172, 98, 39]. The topics presented in this chapter are united by this approach. First in section 7.1 we give a minimal introduction to this method following the papers cited above. Then in section 7.2 we will compare classical curve formulation obtained from the coset model with the quasi-classical limit of QSC and find that they indeed agree. In 7.4 we present a result concerning

the quasiclassical limit of the cusp anomalous dimension computed in the previous chapter. This involves constructing an algebraic curve for an open string. As opposed to closed strings, for the open string theory there is no systematic method of constructing the algebraic curve, and our work can serve as a step for building such a method. Section 7.5 will comment on a certain reciprocity-like property of large L expansion of the cusp anomalous dimension found in [173] after we published our result [11]. Finally in section 7.6 we use this reciprocity-like property to derive the 1-loop correction to classical energy.

7.1 Metsaev-Tseytlin sigma-model

Let us, following [171], rewrite the string action as a coset model. We notice that the symmetry group of $\mathcal{N}=4$ SYM factored by the four-dimensional conformal group and by the R-symmetry form a coset

$$\frac{PSU(2,2|4)}{SO(4,1)\times SO(5)} \tag{7.1}$$

containing $AdS_5\times S^5$ as its bosonic subgroup. This gives us a way of parametrizing the worldsheet: let $g(\sigma,\tau)$ be a supermatrix-valued function of worldsheet coordinates taking values in the coset. Since we are considering closed strings, the function has to be periodic $g(\sigma,\tau)=g(\sigma+2\pi,\tau)$. It also has to satisfy sdet $g=1$. The current $J=-g^{-1}dg$ constructed for $g(\sigma,\tau)$ in this way is flat and traceless by construction:

$$\text{str } J=0,\quad dJ-J\wedge J=0 \tag{7.2}$$

An important property of $\mathfrak{psu}(2,2|4)$ algebra is existence of a $\mathbb{Z}_4$ automorphism Ω ($\Omega^4=1$) [171, 174, 175, 176]. This implies that the algebra can be decomposed into four subspaces according to $\mathbb{Z}_4$ grading:

$$\mathcal{G}=\mathcal{H}+\mathcal{P}+\mathcal{Q}_1+\mathcal{Q}_2 \tag{7.3}$$

In terms of the coset (7.1) $\mathcal{H}$ is the denominator algebra, $\mathcal{P}$ is spanned by the remaining bosonic generators and $\mathcal{Q}_i$ are two copies of (4,4) representation of $\mathcal{H}$.

The Metsaev-Tseytlin action for the GS superstring in $AdS_5\times S^5$ is given by

$$S=\frac{\sqrt{\lambda}}{4\pi}\int \text{str}\left(J^{(2)}\wedge *J^{(2)}-J^{(1)}\wedge J^{(3)}\right)+\Lambda\wedge \text{str}J^{(2)}, \tag{7.4}$$

where $J^{(i)}$ are components of the current belonging to the corresponding subspaces in the decomposition (7.3). The last term ensures that $J^{(2)}$ is supertraceless. Let us now construct a new connection, depending on a parameter x:

$$A(x)=J^{(0)}+\frac{x^2+1}{x^2-1}J^{(2)}-\frac{2x}{x^2-1}(*J^{(2)}-\Lambda)+\sqrt{\frac{x+1}{x-1}}J^{(1)}+\sqrt{\frac{x-1}{x+1}}J^{(3)} \tag{7.5}$$

It turns out that the string equations of motion can be rewritten as the flatness condition of this connection

$$dA - A \wedge A = 0 \tag{7.6}$$

One can construct monodromy of the connection by integrating it around the worldsheet at constant τ

$$\Omega(x) = \mathrm{Pexp} \oint_{\gamma} A(x) \tag{7.7}$$

Since the connection is flat, the monodromy depends only trivially on the path of integration. In particular, shifting τ only changes Ω by a similarity transformation and so the eigenvalues of the monodromy are independent of the path of integration. We parameterize them in the following form:

$$\{e^{i\hat{p}_1(x)}, e^{i\hat{p}_2(x)}, e^{i\hat{p}_3(x)}, e^{i\hat{p}_4(x)} | e^{i\tilde{p}_1(x)}, e^{i\tilde{p}_2(x)}, e^{i\tilde{p}_3(x)}, e^{i\tilde{p}_4(x)}\} \tag{7.8}$$

Since $p_i(x)$ are logarithms of eigenvalues, they can be considered as eight sheets of a Riemann surface parameterized by x. The Riemann surface will have branch points at values of x at which some of the eigenvalues coincide. At such point the values of the corresponding p_i have to differ by a multiple of 2π. The branch points are connected with cuts, which can thus be of different types: a cut connecting sheet i with sheet j will be denoted by $\mathcal{C}_{ij}$. Each type of cuts is associated with different type of excitations. In fact, only the following types of excitation exist in the theory

$$i = \tilde{1}, \tilde{2}, \hat{1}, \hat{2} \quad j = \tilde{3}, \tilde{4}, \hat{3}, \hat{4} \tag{7.9}$$

The sheets of the surface, otherwise called quasimomenta, satisfy

$$p_i - p_j = 2\pi n_{ij}, x \in \mathcal{C}_{ij} \tag{7.10}$$

The integers n_{ij} are called mode numbers.

The number of excitations in each of the cuts $\mathcal{C}_{ij}$ is measured by so-called filling fractions S_{ij}, which are calculated as

$$S_{ij} = \pm \frac{\sqrt{\lambda}}{8\pi^2 i} \oint_{\mathcal{C}_{ij}} \left(1 - \frac{1}{x^2}\right) p_i(x) dx \tag{7.11}$$

It is possible to show that the structure of the coset (7.1) implies the following symmetry of the Riemann surface $p_i(x)$:

$$\tilde{p}_{1,2}(x) = -2\pi m - \tilde{p}_{2,1}(1/x) \tag{7.12}$$

$$\tilde{p}_{3,4}(x) = +2\pi m - \tilde{p}_{4,3}(1/x) \tag{7.13}$$

$$\hat{p}_{1,2,3,4}(x) = -\hat{p}_{2,1,4,3}(1/x) \tag{7.14}$$

As we have mentioned before, the global charges of the solution are encoded in the holomorphic integrals of the curve. The most straightforward way of extracting these charges is to consider the asymptotics at infinity (which, as follows from the equation above, are also related to the expansion at $x = 0$)

$$\left(\begin{array}{c} \hat{p}_1 \\ \hat{p}_2 \\ \hat{p}_3 \\ \hat{p}_4 \\ \hline \tilde{p}_1 \\ \tilde{p}_2 \\ \tilde{p}_3 \\ \tilde{p}_4 \end{array}\right) \approx \frac{2\pi}{x\sqrt{\lambda}} \left(\begin{array}{c} +E - S_1 + S_2 \\ +E - S_1 - S_2 \\ -E - S_1 - S_2 \\ -E + S_1 + S_2 \\ \hline +J_1 + J_2 - J_3 \\ +J_1 - J_2 - J_3 \\ -J_1 + J_2 + J_3 \\ -J_1 - J_2 - J_3 \end{array}\right) \tag{7.15}$$

One can use the framework of a Riemann surface to go beyond the classical limit and consider one-loop corrections, i.e. excitations around the classical solutions [177, 99].

7.2 Classical Limit of QSC

The classical curve presented above was, of course, known long before QSC, but here we will show it can be derived from QSC as its special limit (see section 5 of [8])

It is well known that the classical curve can be obtained not only through the monodromy eigenvalues construction, but also as a classical limit of ABA. This gives the correct result because the wrapping corrections do not contribute to the classical expansion. In order to do so one takes the strong coupling limit, at the same time scaling the length L and the number of excitations of each kind K_i so that L/g, K_i/g are fixed. It is convenient to pack the roots into resolvents

$$H_a(x) = \frac{4\pi}{\sqrt{\lambda}} \frac{x^2}{x^2-1} \sum_j \frac{1}{x - x\left(u_{a,j}\right)} \tag{7.16}$$

In the classical limit the roots condense into cuts. The quasimomenta are then defined through the resolvents and the cuts of the resolvents become cuts connecting some of the eight sheets of the Riemann surface.

This procedure can be applied to ABA described in section 4.5. Consider the ratio $\mathbf{Q}_1^+/\mathbf{Q}_1^-$, which using the ansatz (4.73) can be rewritten as

$$\frac{\mathbf{Q}_1^+}{\mathbf{Q}_1^-} = \frac{R^+_{\emptyset|1} B^+_{12|1}}{R^-_{\emptyset|1} B^-_{12|1}} \frac{B^-_{(-)}}{B^+_{(+)}} \left(\frac{x^+}{x^-}\right)^{L/2} \frac{\sigma^-}{\sigma^+} \tag{7.17}$$

We expand the right hand side at $g \to \infty$, assuming x is fixed and introduce local charges

$$\mathcal{Q}_n = \frac{4\pi}{\sqrt{\lambda}} \sum_j \frac{x^{2-n}(u_{4,j})}{x^2(u_{4,j}) - 1} \tag{7.18}$$

In this notation the ratio above can be written as

$$\frac{\mathbf{Q}_1^+}{\mathbf{Q}_1^-} = \exp i \left(\frac{4\pi \mathcal{J} x}{x^2 - 1} + H_3(1/x) + H_1(x) - H_4(x) + \frac{x\mathcal{Q}_2}{x^2 - 1} \right) \tag{7.19}$$

The right hand side is exactly $e^{ip_1(x)}$, with quasimomentum $p_1(x)$ defined in the previous section. Similar calculations can be performed for all $\mathbf{Q}_i$ and $\mathbf{P}_a$, resulting in

$$\mathbf{P}_a(u) = \mathcal{P}_{a|\emptyset}(u) \exp \left(-g \int_{0+i0}^{u/g} dz p_{\tilde{a}}(z) \right) \tag{7.20}$$

$$\mathbf{Q}_i(u) = \mathcal{P}_{\emptyset|i}(u) \exp \left(-g \int_{0+i0}^{u/g} dz p_{\hat{i}}(z) \right) \tag{7.21}$$

The preexponents can be constrained by relating $\mathbf{P}_a$ with $\mathbf{Q}_i$ through $\mathcal{Q}_{a|i}$, using equations (4.8) and (4.10)-(4.11), which is described in detail in [8].

7.3 Classical string solutions

In the classical limit it is sometimes possible to write down the solution of the string equations of motion explicitly or define it through the algebraic curve. Let us recall that in this limit, when the coupling goes to infinity, the global charges scale as

$$\mathcal{S}_i = S_i/\sqrt{\lambda}, \quad \mathcal{J}_i = J_i/\sqrt{\lambda}, \quad \mathcal{E} = E/\sqrt{\lambda}. \tag{7.22}$$

Often the goal is to find a strong coupling expansion of the string energy (conformal dimension of the state), which looks like

$$E = \sqrt{\lambda} E_0(\mathcal{S}, \mathcal{J}) + E_1(\mathcal{S}, \mathcal{J}) + \frac{1}{\sqrt{\lambda}} E_2(\mathcal{S}, \mathcal{J}) + \dots \tag{7.23}$$

Several classes of solutions are well studied and relevant for the problems we consider in this thesis. One example is called rotating folded string and corresponds to the quasiclassical limit of operators of $\mathfrak{sl}(2)$ sector described in section 4.4. Operators of this sector have three non-zero charges, two in AdS and one on the sphere, which in the quasiclassical limit scale as $S_1 = \sqrt{\lambda}\,\mathcal{S}$, $\Delta = \sqrt{\lambda}\,\mathcal{E}$, and $J_1 = \sqrt{\lambda}\,\mathcal{J}$.

The explicit form of the algebraic curve for this class of solutions was found in [148]. As we said above, in the classical limit the Bethe roots condense and form cuts. The

algebraic curve of the folded string has two symmetric cuts with real branch-points $\pm a$, $\pm b$, which satisfy $1 < a < b$. Two of the sheets are given by

$$\frac{p_{\hat{2}}}{4\pi} = \pi n - \frac{\mathcal{J}}{2}\left(\frac{a}{a^2-1} - \frac{x}{x^2-1}\right)\sqrt{\frac{(a^2-1)(b^2-x^2)}{(b^2-1)(a^2-x^2)}} + \tag{7.24}$$

$$+\frac{2ab\mathcal{S}F_1(x)}{(b-a)(ab+1)} + \frac{\mathcal{J}(a-b)F_2(x)}{2\sqrt{(a^2-1)(b^2-1)}} \tag{7.25}$$

$$\frac{p_{\tilde{2}}}{4\pi} = \frac{\mathcal{J}x}{2(x^2-1)} \tag{7.26}$$

where

$$F_1(x) = iF\left(i\sinh^{-1}\sqrt{\frac{(b-a)(a-x)}{(b+a)(a+x)}}\left|\left(\frac{a+b}{a-b}\right)^2\right.\right), \tag{7.27}$$

$$F_2(x) = iE\left(i\sinh^{-1}\sqrt{\frac{(b-a)(a-x)}{(b+a)(a+x)}}\left|\left(\frac{a+b}{a-b}\right)^2\right.\right) \tag{7.28}$$

The rest of the quasimomenta can are determined by the symmetry relations (7.12). The integer n is called the mode number and is related to the number of spikes of the curve.

The branch points are implicitly determined by the global charges

$$\mathcal{S} = 8\pi n\frac{ab+1}{ab}\left(bE\left(1-\frac{a^2}{b^2}\right) - aK\left(1-\frac{a^2}{b^2}\right)\right) \tag{7.29}$$

$$\mathcal{J} = \frac{16\pi n}{b}K\left(1-\frac{a^2}{b^2}\right)\sqrt{(a^2-1)(b^2-1)} \tag{7.30}$$

$$\mathcal{E} = 8\pi n\frac{ab-1}{ab}\left(bE\left(1-\frac{a^2}{b^2}\right) + aK\left(1-\frac{a^2}{b^2}\right)\right) \tag{7.31}$$

It is worth noting that although the classical solution assumes the global charges are infinite, predictions for strings with finite charges can be obtained from it by taking the limit $\mathcal{S}, \mathcal{J} \to 0$ [179]. In particular, in the limit $\mathcal{S} \to 0$ the square of the classical energy of a folded string has a form [148, 147]

$$\mathcal{D}^2_{\text{classical}} = \mathcal{J}^2 + 2\,\mathcal{S}\,\sqrt{\mathcal{J}^2+1} + \mathcal{S}^2\,\frac{2\mathcal{J}^2+3}{2\mathcal{J}^2+2} - \mathcal{S}^3\,\frac{\mathcal{J}^2+3}{8\left(\mathcal{J}^2+1\right)^{5/2}} + \mathcal{O}\left(\mathcal{S}^4\right)\ , \tag{7.32}$$

where $\mathcal{D}_{\text{classical}} \equiv \Delta_{classical}/\sqrt{\lambda}$.

The one-loop correction to the classical energy obtained by quasi-classical quantization in the same limit is given by

$$\Delta_{sc} \simeq \frac{-\mathcal{S}}{2\left(\mathcal{J}^3+\mathcal{J}\right)} + \mathcal{S}^2\left[\frac{3\mathcal{J}^4+11\mathcal{J}^2+17}{16\mathcal{J}^3\left(\mathcal{J}^2+1\right)^{5/2}} - \sum_{\substack{m>0\\ m\neq n}}\frac{n^3m^2\left(2m^2+n^2\mathcal{J}^2-n^2\right)}{\mathcal{J}^3\left(m^2-n^2\right)^2\left(m^2+n^2\mathcal{J}^2\right)^{3/2}}\right] \tag{7.33}$$

If both J and S are taken to be finite, the energy has the following scaling

$$E = \lambda^{1/4}a_0 + \frac{1}{\lambda^{1/4}}a_2 + \ldots \tag{7.34}$$

In particular, for a folded string from the classical energy and the one-loop correction one gets [148]

$$E = \lambda^{1/4}\sqrt{2S} + \frac{2J^2 + 3S^2 - 2S}{4(2S)^{1/2}\lambda^{1/4}} \tag{7.35}$$

7.4 Algebraic curve for cusped Wilson line

In this section, based on our paper [11], we perform a quasi-classical analysis of the result for the anomalous dimension for a cusped Wilson line with an insertion of a scalar operator at the cusp (6.3). Such an analysis is useful, for example, as a strong coupling test of the result: the cusped Wilson line operator is dual to an open string in $AdS_5 \times S^5$, the classical solution of which was studied in [91, 95] and described here in section 7.4.2. The cusp anomalous dimension is then dual to the energy of the string. As one might recall, the result (6.90) included a ratio of two determinants with sizes proportional to L. This makes taking the classical limit, with $L \to \infty$, not entirely straightforward. The solution to this problem is to reformulate the formula as an expectation value in some matrix model. Then the classical value of Γ_L will be given by the saddle-point approximation of a matrix integral. An elegant way to describe the solution in the classical limit is the algebraic curve method [38, 39, 98, 180, 181] which we described earlier in this chapter. For a more detailed review of the method, see [99]. Let us notice that the algebraic curve construction works in the regime $L \sim \sqrt{\lambda} \to \infty$, otherwise the curve is degenerate, with its cuts collapsing to poles. In the limit of $\theta = 0,\ \phi \ll 1$ the algebraic curve in question was found in [91] (the $L = 0$ case was also considered in [100]) and here we generalize this construction for the general near-BPS case $\phi \approx \theta$.

In section 7.4.1 we reformulate the problem in the language of matrix models, showing how the cusp anomalous dimension can be expressed as an expectation value in the aforementioned matrix model. In section 7.4.2 we review the corresponding classical string solution and in section 7.4.3 we find the algebraic curve for $\theta \approx \phi$ and using it derive the classical energy. We show that our results indeed agree with the known classical expansions for the cusp anomalous dimension.

7.4.1 Matrix model reformulation

Quasiclassical limit in our case means taking L to infinity with $L/\sqrt{\lambda}$ fixed. This becomes considerably easier once we realize that the cusp anomalous dimension (6.5) can be expressed in terms of an expectation value of some operator in a matrix model. In

this section we will show how to use this approach to find the large N expansion of the determinant of $\mathcal{M}_N$ defined in (6.82).

One can check that the quantities I_n^θ defined in (6.75) have the following integral representation

$$I_n^\theta = \frac{1}{2\pi i}\oint \frac{dx}{x^{n+1}} \sinh(2\pi g\,(x+1/x))\, e^{2g\theta(x-1/x)}, \tag{7.36}$$

where the integration contour is the unit circle. This makes it possible to write the determinant of $\mathcal{M}_N$ as

$$\det \mathcal{M}_N = \oint \prod_{i=1}^{N+1} \frac{dx_i}{2\pi i} e^{2g\,\theta\left(x_i-\frac{1}{x_i}\right)} \sinh\left(2\pi g\left(x_i+\frac{1}{x_i}\right)\right) \times \det X, \tag{7.37}$$

where

$$\det X = \begin{vmatrix} x_1^{-2} & x_1^{-1} & \dots & x_1^{N-1} & x_1^{N-2} \\ x_2^{-3} & x_2^{-2} & \dots & x_2^{N} & x_2^{N-1} \\ \vdots & \vdots & \ddots & \vdots & \vdots \\ x_N^{-N-1} & x_N^{-N} & \dots & x_N^{-2} & x_N^{-1} \\ x_{N+1}^{-N-2} & x_{N+1}^{-N-1} & \dots & x_{N+1}^{-3} & x_{N+1}^{-2} \end{vmatrix} = \frac{\prod_{i<j}^{N+1}(x_i-x_j)}{\prod_{i=1}^{N+1} x_i^{i+1}}, \tag{7.38}$$

and we recognize the numerator as the Vandermonde determinant $\Delta(x_i)$. We can further simplify the final result by anti-symmetrizing the denominator, which we can do because everything else in the integrand is anti-symmetric and the integration measure is symmetric w.r.t x_i. Thus by utilizing the identity

$$\sum_\sigma (-1)^{|\sigma|} \prod_{i=1}^{N+1} x_{\sigma_i}^{-i-1} = \frac{\Delta(x_i)}{(N+1)!} \prod_{i=1}^{N+1} x_i^{-N-2}, \tag{7.39}$$

we can replace $\det X$ in the integrand by

$$\det X' = \frac{\Delta^2(x_i)}{(N+1)!} \prod_{i=1}^{N+1} \frac{1}{x_i^{N+2}}. \tag{7.40}$$

Thus finally we get the following expression

$$\det \mathcal{M}_N = \frac{1}{(2\pi i)^{N+1}} \oint \prod_{i=1}^{N+1} \frac{dx_i}{x_i^{N+2}} \frac{\Delta^2(x_i)}{(N+1)!} \sinh(2\pi g\,(x_i+1/x_i))\, e^{2g\theta(x_i-1/x_i)}, \tag{7.41}$$

which indeed has the structure of a partition function of some matrix model[39]. It now becomes a matter of simple algebra to show that the cusp anomalous dimension (6.5) can be written in terms of expectation values in this matrix model, namely

$$\Gamma_L(g) = g\,\frac{\phi-\theta}{2}\left[\left\langle \sum_{i=1}^{2L+1}\left(x_i-\frac{1}{x_i}\right)\right\rangle_{2L+1} - \left\langle \sum_{i=1}^{2L-1}\left(x_i-\frac{1}{x_i}\right)\right\rangle_{2L-1}\right], \tag{7.42}$$

[39] Namely, it is equal to the partition function of a two-matrix model. We thank I.Kostov for discussions related to this question.

where $\langle \dots \rangle_N$ denotes the normalized expectation value in the matrix model of size N with the partition function defined in (7.41). Note that this formula is exact and we have not yet taken any limits.

Saddle point equations In this section we will explore the classical $L \sim \sqrt{\lambda} \to \infty$ limit of the matrix model (7.41). As usual in matrix models, when the size of matrices becomes large, the partition function is dominated by the solution of the saddle point equations. In the leading order it is just equal to the value of the integrand at the saddle point. Here we work in this approximation, leaving the corrections (beyond the first one calculated in section 7.6) for future work.

The partition function (7.41) can be recast in the form [40]

$$\det \mathcal{M}_{2L} = \frac{1}{(2\pi i)^{2L+1}} \frac{1}{(2L+1)!} \oint \prod_{i=1}^{2L+1} dx_i \, e^{-S(x_1,x_2,\dots,x_{2L+1})}, \tag{7.43}$$

where the action is given by

$$\begin{aligned} S &= \sum_{i=1}^{2L+1} \left[2g\theta \left(x_i - \frac{1}{x_i} \right) - (2L+2) \log x_i \right] + 2 \sum_{i<j}^{2L+1} \log(x_i - x_j) + \\ &+ \sum_{i=1}^{2L+1} \log \sinh \left(2\pi g \left(x_i + \frac{1}{x_i} \right) \right). \end{aligned} \tag{7.44}$$

The saddle point equations $\partial S / \partial x_j = 0$ now read[41]

$$g\theta \left(1 + \frac{1}{x_j^2} \right) - \frac{L}{x_j} + \sum_{i \neq j}^{2L+1} \frac{1}{x_j - x_i} + \pi g \left(1 - \frac{1}{x_j^2} \right) \coth \left(2\pi g \left(x_j + \frac{1}{x_j} \right) \right) = 0. \tag{7.45}$$

We can further simplify them by noting that a large coupling constant g appears inside the cotangent and since the roots x_i are expected to be of order 1, with exponential precision it is possible to replace

$$\coth \left(2\pi g \left(x_j + \frac{1}{x_j} \right) \right) \approx \operatorname{sgn}(\operatorname{Re}(x_j)). \tag{7.46}$$

Finally we bring the equations to a more canonical and convenient form and get the following result,

$$-\theta \frac{x_j^2 + 1}{x_j^2 - 1} + \frac{L}{g} \frac{x_j}{x_j^2 - 1} - \frac{1}{g} \frac{x_j^2}{x_j^2 - 1} \sum_{i \neq j}^{2L+1} \frac{1}{x_j - x_i} = \pi \operatorname{sgn}(\operatorname{Re}(x_j)). \tag{7.47}$$

An alternative way of finding these values x_i is to consider the function $P_L(x)$ defined by (6.84), which played an important role in chapter (6). The numerator of (6.84) is the same

[40] we take $N = 2L$.

[41] Technically the x_j^{-1} term has a coefficient of $L+1$, but since we are taking $L \to \infty$ we chose to neglect it for simplicity.

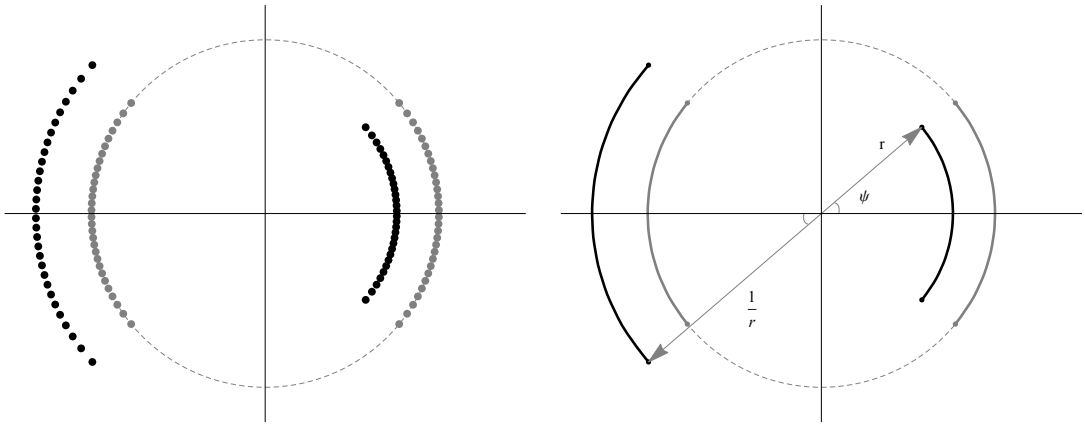

Figure 10: **Distribution of roots on the complex plane** for $\theta = 0$ (gray) and $\theta = 1$ (black) on the left and the condensation of the roots to corresponding smooth cuts on the right with the algebraic curve parameters r and ψ identified. The dashed circle is the unit circle.

as $\det \mathcal{M}_{2L}$ except in the last line x_{2L+1} is replaced by x which is not integrated over. In the classical limit all integrals are saturated by their saddle point values, i.e. one can remove the integrals by simply replacing $x_i \to x_i^{cl}$. If we replace x with any saddle point value x_i^{cl} the determinant will contain two identical rows and will automatically become zero, thus the zeros of $P_L(x)$ are the saddle point values. On the complex plane they are distributed on two arcs as shown in Fig. 10. As expected, for the case $\theta = 0$ we recover two symmetric arcs on the unit circle [91].

Now, following [39, 38, 91], we introduce the quasimomentum $p(x)$ as

$$p_{2L+1}(x) = -\theta \frac{x^2+1}{x^2-1} + \frac{L}{g}\frac{x}{x^2-1} - \frac{2L}{g}\frac{x^2}{x^2-1} G_{2L+1}(x), \tag{7.48}$$

where the resolvent $G_{2L+1}(x)$ is

$$G_{2L+1}(x) = \frac{1}{2L}\sum_{k=1}^{2L+1} \frac{1}{x - x_k}. \tag{7.49}$$

Sometimes we will omit the index of p_{2L+1}. The motivation for introducing $p(x)$ is that the saddle point equations (7.47) expressed through $p(x)$ take a very simple form

$$\frac{1}{2}\left(p(x_i + i\epsilon) + p(x_i - i\epsilon)\right) = \pi \,\mathrm{sgn}(\mathrm{Re}(x_i)). \tag{7.50}$$

In the classical limit the poles of the quasimomentum condense and form two cuts. In anticipation of this fact we introduce the shifts $\pm i\epsilon$ in the equation above, which in the classical limit will refer to taking the argument of the quasimomentum to one or the other side of the cut.

Explicit formula for the algebraic curve The quasimomentum (7.48) introduced in the previous section is a convenient object to consider when taking the classical limit $L \sim \sqrt{\lambda} \to \infty$, because in this limit it is related to the algebraic curve of the corresponding classical solution. In this section we will construct this curve explicitly.

In the classical limit the poles of $p(x)$, which we denote as x_i, are governed by the saddle-point equation and condense on two cuts in the complex plane, as shown in Fig. 10. The saddle-point equation (7.47) has a symmetry $x \to -1/x$, so does the set of poles x_i. For the quasimomentum (7.48) this symmetry manifests as the identity $p(x) = -p(-1/x)$. Thus we conclude that the two cuts are related by an $x \to -1/x$ transformation. This and the invariance of the saddle-point equation under complex conjugation implies that the four branch points can be parameterized as $\{r\, e^{i\psi}, r\, e^{-i\psi}, -1/r\, e^{i\psi}, -1/r\, e^{-i\psi}\}$. Note that in the case $\theta = 0$ the symmetry is enhanced to $p(x) = -p(-x)$ and $p(1/x) = p(x)$, which is not true for arbitrary θ.

An important observation which will help us build an explicit formula for the curve is that while $p(x)$ satisfies the equation (7.50) which has different constants on the right hand side for the two different cuts, the corresponding equation for $p'(x)$ has a zero on the right hand side for both cuts[42], thus we expect $p'(x)$ to have a simpler form than $p(x)$. Thus one can write down an ansatz for the derivative $p'(x)$ using the symmetries and analytical properties of $p(x)$ and then integrate it. The form of the expression we get is analogous to the curve constructed in [98], which also helps us to construct the ansatz.

First, $p(x)$ has four branch points and according to (7.50) its derivative changes sign on each cut, hence all the cuts are of square-root type. One can write $p'(x) \propto 1/y(x)$, where

$$y(x) = \sqrt{x - re^{i\psi}}\sqrt{x - re^{-i\psi}}\sqrt{x + \frac{1}{r}e^{i\psi}}\sqrt{x + \frac{1}{r}e^{-i\psi}}. \tag{7.51}$$

Second, since the algebraic curve is obtained from (7.48) in the classical limit, $p(x)$ should have simple poles at $x = \pm 1$. Finally, from (7.48) we can get the behaviour at infinity:

$$p'(x) \approx \frac{L}{g}\frac{1}{x^2} + \mathcal{O}\left(\frac{1}{x^3}\right). \tag{7.52}$$

By using the knowledge about these singularities and asymptotics we can fix $p(x)$ completely. Based on what we know up to now we write down our ansatz for the derivative

$$p'(x) = \frac{A_1x^4 + A_2x^3 + A_3x^2 + A_4x + A_5}{(x^2-1)^2\sqrt{x - re^{i\psi}}\sqrt{x - re^{-i\psi}}\sqrt{x + \frac{1}{r}e^{i\psi}}\sqrt{x + \frac{1}{r}e^{-i\psi}}}. \tag{7.53}$$

[42] The sign function in the right hand side of (7.50) has a non-zero derivative only on the imaginary axis, i.e. away from the cuts.

The polynomial in the numerator is of order four in order to maintain the correct asymptotics, and below we fix its coefficients using the properties of the quasimomentum.[43]

The $x \to -1/x$ symmetry for the derivative implies that $A_1 = A_5$ and $A_2 = -A_4$. Next, the condition that $p(x)$ has only simple poles at $x = \pm 1$ requires the residues of the order-one poles of $p'(x)$ to vanish, which fixes A_2 to be

$$A_2 = -\frac{(2A_1 + A_3)\, r\, (r^2 - 1) \cos\psi}{r^4 - 2\, r^2\, \cos 2\psi + 1}. \tag{7.54}$$

We fix the two remaining unknowns A_1 and A_3 after integrating the $p'(x)$. We do not write the intermediate results of the integration as the expressions are enormous without any apparent structure. Looking back at (7.50) we see that at the branchpoints

$$p(x_{bp}) = \pm\pi. \tag{7.55}$$

We use this condition to fix A_1 and we get

$$A_1 = \frac{A_3}{2} \frac{K_1 - E_1}{E_1 + K_1 - 2\, a_r^2\, K_1 \cos^2(\psi)}, \tag{7.56}$$

where

$$E_1 = \mathbb{E}\left(a_r^2 \sin^2(\psi)\right),\ K_1 = \mathbb{K}\left(a_r^2 \sin^2(\psi)\right),\ a_r = \frac{2r}{r^2+1}. \tag{7.57}$$

Finally, imposing $x \to -1/x$ symmetry on the quasimomentum (before it was only imposed on $p'(x)$) yields

$$A_3 = \frac{8}{a_r}\left(E_1 + K_1 - 2\, a_r^2\, \cos^2(\psi) K_1\right). \tag{7.58}$$

As expected, after plugging these coefficients into $p(x)$ (and using the identities from appendix C) the whole expression simplifies enormously and we are left with the following result

$$p(x) = \pi - 4\, i\, E_1\, \mathbb{F}_1(x) + 4\, i\, K_1\, \mathbb{F}_2(x) - a_r \left(\frac{x + r e^{-i\psi}}{x + \frac{1}{r} e^{i\psi}}\right) \left(\frac{2/r\, e^{i\psi}}{x^2 - 1}\right) y(x)\, K_1, \tag{7.59}$$

where

$$\mathbb{F}_1(x) = \mathbb{F}\left(\sin^{-1} \sqrt{\left(\frac{x - r e^{-i\psi}}{x + \frac{1}{r} e^{i\psi}}\right) \left(\frac{e^{i\psi}}{i a_r\, r \sin\psi}\right)} \,\middle|\, a_r^2 \sin^2(\psi)\right), \tag{7.60}$$

$$\mathbb{F}_2(x) = \mathbb{E}\left(\sin^{-1} \sqrt{\left(\frac{x - r e^{-i\psi}}{x + \frac{1}{r} e^{i\psi}}\right) \left(\frac{e^{i\psi}}{i a_r\, r \sin\psi}\right)} \,\middle|\, a_r^2 \sin^2(\psi)\right). \tag{7.61}$$

We verified this result numerically by comparing it to the extrapolation of the discrete quasimomentum (7.48) at large L and got an agreement up to thirty digits. We also

[43] Comparing with the asymptotic one can immediately see that $A_1 = L/g$, however our objective is to express $p(x)$ solely in terms of r and ψ, which parameterize the algebraic curve.

compared this expression at $\theta = 0$ with the quasimomentum obtained in [91] and the expressions agree perfectly.

The resulting quasimomentum is parameterized in terms of the branchpoints, i.e. the parameters are the radius r and angle ψ. They are determined in terms of L/g and θ, which are parameters of the matrix model. We already mentioned that L/g is simply the constant A_1, which we found to be

$$\frac{L}{g} = 4\,\frac{K_1 - E_1}{a_r}, \tag{7.62}$$

and looking back at (7.48) we see that $\theta = p(0) = -p(\infty)$, hence

$$\begin{aligned}\theta &= -\pi + \frac{2a_r}{r}\,e^{i\psi}K_1 \\ &- 4\,i\,K_1\,\mathbb{E}\left(\sin^{-1}\sqrt{\frac{e^{i\psi}}{ia_r\,r\sin\psi}}\,\middle|\, a_r^2\sin^2(\psi)\right) \\ &+ 4\,i\,E_1\,\mathbb{F}\left(\sin^{-1}\sqrt{\frac{e^{i\psi}}{ia_r\,r\sin\psi}}\,\middle|\, a_r^2\sin^2(\psi)\right).\end{aligned} \tag{7.63}$$

In the next section the two equations above will be matched with two analogous equations following from the classical string equations of motion.

7.4.2 Classical string solution

As we have mentioned before, in the classical $L \sim \sqrt{\lambda} \to \infty$ limit $\Gamma_L(\lambda)$ can be matched with the energy of an open string. In this section we will describe the corresponding classical string solution and find its energy.

The class of string solutions we are interested in was introduced in [95] and generalized in [91]. It is a string in $\mathrm{AdS}_3 \times S^3$ governed by the parameters θ, ϕ, AdS_3 charge E and S^3 charge L; the four parameters are restricted by the Virasoro constraint. The ansatz for the embedding coordinates of AdS_3 and S^3 is

$$y_1 + iy_2 = e^{i\kappa\tau}\sqrt{1 + r^2(\sigma)}, \;\; y_3 + iy_4 = r(\sigma)e^{i\phi(\sigma)}, \tag{7.64}$$

$$x_1 + ix_2 = e^{i\gamma\tau}\sqrt{1 + \rho^2(\sigma)}, \;\; x_3 + ix_4 = r(\sigma)e^{if(\sigma)}. \tag{7.65}$$

The range of the worldsheet coordinate is $-s/2 < \sigma < s/2$, where s is to be found dynamically. The angles θ and ϕ parameterizing the cusp enter the string solution through the boundary conditions $\phi(\pm s/2) = \pm(\pi - \phi)/2$ and $f(\pm s/2) = \pm\theta/2$. The equations of motion and Virasoro constraints lead to the following system of equations (see appendix

E of [91] for more details, also [182]):

$$h_1(\gamma, l_\theta) = h_1(\kappa, l_\phi), \tag{7.66}$$

$$h_2(\gamma, l_\theta) = \theta, \;\; h_2(\kappa, l_\phi) = \phi, \tag{7.67}$$

$$h_3(\gamma, l_\theta) = L/g, \;\; h_3(\kappa, l_\phi) = E/g, \tag{7.68}$$

where

$$h_1(\gamma, l) = \frac{2\sqrt{2}}{\sqrt{\gamma^2+k^2+1}}\,\mathbb{K}\left(\frac{-k^2+\gamma^2+1}{k^2+\gamma^2+1}\right), \tag{7.69}$$

$$h_2(\gamma, l) = \frac{2l}{k(1+k^2-\gamma^2)}\left[(1+\gamma^2+k^2)\,\Pi\left(\frac{k^2-2l^2-\gamma^2+1}{2k^2}\middle|\frac{k^2-\gamma^2-1}{2k^2}\right) - \right.$$
$$\left. -2\gamma^2\,\mathbb{K}\left(\frac{k^2-\gamma^2-1}{2k^2}\right)\right], \tag{7.70}$$

$$h_3(\gamma, l) = -2\sqrt{2}\,\frac{\sqrt{\gamma^2+k^2+1}}{\gamma}\left[\mathbb{E}\left(\frac{-k^2+\gamma^2+1}{k^2+\gamma^2+1}\right) - \mathbb{K}\left(\frac{-k^2+\gamma^2+1}{k^2+\gamma^2+1}\right)\right], \tag{7.71}$$

$$k^4 = \gamma^4 - 2\gamma^2 + 4\,\gamma^2 l^2 + 1.$$

One can see that the variables θ, l_θ, γ and L govern the S^3 part of the solution, while ϕ, l_ϕ, κ and E are their analogues for AdS_3. The two parts of the solution are connected only by the Virasoro condition which leads to (7.66). We are interested in the limit when $\theta \approx \phi$. In this limit the two groups of variables responsible for S^3 and AdS_3 parts of the solution become close to each other, namely $l_\theta \approx l_\phi$ and $E \approx L$. The classical dimension of the observable W_L is L, hence the cusp anomalous dimension should be matched with $E - L$. To find $E - L$ we linearize the system (7.69),(7.70),(7.71) around $\phi \approx \theta$, which yields

$$E - L = (\phi - \theta)\left|\frac{\partial(h_3, h_1)}{\partial(l, \kappa)}\right| \Big/ \left|\frac{\partial(h_2, h_1)}{\partial(l, \kappa)}\right|. \tag{7.72}$$

Plugging in here the explicit form of h_1, h_2 and h_3 one gets as a result an extremely complicated expression with a lot of elliptic functions. However, there exists a parametrization in which the result looks surprisingly simple: this parametrization comes from comparison of the string conserved charges with the corresponding quantities of the algebraic curve. One can notice that the equations for θ and L/g in the end of the last section have the same structure as the equations (7.67) and (7.68). Indeed, it is possible to match them precisely if one chooses the correct identification of parameters of the string solution l_θ, γ with the parameters of the algebraic curve r, ψ. We used the elliptic identities presented in appendix C to bring the equations to identical form after the following identifications

$$\gamma = \frac{2r}{\sqrt{r^4 - 2r^2\cos 2\psi + 1}}, \;\; l_\theta = \frac{(r^2-1)\cos\psi}{\sqrt{r^4 - 2r^2\cos 2\psi + 1}}. \tag{7.73}$$

As another confirmation of correctness of this identification, after plugging it into (7.72) the complicated expression reduces to the following simple formula for the classical energy

$$E - L = g(\phi - \theta)(r - 1/r)\cos\psi. \tag{7.74}$$

Notice that this can be rewritten as a sum over the branch points of the algebraic curve

$$E - L = \frac{g}{2}(\phi - \theta)\sum_i b_i, \tag{7.75}$$

where $b_i = \{r\, e^{i\psi}, r\, e^{-i\psi}, -1/r\, e^{i\psi}, -1/r\, e^{-i\psi}\}$.

7.4.3 The energy from the quasimomentum

In this section we will find the classical limit of the cusp anomalous dimension from the algebraic curve. At large L the formula (6.5) can be rewritten as

$$\Gamma_L(g) = \frac{\phi - \theta}{4}\partial_\theta \partial_L \det \mathcal{M}_{2L}. \tag{7.76}$$

Use the integral representation (7.41) for $\det \mathcal{M}_L$ we can notice that

$$\partial_\theta \log\det \mathcal{M}_L = \left\langle 2g \sum_{i=1}^{2L}(x_i - 1/x_i) \right\rangle, \tag{7.77}$$

where by the angular brackets we denoted an expectation value in the matrix model with the partition function (7.41). In the quasiclassical approximation the expectation value is determined by the saddle-point, i.e. the previous expression is equal to $2g\sum\limits_{i=1}^{2L}(x_i - 1/x_i)$, where the roots x_i are the solutions of the saddle-point equation (7.47). Since the set of the roots has a $x \to -1/x$ symmetry, the two terms in the sum give the same contribution. Thus

$$\partial_\theta \log\det \mathcal{M}_L = -4g\sum_{i=1}^{2L}\frac{1}{x_i} = 8\, g\, L\, G(0), \tag{7.78}$$

where we used the resolvent (7.49).

Using the relation (7.48) between the resolvent and the quasimomentum we find $G(0) = \frac{g}{L}\,(p''(0)/4 - \theta)$, so the final expression for the cusp anomalous dimension in terms of the quasimomentum is

$$\Gamma_L(g) = -\frac{g^2}{2}\left(p''_{2L+1}(0) - p''_{2L-1}(0)\right) \tag{7.79}$$

or, neglecting $1/L$ corrections

$$\Gamma_L(g) = -\frac{g^2}{2}\partial_L p''_{2L}(0). \tag{7.80}$$

The formula for $p(x)$ presented in the previous section is given in terms of the parameters of the branch points r and ψ. They are implicitly defined through L/g and θ by the equations (7.62) and (7.63). In order to get Γ_L we express ∂_L though ∂_r and ∂_ψ and then apply (7.80) to (7.59). Finally we obtain a very simple result in terms of r and ψ

$$\Gamma_L(g) = g(\phi - \theta)\,(r - 1/r)\cos\psi, \tag{7.81}$$

which exactly coincides with the calculation from the string solution!

Comparison with the small angle limit Here we will check our formula (7.81) in the limit $\phi = 0$ and $\theta \to 0$ considered in section E.2 of [91]. As the angles go to zero, the branch points approach the unit circle: $r \to 1$, thus the formula (7.81) gives

$$\Gamma_L(g) = 2\,g\,(\theta - \phi)(r - 1)\cos\psi. \tag{7.82}$$

In this limit $r - 1 \propto \theta$, and the coefficient of proportionality can be found by expanding the equation (7.63) for θ around $r = 1$:

$$2(1 - r)\frac{\mathbb{E}\left(\sin^2\psi\right)}{\cos\psi} = \theta. \tag{7.83}$$

and using this formula to express $r - 1$ in (7.82) we get

$$\Gamma_L(g) = g\,(\theta - \phi)\theta\,\frac{\cos^2\psi}{2\mathbb{E}\left(\sin^2\psi\right)}. \tag{7.84}$$

Now we are almost ready to compare with the result of [91] except for one detail: since our result is written in the leading order in $\theta - \phi$, the terms of order $\mathcal{O}(\theta^2)$ might be lost, whereas the result of [91] is of order $\mathcal{O}(\theta^2)$ itself. To make the comparison possible, let us rewrite the last formula keeping track of all the infinitesimally small quantities

$$\Gamma_L(g) = g\,(\theta - \phi)(\theta + \mathcal{O}(\theta^2))\,\frac{\cos^2\psi}{2\mathbb{E}\left(\sin^2\psi\right)} + \mathcal{O}((\theta - \phi)^2). \tag{7.85}$$

On the other hand, we know [95] that at $\theta \approx \phi$ the energy behaves as

$$\Gamma_L(g) = (\theta^2 - \phi^2)A(\phi) + \mathcal{O}((\theta^2 - \phi^2)^2). \tag{7.86}$$

From comparing the last two expressions, one can conclude that

$$\Gamma_L(g) = g\,(\theta - \phi)(\theta + \phi)\,\frac{\cos^2\psi}{2\mathbb{E}\left(\sin^2\psi\right)} + \mathcal{O}((\theta - \phi)^2). \tag{7.87}$$

In this expression we can take the limit $\phi = 0$, $\theta \to 0$ and get the result

$$\Gamma_L(g) = g\,\theta^2\,\frac{\cos^2\psi}{2\mathbb{E}\left(\sin^2\psi\right)}, \tag{7.88}$$

which perfectly agrees with (190) of [91].

7.5 Comment on discrete symmetry of $1/L^2$ expansion and Matrix Models

Soon after our result (6.91) appeared in [10], a curious property of its strong coupling expansion was pointed out in [173]. Namely, it was noticed that the expansion (6.113) is odd under a discrete transformation $L \to -1-L$, $g \to -g$. This symmetry has implications for the expansion of the energy in the quasiclassical limit, when $L \to \infty$ and $\mathcal{L} = L/g$ is fixed:

$$\frac{\Gamma(g)}{\theta - \phi} = g \sum_{p=0}^{\infty} g^{-p} b_p(\mathcal{L}) + \text{non-perturbative terms.} \tag{7.89}$$

Namely, the odd terms of the expansion are determined by the even ones

$$b_1(\mathcal{L}) = \frac{1}{2}\frac{d}{d\mathcal{L}} b_0(\mathcal{L}) \tag{7.90}$$

$$b_3(\mathcal{L}) = \frac{1}{2}\frac{d}{d\mathcal{L}} b_2(\mathcal{L}) - \frac{1}{24}\frac{d^3}{d\mathcal{L}^3} b_0(\mathcal{L}) \tag{7.91}$$

$$b_5(\mathcal{L}) = \frac{1}{2}\frac{d}{d\mathcal{L}} b_4(\mathcal{L}) - \frac{1}{24}\frac{d^3}{d\mathcal{L}^3} b_2(\mathcal{L}) + \frac{1}{240}\frac{d^5}{d\mathcal{L}^5} b_0(\mathcal{L}) \tag{7.92}$$

$$\dots$$

The symmetry was noticed empirically, although the proof was missing; now we have at least two ways to prove it. The first one is based on QSC[44]: as we have seen in this thesis before, L only enter the QSC equation through the asymptotics of $\mathbf{P}_a$. Looking at formulas (4.50), (4.51) for the leading coefficients and (4.48) for powers, one can easily notice that the transformation $J \to -1 - J$ just swaps $\mathbf{P}_1$ with $\mathbf{P}_4$ and $\mathbf{P}_2$ with $\mathbf{P}_3$. Thus this discrete transformation is the symmetry of the system.

The other way to understand the symmetry in question is from the point of view of matrix model reformulation described in this chapter[45]. It is well known that large N expansion of expectation values in matrix models goes in $1/N^2$, where N is the size of the matrix, thus being invariant under $N \to -N$ symmetry. Since the result (7.89) involves matrix integrals of sizes $2L+1$ and $2L-1$, one would expect that this would translate into a discrete symmetry in L. Let us make the argument precise now. Suppose L is large but finite and come back to the formula (7.79). To all orders in $1/N$ the quasimomentum $p_N(x)$ can be computed as one-point function in a matrix model of size $N+1$ and thus it

[44] The version of QSC relevant here is so-called "boundary" or twisted QSC [166, 109] (see also section 6.3)

[45] We thank Ivan Kostov for the idea that the discrete symmetry in question should be related to the $1/N^2$ expansion in Matrix Models

has expansion in $1/(N+1)^2$:

$$p(v,g,N) = \sum_{m=0}^{\infty} (N+1)^{-2m} p^{(m)}\left(v, \frac{N+1}{2g}\right) \tag{7.93}$$

Then plugging the expansion (7.93) into (7.79) we get

$$\frac{\Gamma_L}{\phi-\theta} = -\frac{g^2}{2}\frac{\partial^2}{\partial v^2}|_{v=0}\left[p(v,g,2L+1) - p(v,g,2L-1)\right] = \tag{7.94}$$

$$= -\frac{g^2}{2}\frac{\partial^2}{\partial v^2}|_{v=0} \sum_{m=0}^{\infty}\left[(2g\mathcal{L}+2)^{-2m} p^{(m)}\left(v, \mathcal{L}+\frac{1}{g}\right) - (2g\mathcal{L})^{-2m} p^{(m)}\left(v,\mathcal{L}\right)\right] \tag{7.95}$$

Expanding it in g we get

$$\frac{\Gamma_L}{\phi-\theta} = \frac{\partial^2}{\partial v^2}|_{v=0}\left[-\frac{1}{2}g\partial_{\mathcal{L}} p^{(0)}(v,\mathcal{L}) - \frac{1}{4}\partial^2_{\mathcal{L}} p^{(0)}(v,\mathcal{L}) + \right.$$
$$\left. + g^{-1}\left(\frac{p^{(1)}(v,\mathcal{L})}{4\mathcal{L}^3} - \frac{\partial_{\mathcal{L}} p^{(1)}(v,\mathcal{L})}{8\mathcal{L}^2} - \frac{\partial^3_{\mathcal{L}} p^{(0)}(v,\mathcal{L})}{12}\right) + \dots\right] \tag{7.96}$$

One can identify coefficients of the expansion (7.96) with b_i from (7.89) and see that b_i generated in this way automatically satisfy the relations (7.90)-(7.92).

7.6 The one-loop correction to the classical energy

The discrete symmetry of the formula for $\Gamma_L(g)$ found in [173] and proven in the previous section allows us to express the even terms in the expansion (7.89) through the odd ones. In particular, b_1 can be obtained from b_0 by differentiating with respect to $\mathcal{L}$. Since the classical energy is

$$\Gamma^{cl}_L(g) = g\,(\phi-\theta)\,(r-1/r)\cos\psi \tag{7.97}$$

by differentiating it with respect to $\mathcal{L}$ we find that the perturbative part of energy in the first two orders in the classical expansion is

$$\Gamma_L(g) = g\,(\phi-\theta)\,(r-1/r)\cos\psi\left(1+\frac{1}{g}f(r,\psi)\right), \tag{7.98}$$

where

$$f(r,\psi) = \frac{r+1/r}{4}\frac{\left|r^2e^{2i\psi}+1\right|^2 K_1 - r^2\left|r+\frac{1}{r}+e^{i\psi}-e^{-i\psi}\right|^2 E_1}{\left|\left(r+\frac{1}{r}\right)\left(r^2e^{2i\psi}-1\right)E_1 - \left(r-\frac{1}{r}\right)\left(r^2e^{2i\psi}+1\right)K_1\right|^2}, \tag{7.99}$$

and E_1, K_1 are defined in (7.57). We have checked this formula and the classical energy (7.74) against a numerical extrapolation of the exact expression (6.5) and found an agreement up to more than thirty digits.

8 Solving QSC numerically

In the previous chapters we have described several applications of QSC which allow to obtain certain results analytically. Naturally, another important range of applications of the QSC is the numerical investigation of the spectrum at finite coupling.

Spectrum of $\mathcal{N} = 4$ SYM at finite coupling was investigated numerically before by solving the TBA equation. Although this approach was restricted to only a few operators [46] and low precision and convergence rate, it nevertheless gave several very important results. In particular, the anomalous dimension of a nonprotected (Konishi) operator at finite coupling was computed in [156]. Numerics also gave a prediction for the strong coupling Konishi anomalous dimension which was later confirmed by several methods [183, 184, 148, 115, 9, 147, 149, 185]. The main goal of the work presented in this chapter, based on [12], is to remove the limitations of the previously known methods by developing an algorithm for a numerical solution of the QSC.

The low precision and performance of the TBA-based approach was mainly due to the complicated infinite system of equations and cumbersome integration kernels. The QSC includes only a few unknown functions and thus can be expected to give highly precise numerical results. However, the QSC equations are functional equations supplemented with some analyticity constraints of a novel type which makes it a priori a nontrivial task to develop a robust numerical approach.

Below we first describe the method and then illustrate it by a few examples. Among the several equivalent formulations of the QSC we identified the equations which are best-suited for numerical solution. Even when implemented in relatively slow *Mathematica*, our algorithm gives a massive increase in efficiency compared to the TBA or FiNLIE systems [156, 94, 149, 165]. With one iteration taking about 2 seconds we only need $2-3$ iterations (depending on the starting points) to reach at least 10 digits of precision. Quite expectedly, the precision gets lost for very large values of the 't Hooft coupling. Nevertheless, without any extra effort we reached $\lambda \sim 1000$ keeping a good precision, which should be more than enough for any practical goal.

Not only does our approach work for any finite length single trace operator and in particular for any value of the spin, it also works with minimal changes even away from

[46] Only for a few operators the complicated structure of the "driving terms" was deduced explicitly in a closed form. Even for those operators the driving terms may change depending on the value of the coupling.

integer quantum numbers! We demonstrate this in the particularly interesting case of the $\mathfrak{sl}(2)$ twist-two operators. Their anomalous dimension analytically continued to complex values of the spin S is known to have a very rich structure, in particular the region $S \simeq -1$ is described by BFKL physics (see chapter 9). As we show, within the framework of QSC it is not hard to specify any value of the Lorentz spin S as the conserved charges enter the equations through the asymptotics which can in principle take any complex values. Then we can compute the analytically continued scaling dimension Δ *directly* for complex S (or even interchange their roles and study S as a function of Δ). The result of this calculation can be seen on Fig. 11.

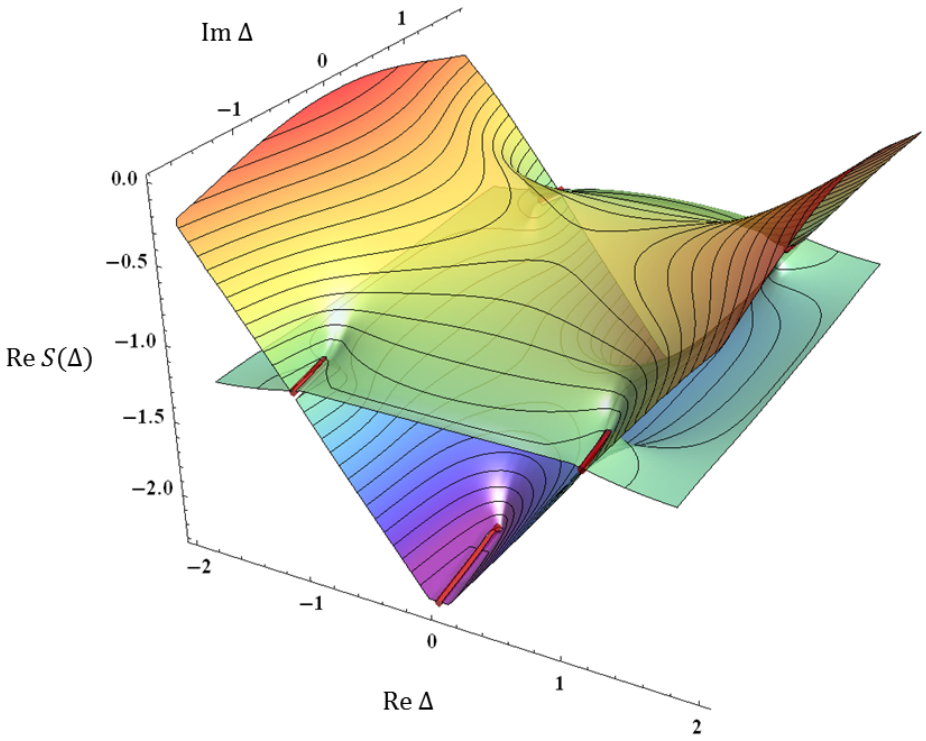

Figure 11: **Riemann surface of the function $S(\Delta)$ for twist-two operators.** Plot of the real part of $S(\Delta)$ for complex values of Δ, generated from about 2200 numerical data points for $\lambda \approx 6.3$. We have mapped two Riemann sheets of this function. The thick red lines show the position of cuts. The upper sheet corresponds to physical values of the spin. Going through a cut we arrive at another sheet containing yet more cuts.

8.1 Method description

8.1.1 Step 1: Find $\mathcal{Q}_{a|i}$

The quantity $\mathcal{Q}_{a|i}$, defined in (4.9), is at the heart of our procedure. In this section we will demonstrate how this set of 16 functions can be found for arbitrary $\mathbf{P}_a$ and $\mathbf{P}^a$. In this procedure the precise ansatz for $\mathbf{P}$ is not important. However, as we will see later, we should be able to compute the combination $\mathbf{P}_a(u)\mathbf{P}^b(u)$ on the upper sheet for u with large imaginary part. In practice it is not difficult to come up with an ansatz for $\mathbf{P}_a$. They have power-like behavior at infinity and one Zhukovsky cut on the main sheet. This implies that on the main sheet they can be represented as (truncated) series in $x(u)$

$$\mathbf{P}_a(u) = \sum_{n=\tilde{M}_a}^{\infty} c_{a,n} x^n(u) \ . \tag{8.1}$$

Using this representation for $\mathbf{P}_a$ we can efficiently evaluate the combination above everywhere on the upper sheet numerically.

The process of finding $\mathcal{Q}_{a|i}$ is divided into two stages. Firstly, we find a good approximation for $\mathcal{Q}_{a|i}$ at some u with large imaginary part (in the examples we will need Im $u \sim 10 - 100$). At the next step we apply to this large u approximation of $\mathcal{Q}_{a|i}$ a recursive procedure which produces $\mathcal{Q}_{a|i}$ at $u \sim 1$.

Large u approximation. For Im $u \sim 10 - 100$ we can build the solution of (8.3) as a $1/u$ expansion. This is done by plugging the (asymptotic) series expansion of $\mathcal{Q}_{a|i}$

$$\mathcal{Q}_{a|i}(u) = u^{\hat{M}_i - \tilde{M}_a} \sum_{n=0}^{N} \frac{B_{a|i,n}}{u^n}, \tag{8.2}$$

where N is some cutoff (usually $\sim 10 - 20$), into

$$\mathcal{Q}_{a|i}(u + \tfrac{i}{2}) - \mathcal{Q}_{a|i}(u - \tfrac{i}{2}) = -\mathbf{P}_a(u)\mathbf{P}^b(u)\mathcal{Q}_{b|i}(u + \tfrac{i}{2}), \tag{8.3}$$

which is a consequence of (4.8) and (4.11). This produces a simple linear problem for the coefficients $B_{a|i,n}$, which can be even solved analytically to a rather high order. The leading order coefficients of $\mathcal{Q}_{a|i}$ can be chosen arbitrarily. After that the linear system of equations becomes non-homogeneous and gives a unique solution in a generic case.[47]

[47] The matrix of this system may become non-invertible unless certain constraint (which is not hard to find) on the coefficients $c_{a,n}$ is satisfied. This constraint is fulfilled trivially for LR-symmetric sector, which contains all our operators in this chapter. There is also no such problem for the situation with generic twists (similar to $\beta-$ or γ-deformations, see the review [186]). Adding twists should correspond

Finite u approximation. Once we have a good approximation at large u we can simply use the equation (8.3) to recursively decrease u. Indeed, defining a 4×4 matrix

$$U_a{}^b(u) = \delta_a^b + \mathbf{P}_a(u)\mathbf{P}^b(u) \tag{8.4}$$

we have

$$\mathcal{Q}_{a|i}(u - \tfrac{i}{2}) = U_a{}^b(u)\mathcal{Q}_{b|i}(u + \tfrac{i}{2}). \tag{8.5}$$

Iterating this equation we get, in matrix notation

$$\mathcal{Q}_{a|i}(u - \tfrac{i}{2}) = [U(u)U(u+i)\dots U(u+iN)]_a{}^b \; \mathcal{Q}_{b|i}(u + iN + \tfrac{i}{2}) \; . \tag{8.6}$$

For large enough N we can use the large u approximation (8.2) for $\mathcal{Q}_{b|i}$ in the right hand side. As a result we obtain the functions $\mathcal{Q}_{a|i}$ for finite u with high precision.

8.1.2 Step 2: Recover ω_{ab}

Let us rewrite here (4.10) and its consequence:

$$\mathbf{Q}_i = -\mathbf{P}^a \mathcal{Q}^+_{a|i}, \tag{8.7}$$

$$\tilde{\mathbf{Q}}_i = -\tilde{\mathbf{P}}^a \mathcal{Q}^+_{a|i}. \tag{8.8}$$

Using these two equations and our numerical approximation for $\mathcal{Q}_{a|i}(u)$ we can compute $\mathbf{Q}_i$ and $\tilde{\mathbf{Q}}_i$ and plug them into the discontinuity of ω_{ij} (4.25). After that we can recover ω_{ij} from its discontinuity modulo an analytic function using its spectral representation

$$\omega_{ij}(u) = \frac{i}{2} \int_{-2g}^{2g} dv \coth(\pi(u-v)) \left[\tilde{\mathbf{Q}}_i(v)\mathbf{Q}_j(v) - \mathbf{Q}_i(v)\tilde{\mathbf{Q}}_j(v)\right] + \omega^0_{ij}(u) \tag{8.9}$$

where the "zero mode" $\omega^0_{ij}(u)$ is the analytic part of ω_{ij} — it has to be periodic, antisymmetric in i, j and should not have cuts. We will fix it below. We note that we only need to know values of $\mathbf{Q}$ and $\tilde{\mathbf{Q}}$ on the cut. In our implementation we use a finite number of sampling points on the cut given by zeros of Chebyshev polynomials. One can then fit the values of $\tilde{\mathbf{Q}}_i\mathbf{Q}_j - \mathbf{Q}_i\tilde{\mathbf{Q}}_j$ at those points with a polynomial times the square root $\sqrt{u^2 - 4g^2}$. After that we can use precomputed integrals of the form $\int_{-2g}^{2g} \coth(\pi(u_i - v))v^n\sqrt{v^2 - 4g^2}dv$ to evaluate (8.9) with high precision by a simple matrix multiplication, which produces the result at the sampling points u_A in an instant.

[8] to allowing exponential factors $e^{\alpha_a u}, e^{\beta_i u}$ in the asymptotics of $\mathbf{P}_a$ and $\mathbf{Q}_i$, making everything less degenerate and providing a useful regularization. QSC with twists is considered in [166, 109] and briefly in section 6.3 of this thesis.

One more point to mention here is that in our implementation we only compute $\omega_{ij}^{reg} = \frac{1}{2}(\omega_{ij} - \tilde{\omega}_{ij})$ at the sampling points to avoid the problem of dealing with the singularity of the integration kernel. Note that ω_{ij}^{reg} can be used instead of ω_{ij} in the equations like (4.25),(4.24), because the difference is proportional to $\mathbf{Q}_i\mathbf{Q}^i$ which is zero due to orthogonality relations (4.13).

Finding zero modes. It only remains to fix $\omega_{ij}^0(u)$. First we notice that for all physical operators ω_{ij} should not grow faster than constant at infinity [8]. As the integral part of (8.9) does not grow either and since $\omega_{ij}^0(u)$ is i-periodic it can only be a constant. To fix this constant we use the following observation [8]: the constant matrix α_{ij}^+ which ω_{ij} approaches at $u \to +\infty$ and the constant matrix α_{ij}^- which it reaches at $u \to -\infty$ are restricted by the quantum numbers. To see this we can pick some point on the real axis far away from the origin and shift it slightly up into the complex plane, then from (4.24) we have

$$\omega_{ij}\mathbf{Q}^j(u+i0) = \alpha_{ij}^+\mathbf{Q}^j(u+i0) = \tilde{\mathbf{Q}}_i(u+i0) = \mathbf{Q}_i(u-i0). \tag{8.10}$$

Similarly for $-u$ we get

$$\alpha_{ij}^-\mathbf{Q}^j(-u+i0) = \mathbf{Q}_i(-u-i0). \tag{8.11}$$

Next, notice that since $\mathbf{Q}^j$ is analytic everywhere except the cut on the real axis, it can be replaced by its asymptotics above the real axis, i.e. $\mathbf{Q}^j(u+i0) \sim B^j u^{-\hat{M}_j}$, and also $\mathbf{Q}^j(-u+i0) \sim B^j u^{-\hat{M}_j} e^{-i\pi\hat{M}_j}$, as we find from the previous expression by a rotation by π in the complex plane. As a result we get the asymptotics of $\mathbf{Q}_i$ at infinities and slightly below the real axis

$$\mathbf{Q}_i(u-i0) = \alpha_{ij}^+ B^j u^{-\hat{M}_j} \;\;,\;\; \mathbf{Q}_i(-u-i0) = \alpha_{ij}^- B^j u^{-\hat{M}_j} e^{-i\pi\hat{M}_j} \;. \tag{8.12}$$

Now we can analytically continue the first equation in the lower half plane and get

$$\mathbf{Q}_i(-u-i0) = \alpha_{ij}^+ B^j u^{-\hat{M}_j} e^{+i\pi\hat{M}_j} \;. \tag{8.13}$$

Combining this with the second one we find

$$\alpha_{ij}^+ = \alpha_{ij}^- e^{-2i\pi\hat{M}_j} \;. \tag{8.14}$$

At the same time from (8.9) we get

$$\alpha_{ij}^\pm = \pm I_{ij} + \omega_{ij}^0 \;\;,\;\; I_{ij} \equiv \frac{i}{2}\int_{-2g}^{2g} dv \left[\tilde{\mathbf{Q}}_i(v)\mathbf{Q}_j(v) - \mathbf{Q}_i(v)\tilde{\mathbf{Q}}_j(v)\right], \tag{8.15}$$

which implies that

$$\omega^0_{kl} = -iI_{kl} \cot \pi \hat{M}_l. \tag{8.16}$$

We see that the zero modes can be also computed from the values of $\mathbf{Q}$ and $\tilde{\mathbf{Q}}$ on the cut.

Note also that the right hand side is not explicitly antisymmetric. Imposing the antisymmetry gives

$$I_{kl}(\cot \pi \hat{M}_l - \cot \pi \hat{M}_k) = 0, \tag{8.17}$$

so either $I_{kl} = 0$ or $\cot \pi \hat{M}_l = \cot \pi \hat{M}_k$. As Pf $\omega = 1$, all I_{kl} can not be equal to zero simultaneously. Having I_{kl} non-zero implies quantization of charges: for example, the choice $I_{12} \neq 0$ and $I_{34} \neq 0$, which is consistent with perturbative data, requires $\cot \pi \hat{M}_1 = \cot \pi \hat{M}_2$ and $\cot \pi \hat{M}_3 = \cot \pi \hat{M}_4$, and so S_1, S_2 have to be integer or half integer. In section 8.3 we will see how to relax this condition and do an analytic continuation in the spin S_1 to the whole complex plane.

8.1.3 Step 3: Solve the optimization problem

Having ω_{ij} and $\mathbf{Q}_{a|i}$ at hand we can try to impose the remaining equations of the QSC (4.24). We notice that there are two different ways of computing $\tilde{\mathbf{Q}}_i$, which should give the same result when we have a true solution: (8.8) and (4.24). Their difference, which at the end should be zero, is

$$F_i(u) = \tilde{\mathbf{P}}^a(u)\ \mathcal{Q}_{a|i}(u + i/2) + \omega_{ij}(u)\ \mathcal{Q}^{a|j}(u + i/2)\mathbf{P}_a(u)\ . \tag{8.18}$$

The problem is now to find $c_{a,n}$ for which $F_i(u)$ is as close as possible to zero. Here we have some freedom in how to measure its deviation from zero, but in our implementation we use the sum of squares of F_i at the sampling points u_A. Then the problem reduces to the classical optimization problem of the least squares type. In our implementation we found it to be particular efficient to use the Levenberg-Marquardt algorithm (LMA), which we briefly describe in the next section. The LMA is known to have a Q-quadratic convergence rate, which means that the error ϵ_n decreases with the iteration number n as fast as $e^{-c\,2^n}$. The convergence is indeed so fast that normally it is enough to do 2 or 3 iterations to get the result with 10 digits precision. We give some examples in the next section.

Levenberg-Marquardt algorithm Our problem can be reformulated as follows: given a vector function $f_i(c_a)$ of a set of variables c_a (which we can always assume to be real)

find the configuration which minimizes

$$S(c_a) \equiv \sum_i |f_i(c_a)|^2 \ . \tag{8.19}$$

Assuming we are close to the minimum we can approximate f_i by a linear function:

$$f_i(\tilde{c}_a) \simeq f_i(c_a) + (\tilde{c}_a - c_a) J_{ai} \ \ , \ \ J_{ai} \equiv \partial_{c_a} f_i(c_a) \tag{8.20}$$

which gives the following approximation for $S(\tilde{c}_a)$:

$$S(\tilde{c}_a) = [f_i(c_a) + (\tilde{c}_a - c_a) J_{ai}] \left[\bar{f}_i(c_a) + (\tilde{c}_a - c_a) \bar{J}_{ai}\right] \tag{8.21}$$

The approximate position of the minimum is then at $\partial_{\tilde{c}_a} S = 0$ for which we get

$$J_{ai} \left[\bar{f}_i(c_a) + (\tilde{c}_a - c_a) \bar{J}_{ai}\right] + [f_i(c_a) + (\tilde{c}_a - c_a) J_{ai}] \, \bar{J}_{ai} = 0 \tag{8.22}$$

from which, in matrix notation,

$$\tilde{c} = c - (J\bar{J}^T + \bar{J}J^T)^{-1} (\bar{J} f + J \bar{f}) \ . \tag{8.23}$$

We see that for this method we should also know the derivatives of our $F_a(u)$ w.r.t. the parameters $c_{a,n}$, which in our implementation is found numerically by shifting a bit the corresponding parameter.

In some cases, when the starting points are far away from the minimum, the above procedure may start to diverge. In such cases one can switch to a slower, but more stable, gradient descent method for a few steps. The Levenberg-Marquardt algorithm provides a nice way to interpolate between the two algorithms by inserting a positive parameter Λ into the above procedure,

$$c_{n+1} = c_n - (J\bar{J}^T + \bar{J}J^T + \Lambda I)^{-1} (\bar{J} f + J \bar{f}) \ . \tag{8.24}$$

The point is that for large Λ this is equivalent to the gradient descent method. Thus one can try to increase Λ from its zero value until $S(c_{n+1}) < S(c_n)$ and only then accept the new value c_{n+1}. This helps a lot to ensure stable convergence.

In the next section we demonstrate the performance of our numerical method by applying it to the twist-two operators in $\mathfrak{sl}(2)$ sector.

8.2 Implementation for the $\mathfrak{sl}(2)$ sector and comparison with existing data

The $\mathfrak{sl}(2)$ sector in the QSC framework Although our method can be used for any state of the $\mathcal{N}=4$ SYM theory, the examples we provide in this thesis are for left-right symmetric states, more precisely for the states in the $\mathfrak{sl}(2)$ subsector,

$$\mathcal{O} = \mathrm{Tr}\left(D^S Z^L\right) + \ldots, \tag{8.25}$$

described in section 4.4. In this section we will discuss the physical operators which have integer spin, and as a demonstration of our numerical method apply it to the Konishi operator. Then in section 8.3 we will show how the algorithm is modified for states with non-integer S.

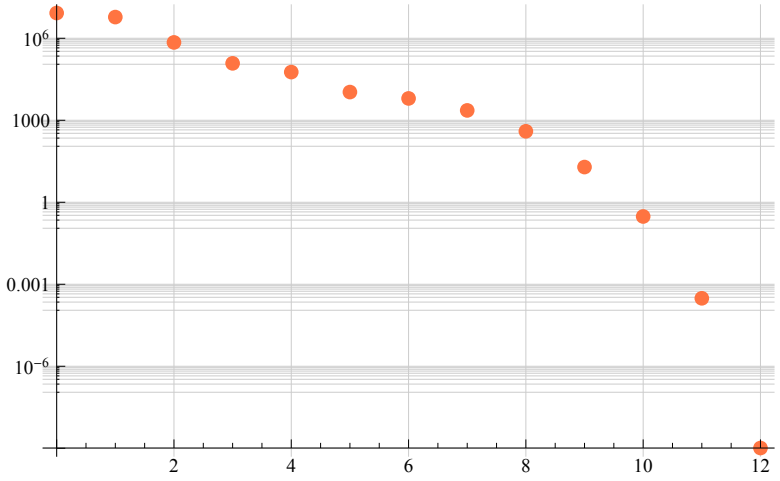

Figure 12: **Convergence of the algorithm.** The error ϵ_n as measured by the value of (8.19) reduces at the quadratic rate $\epsilon_n \sim e^{-c\,2^n}$ as a function of the iteration number. In most cases our program managed to find the solution from a very remote starting point. On the picture we started from all free parameters $c_{a,n}$ set to zero and with the initial value for the energy $\Delta_0 = 4.1$. After 12 iterations it correctly reproduced $\Delta = 4.4188599$ at $\lambda = 16\pi^2(0.2)^2 \simeq 31.6$. With each iteration taking about 1.5sec the whole procedure took about 20 sec on a Laptop with Intel i7 2.7GHz processor.

Implementation for Konishi Here we discuss the convergence on a particular example of an operator belonging to the $\mathfrak{sl}(2)$ sector — the Konishi operator which corresponds to $S=2, L=2$. The reason we start from this operator is because it is very well studied both analytically at weak and strong coupling and also numerically. So we will have lots of data to compare with.

To start the iteration process described in the previous sections, we need some reasonably good starting points for the coefficients $c_{a,n}$. For the iterative methods, like, for

$\frac{\sqrt{\lambda}}{4\pi}$	$\Delta_{S=2}(\lambda)$	$\frac{\sqrt{\lambda}}{4\pi}$	$\Delta_{S=2}(\lambda)$
0.1	4.115 506 377 945	0.2	4.418 859 880 802
0.3	4.826 948 662 284	0.4	5.271 565 182 595
0.5	5.712 723 424 787	0.6	6.133 862 814 488
0.7	6.531 606 077 852	0.8	6.907 504 206 024
0.9	7.264 169 587 439	1.	7.604 070 717 047

Table 2: Conformal dimension of Konishi operator

instance, Newton's method, good starting points are normally very important. Depending on them the procedure may converge very slowly or even diverge. We made a rather radical test of the convergence of our method by setting all coefficients to zero except for the leading ones, which are fixed by the charges. For Δ we took the initial value 4.1 at the value of 't Hooft coupling $g = 0.2$. To our great surprise it took only 12 steps to converge from the huge value of $S(c_a) \sim 10^{+7}$ (defined in (8.19)) to $S(c_a) \sim 10^{-9}$. The whole process took about 20 seconds on a usual laptop (see Fig. 12), producing the value $\Delta = 4.4188599$, consistent with the best TBA estimates [156, 149].

After that we used the obtained coefficients as starting points for other values of the coupling to produce Tab. 8.2. All the values obtained are consistent with the TBA results within the precision of the latter, being considerably more accurate at the same time.

The reason for such an excellent convergence is the Q-quadratic convergence rate of the algorithm we use. It means that the number of exact digits doubles with each iteration, or that the error decreases as $e^{-c\,2^n}$ at the step n, if the starting point is close enough. What is perhaps surprising is that the algorithm converges from a very remote starting point.

Another indicator of the convergence is the plot of $\tilde{\mathbf{Q}}_a$ computed in two different ways, i.e. (8.8) and (4.24). On the true solution of the QSC both should coincide. On Fig. 5 we show how fast the difference between them vanishes with iterations, i.e. how fast we approach the exact solution of the QSC.

In the next section we discuss the analytic continuation in S away from its integer values. This is an important calculation which bring us to a highly accurate numerical estimate for the pomeron intercept at finite coupling in section 9.5 — a quantity which can be studied exclusively by our methods.

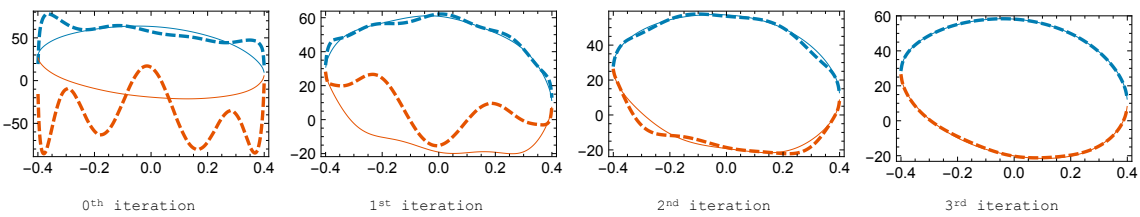

Figure 13: **Q-functions at the first several iterations.** Here we show how $\mathbf{Q}_3$ converges to the solution in just four iterations when calculating the Konishi anomalous dimension. At each picture solid and dashed blue lines show $\mathbf{Q}_3$ slightly below the cut calculated with (4.24) and (8.8) respectively, which should coincide on the solution. Red lines show the same slightly above the cut.

8.3 Generalization to non-integer spin

In this section we explain which modifications are needed in order to extend our method to non-integer values of spin S, and give a specific example of a calculation for such S.

8.3.1 Modification of the algorithm for non-integer spin

First we need to discuss how non-integer S modifies the procedure of fixing zero modes of the ω's described in section 8.1.2. As we already know from chapter 5, the analytic continuation to non-integer S changes the asymptotic behavior of ω_{ij}, μ_{ab}, and Q-functions at large u. The modification of μ_{ab} was described in section 5.2. Since our algorithm works more with the $\mathbf{Q}\omega$-system than with the $\mathbf{P}\mu$-system, we need to understand the asymptotics of ω_{ij} for non-integer S. As described in [9, 110, 15], for non-integer S some components of ω have to grow exponentially (as opposed to constant asymptotics for integer S). Without this modification the system has no solution: indeed, in section 8.1.3 we assumed constant asymptotics of all ω's and derived the quantization condition for global charges.

A minimal modification would be to allow exponential asymptotics in one of the components of ω. In order to understand which of the components can it be, let us recall the Pfaffian constraint satisfied by ω_{ij}

$$\mathrm{Pf}\,\omega = \omega_{12}\omega_{34} - \omega_{13}\omega_{24} + \omega_{14}^2 = 1. \tag{8.26}$$

First, it is clear ω_{14} alone can not have exponential asymptotics. Second, in the case of integer S both ω_{12} and ω_{34} are non-zero constants at infinity [110, 9]; then shifting

S infinitesimally away from an integer we see that it would be impossible to satisfy the condition (8.26) if we allow one of them to have exponential asymptotics at infinity: this exponent will multiply the constant in the other one. So the only two possibilities left are ω_{13} and ω_{24}, which are both zero at infinity for integer S. From perturbative data we know that it is ω_{24} which should have exponential asymptotics. Thus we formulate the "minimal" prescription for analytic continuation of Q-system to non-integer S: $e^{2\pi|u|}$ asymptotic has to be allowed in ω_{24}. This prescription was tested thoroughly on a variety of examples [124, 125, 110, 9, 15], but it would be interesting to derive it rigorously and generalize it to states outside of the $\mathfrak{sl}(2)$ sector. Of course, one can also consider adding exponents to more than one component of ω_{ij}: in this case the solution will not be unique. A complete classification of solutions of the Q-system according to exponents in their asymptotics might be interesting. For example it is known that allowing for an exponent in some other components corresponds to the generalized cusp anomalous dimension [9, 166].

Because of the exponential asymptotics of ω_{24}, the argument in section 8.1.2, which fixes the zero modes of ω, has to be modified. First, formula (8.16) still holds true for $i = 1$ or $i = 3$, as ω_{24} does not enter anywhere in the derivation. Thus

$$\omega_{12} = -iI_{12}\cot\frac{\pi\,(S+\Delta)}{2},\ \omega_{34} = -iI_{34}\cot\frac{\pi\,(S-\Delta)}{2}. \tag{8.27}$$

Consequently, one can use (8.16) for both ω_{13} and ω_{31}, and reproduce the quantization condition (8.17) for global charges, which in this case implies that either $\Delta = 0$ or $\omega_{13} = 0$. Equation (8.16) can also be used for ω_{14} and ω_{23} (which are equal) and imposes that either $\Delta = 0$ or $\omega_{14} = 0$.

It remains to fix the zero mode in ω^0_{24}, for which we use an ansatz

$$\omega^0_{24} = a_1 e^{2\pi u} + a_2 + a_3 e^{-2\pi u}. \tag{8.28}$$

The constants a_1, a_2, a_3 can be found from the Pfaffian constraint (8.26). To this end we expand the hyperbolic cotangent in (8.9) to get

$$\omega_{ij} = \omega^0_{ij} + I_{ij} + 2e^{-2\pi u} I^{+}_{ij} + 2e^{-4\pi u} I^{++}_{ij} + \ldots,\ u \to +\infty, \tag{8.29}$$

where the terms of the expansion are integrals similar to I_{ij} with additional factors of $e^{2\pi u}$ or $e^{4\pi u}$ in the integrand[48]. Analogous expansion can be obtained at $u \to -\infty$. Then plugging these expansions into (8.26) we get formulas for the coefficients a_1, a_2, a_3. For

[48] Actually, these integrals can be evaluated analytically in terms of Bessel functions

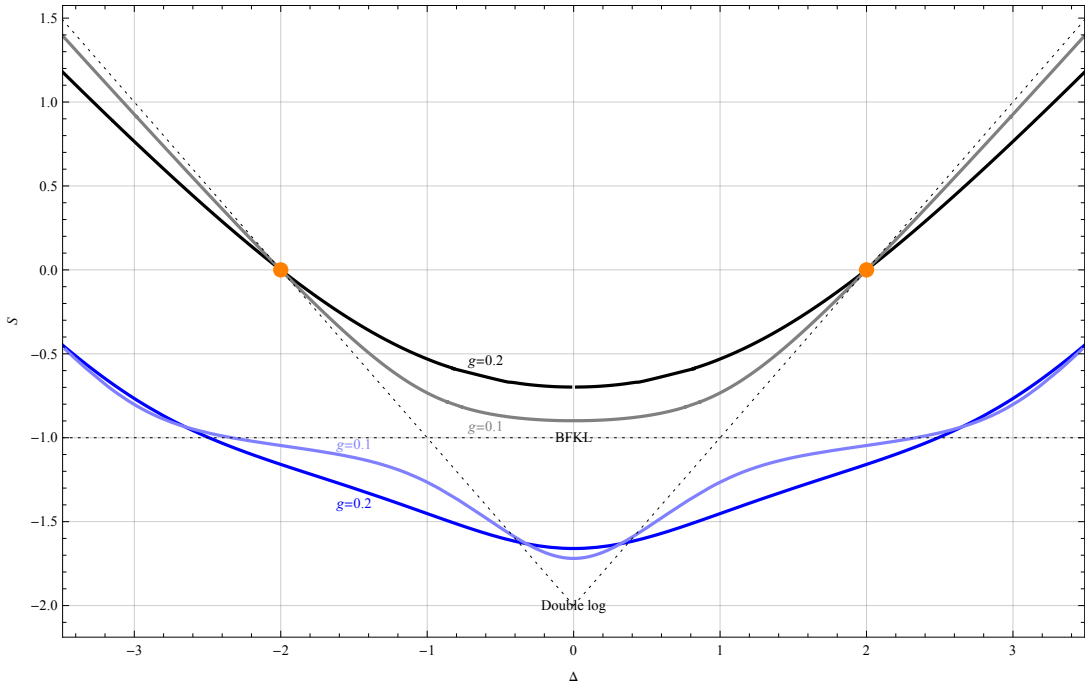

Figure 14: **Section of the Riemann surface $S(\Delta)$ along** Im $\Delta = 0$ **for different values of coupling** g. The upper two solid curves, shown in black and grey, represent the BFKL eigenvalue (see section 9) as a function of Δ, whereas the lower two come from the unphysical sheet which can be accessed from the upper one by going through the cuts. The dashed line shows the zero-coupling limit of the curve. Orange dots mark BPS states $\mathrm{Tr}(ZZ)$.

example,

$$a_1 = 2i\frac{1+\frac{I_{12}I_{34}}{4}\left(1+i\cot\frac{\pi(\Delta+S)}{2}\right)\left(1-i\cot\frac{\pi(\Delta-S)}{2}\right)}{I_{13}^{+}}\,. \tag{8.30}$$

With these modifications we can reconstruct all ω_{ij} including the zero modes and then proceed with our algorithm as in the case of integer S.

8.3.2 Exploring complex spin

In this section we briefly describe the results of our numerical exploration of $\Delta(S)$ as an analytic function of a complexified spin S. As explained in the previous section the generalization of our numerical method to arbitrary values of spin requires minimal modifications in the code. Thus we are able to generate numerous values of the anomalous dimension for any S with high precision in seconds. In fact both S and Δ enter the QSC formalism on almost equal footing and we can also switch quite easily to finding S for given Δ. This is what is adopted in the vast literature on the subject and what we are

going to consider below. This viewpoint is additionally convenient due to the symmetry $\Delta \to -\Delta$.

Starting from $S = 2$ (Konishi operator) we decreased the value of S or Δ in small steps each time using the solution at the previous step as a starting point for the next value. In this way we built the upper two curves on Fig. 14. Let us point out one curious technical problem – one can see for instance from (8.30) that the lines $S = \pm\Delta + \mathbb{Z}$ are potentially dangerous due to the divergence. The divergence is cancelled because of the vanishing $I_{12}I_{34}$ factor, but this affects the convergence "radius" of our iterative procedure. Thus we found it quite complicated to cross those lines, even though in very small steps we were able to reach close to them. The solution is to go around these lines in the complex plane Δ instead of crossing them.

To make sure there is no true singularity or branch point we also explored a big patch of the complex plane Δ, indeed finding some branch points, but deep inside the complex plane, having nothing to do with these lines. For example when $g = 0.2$ we found 4 closest branch points at roughly $\pm 1 \pm i$, see Fig. 11. By making an analytic continuation (described above) through those cuts we found another sheet of the Riemann surface $S(\Delta)$. On this sheet we have found four cuts: two are connecting it to the first sheet and two other ones, located symmetrically on the imaginary axis, lead to further sheets. We expect an infinite set of sheets hidden below and also more cuts on both sheets outside of the area that we have explored.

It is instructive to see how this Riemann surface behaves as $g \to 0$. First, the real parts of branch points on the physical sheet are very close to ± 1, but the imaginary part goes to zero. Thus at infinitely small g the cuts collide, isolating the region $|\mathrm{Re}\ \Delta| < 1$ from the rest of the complex plane. These two separated regions become then the areas of applicability of two different approximations: for $|\mathrm{Re}\ \Delta| > 1$ one can apply the usual perturbation theory and Beisert-Eden-Staudacher Asymptotic Bethe Ansatz, whereas the region $|\mathrm{Re}\ \Delta| < 1$ is described by BFKL approximation and so-called Asymptotic BFKL Ansatz [15].

The presence of the cut can be to some extent deduced from perturbative perspective in each region: in the regime of usual perturbation theory

$$\Delta(S) = 2 + S - 8g^2 H_S + \mathcal{O}(g^4), \tag{8.31}$$

where H_S is the harmonic number. It has poles for all negative integer values of S — these poles are weak-coupling remnants of the cuts we see at finite coupling. In the BFKL

regime one should instead look at the leading order BFKL equation [192, 193, 187]

$$S(\Delta) = -1 + 4g^2 \left[\psi\left(\frac{1+\Delta}{2}\right) + \psi\left(\frac{1-\Delta}{2}\right) - 2\psi(1) \right] + \mathcal{O}(g^4) \,. \tag{8.32}$$

To make sense of this equation one has to take the limit $g \to 0$, $S \to -1$ so that the l.h.s stays finite. Then the ψ-functions in the r.h.s generate poles at odd values of Δ, which, again, are cuts degenerated at weak coupling.

BFKL physics which gives rise to (8.32) is a rich topic to explore. In particular, it connects the spectral problem to Regge behaviour of scattering cross-sections and will be discussed in details in the next chapter.

Fig. 14 represents a section of the Riemann surface by the plane Im $u = 0$, i.e. dependence of S on Δ for real Δ, which, of course, consists of two curves, originating from the two sheets we explored. At weak coupling the upper curve becomes piecewise linear, approaching different parts of the dotted line: for $|\Delta| > 1$ it coincides with $S = \pm\Delta - 2$ and for $|\Delta| < 1$ it becomes $S = -1$. One could expect a similar piecewise linear behavior for the lower curve: it approaches $S = \pm\Delta - 2$ for $|\Delta| < 1$, approaches $S = 0$ in some region outside of $|\Delta| < 1$ and becomes a certain linear function even further away from $\Delta = 0$. It would be interesting to explore the complete analytic structure of this Riemann surface, and understand what describes its asymptotics when $g \to 0$. It should produce a hierarchy of "Asymptotic Bethe Ansätze" each responsible for its own linear part of the limiting surface.

* * *

The numerical method described in this chapter can of course be improved in many ways. The most obvious thing to do is to rewrite the algorithm, which is now written in Mathematica, in a lower-level language such as C++. Since our algorithms only uses simple matrix operations, this should not be too difficult and will give a significant increase in speed. Also the of applications of our algorithm can be vastly extended. Up to now we have only demonstrated how it works in $\mathfrak{sl}(2)$ sector of $\mathcal{N} = 4$ SYM . However, in principle it should work for any state of $\mathcal{N} = 4$ SYM , including non-symmetric ones. For example, the wider class of $\mathfrak{sl}(2, \mathbb{C})$ operators (identified in [15]), also exhibiting a BFKL regime, could be a good candidate to begin with. Moreover, since spectrum of ABJM theory can also be described by QSC [194] (presented in section 10), our numerical method is also applicable there.

9 BFKL regime

In this chapter we will apply of QSC method to long-standing problems of BFKL physics. First, in section 9.1 we will briefly describe BFKL regime, its importance, and summary of known results. Then in section 9.2 we will present the LO order solution of QSC and use it to reproduce the known result for LO BFKL eigenvalue. In chapter 9.3, which is based on our paper [13], we find a new, NNLO term in BFKL expansion using analytical solution of QSC. In section 9.4 we find two new terms in the strong coupling expansion of BFKL intercept. Finally, in section 9.5 we use the numerical method developed in the previous chapter in order to compute BFKL intercept at finite values of coupling.

9.1 Introduction to BFKL physics

One of the limits often studied in QFTs is the Regge limit: high energy scattering with fixed momentum transfer, $s \gg |t|$. In this regime the usual perturbation theory can not be applied directly, because each order in the coupling constant contains powers of large logarithms of the ratio of energy scales: $(g \log t/s)^n$. In order to obtain a meaningful result, one has to resum large logarithms in all orders in perturbation theory. This can be seen as a disadvantage, because it makes obtaining any result in this regime much more difficult. However, it also makes the Regge limit extremely interesting, because one can probe all orders of perturbation theory at once. This resummation of leading logarithms often leads to power-law behaviour of the cross-sections, which one might hope to see experimentally. This is the case, for example, in small x regime of deep inelastic scattering in QCD, where the cross-section depends on the energy like

$$\sigma \propto s^{j(0)-1}. \tag{9.1}$$

The quantity $j(0)$, which will play an important role in this chapter, is called the pomeron intercept.

In order to see how this power-law comes about one notices that the BFKL regime is characterized by separation of physics in the plane of collision and in the transversal plane. The process of scattering of two partonic jets factorizes into two vertex contributions, depending only on the small transverse momenta, and the non-trivial part $f(\Delta y, p_\perp)$ which also depends on the large rapidity separation Δy [195]. The process receives contributions from diagrams including emission of arbitrary number of intermediate gluons. Each new

gluon's momentum k needs to be integrated over the transverse plane with the measure of d^2k/k^2 — and that is where the logarithms come from. Thus $f(\Delta y, p_\perp)$ satisfies an integral equation of Bethe-Salpeter type, whose solution can be schematically represented as

$$f(\Delta y, p_\perp) = \sum_{n=-\infty}^{+\infty} e^{in\tilde{\phi}} \int_{-\infty}^{\infty} d\nu \, Q_\nu(p_\perp) e^{4g^2\chi(n,\nu)\Delta y}. \tag{9.2}$$

We see that in the limit of very large rapidity separation Δy the integral can be taken by the saddle-point approximation and indeed produces the power-law.

In the formula above $Q_\nu(p_\perp)$ absorbs the trivial dependence on the transverse momenta and the nontrivial part $\chi(n,\nu)$ is the eigenvalue of the leading order BFKL Hamiltonian. In order to define the Hamiltonian it is convenient to introduce transverse coordinates and their corresponding momenta:

$$\rho_k = x_k + iy_k, \quad \rho_k^* = x_k - iy_k \tag{9.3}$$

$$p_k = i\frac{\partial}{\partial \rho_k}, \qquad p_k^* = i\frac{\partial}{\partial \rho_k^*} \tag{9.4}$$

In terms of these variables the LO BFKL Hamiltonian takes the form

$$H = \ln|p_1 p_2|^2 + \frac{1}{p_1 p_2^*}\left(\ln|\rho_{12}|^2\right) p_1 p_2^* + \frac{1}{p_1^* p_2}\left(\ln|\rho_{12}|^2\right) p_1^* p_2 - 4\psi(1), \tag{9.5}$$

where $\rho_{12} = \rho_1 - \rho_2$. One can see that the Hamiltonian enjoys symmetry under Mobius transformations in the transversal plane

$$\rho_k \to \frac{a\rho_k + b}{c\rho_k + d}. \tag{9.6}$$

Thus its eigenvalues are classified by a pair m, $\bar{m}$ which parametrize representations of $\mathfrak{sl}(2,\mathbb{C})$. They are related to ν and conformal spin n by

$$m = \frac{1}{2} + i\nu + \frac{n}{2}, \quad \tilde{m} = \frac{1}{2} + i\nu - \frac{n}{2} \tag{9.7}$$

In this notation the LO eigenvalue can be written as

$$\chi^{LO}(n,\nu) = 2\psi(1) - \psi\left(\frac{n+1+i\nu}{2}\right) - \psi\left(\frac{n+1-i\nu}{2}\right) \tag{9.8}$$

In this thesis we will be working with $n = 0$, leaving the operators with non-vanishing conformal spin for further work.

Taking into account Next-to-Leading, Next-to-Next-to-Leading corrections we get a structure similar to (9.2), where the BFKL eigenvalue χ in the exponent gets corrected. One usually introduces $j(i\nu)$, which in the LO is related to the BFKL eigenvalue as $j = 1 + 4g^2\chi$ and beyond the LO has an expansion in g^2 which can be represented as

$$j(i\nu) = 1 + \sum_{\ell=1}^{\infty} g^{2\ell}\left[F_\ell\left(\frac{i\nu-1}{2}\right) + F_\ell\left(\frac{-i\nu-1}{2}\right)\right], \tag{9.9}$$

From the point of view of effective physical description one can say that this regime is dominated by exchange of an quasi-particle — BFKL pomeron, which is a bound state of two reggized gluons. In the leading order BFKL pomeron is just a pair of gluons in a color singlet, which explains why $j(0) = 1$ at zero coupling. The LO correction is given by (9.8); NLO BFKL ($F_2(x)$ in the formula above) was obtained after 9 years laborious calculations in [196, 197, 198, 187]; the result in modern notation is presented below in the text (9.14). The corrections turned out to be numerically rather large compared to the LO, which makes one question the validity of the whole BFKL resummation procedure and its applicability for phenomenology. Moreover, the sign of NLO is such that at some finite value of coupling it completely cancels the LO correction and then changes the sign of the BFKL intercept, meaning that, for example, partonic cross-sections will increase, and not decrease with energy. All this points out that just NLO is not enough to match experimental predictions: it is important to understand the general structure of BFKL expansion terms and find a meaningful way of resummation. As a first step towards this goal in the last part of this chapter we present a result for NNLO BFKL eigenvalue in $\mathcal{N} = 4$ SYM .

Notably, it was observed in [187] that the $\mathcal{N} = 4$ SYM reproduces correctly a part of the QCD result with maximal transcendentality. In particular the LO coincides exactly in the two theories. Since this thesis deals with supersymmetric gauge theories, we will consider Regge limit of $\mathcal{N} = 4$ SYM , sometimes making comparison with QCD.

Since in this thesis we work with QSC formalism, which is designed for solving the spectral problem, it is crucial for us that [198] related BFKL pomeron to a certain analytical continuation of twist-two operators. To be more precise, for an operator of the form tr $(ZD^S Z)$ the spin S and conformal dimension Δ are related to j and ν in formulas above as

$$S = j(i\nu) - 2, \quad \Delta = i\nu \tag{9.10}$$

The anomalous dimension as a function of spin has singularities at negative integer values. The first pole at $S = -1$ corresponds to the BFKL regime. In order to explore the weak coupling BFKL expansion we approach the singularity in the scaling

$$\Lambda \equiv \frac{g^2}{S+1} = \text{fixed}, \ S \to -1, \ g \to 0 \tag{9.11}$$

This gives us the leading order relation between spin and anomalous dimension as

$$\frac{1}{4\Lambda} = \chi^{LO}(\Delta) + g^2 \chi^{NLO}(\Delta) + g^4 \chi^{NNLO}(\Delta) + \dots, \tag{9.12}$$

where χ^{LO} is LO BFKL eigenvalue, χ^{NLO} is NLO BFKL eigenvalue and so on.

It was noticed in [189] that both LO and NLO BFKL eigenvalues can be expressed in terms of the so-called nested harmonic sums $S_{a_1,\dots,a_k}$. These functions are defined recursively for even integer arguments

$$S_{a_1,a_2,\dots,a_n}(x) = \sum_{y=1}^{x} \frac{(\text{sign}\,(a_1))^y}{y^{|a_1|}} S_{a_2,\dots,a_n}(y), \quad S(x) = 1.$$

Below we use nested harmonic sums of complex argument, understanding them as analytical continuation of the expression above in the complex plane. In practice this continuation can be performed by expressing harmonic sums through η-functions defined in (9.44). Having defined the harmonic sums in this way we can rewrite F_l from (9.9) in the first two orders as

$$F_0(x) = -S_1(x) \tag{9.13}$$

$$F_1(x) = -\frac{3}{2}\zeta(3) + \pi^2 \ln 2 + \frac{\pi^2}{3} S_1(x) + 2S_3(x) + \pi^2 S_{-1}(x) - 4S_{-2,1}(x) \tag{9.14}$$

In the last part of this chapter we show how the assumption that χ^{NNLO} can also be written in this form allows us to find its exact analytical form — a result which is virtually impossible to reach by the usual perturbation theory.

9.2 LO solution of QSC in the BFKL regime

In this section we will sketch the derivation of the LO BFKL eigenvalue from QSC. In order to do this we consider twist-two operators near $S = -1$ and find some Q-functions to the LO and some to NLO. The derivation will closely follow [110].

As we mentioned before, the BFKL eigenvalue is accessible as an anomalous dimension of twist-two operators in the limit (9.11). All quantities of the Q-system will be presented as series expansions in $\omega = S+1$, so the first thing to do before looking for the solution is to determine scaling of different variables with ω. We will not derive this scaling rigorously, but rather give an empirical argument for a particular scaling and later check that there indeed exists a solution with this scaling. Let us start with $\mathbf{P}_a$: from the formulas (4.50) one can see that their leading coefficients A_a stay finite when $\omega \to 0$; same holds for $\mathbf{Q}_i$. So we assume that

$$\mathbf{P}_a \sim 1, \mathbf{Q}_i \sim 1 \tag{9.15}$$

We also know that $\mathbf{P}_a$ have singularities at $u = 0$: the strongest in the leading order is $\mathbf{P}_1 \sim u^{-2}$. This singularities is what remains of short cuts after expansion in ω. Thus if we "zoom in" close enough to the cut, on the scale of order ω the singularities have a

cut-off and match the value of $\mathbf{P}_a$ on the other sheet, i.e. $\tilde{\mathbf{P}}_a$. This leads to the conclusion that at least some of $\tilde{\mathbf{P}}_a$ scale as ω^{-2}. Taking into account the equation (4.17) and the fact that $\mathbf{P}_a$ are finite, we see that the factor of ω^{-2} can only come from μ_{ab}. So we conjecture the following scaling for all μ_{ab}

$$\mu_{ab} \sim \omega^{-2} \tag{9.16}$$

From (4.23) we see that μ_{ab} and ω_{ij} are related by $Q_{ab|ij}$, which can be expressed through $\mathbf{P}_a$ and $\mathbf{Q}_i$ and so is of order 1. Thus at least some ω_{ij} have to diverge as $\omega \to 0$. We found the following scaling consistent:

$$\omega_{24} \sim \omega^{-2},\ \omega_{13} \sim \omega^2, \tag{9.17}$$

$$\omega_{12}, \omega_{14}, \omega_{34} \sim 1, \tag{9.18}$$

Now that the scaling of all functions in established, let us find an ansatz for the solution, starting with $\mathbf{P}_a$. As it was argued in the previous chapter, $\mathbf{P}_a$ can be represented as series in $x(u)$ on the main sheet:

$$\mathbf{P}_a = \sum_{n=-1}^{\infty} \frac{c_{a,n}}{x^n} \tag{9.19}$$

Since $\tilde{x} = 1/x$, the corresponding series on the other second sheet is

$$\tilde{\mathbf{P}}_a = \sum_{n=-1}^{\infty} c_{a,n} x^n \tag{9.20}$$

In fact, in series above only every second coefficient is non-zero: since we are in a left-right symmetric situation, each $\mathbf{P}_a$ has a definite parity which can be deduced its asymptotics.

We will also need an ansatz for the leading order μ_{ab}. Notice that up to a periodic function μ_{ab} has polynomial asymptotics. Also it can not have a singularity at zero, otherwise $\tilde{\mathbf{P}}_a$ would be singular in the leading order. Finally, one can show that μ^+_{ab} should have definite parity defined, again, by the asymptotics[49].

Thus we write down the following ansatz: $\mu_{ab} = \frac{q_{ab}}{\omega^2}\mathcal{P}$, where q_{ab} is a polynomial and $\mathcal{P}$ is a periodic function. Under assumption of absence of higher-frequency modes we can parameterize $\mathcal{P}$ in terms of two coefficients

$$\mathcal{P} = C_1 + C_2 \sinh^2(\pi u) \tag{9.21}$$

Having an ansatz for $\mathbf{P}_a$ and μ_{ab}, we can try to constraint its coefficients by equations (4.17) and (4.18). We find that, indeed, for the leading order of μ_{ab} and the first two

[49]Here we assume that μ has long cuts. Definite parity of μ^+ with long cuts follows from definite parity of μ with short ones

orders of $\mathbf{P}_a$ there is a consistent solution, which we present here without going into the details of calculations:

$$\mathbf{P}_1 \simeq \frac{1}{u^2} + \frac{2\Lambda\omega}{u^4} \tag{9.22}$$

$$\mathbf{P}_2 \simeq \frac{1}{u} + \frac{2\Lambda\omega}{u^3} \tag{9.23}$$

$$\mathbf{P}_3 \simeq A_3^{(0)} + A_4^{(1)}\omega \tag{9.24}$$

$$\mathbf{P}_4 \simeq A_4^{(0)}u - \frac{i(\Delta^2-1)^2}{96u} + \left(A_4^{(1)}u + \frac{c_{4,1}^{(2)}}{u\Lambda} - \frac{i(\Delta^2-1)^2\Lambda}{48u^3}\right)\omega, \tag{9.25}$$

where $c_{4,1}^{(2)} = -\frac{i\Lambda}{24}\left(\Delta^2-1\right)\left[2\left(\Delta^2-1\right)\Lambda - 1\right]$.

The corresponding μ_{ab}'s are

$$\mu_{12}^{+} \simeq +\frac{\mathcal{P}}{\omega^2}, \tag{9.26}$$

$$\mu_{13}^{+} \simeq -\frac{\mathcal{P}}{16\omega^2} iu\left(\Delta^2-1\right)^2, \tag{9.27}$$

$$\mu_{14}^{+} \simeq -\frac{\mathcal{P}}{128\omega^2} i\left(4u^2+1\right)\left(\Delta^2-1\right)^2, \tag{9.28}$$

$$\mu_{24}^{+} \simeq -\frac{\mathcal{P}}{192\omega^2} iu\left(4u^2+1\right)\left(\Delta^2-1\right)^2, \tag{9.29}$$

$$\mu_{34}^{+} \simeq -\frac{\mathcal{P}}{49152\omega^2} i\left(4u^2+1\right)\left(4u^2-3\right)\left(\Delta^2-1\right)^4. \tag{9.30}$$

With $\mathbf{P}_a$ given above we can write down the fourth-order equation (4.29) explicitly in the first two orders in ω. It turns out that the finite-difference operator in the left hand side can be factorized into two second-order ones, i.e. two of the solutions satisfy a second order equation:

$$\mathbf{Q}_j\left(\frac{\Delta^2-1-8u^2}{4u^2} + \omega\frac{(\Delta^2-1)\Lambda - u^2}{2u^4}\right) + \mathbf{Q}_j^{--}\left(1 - \frac{i\omega/2}{u-i}\right) + \mathbf{Q}_j^{++}\left(1 + \frac{i\omega/2}{u+i}\right) = 0 \tag{9.31}$$

By comparing the asymptotics one can conclude that these two solutions are $\mathbf{Q}_1$ and $\mathbf{Q}_3$. They can be written in terms of hypergeometric functions, the leading order being

$$\mathbf{Q}_1(u) = 2iu\,{}_3F_2\left(iu+1, \frac{1-\Delta}{2}, \frac{1+\Delta}{2}; 1, 2; 1\right), \tag{9.32}$$

$$\mathbf{Q}_3(u) = \frac{\mathbf{Q}_1(-u)}{\cos\frac{\pi\Delta}{2}} + \mathbf{Q}_1(u)\left[-i\coth(\pi u) + \tan\frac{\pi\Delta}{2}\right] \tag{9.33}$$

The leading order solution of the Baxter equation is found, but to obtain from it the LO BFKL eigenvalue we still need to perforrms several additional steps.

First, we need to analyse the singular behaviour of $\mathbf{Q}_j$ near $u = 0$. To do this, recall that $\mathbf{Q}_i$ can have singularities at zero and below, but not in the upper half plane. Thus, considering the equation (9.31) near $u = i$ we conclude that

$$\frac{\mathbf{Q}_j^{(1)}(u)}{\mathbf{Q}_j^{(0)}(u)} = \frac{i\omega}{2u} + \mathcal{O}(u^0)\ ,\ j = 1, 3 \tag{9.34}$$

where $\mathbf{Q}_j = \mathbf{Q}_j^{(0)} + \omega \mathbf{Q}_j^{(1)} + \mathcal{O}(\omega^2)$.

Second, it is important to understand the properties of $\mathbf{Q}_i$ under reflection in u. Since $\mathbf{Q}_i(-u)$ and $\tilde{\mathbf{Q}}_i(u)$ have identical analytical properties, they can be expressed though each other with constant coefficients. Without going into detail, we state that

$$\tilde{\mathbf{Q}}_1(u) = -\mathbf{Q}_1(-u) \tag{9.35}$$

$$\tilde{\mathbf{Q}}_3(u) = +\mathbf{Q}_3(-u) - 2\tan\left(\frac{\pi\Delta}{2}\right)\mathbf{Q}_1(-u) \tag{9.36}$$

Finally, to put the two arguments together, notice that the combinations $\mathbf{Q}_1 + \tilde{\mathbf{Q}}_1$ and $\frac{\mathbf{Q}_1 - \tilde{\mathbf{Q}}_1}{\sqrt{u^2-4\omega\Lambda}}$ are regular. Using this fact one can separate $\mathbf{Q}_1$ into singular and regular parts in the following way

$$\mathbf{Q}_1 = \frac{\mathbf{Q}_1 - \tilde{\mathbf{Q}}_1}{2\sqrt{u^2-4\omega\Lambda}}\sqrt{u^2-4\omega\Lambda} + \frac{\mathbf{Q}_1 + \tilde{\mathbf{Q}}_1}{2} = \frac{\mathbf{Q}_1 - \tilde{\mathbf{Q}}_1}{\sqrt{u^2-4\omega\Lambda}}\left(-\frac{\Lambda\omega}{u} - \frac{\Lambda^2\omega^2}{u^3} + \dots\right) + \text{reg} \tag{9.37}$$

But from (9.35) and the explicit form of the solution (9.32) one finds that

$$\frac{\mathbf{Q}_3 - \tilde{\mathbf{Q}}_3}{\sqrt{u^2-4g^2}} = 2i\mathbf{Q}_3(0)\left[\psi\left(\frac{1-\Delta}{2}\right) + \psi\left(\frac{1+\Delta}{2}\right) - 2\psi(1)\right] + \mathcal{O}(\omega) + \mathcal{O}(u) \tag{9.38}$$

which, plugged into (9.37) and compared with (9.34), yields the LO BFKL formula

$$-\frac{1}{4\Lambda} = \psi\left(\frac{1-\Delta}{2}\right) + \psi\left(\frac{1+\Delta}{2}\right) - 2\psi(1) \tag{9.39}$$

9.3 NNLO BFKL eigenvalue

Here we will describe how the iterative analytical solution of QSC allowed us to find a previously unknown, NNLO term of the weak coupling expansion of BFKL eigenvalue in [13]. The method for the analytical iterative solution is based on principles which are similar but not identical to those of the numerical method described in the previous chapter. Therefore we present here a brief description of the method, the result and its numerical verification.

The crucial assumption of our calculation is that, similar to LO and NLO, the NNLO correction can also be written as a combination of nested harmonic sums of fixed transcendentality. Assuming this, we have only finite number of coefficients to fix, and we do this by solving QSC iteratively in two small expansion parameters. The first expansion is in coupling g; the second is in Δ around certain integer positive values Δ_0 of conformal dimension at which QSC simplifies.

9.3.1 Analytic constraints from QSC

We describe now the details of our analytical method. We will focus on some particular points $\Delta_0 = 1, 3, 5, 7$. It can be seen already from the LO (9.8) that the function $S(\Delta)$ is singular at these points, however the coefficients of the expansion are relatively simple and are given by ζ-functions. We will perform a double expansion first in g up to the order g^6 and then in $\delta = \Delta - \Delta_0$.

General iterative procedure for solving QSC. We describe a procedure which for some given $\mathbf{P}_a$ (or equivalently $c_{a,n}$ from the expansion (8.1)) takes as an input some approximate solution of (8.3) $\mathcal{Q}^{(0)}_{a|i}$ valid up to the order ϵ^n (where ϵ is some small expansion parameter) and produces as an output new $\mathcal{Q}_{a|i}$ accurate to the order ϵ^{2n}. The method is very general and in particular is suitable for perturbative expansion around any background.

Let dS be the mismatch in the equation (8.3), i.e.

$$\mathcal{Q}^{(0)}_{a|i}(u + \tfrac{i}{2}) - \mathcal{Q}^{(0)}_{a|i}(u - \tfrac{i}{2}) + \mathbf{P}_a \mathbf{P}^b \mathcal{Q}^{(0)}_{b|i}(u + \tfrac{i}{2}) = dS_{a|i}, \tag{9.40}$$

where $dS_{a|i}$ is small $\sim \epsilon^n$. We can always represent the exact solution in the form

$$\mathcal{Q}_{a|i}(u) = \mathcal{Q}^{(0)}_{a|i}(u) + b_i{}^j(u + \tfrac{i}{2})\ \mathcal{Q}^{(0)}_{a|j}(u) \tag{9.41}$$

where the unknown functions $b_i{}^j$ are also small. After plugging this ansatz into the equation (9.40) we get

$$\Big(b_i{}^j(u) - b_i{}^j(u + i)\Big)\ \mathcal{Q}^{+(0)}_{a|j} = dS_{a|i} + dS_{a|j} b_i{}^j\ . \tag{9.42}$$

Since $b_i{}^j$ is small it can be neglected in the right hand side where it multiplies another small quantity. Finally, multiplying the equation by $\mathcal{Q}^{(0)a|k}$ and using the orthogonality relation (4.12) we arrive at

$$b_i^k(u + i) - b_i^k(u) = -dS_{a|i}(u) \mathcal{Q}^{(0)a|k}\left(u + \tfrac{i}{2}\right) + \mathcal{O}(\epsilon^{2n})\ .$$

We see that the right hand side contains only the known functions dS and $\mathcal{Q}^{(0)}$ and does not contain b which means that the original 4th order finite difference equation is reduced to a set of independent 1st order equations! In most interesting cases the first order equation can be easily solved. After $\mathcal{Q}_{a|i}$ is found one can use (8.8) to find $\mathbf{Q}_i$.

Iterations at weak coupling. For our particular problem we will take either $\epsilon = g$ or $\epsilon = \delta$. Applying this procedure a few times we generate $\mathbf{Q}_i$ for sufficiently high order both

in g and in δ. Finally, by "gluing" $\mathbf{Q}_i$ and $\tilde{\mathbf{Q}}_i$ on the cut we find $c_{a,n}$ and $S(\Delta)$ also as a double expansion.

For the above procedure we need the leading order $\mathcal{Q}^{(0)}_{a,i}$. One can expect that to the leading order in g the solution should be very simple, because the branch cuts collapse to a point making most of the functions polynomial or having very simple singular structure. Also one can use that to the leading order in g functions $\mathbf{P}_a$ are very simple and are already known from [110] for any Δ. By making a simple ansatz for $\mathbf{Q}_i$ we found for $\Delta_0 = 1$ to the leading order

$$\mathbf{Q}_1 \simeq u,\ \mathbf{Q}_2 \simeq 1/u,\ \mathbf{Q}_3 \simeq 1,\ \mathbf{Q}_4 \simeq 1/u^2\ . \tag{9.43}$$

For $\Delta_0 = 3, 5, \dots$ the solution involves also the η-functions introduced in the QSC context in [136, 199]

$$\eta_{s_1,\dots,s_k}(u) = \sum_{n_1>n_2\dots n_k\geq 0} \frac{1}{(u+in_1)^{s_1}\dots(u+in_k)^{s_k}}. \tag{9.44}$$

which are related in a simple way to the nested harmonic sums. For $\Delta = 3$ we found

$$\begin{aligned} &\mathbf{Q}_1 \simeq u^2,\ \mathbf{Q}_2 \simeq u^2\eta_{1,3} - i - \frac{1}{2u}, \\ &\mathbf{Q}_3 \simeq u^2\eta_{1,2} - iu - \frac{1}{2},\ \mathbf{Q}_4 \simeq u^2\eta_{1,4} - \frac{i}{u} - \frac{1}{2u^2}\ , \end{aligned} \tag{9.45}$$

which reflects the general structure of the expansion of $\mathbf{Q}_i$ around integer Δ's which contain only $\eta_{1,2}$, $\eta_{1,3}$ and $\eta_{1,4}$ with polynomial coefficients.

Let us introduce a class of functions called η-polynomials — linear combinations of η-functions with polynomial coefficients. As explained in [136, 199], it is closed under all essential for us operations. Indeed, the product of any two η-functions can be written as a sum of η-functions, and, most importantly, one can easily solve equations of the type

$$f(u+i) - f(u) = u^n \eta_{s_1,\dots,s_k} \tag{9.46}$$

for any integer n again in terms of η-polynomials. For example for $n = -1$ and $k = 1$, $s_1 = 1$ we get $f = -\eta_2 - \eta_{1,1}$. Thus starting with LO expressed in terms of η-polynomials we are guaranteed to get η-polynomials on each step of the iterative procedure described above.

Proceeding in this way we computed $\mathbf{Q}_i$ up to the order g^6 and δ^{10} for $\Delta = 3, 5, 7$. After that we fix the coefficients in the ansatz for $\mathbf{P}_a$ from analyticity requirements described below.

Fixing remaining parameters. Here we will describe how to use $\mathbf{Q}_i$ found before to finally extract a relation between S and Δ and the constants $c_{a,n}$. This is done by using

a relation between $\mathbf{Q}_i$ and their analytical continuations $\tilde{\mathbf{Q}}_i$. On the one hand we have the relation (4.24). On the other hand we can use the $u \to -u$ symmetry[50] of the twist-two operators to notice that $\mathbf{Q}_i(-u)$ should satisfy the same finite difference equation as $\mathbf{Q}_i(u)$ and thus we should have $\mathbf{Q}_i(u) = \Omega_i^j(u)\mathbf{Q}_j(-u)$ where $\Omega_i^j(u)$ is a set of periodic coefficients. As $\mathbf{Q}_i(u)$ has a power-like behavior at infinity, $\Omega_i^j(u)$ should not grow faster than a constant. Furthermore, since $\mathbf{Q}_i$ has a definite asymptotic (8.2) only diagonal elements of $\Omega_i^i(u)$ can be nonzero at infinity. Combining these relations we find

$$\tilde{\mathbf{Q}}_A(u) = \alpha_A^i \mathbf{Q}_i(-u) \ , \quad A = 1, 3 \ , \tag{9.47}$$

where $\alpha_A^j = \omega_{Ai}\chi^{ik}\Omega_k^j$ are i-periodic (as a combination of i-periodic functions), analytic (as both $\tilde{\mathbf{Q}}_a(u)$ and $\mathbf{Q}_a(-u)$ should be analytic in the lower-half-plane) and growing not faster than a constant at infinity which implies that they are constants. Furthermore most of them are zero because only ω_{12}, ω_{34} and Ω_i^i are non-zero at infinity. Thus we simply get

$$\tilde{\mathbf{Q}}_1(u) = \alpha_{13}\mathbf{Q}_3(-u) \ , \quad \tilde{\mathbf{Q}}_3(u) = \alpha_{31}\mathbf{Q}_1(-u) \ . \tag{9.48}$$

Next we note that if we analytically continue this relation and change $u \to -u$ we should get an inverse transformation which implies $\alpha_{13} = 1/\alpha_{31} \equiv \alpha$. The coefficient α depends on relative normalization of $\mathbf{Q}_1$ and $\mathbf{Q}_3$. Let us see how to use the identity (9.48) to constrain the constants $c_{a,n}$ of the expansion (8.1) of $\mathbf{P}_a$. We observed that all the constants are fixed from the requirement of regularity at the origin of the combinations $\mathbf{Q}_1 + \tilde{\mathbf{Q}}_1$ and $\frac{\mathbf{Q}_1 - \tilde{\mathbf{Q}}_1}{\sqrt{u^2-4g^2}}$, which now can be written as

$$\mathbf{Q}_1(u) + \alpha\mathbf{Q}_3(-u) = \text{reg} \ , \quad \frac{\mathbf{Q}_1(u) - \alpha\mathbf{Q}_3(-u)}{\sqrt{u^2-4g^2}} = \text{reg} \ .$$

This relation is used in the following way: one first expands in g the left hand side and then in u around the origin. Then requiring the absence of the negative powers will fix α, all the coefficients $c_{a,n}$, and the function $\Delta(S)$! So we can completely ignore ω_{ij}, $\mathbf{Q}_2$, and $\mathbf{Q}_4$ in this calculation. This observation can be used in more general situations and allows avoiding construction of ω_{ij}, and in particular could considerably simplify the numerical algorithm of chapter 8.

Constraints from poles. We use the procedure described above to compute the expansion of $S(\Delta)$ around $\Delta_0 = 3, 5, 7$. In particular for $\Delta = 5 + \epsilon$ we computed the first 8

[50] More generally one can also use complex conjugation symmetry

terms

$$\begin{aligned}
\chi^{\text{NNLO}} &= -\frac{1024}{\epsilon^5} + \frac{64\left(4\pi^2-33\right)}{3\epsilon^3} + \frac{16\left(-36\zeta_3+2\pi^2+31\right)}{\epsilon^2} \\
&+\frac{-288\zeta_3+\frac{232\pi^4}{45}-16\pi^2-296}{\epsilon} - \frac{2}{15}\left[20\left(4\pi^2-75\right)\zeta_3+6300\zeta_5+\pi^4-215\pi^2+285\right] \\
&+\epsilon\left[40\zeta_3^2+2\left(8\pi^2-123\right)\zeta_3-396\zeta_5+\frac{373\pi^6}{945}+\frac{11\pi^4}{9}-26\pi^2+\frac{1771}{4}\right] . \\
&+\epsilon^2\left[-48\zeta_3^2+\left(\frac{505}{2}-6\pi^2+\frac{43\pi^4}{45}\right)\zeta_3+\left(329+\frac{4\pi^2}{3}\right)\zeta_5\right. \\
&\left.-\frac{1001\zeta_7}{4}+\frac{31\pi^6}{252}+\frac{27\pi^4}{40}+\frac{147\pi^2}{8}-\frac{12387}{16}\right] \\
&+\epsilon^3\left[-\frac{2}{3}\left(\pi^2-30\right)\zeta_3^2+\left(218\zeta_5+\frac{7\pi^4}{5}+\frac{4\pi^2}{3}-\frac{1779}{8}\right)\zeta_3+\left(8\pi^2-\frac{1161}{4}\right)\zeta_5\right. \\
&\left.-\frac{2715\zeta_7}{8}+\frac{78S_{5,3}(\infty)}{5}-\frac{14233\pi^8}{3402000}-\frac{223\pi^4}{144}-\frac{557\pi^2}{48}+\frac{7625}{8}\right]+O\left(\epsilon^4\right) . \qquad (9.49)
\end{aligned}$$

We also reproduced expansions extracted from [200] for $\Delta = 1$.

9.3.2 Result for NNLO BFKL

One can notice that formulas (9.13), (9.14) for LO and NLO have uniform transcendentality if one assigns to $S_{a_1,\ldots,a_k}$ transcendentality equal to $\sum_{j=1}^{k}|a_j|$. As usual, transcendentality of a product is the sum of transcendentalities of the factors, transcendentalities of ζ_n and $\text{Li}_n\left(\frac{1}{2}\right)$ are both n, transcendentalities of $\log 2$ and π are both 1. The principal assumption of our calculation states that $F_3(x)$ can also be written as a linear combination of nested harmonic sums with coefficients made out of several transcendental constants $\pi^2, \log(2), \zeta_3, \zeta_5, \text{Li}_4\left(\frac{1}{2}\right), \text{Li}_5\left(\frac{1}{2}\right)$ of uniform transcendentality 5. The final basis obtained after taking into account the constants contains 288 elements.

Hence we build the linear combination of these basis elements with free coefficients and constrained them by imposing the expansion at $\Delta = 1, 3, 5, 7$ to match the results of the analytic expansion of QSC (in particular, requiring (9.49)). This gave an overdefined system of linear equations for the unknown coefficients which happen to have a unique

solution presented below:

$$\begin{aligned}
\frac{F_3(x)}{256} &= -\frac{5S_{-5}}{8} - \frac{S_{-4,1}}{2} + \frac{S_1 S_{-3,1}}{2} + \frac{S_{-3,2}}{2} - \frac{5S_2 S_{-2,1}}{4} \\
&+\frac{S_{-4}S_1}{4} + \frac{S_{-3}S_2}{8} + \frac{3S_{3,-2}}{4} - \frac{3S_{-3,1,1}}{2} - S_1 S_{-2,1,1} \\
&+S_{2,-2,1} + 3S_{-2,1,1,1} - \frac{3S_{-2}S_3}{4} - \frac{S_5}{8} + \frac{S_{-2}S_1S_2}{4} \\
&+\pi^2\left[\frac{S_{-2,1}}{8} - \frac{7S_{-3}}{48} - \frac{S_{-2}S_1}{12} + \frac{S_1S_2}{48}\right] - \pi^4\left[\frac{2S_{-1}}{45} - \frac{S_1}{96}\right] \\
&+\zeta_3\left[-\frac{7S_{-1,1}}{4} + \frac{7S_{-2}}{8} + \frac{7S_{-1}S_1}{4} - \frac{S_2}{16}\right] \\
&+\left[2\mathrm{Li}_4\left(\tfrac{1}{2}\right) - \frac{\pi^2\log^2 2}{12} + \frac{\log^4 2}{12}\right](S_{-1} - S_1) \\
&+\frac{\log^5 2}{60} - \frac{\pi^2\log^3 2}{36} - \frac{2\pi^4\log 2}{45} - \frac{\pi^2\zeta_3}{24} + \frac{49\zeta_5}{32} - 2\mathrm{Li}_5\left(\tfrac{1}{2}\right) \ .
\end{aligned} \tag{9.50}$$

The simplicity of the final result is quite astonishing: only 37 coefficients out of 288 turned out to be nonzero. Furthermore, they are significantly simpler than the coefficients appearing in the series expansion around the poles (9.49). These are all clear and expected indications of the correct result similar to what was observed in the usual perturbation theory [81]. In addition we also performed the numerical test described below.

9.3.3 Numerical tests

Using the method of [12], described in chapter 8, we evaluated 40 values of spin S for various values of the coupling g in the range $(0.01, 0.025)$ with 80 digits precision and then fit this data to get the following prediction for the N^{n}LO BFKL coefficients at the fixed value of $\Delta = 0.45$:

	value	error
N^{2}LO	10775.6358188471766379575931271924 5699592917094805765378342453322 9	10^{-61}
N^{3}LO	−366392.2052053917038937903507478 5 4454993553195933391916340383 6	10^{-56}
N^{4}LO	1.3327364556811269156940443103698 2 8561521940588979476878854 × 10^7	10^{-51}
N^{5}LO	−4.9217401266579165009139555520750 7006072145095843655987 6 × 10^8	10^{-47}

We found that our result (9.50) reproduces perfectly the first line in the table within the numerical error 10^{-61} which leaves no room for doubt in the validity of our result.

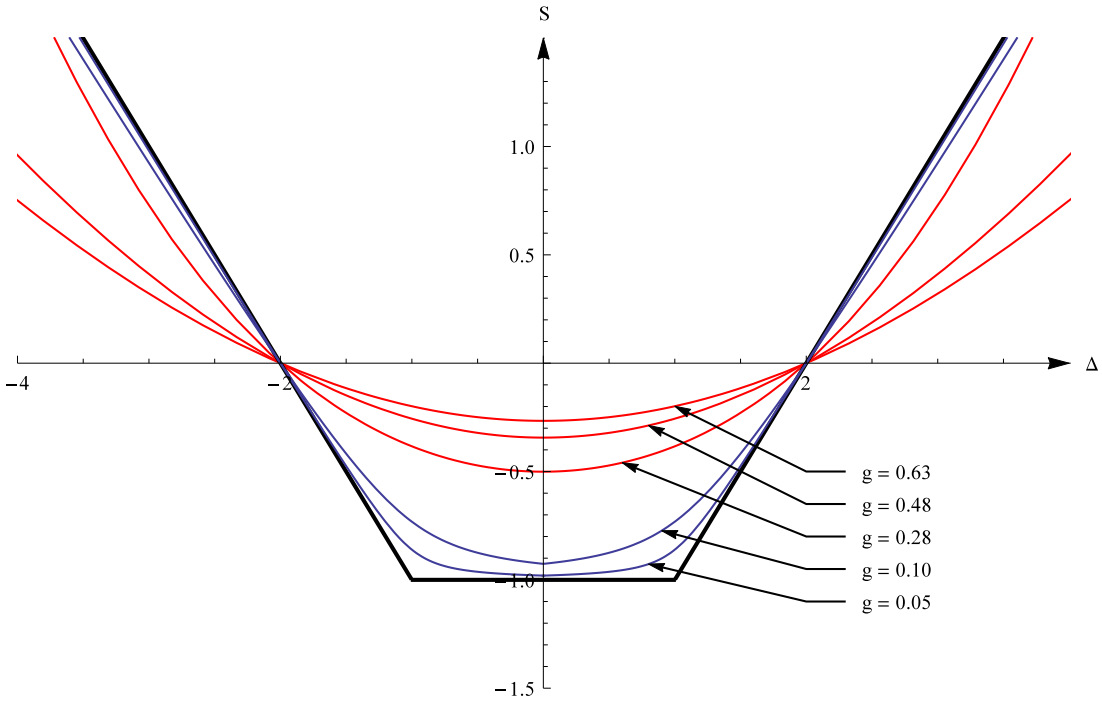

Figure 15: **The BFKL trajectories $S(\Delta)$ at various values of the coupling.** Blue lines are obtained using the known two loop weak coupling expansion [188, 187] and red lines are obtained using the strong coupling expansion [189, 190, 191].

9.4 Strong coupling regime of BFKL pomeron

Another interesting problem is to determine the strong coupling expansion of the BFKL pomeron intercept at strong coupling. At strong coupling the quasiparticle can be described as a graviton in AdS, thus $j(\lambda)$ approaches 2, as can be seen on Fig. 16.

As shown in [201], when $\lambda \to \infty$ the expansion of $j(\nu)$ has the following form

$$j(\nu) = 2 - \frac{2+2\nu^2}{\sqrt{\lambda}} \left(1 + \sum_{n=2}^{\infty} \frac{\tilde{j}_n\left(\nu^2\right)}{\lambda^{\frac{n-1}{2}}}\right), \tag{9.51}$$

where $\tilde{j}_n(\nu^2)$ is a polynomial of order $n-2$.

One can also use the same techniques as in section 5.5.3 to calculate the coefficients of this expansion. As mentioned before, the intercept of a BFKL trajectory $j(\Delta)$ is simply $j(0)$ and we already wrote down an ansatz for $S(\Delta)$ in (5.128). Obviously, the coefficients α_i, β_i, ... are in one-to-one correspondence with the coefficients A_i, B_i, ... from (5.130), values of which we found in chapter 5. Using this relation we find

$$\alpha_1 = 1/2,\ \alpha_2 = 1/4,\ \alpha_3 = -1/16\ ,\ \alpha_4 = -\frac{3\zeta_3}{2} - \frac{1}{2}, \tag{9.52}$$

$$\alpha_5 = -\frac{9\zeta_3}{2} - \frac{361}{256},\ \alpha_6 = -\frac{39\zeta_3}{4} - \frac{447}{128} \tag{9.53}$$

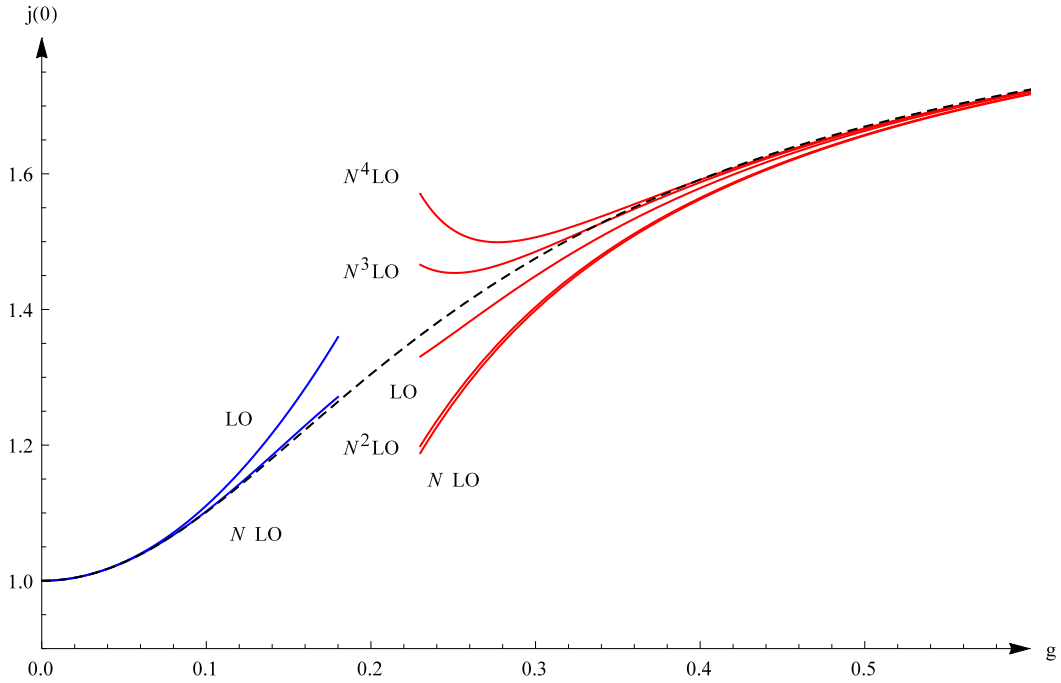

Figure 16: **The BFKL intercept** dependence on the coupling constant g at two orders at weak coupling (blue lines), four orders at strong coupling (red lines) and a Padé type interpolating function in between (dashed line).

$$\beta_3 = -3/16,\ \beta_4 = \frac{3\zeta_3}{8} - \frac{21}{64},\ \beta_5 = \frac{9\zeta_3}{8} - \frac{51}{128},\ \beta_6 = \frac{45\zeta_3}{8} + \frac{15\zeta_5}{16} + \frac{13}{512} \tag{9.54}$$

$$\gamma_5 = \frac{21}{128},\ \gamma_6 = -\frac{51\zeta_3}{64} - \frac{15\zeta_5}{64} + \frac{137}{256} \tag{9.55}$$

Furthermore, setting $\Delta = 0$ we find the intercept to be

$$\begin{aligned} j(0) = 2 + S(0) \quad &= \quad 2 - \frac{2}{\lambda^{1/2}} - \frac{1}{\lambda} + \frac{1}{4\,\lambda^{3/2}} + (6\zeta_3 + 2)\,\frac{1}{\lambda^2} \\ &+ \quad \left(18\,\zeta_3 + \frac{361}{64}\right)\frac{1}{\lambda^{5/2}} + \left(39\,\zeta_3 + \frac{447}{32}\right)\frac{1}{\lambda^3} + \mathcal{O}\left(\frac{1}{\lambda^{7/2}}\right). \end{aligned} \tag{9.56}$$

The first four terms successfully reproduce known results [189, 190, 191] and the last two terms of the series are a new prediction (their derivation relies on the knowledge of the constants $B_{3,4;J=2}$ found in section 5.5.3).

9.5 Numerical calculation of the Pomeron intercept

In the previous sections of this chapter we saw how QSC can be used to obtain perturbative analytic results in the BFKL regime at weak and strong coupling. Here we take an alternative approach and solve QSC numerically at intermediate values of the coupling, which are unaccessible by analytical methods. Namely, we will apply the numerical algorithm of

the previous chapter to determine the BFKL intercept numerically at intermediate values of coupling.

As explained earlier, the problem of determining $j(i\nu)$ can be mapped to the spectral problem for twist-two operators. In this approach the intercept will be defined as $j = S(\Delta = 0) + 2$, where S is the spin of the twist-two operator such that $\Delta(S) = 0$. Having formulated the problem like this, we can in principle apply the algorithm described in chapter 8 to find the correct value of S, while keeping Δ at zero. However, one may already suspect that the point $\Delta = 0$ is special. Indeed, we know that for any solution of QSC there is always another one related by $\Delta \to -\Delta$ symmetry. At the level of $\mathbf{Q}_i$ functions this allows simultaneously interchanging $\mathbf{Q}_1 \leftrightarrow \mathbf{Q}_3$ and $\mathbf{Q}_2 \leftrightarrow \mathbf{Q}_4$ as one can see from the asymptotics (4.49). From this we see that at small Δ two different solutions of QSC (related by the symmetry) approach each other, making the convergence slow, exactly like Newton's method becomes inefficient for degenerate zeros. In other words, in the limit $\Delta \to 0$ the $\mathbf{Q}$'s related by the symmetry become linearly dependent in the leading order. Furthermore, since the matrix $\mathcal{Q}_{a|i}$ should stay invertible, the leading coefficients B_i of asymptotic expansion of $\mathbf{Q}_i$ diverge at $\Delta \to 0$.

To lift the degeneracy we perform a linear transformation of $\mathbf{Q}$'s preserving the equations: it will replace two of them by linear combinations $\mathbf{Q}_3 - \gamma\mathbf{Q}_1$ and $\mathbf{Q}_4 + \gamma\mathbf{Q}_2$ with some coefficient γ, so that the divergent leading order cancels and the four functions $\mathbf{Q}_i$ become linearly independent. This will be a particular case of H-transformations (4.14), analogous to the γ-transformation (4.61) for $\mathbf{P}_a$. For the gauge choice in which $B_1 = B_2 = 1$ the transformation acts on i-indices of Q-functions with a matrix

$$H_i{}^j = \begin{pmatrix} 1 & 0 & 0 & 0 \\ 0 & 1 & 0 & 0 \\ -\gamma & 0 & 1 & 0 \\ 0 & \gamma & 0 & 1 \end{pmatrix}, \ \gamma = \frac{i(S-4)(S-2)S(S+2)}{16(S-1)^2\Delta}. \tag{9.57}$$

One can check that rotation by this matrix will render $\mathcal{Q}_{a|i}$ finite and linearly independent, and moreover, preserve relations (4.42). After this one can apply the standard procedure from chapter 8 with the only modification that the large u expansion of $\mathcal{Q}_{a|i}$ will contain $\log u/u^n$ terms in addition to the usual $1/u^n$.

Having done this, we can readily generate lots of numerical results. In particular we numerically built the function $j(\lambda)$ which interpolates perfectly between the weak and strong coupling predictions. We have found $j(\lambda)$ with high precision (up to 20 digits) for a wide range of 't Hooft coupling (going up to $\lambda \simeq 1000$). The results are also summarized

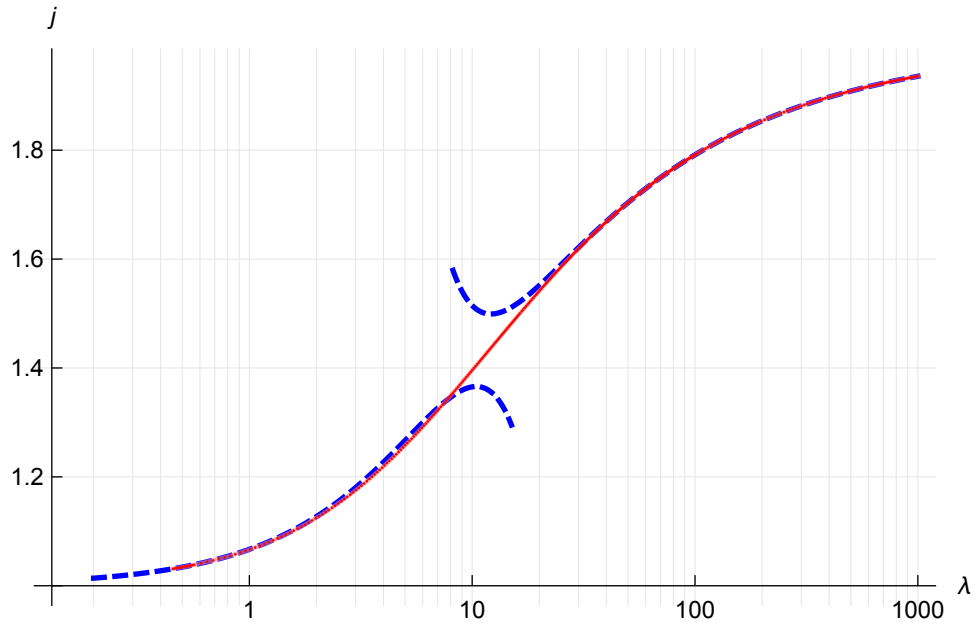

Figure 17: **The BFKL intercept j as a function of coupling λ from numerics**. The red solid line with tiny red dots is obtained by our numerical procedure. It interpolates perfectly between the known perturbative predictions (the blue dashed lines) at weak [187, 188] and strong coupling [189, 190, 191, 9].

in Tab. 3 and Fig. 17.

Tab. 3 represents a small portion of all data we generated. In particular we generated ~ 100 points with small g in the range $0.017 \ldots 0.1$, each with more than 20 digits precision. Fitting this data with powers of g^2 we found

$$j = 1 + 11.090354888959124950 68 g^2 - 84.078566807464919912295 g^4$$
$$-2543.048165180449429535212 9 g^6 + 156244.808630434501576429 24 g^8$$

where the first 3 terms are known analytically from Feynman diagram perturbation theory calculations [187, 188] and their numerical values coincide in all digits with our prediction above. The g^6 term agrees the NNLO formula we presented in the previous section to all significant digits. The last term gives a numerical prediction for the numerical values of the NNNLO BFKL pomeron intercept. Our fit also gives predictions for the higher corrections, but with smaller precision.

$\frac{\sqrt{\lambda}}{4\pi}$	$j(\lambda)$	$\frac{\sqrt{\lambda}}{4\pi}$	$j(\lambda)$
0.	1.000 000 000 000 000 000 0	0.1	1.101 144 978 997 772 874 8
0.2	1.301 794 032 258 782 208 7	0.3	1.470 445 240 989 187 630 6
0.4	1.587 128 066 254 129 730 4	0.5	1.666 438 709 974 061 852 3
0.6	1.721 917 842 815 631 353 9	0.7	1.762 239 296 816 453 814 3
0.8	1.792 626 253 069 403 59	0.9	1.816 252 952 807 284 11
1.	1.835 109 464 032 173 0	1.1	1.850 489 553 739 522 8
1.2	1.863 264 346 392 640 4	1.3	1.874 039 320 799 460
1.4	1.883 247 290 966 33	1.5	1.891 205 346 040 23
1.6	1.898 150 851 852 49	1.7	1.904 264 892 928 17
1.8	1.909 687 948 271 74	1.9	1.914 530 628 017 38
2.	1.918 881 187 304 9	2.1	1.922 810 887 750
2.2	1.926 377 890 67	2.3	1.929 630 129 41
2.4	1.932 607 459 1	2.5	1.935 343 287 2

Table 3: Numerical data for the pomeron intercept for various values of the 't Hooft coupling.

10 Integrability in $\mathbf{AdS_4/CFT_3}$

The main part of this thesis deals with integrability in $\mathrm{AdS}_5/\mathrm{CFT}_4$. However, AdS/CFT dualities in lower dimensions can also manifest integrability in the planar limit. In this chapter we will discuss the case of $\mathrm{AdS}_4/\mathrm{CFT}_3$ duality, which relates a three-dimensional supersymmetric gauge theory called ABJM to type IIA string theory on a curved background. The duality is briefly described in section 10.1. In section 10.2 we make an overview of the integrability tools in ABJM with emphasis on differences and similarities with respect to the $\mathrm{AdS}_5/\mathrm{CFT}_4$ case (for more details see [202]). As in the case of $\mathrm{AdS}_5/\mathrm{CFT}_4$, in ABJM the integrability properties of the theory are compactly encoded into a version of QSC which we discuss in section 10.3. However, ABJM possesses one important feature which differs it from $\mathcal{N} = 4$ SYM — in this theory all integrability-based calculations are performed in terms of one unknown function of coupling, so-called interpolating function $h(\lambda)$. For a long time this function was known only in its weak and strong coupling expansions. In section 10.4 we solve QSC in a near-BPS limit and in section 10.5 show how this solution allows us to make a conjecture about the exact form of the interpolating function.

10.1 Overview of AdS$_4$/CFT$_3$

The AdS$_4$/CFT$_3$ duality was proposed in [49] and relates a three-dimensional $\mathcal{N} = 6$ supersymmetric gauge theory named ABJM to type IIA string theory on $AdS_4 \times \mathbb{C}P^3$. The QFT side of the duality, ABJM theory consists of two copies of Chern-Simons theory with gauge groups $U(N)$ at levels k and $-k$ and the matter. The matter is composed of four complex scalars Y^A and four Weyl spinors ψ_A, which transform in the bi-fundamental representation of $U(N)$ and their counterparts $Y^{\dagger A}$ and $\psi^\dagger_A$ in the anti-bi-fundamental. To complete the field content one has to also include gauge fields A_μ and $\hat{A}_\mu$ of the two copies of $U(N)$, which transform in the adjoint. The explicit action can be written in the form [203]

$$\begin{aligned}\mathcal{S} = \frac{k}{4\pi}\int d^3x \Big[\epsilon^{\mu\nu\lambda}\mathrm{tr}\ \left(A_\mu\partial_\nu A_\lambda + \frac{2i}{3}A_\mu A_\nu A_\lambda\right) \\ -\mathrm{tr}\ (D_\mu Y)^\dagger D^\mu Y - i\mathrm{tr}\ \psi^\dagger D\psi - V_{ferm} - V_{bos}\Big]\end{aligned} \tag{10.1}$$

where

$$\begin{aligned}V_{bos} = -\frac{1}{12}\mathrm{tr}\ \Big[Y^A Y^\dagger_A Y^B Y^\dagger_B Y^C Y^\dagger_C + Y^\dagger_A Y^A Y^\dagger_B Y^B Y^\dagger_C Y^C \\ +4Y^A Y^\dagger_B Y_C Y^\dagger_A Y^B Y^\dagger_C - 6Y^A Y^\dagger_B Y^B Y^\dagger_A Y^C Y^\dagger_C\Big]\end{aligned} \tag{10.2}$$

and

$$\begin{aligned}V_{ferm} = \frac{i}{2}\mathrm{tr}\ \Big[Y^\dagger_A Y^A \psi^{\dagger B}\psi_B - Y^A Y^\dagger_A \psi_B \psi^{\dagger B} + 2Y^A Y^\dagger_B \psi_A \psi^{\dagger B} - 2Y^\dagger_A Y^B \psi^{\dagger A}\psi_B \\ -\epsilon^{ABCD}Y^\dagger_A \psi_B Y^\dagger_C \psi_D + \epsilon_{ABCD}Y^A \psi_{\dagger B} Y^C \psi^{\dagger D}\Big]\end{aligned} \tag{10.3}$$

Here the covariant derivative acts on the bi-fundamental fields as $D_\mu Y = \partial_\mu Y + iA_\mu Y - iY\hat{A}_\mu$.

This action possesses $OSp(6|4)$ symmetry and an additional "barionic" $U(1)$ under which bi-fundamental, anti-bi-fundamental and adjoint fields transform with charges 1, -1, and 0 respectively. The $OSp(6|4)$ group contains as a bosonic subgroups three-dimensional conformal group $Sp(4) \cong SO(2,3)$ and R-symmetry $SO(6) \cong SU(4)$. It also contains $\mathcal{N} = 6$ SUSY transformations.

The parameters of the gauge theory, N and k, are related to the parameters of the string theory, string coupling g_s and the radius R of CP^3, which is twice the radius of AdS_4

$$g_s = \left(N/k^4\right)^{1/4} = (\lambda/k^3)^{1/4},\ R^2/\alpha' = 4\pi\sqrt{2\lambda} \tag{10.4}$$

where $\lambda = N/k$. One can see that in the strong coupling limit ($\lambda \to \infty$) the string background becomes flat and strings propagate classically. On the other hand, in the small coupling limit the background becomes highly curved and the strings are quantum.

10.2 Integrability in AdS_4/CFT_3

Fields in the action (10.1) can be rescaled in such a way that the quadratic terms will come without a factor of k and the interaction terms will be suppressed by powers of $1/k$. This means that effectively $1/k$ can be treated as a coupling constant. In analogy with $\mathcal{N} = 4$ SYM one can consider 't Hooft limit, otherwise called the planar limit: weak coupling and large rank of the gauge group. In the context of ABJM this will mean

$$\lambda = N/k = \text{fixed},\ N \to \infty,\ k \to \infty. \tag{10.5}$$

As one can see from (10.4), on the string side the planar limit corresponds to $g_s \to 0$. In other words, the string interactions are suppressed and only tree-level amplitudes survive. As the $\mathcal{N} = 4$ SYM , in the planar limit ABJM becomes integrable. A similar hierarchy of integrability-based methods was developed, which we will very briefly describe here. The starting point is, as before, to map the spectral problem for the dilatation operator at weak coupling to spin chain spectral problem. Because the matter in ABJM transforms in (anti-)bi-fundamental representation, the spin chain should be alternating — fields $Y^A, \psi_{A\alpha}$ live on odd sites and $Y^\dagger_A, \psi^{\dagger A}_\alpha$ live on even sites. The Hamiltonian at two loops in $\mathfrak{su}(4)$ sector was found in [204, 205]

$$H = \frac{\lambda^2}{2} \sum_{l=1}^{2L} (2 - 2P_{l,l+2} + P_{l,l+2}K_{l,l+1} + K_{l,l+1}P_{l,l+2}) \tag{10.6}$$

It was shown to be integrable and the Bethe equations at two loops were derived, which were later generalized to all operators in [206] and [207].

As in $\mathcal{N} = 4$ SYM , the Asymptotic Bethe Ansatz — all-loop Bethe equations valid in the infinite volume limit were derived in [208]. One of its peculiarities was presence of two types of momentum-carrying roots, originating from the alternating nature of the spin-chain. Another feature which differs the ABA and, more broadly, the whole integrability picture in ABJM from that of $\mathcal{N} = 4$ SYM is that in ABJM symmetries and crossing-relations do not fix the S-matrix completely, but up to one unknown function $h(\lambda)$. This function first appears in one-magnon dispersion relation

$$E(p) = \sqrt{Q^2 + 4h^2(\lambda)\sin^2 p/2}, \tag{10.7}$$

where Q is the magnon charge equal to 1 in $\mathcal{N}=4$ SYM and 1/2 in ABJM. The real difference comes from the fact that whereas in $\mathcal{N}=4$ SYM the function $h(\lambda)$ is known and equal to $\sqrt{\lambda}/4\pi$ (the argument for its non-renormalization was given in [209]), in ABJM until recently only its weak and strong expansions were known. In section 10.5 we propose a conjecture for the exact form of this function.

On the classical side the string action was formulated and written as a coset model [210, 211, 212]

$$\frac{OSp(6|4)}{SO(1,2)\times U(3)} \tag{10.8}$$

As in $\mathcal{N}=4$ SYM case, it possesses $\mathbb{Z}_4$ grading and allows to construct an algebraic curve. In this case the algebraic curve is a ten-sheeted Riemann surface parametrized by Zhukovsky variable x satisfying

$$p_{1,2,3,4,5}(x) = -p_{10,9,8,7,6}(x) \tag{10.9}$$

These all are perturbative tools, at weak and strong coupling. The thermodynamic Bethe Ansatz, working for any value of coupling for finite length operators was developed in ABJM in [96, 97]. Finally, the cumbersome system of TBA equations was reformulated as Quantum Spectral Curve in [194]. This is our main tool and we will describe it in the next section.

10.3 Quantum Spectral Curve for ABJM

In this section we describe the Quantum Spectral Curve (QSC) also known as $\mathbf{P}\mu$-system for the ABJM model of [194]. The structure found in [194] has an unexpected and intriguing relation to that of QSC of $\mathcal{N}=4$ SYM described in the previous chapters of the thesis. Here we briefly describe the part of the construction essential for our applications.

As in $\mathcal{N}=4$ SYM , TBA can be reduced to Hirota equation for T-functions supplemented by some analyticity constraints. Then Q-functions originate as a parametrization of a general solution of this Hirota equation on given lattice. As a consequence of a different symmetry algebra, the form of a lattice here is different from that of $\mathcal{N}=4$ SYM [96, 97]. The set of Q-functions is modified as well. We do not describe here the whole Q-system, but only its $\mathbf{P}\mu$-part, essential for our calculation.

The main objects are 5 functions $\mathbf{P}_A,\ A=1,\dots,5$ and 4 function $\nu_a,\ a=1,\dots,4$ of the spectral parameter u. $\mathbf{P}_A$ are restricted by a quadratic constraint $\mathbf{P}_5=\sqrt{1-\mathbf{P}_1\mathbf{P}_4+\mathbf{P}_2\mathbf{P}_3}$. Depending on the choice of the branch cuts ν_a could be made i-periodic. However, for our

calculation it will be more convenient to choose the branch of $\nu_a(u)$ with infinitely many cuts going from $-2h+in$ to $2h+in$ for any integer n. In this case ν_a are quasi-periodic and satisfy

$$\nu_a(u+i) = -\mathbf{P}_{ab}(u)\nu^b(u), \tag{10.10}$$

where $\nu^1 = -\nu_4,\ ,\nu^2 = \nu_3,\ \nu^3 = -\nu_2,\ \nu^4 = \nu_1$ and $\mathbf{P}_{ab}$ is a 4×4 matrix built out of $\mathbf{P}_A$:

$$\mathbf{P}_{ab} = \begin{pmatrix} 0 & -\mathbf{P}_1 & -\mathbf{P}_2 & -\mathbf{P}_5 \\ \mathbf{P}_1 & 0 & -\mathbf{P}_5 & -\mathbf{P}_3 \\ \mathbf{P}_2 & \mathbf{P}_5 & 0 & -\mathbf{P}_4 \\ \mathbf{P}_5 & \mathbf{P}_3 & \mathbf{P}_4 & 0 \end{pmatrix}_{ab} . \tag{10.11}$$

Analytical continuation of ν_a under the cut $[-2h, 2h]$, denoted as $\tilde{\nu}_a$, is related to ν_a itself simply by $\tilde{\nu}_a(u) = \nu_a(u+i)$. Finally, functions $\mathbf{P}_A$ have only one cut $[-2h, 2h]$ and their analytical continuation $\tilde{\mathbf{P}}_A$ under this cut is given by

$$\tilde{\mathbf{P}}_{ab} = \mathbf{P}_{ab} + \nu_a\tilde{\nu}_b - \nu_b\tilde{\nu}_a\ . \tag{10.12}$$

It is easy to notice that this construction is very similar to that of $\mathcal{N}=4$ SYM : indeed, replace $\mathbf{P}_{ab}$ by $\mu_{ab}^{\mathcal{N}=4}$ and ν_a by $\mathbf{P}_a^{\mathcal{N}=4}$ and compare the equations (10.12) and (10.10) with (4.18) and (4.17) respectively. Algebraically, we get exactly the same equations! However, their analytical properties are interchanged (see [194] for more details).

Finally, we have to specify how the quantum numbers of a state enter into this construction. Here we focus on $\mathfrak{sl}(2)$ subsector (analogue of $\mathfrak{sl}(2)$ subsector of $\mathcal{N}=4$ SYM described in 4.4) which includes single trace operators of the type $\mathrm{tr}[D_+^S(Y^1Y_4^\dagger)^L]$ [51], thus there are 3 quantum numbers to specify: L, S, and the scaling dimension $\Delta = L+S+\gamma$, where γ denotes its anomalous part. As usual, the quantum numbers enter QSC through the large u asymptotics

$$\mathbf{P}_A \sim (A_1u^{-L}, A_2u^{-L-1}, A_3u^{+L+1}, A_4u^{+L}, A_5u^0) \tag{10.13}$$

and Δ and S are encoded into the coefficients as

$$\begin{aligned} A_1A_4 &= -\frac{2\left((\mathbf{L}-S)^2-\mathbf{\Delta}^2\right)\left((\mathbf{L}+S-1)^2-\mathbf{\Delta}^2\right)}{(1-2\mathbf{L})^2\mathbf{L}}, \\ A_2A_3 &= -\frac{2\left((\mathbf{L}+S)^2-\mathbf{\Delta}^2\right)\left((\mathbf{L}-S+1)^2-\mathbf{\Delta}^2\right)}{(1+2\mathbf{L})^2\mathbf{L}}, \end{aligned} \tag{10.14}$$

where we introduced $\mathbf{\Delta} = \Delta + \frac{1}{2}$ and $\mathbf{L} = L + \frac{1}{2}$.

[51] Strictly speaking these operators could also mix with fermions, for a detailed description see [202]

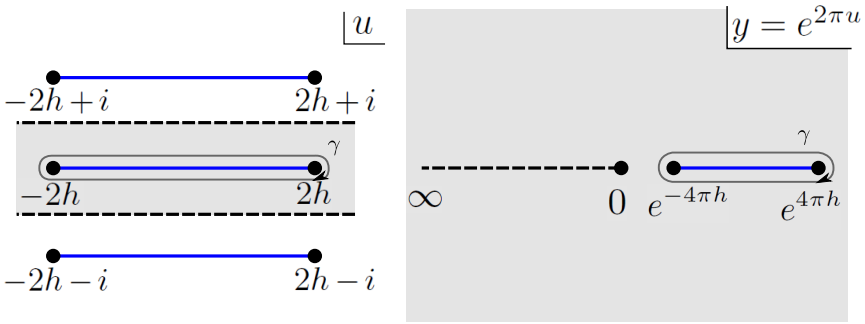

Figure 18: **Mapping the cuts.** Antiperiodic functions $\rho_{2,3}(u)$ have infinitely many short cuts. In the variable $y = e^{2\pi u}$ only two cuts remain.

10.4 Slope function

In this section we compute the slope function exactly as a function of the effective coupling $h(\lambda)$. This observable is close to the BPS point in the parameter space. Similar observables — slope and curvature — were studied in $\mathcal{N} = 4$ SYM in chapter 5 and an enormous simplification of the QSC system equations was observed there, which allowed for an exact explicit solutions for any value of 't Hooft coupling. For us the BPS operator is $\mathrm{tr}[(Y^1 Y_4^\dagger)^L]$ so in order to be close to the protected point we have to take the number of derivatives S small. The expansion coefficients in small S are expected to be exactly computable, and we will find the first such coefficient, called slope function. In $\mathcal{N} = 4$ SYM it was first computed by Basso [115]. There the situation was *a priori* simpler as in $\mathcal{N} = 4$ the slope function is not affected by wrapping effects which means that the result can be calculated solely from a simple algebraic set of equations called asymptotic Bethe ansatz. At the same time in the QSC formalism the wrapping corrections are incorporated automatically and both theories can be treated very similarly. As we will show in many ways the calculation in ABJM based on QSC is similar to that for the curvature function in $\mathcal{N} = 4$ SYM described in [9] and section 5.3 of this thesis.

To see that there is a simplification in the limit $S \to 0$, we notice that in this limit $\Delta \simeq L$ and thus $A_1 A_4 \sim A_2 A_3 \sim S$. Like in $\mathcal{N} = 4$ case we can assume that $\mathbf{P}_a \sim \sqrt{S}$, $a = 1, \ldots, 4$ and due to the constraint we must have $\mathbf{P}_5 \simeq 1$. Based on this, we found that the consistent scaling of ν_a is $\nu_1, \nu_4 \sim 1$, $\nu_2, \nu_3 \sim \sqrt{S}$. Then in the leading order of

the equations for the monodromy of ν_a become

$$\begin{pmatrix} \tilde{\nu}_1 \\ \tilde{\nu}_2 \\ \tilde{\nu}_3 \\ \tilde{\nu}_4 \end{pmatrix} = \begin{pmatrix} 1 & 0 & 0 & 0 \\ \mathbf{P}_3 & -1 & 0 & \mathbf{P}_1 \\ \mathbf{P}_4 & 0 & -1 & \mathbf{P}_2 \\ 0 & 0 & 0 & 1 \end{pmatrix} \begin{pmatrix} \nu_1 \\ \nu_2 \\ \nu_3 \\ \nu_4 \end{pmatrix}, \tag{10.15}$$

from where we see that to the leading order ν_1 and ν_4 do not have cuts whereas ν_2 and ν_3 are nontrivial. There is still certain freedom in the construction which allows, for example, to shift $\mathbf{P}_4 \to \mathbf{P}_4 + \alpha \mathbf{P}_2$ with arbitrary constant α. We use this freedom to set $\nu_1 = 1$ and $\nu_4 = 0$ [194]. The equations for the monodromy of $\mathbf{P}_a$ take the form

$$\begin{aligned} &\mathbf{P}_1 - \tilde{\mathbf{P}}_1 = \tilde{\nu}_2 - \nu_2, \ \tilde{\mathbf{P}}_3 = \mathbf{P}_3, \\ &\mathbf{P}_2 - \tilde{\mathbf{P}}_2 = \tilde{\nu}_3 - \nu_3, \ \tilde{\mathbf{P}}_4 = \mathbf{P}_4. \end{aligned} \tag{10.16}$$

From (10.15), (10.16) one can see that the equations for $\mathbf{P}_2, \mathbf{P}_4, \nu_3$ decouple from $\mathbf{P}_1, \mathbf{P}_3, \nu_2$. The two groups of equations differ only by asymptotics of $\mathbf{P}_a$, so here we only give details on the solution of the first one, i.e. $\tilde{\nu}_3 + \nu_3 = \mathbf{P}_4, \ \mathbf{P}_2 - \tilde{\mathbf{P}}_2 = \tilde{\nu}_3 - \nu_3$, which together with periodicity gives $\nu_3(u+i) + \nu_3(u) = \mathbf{P}_4(u)$. There is another important difference between ν_2 and ν_3 – we have to assume that asymptotics of ν_3 grows as $e^{\pi u}$ and ν_2 decays at infinity. This is a peculiarity of analytical continuation in S to non-integer values, described for $\mathcal{N} = 4$ SYM in [9] in detail.

Taking into account that $\mathbf{P}_4$ does not have a cut according to (10.16) and also its asymptotic behavior (10.13), we conclude that it is a polynomial in u of degree L. Introducing notations

$$\nu_3(u + \tfrac{i}{2}) = \rho_3(u + \tfrac{i}{2}) + Q_3(u), \tag{10.17}$$

where $Q_3(u)$ is a polynomial such that $Q_3(u + \frac{i}{2}) + Q_3(u - \frac{i}{2}) = \mathbf{P}_4(u)$, we get

$$\rho_3(u+i) = -\rho_3(u) \ , \ \ \tilde{\rho}_3 + \rho_3 = Q_3^+ - Q_3^- \equiv q_3 \ , \tag{10.18}$$

i.e. ρ_3 is antiperiodic. It is convenient to make a change of variables $y = e^{2\pi u}$, which maps infinitely many cuts of ν_i or ρ_i into one cut and introduces a quadratic cut from 0 to $-\infty$, see Fig. 18.

In order to resolve equations of the form $\tilde{g} + g = f$ like in (10.18) we define the following Hilbert transformation H as

$$H[f](z) = \frac{1}{2} \oint_\gamma \frac{dy}{2\pi i} \frac{\sqrt{z - e^{4\pi h}}\sqrt{z - e^{-4\pi h}}}{\sqrt{y - e^{4\pi h}}\sqrt{y - e^{-4\pi h}}} \frac{f(y)}{y - z}, \tag{10.19}$$

which gives a solution of this equation with non-growing asymptotics at infinity with one cut $[e^{-4\pi h}, e^{+4\pi h}]$. Note, however, that $\rho_3(z)$ has another cut $(-\infty, 0)$ on which it simply changes its sign. We can overcome this problem by dividing it by $\sqrt{z}$. After that we can use (10.19) to get

$$\rho_3(z) = \frac{C}{\sqrt{z}} + \sqrt{z} H\left[\frac{1}{\sqrt{y}} q_3\left(\frac{\log y}{2\pi}\right) - \frac{2C}{y}\right] . \tag{10.20}$$

The term proportional to C is added here, because it is not prohibited by the asymptotics: ν_3 can grow as $e^{\pi u}$ at infinity. The constant C is fixed at the end from the condition that $\rho_3(u)$ should be even.

Next, knowing ρ_3 and thus ν_3 in terms of the yet to be fixed polynomial $\mathbf{P}_4$, we can find $\mathbf{P}_2$ as a solution of corresponding equation in (10.16). As $\mathbf{P}_2$ is a function with one cut we simply use the Cauchy kernel

$$\mathbf{P}_2(v) = -\oint \frac{dz}{2\pi i z} \frac{\rho_3(z)}{\log z - 2\pi v}. \tag{10.21}$$

Thus we found all the objects in terms of a few coefficients of the polynomial $\mathbf{P}_4$. To extract $\gamma_L(h)$ we have to find these coefficients. Consider first, for simplicity, $L = 1$. In this case $\mathbf{P}_4 = A_4 u$, so $q_3 = i\frac{A_4}{2}$ and

$$\mathbf{P}_2 = A_4 \oint \frac{dz}{4\pi\sqrt{z}} \frac{H[y^{-1/2}]}{2\pi v - \log z}. \tag{10.22}$$

Thus considering the leading asymptotics of $\mathbf{P}_2$ we can obtain

$$A_2/A_4 = \oint \frac{dz \log z}{2(2\pi)^3\sqrt{z}} H[y^{-\frac{1}{2}}] \tag{10.23}$$

and similarly $\mathbf{P}_1$ gives A_1/A_3. On the other hand, expanding equations (10.14) to the first order in S yields $\gamma_1 = \frac{-2S}{1+\frac{L}{L+1}\frac{A_1 A_4}{A_3 A2}}$ and substituting the ratios of the coefficients we get

$$\gamma_1(h) = -2S \frac{\partial_\alpha I_{-\frac{1}{2},-\frac{1}{2}}}{\partial_\alpha I_{-\frac{1}{2},-\frac{1}{2}} + \partial_\beta I_{-\frac{1}{2},-\frac{1}{2}}}, \tag{10.24}$$

where

$$I_{\alpha,\beta} = \oint_\gamma dy \oint_\gamma dz \frac{\sqrt{y - e^{4\pi h}}\sqrt{y - e^{-4\pi h}}}{\sqrt{z - e^{4\pi h}}\sqrt{z - e^{-4\pi h}}} \frac{y^\alpha z^\beta}{z - y}. \tag{10.25}$$

Both integrals go around the cut $[e^{-4\pi h}, e^{4\pi h}]$. Another convenient representation of $I_{\alpha,\beta} e^{4\pi h(\alpha+\beta+1)}$ is

$$\pi^2 \beta \int_0^{e^{8\pi h}-1} {}_2F_1\left(\tfrac{3}{2}, -\alpha; 2; -S\right) {}_2F_1\left(\tfrac{3}{2}, 1-\beta; 2; -S\right) S dS. \tag{10.26}$$

For odd $L > 1$ there are $\frac{L+1}{2}$ constants in q_3. To fix them we use $\frac{L-1}{2}$ conditions of the form $\oint \frac{du}{2\pi i} u^k \gamma_3(u) = 0$ for $k = 1, 3 \ldots L-2$, which ensure that asymptotics of $\mathbf{P}_2$ at

infinity is $\mathcal{O}\left(u^{-L-1}\right)$. These conditions take a form of a system of linear equations for constants entering q_3 with coefficients of the form $s_{n,k} = \partial_\alpha^k \partial_\beta^n I_{-1/2,-1/2}$. The solution for this system takes form of a ratio of determinants made of $s_{n,k}$. A similar strategy also applies to $\mathbf{P}_1, \mathbf{P}_3$ and ν_2.

Using again the formula for γ_L in terms of A_1/A_3, A_2/A_4 we get that the result for any L [52] is

$$\gamma_L = -\frac{2S}{1 + r_L/r_{L-2}}\,, \tag{10.27}$$

where

$$r_L = \frac{\det s_{L-2i-1,L-2j}}{\det s_{L-2i,L-2j-1}},\ i,j = 0\ldots\lfloor\tfrac{L}{2}\rfloor,\ L \geq 0 \tag{10.28}$$

We define $s_{k,n}$ as

$$s_{k,n} = \partial_\alpha^k \partial_\beta^n I_{-1/2,-1/2},\quad k,n \geq 0, \tag{10.29}$$

and

$$s_{k,-1} = \partial_\alpha^k I_{-1/2,-1}, \tag{10.30}$$

$$s_{-1,n} = \frac{1}{2}\partial_\beta^n \left(e^{4\pi\beta h}{}_2F_1\left(\frac{1}{2},-\beta;1,1-e^{8\pi h}\right)\right)\Big|_{\beta=-1/2}. \tag{10.31}$$

Equation (10.27) is our result for the slope function which we now test at weak and strong coupling.

Weak coupling. At weak coupling it is convenient to use (10.26). Up to the order h^{2L} we can compare our result against the slope function $\gamma_L^{ABA} = S\frac{2\pi h}{L}\frac{I_{J+1}(2\pi h)}{I_J(2\pi h)}$ of $\mathcal{N}=4$ SYM [115] which does not take into account the wrapping effects. These effects appear at the order $\mathcal{O}\left(h^{2L+2}\right)$ and the leading deviation can be compared with the Lüscher correction which we found as a generalization of [213, 214]:

$$\gamma_L^{wrap} = -Sh^{2L+2}\frac{4\pi^{3/2}(4^L-2)\zeta_{2L}\Gamma\left(L+\frac{1}{2}\right)}{L\Gamma(L+2)}. \tag{10.32}$$

We found a perfect agreement with our exact formula for $L = 1,\ldots,5$ and 7.

Strong coupling. At strong coupling we notice an interesting phenomenon – our result can be written explicitly as a rational function of h with exponential precision. For example $\gamma_{L=1} = \frac{4\mathbf{g}^3-12\mathbf{g}^2+12\mathbf{g}-3\zeta_3}{6\mathbf{g}^2-6\mathbf{g}}S + \mathcal{O}(e^{-4\mathbf{g}})$ where $\mathbf{g} = 2\pi h + \log 2$. To get this expression we

[52] the procedure for odd L, which we do not describe here, is analogous.

have evaluated the integral (10.25) with exponential precision

$$I_{\alpha\beta} \simeq -\frac{2\pi\Gamma\left(\alpha+\frac{1}{2}\right)\Gamma\left(-\beta-\frac{1}{2}\right)e^{4\pi h(\alpha-\beta)}}{\Gamma(\alpha+2)\Gamma(-\beta)} \\ -\frac{4\pi\left(\beta+\frac{1}{2}\right)\Gamma\left(-\alpha-\frac{1}{2}\right)\Gamma\left(-\beta-\frac{1}{2}\right)e^{4\pi h(-\alpha-\beta-1)}}{(\alpha+\beta+1)\Gamma(-\alpha)\Gamma(-\beta)} \\ +\frac{4\pi(\alpha+\frac{1}{2})\Gamma\left(+\alpha+\frac{1}{2}\right)\Gamma\left(+\beta+\frac{1}{2}\right)e^{4\pi h(+\alpha+\beta+1)}}{(\alpha+\beta+1)\Gamma(\alpha+2)\Gamma(\beta)}\,. \tag{10.33}$$

We found that for any L the result is some rational function of $\mathbf{g}$ of a growing with L complexity. However, the large $\mathbf{g}$ expansion coefficients can be found explicitly for any L to be

$$\frac{\gamma_L}{S} = \frac{\mathbf{g}-L-1}{L+\frac{1}{2}} + \left(\frac{1}{2\mathbf{g}} - \frac{3\zeta_3-4}{8\mathbf{g}^2}\right)\frac{L^2+L}{L+\frac{1}{2}} + \mathcal{O}(\mathbf{g}^{-3}). \tag{10.34}$$

To test our result we take the quasi-classical limit $L \sim \mathbf{g} \gg 1$. Introducing $\mathcal{J} = \frac{L+1/2}{\mathbf{g}} \sim 1$ and $\mathcal{S} = \frac{S}{\mathbf{g}}$ and expanding at large $\mathbf{g}$ in (10.34) we find

$$\frac{\Delta - L}{S} \simeq \left(\frac{1}{\mathcal{J}} + \frac{\mathcal{J}}{2} + \dots\right) + \frac{1}{\mathbf{g}}\left(\frac{-1}{2\mathcal{J}} + \mathcal{J}\frac{4-3\zeta_3}{8} + \dots\right)$$

which reproduces the corresponding terms in the tree level and one-loop quasi-classical folded string quantization [215]. Note that with our definition of $\mathcal{J}$ all $\log 2$ terms and all even powers of $\mathcal{J}$ disappear from the one-loop terms of [215]. From that we can see that $\mathbf{L} \equiv L + 1/2$, which appears in denominator of (10.34), and $\mathbf{\Delta} \equiv \Delta + 1/2$ are natural combinations as is already clear at the level of (10.14) which only depends on $\mathbf{\Delta}^2$ and where under the change of sign of $\mathbf{L}$ the two lines in (10.14) simply interchange. This hints the following ansatz for double expansion at large $\mathbf{g}$ and small S, similar to the result (5.129) for $\mathcal{N} = 4$ SYM [115]

$$\mathbf{\Delta}^2 - \mathbf{L}^2 = \sum_{n,k=1} A_{n,k}(\mathbf{L}^2) S^n \mathbf{g}^{-n-k+3} \tag{10.35}$$

where the coefficients $A_{n,k}$ are polynomials of degree $\lfloor \frac{k}{2} \rfloor$ in $\mathbf{L}^2$. By comparison with (10.34) and with quasi-classics [216] we find $A_{1,1} = 2$, $A_{1,2} = -1$, $A_{1,3} = \mathbf{L}^2 - \frac{1}{4}$, $A_{1,4} = (\mathbf{L}^2 - \frac{1}{4})(1 - \frac{3\zeta_3}{4})$, $A_{2,1} = \frac{3}{2}$, $A_{2,2} = \frac{5}{8} - \frac{9\zeta_3}{4}$. Next we can re-expand (10.35) sending $\mathbf{g} \to \infty$ like in [115]. For example at $L = 1, S = 2$ we get (10.35)

$$\Delta_{L=1,S=2} = 2\sqrt{\mathbf{g}} - \frac{1}{2} + \frac{25}{16\sqrt{\mathbf{g}}} + \left(\frac{271}{1024} - \frac{9\zeta_3}{4}\right)\mathbf{g}^{-3/2} + \dots\,. \tag{10.36}$$

which gives a prediction for a strong coupling expansion of the anomalous dimension of a short operator. As we see this result can be trivially generalized to any S and L, but the expression we found is rather bulky. We also note that the third term disagrees with [216], which is most likely due to the different ansatz used in [216]. As our ansatz is

based on an extra insight about the structure of the spectrum coming from QSC and the symmetries of (10.14) our result is likely to be the correct one. It would be interesting to use the methods of [185] to check this result. That is important to note that it is not expected that this result holds for odd S, as operators with odd S belong to a different trajectory, as can be seen already at weak coupling [207, 217]. In particular the analytical continuation of γ from odd S does not go through the BPS point and does not vanish at $S = 0$ and thus should be treated differently [53].

10.5 Comparison with localization and $h(\lambda)$

Here we compare the structure of our result for the slope function with the result of [218, 219, 220] obtained using localization [221, 222]. The quantity calculated in [218] is the expectation value of 1/6 BPS Wilson loop, which in $\mathcal{N} = 4$ is known to similar to the slope function. Although in ABJM these quantities are not related that closely, we still expect similarity in structure, which allow us to make a conjecture about $h(\lambda)$. The result of [218] can be written in a parametric form in terms of κ as an integral over the matrix-model eigenvalue $\log Z$

$$\langle W^{1/6}_{m=1} \rangle = \int_{\frac{1}{A^+}}^{A^+} \frac{dZ}{2\pi^2 i\lambda} \arctan \sqrt{\frac{2 + i\kappa - Z - \frac{1}{Z}}{2 - i\kappa + Z + \frac{1}{Z}}} \tag{10.37}$$

we see that the argument of arctan has 4 branch-points. The integration goes between the branch-points from the numerator are A^+ and $1/A^+$ and those from the denominator, which we denote A^- and $1/A^-$ where

$$A^{\pm} = \pm\tfrac{1}{2}\left(2 \pm i\kappa + \sqrt{\kappa(\pm 4i - \kappa)}\right) \tag{10.38}$$

and the parameter κ is related to the 't Hooft coupling by [218]

$$\lambda = \frac{\kappa}{8\pi} {}_3F_2\left(\frac{1}{2}, \frac{1}{2}, \frac{1}{2}; 1, \frac{3}{2}; -\frac{\kappa^2}{16}\right). \tag{10.39}$$

The main observation is that the integral (10.37) is similar to the main ingredient of our result (10.25). To make the similarity more clear, one can make a change of variable with a suitable Mobius transformation which will map the branch points $A^- \to \infty, 1/A^- \to 0$ and $A^+ \to G, 1/A^+ \to 1/G$ like on Fig.18. There is a unique Mobius transformation with this property. Furthermore, it fixes uniquely the value of G in terms of κ as $G = \left(\frac{1}{4}(\sqrt{\kappa^2 + 16} + \kappa)\right)^2$, which is easy to find from the cross-ratio of the branch points before

[53] We thank B.Basso for pointing this subtlety out to us.

and after the transformation. Thus to relate (10.37) with (10.25) we set $G = e^{4\pi h}$ which leads to our conjecture

$$\lambda = \frac{\sinh(2\pi h)}{2\pi} {}_3F_2\left(\frac{1}{2}, \frac{1}{2}, \frac{1}{2}; 1, \frac{3}{2}; -\sinh^2(2\pi h)\right) . \tag{10.40}$$

Expansion at weak/strong coupling gives

$$\begin{aligned} h(\lambda) &= \lambda - \frac{\pi^2\lambda^3}{3} + \frac{5\pi^4\lambda^5}{12} - \frac{893\pi^6\lambda^7}{1260} + \mathcal{O}(\lambda^9), \\ h(\lambda) &= \sqrt{\frac{1}{2}\left(\lambda - \frac{1}{24}\right)} - \frac{\log 2}{2\pi} + \mathcal{O}\left(e^{-\pi\sqrt{8\lambda}}\right), \end{aligned} \tag{10.41}$$

which reproduces all known coefficients at weak and at strong coupling i.e. in total 4 nontrivial coefficients [223, 224, 225, 226, 227]. Curiously, the shift by $-\frac{1}{24}$ at strong coupling coincides with the anomalous radius shift of AdS found in [228], as also noticed in [220].

Of course such identification at the level of the integrands is not completely rigorous and in order to derive $h(\lambda)$ one should apply the method of the QSC to the Bremsstrahlung function like in [155, 95, 91, 7] and compare it to the result from localization [219, 229, 230] for *the same* quantity (for recent results on weak and strong coupling expansions of Bremsstrahlung function see [231, 232]).

A non-trivial perturbative check supporting our conjecture appeared in [233], where null cusp anomalous dimension was computed at two loops at strong coupling.

Part III

Conclusions and appendices

11 Conclusions and perspectives

In this thesis we studied the Quantum Spectral Curve method in application to AdS_5/CFT_4 and AdS_4/CFT_3 .

After reviewing the AdS_5/CFT_4 duality and the previously existing integrability methods in it, we presented a brief, but self-sufficient description of the Quantum Spectral Curve method. This method yields the ultimate simplification of the spectral problem in planar AdS/CFT: it allows to compute conformal dimensions of arbitrary operators at arbitrary values of the coupling. Namely, it reduces this computation to a system of equations in terms of monodromies of several functions of the spectral parameter in the complex plane.

In the rest of the thesis we consider different limits of this system and apply it to various problems in $\mathrm{AdS}_5/\mathrm{CFT}_4$ and $\mathrm{AdS}_4/\mathrm{CFT}_3$

The first limit we consider is a near-BPS, small spin limit of twist-two operators and compute the quadratic correction in spin which we call *the curvature function*. From this finite coupling result we extract several perturbative predictions, in particular new term in the strong coupling expansion of Konishi operator and two new terms in the strong coupling expansion of BFKL intercept.

Then we consider a different kind of observable, but also in a near-BPS limit: a cusped Wilson line with insertion of scalar operators at the cusp. We calculate the cusp anomalous dimension using two methods: first, using the Thermodynamical Bethe Ansatz and then in a such simpler computation using QSC method. The result for general length L of the inserted operator turns out to be expressed through determinants of matrices of sizes proportional to L. The quasiclassical limit of this kind of expression is an interesting problem in itself because of its relation to Matrix Models and, of course, it helps to compare against strong coupling perturbative results. We found the corresponding classical algebraic curve, which for open string solutions is a non-trivial task, because there is no general method analogous to the monodromy construction for closed strings.

Although analytical calculations with QSC are much easier than with previously existing techniques, their scope of applications is still restricted to particular limiting cases. Thus we developed an efficient numerical method for solving the QSC and demonstrate its power by exploring operators from $\mathfrak{sl}(2)$ sector for physical values of spin and away from them: see, for example, Fig. 11 which shows the dependence of S on Δ in the complex plane.

An extremely interesting regime to study is the high energy Regge scattering, which is related to the spectral problem for twist operators analytically continued to negative values of spin, and thus can be studied by the method of QSC. We review the previously existing results and present a new one — NNLO correction to BFKL eigenvalue, a quantity which is practically unaccessible to perturbative calculations.

Finally, QSC was also developed in $\mathrm{AdS}_4/\mathrm{CFT}_3$. There we again consider small spin limit of twist operators and calculate the linear in spin contribution to the anomalous dimension. Moreover and more importantly, by comparing our result with a certain localization computation, we were able to extract the so-called interpolating function $h(\lambda)$ — an important and previously missing ingredient of the integrability picture in $\mathrm{AdS}_4/\mathrm{CFT}_3$.

The method of QSC has clearly proved its efficiency, but there are plenty of directions in which it can be developed.

The first and obvious one is formulating the QSC for lower-dimensional AdS/CFT. A partial description of QSC for AdS_4/CFT_3 appeared in [194]. The AdS_3/CFT_2 case was for a long time a challenge for researchers: a large body of work on it was done [234, 235, 236, 237, 238, 239, 240, 241, 242], however until very recently even the all-loop Bethe Ansatz was not known in this case. Since the dressing phase necessary to write down such an ansatz was found in [243], one might hope that QSC will soon be found for this system as well. It is also worth mentioning that a variant of QSC has been developed for Hubbard model [244].

The standard way to derive QSC is from Thermodynamical Bethe Ansatz. However, the equations of TBA are much more cumbersome then those of QSC: instead of equations for monodromy of several functions with known analytical properties you have an infinite system of non-linear integral equations. Hence one might try to derive the elegant QSC description directly from first principles and symmetry considerations.

As have been mentioned before, $\mathcal{N} = 4$ SYM is a conformal theory, and this means that data from the two-point functions (conformal dimensions of the fields) and from three-point functions (structure constants) will be enough, at least in principle, to define the whole theory, in particular, an n-point correlator. While large progress has been achieved in applying QSC to the first part — the spectral problem — there has not been any applications of QSC to three-point functions yet. However, work in progress suggests that such application is possible in combination with Sklyanin's Separation of Variables method. In particular, there are indication that in this approach $\mathbf{P}_a$ play the role of wave-functions. This direction is particularly promising because of the huge progress achieved recently for three-point function with SoV and Spin Vertex approach [245, 246, 247, 248] as well as with OPE approach [249].

Finally, after we have several example of Quantum Spectral Curve for different systems it is not improbable that some general rule can be derived which could tell us how QSC should look like based on the symmetry of the system.

In addition to these global problems there are a lot of smaller ones which arise as a natural development of the problem developed in this thesis. We will only name several most interesting ones.

After we have found an analytical form of NNLO BFKL, which seem to be unaccessible for so manly years, it would be interesting to move further in this direction. First of all,

it is apparent that our initial conjecture that the result is expressed in terms of harmonic sums can be made much stronger: since only 37 of possible 288 function enter the basis, it is clear that we only need a certain subclass of all possible harmonic sums of given transcendentality. Once this subclass is identified, it would not be very hard to calculate further corrections; more importantly, it will tell us something about the structure of the general term in the expansion and possibility of resummation.

We have described an algorithm solving QSC numerically and demonstrated its application to some simple examples. There is obviously a lot of work to be done here. First, the algorithm, which is now written in Mathematica, can be rewritten in a lower-level language, such a C and optimized, which should strongly increase its performance. Second, although the method was described for any local operator, the computations we presented all lie in the $\mathfrak{sl}(2)$ sector. Numerical studies of states outside of this sector is the goal of the nearest future.

Everywhere in the thesis we working in the planar limit. However, if we want to approach QCD, which has $N = 3$, we have to find way to go beyond this limit. It is a general understanding that beyond for finite N integrability probably breaks down. Can some of the results obtained with integrability give us a hint of what happens for finite N? To try and answer this question we recall that localization techniques allow to described expectation values of certain supersymmetric enough observables as integrals in matrix models of size N. In the large N limit the eigenvalues which are integrated over condense into cuts. In section 10, based on our paper [14], we used a map of these cuts onto the Zhukovsky cuts appearing in integrability calculations. This map seems to make physical sense: it produces a conjecture for the interpolating function $h(\lambda)$ which is supported by independent perturbative tests. So one might propose a hypothesis that Zhukovsky cuts are actually formed at large N by condensed eigenvalues of a particular matrix model which would describe the system at finite N. We will certainly check this hypothesis in our future work.

An important and still unexplored field of work can be trying to relate integrability-based approach with another, parallel one — on-shell methods of computing scattering amplitudes and emerged from there positive Grassmannian. Both approaches study the same theory, $\mathcal{N} = 4$ SYM , and both reveal beautiful mathematical structures, however different ones. Some work in this direction was done in the series of papers [250, 251, 252, 253, 254, 255] but still the connection between the two approaches is far from clear.

Another possible approach connecting integrability to scattering amplitude studies is

the limit of strong coupling where amplitudes are determined by areas of minimal surfaces with null-polygonal boundary. These areas are described by so-called "Thermodynamical Bubble Ansatz" [256, 257, 258] which was noticed to have formal similarity to TBA. Understanding the possible connection between these two Ansätze can tell us if some form of TBA (and as a consequence QSC) can be applied to calculation of scattering amplitudes.

A Appendices to chapter 5

A.1 Summary of notation and definitions

In this appendix we summarize some notation used throughout chapter 5.

Laurent expansions in x

We often represent functions of the spectral parameter u as a series in x

$$f(u) = \sum_{n=-\infty}^{\infty} f_n x^n \tag{A.1}$$

We denote by $[f]_+$ and $[f]_-$ part of the series with positive and negative powers of x:

$$[f]_+ = \sum_{n=1}^{\infty} f_n x^n, \tag{A.2}$$

$$[f]_- = \sum_{n=1}^{\infty} f_{-n} x^{-n}. \tag{A.3}$$

Functions $\sinh_\pm$ and $\cosh_\pm$

We define $I_k = I_k(4\pi g)$, where $I_k(u)$ is the modified Bessel function of the first kind. Then

$$\sinh_+ = [\sinh(2\pi u)]_+ = \sum_{k=1}^{\infty} I_{2k-1} x^{2k-1}, \tag{A.4}$$

$$\sinh_- = [\sinh(2\pi u)]_- = \sum_{k=1}^{\infty} I_{2k-1} x^{-2k+1}, \tag{A.5}$$

$$\cosh_+ = [\cosh(2\pi u)]_+ = \sum_{k=1}^{\infty} I_{2k} x^{2k}, \tag{A.6}$$

$$\cosh_- = [\cosh(2\pi u)]_- = \sum_{k=1}^{\infty} I_{2k} x^{-2k}. \tag{A.7}$$

In some cases we denote for brevity

$$\mathrm{sh}_-^x = \sinh_-(x), \quad \mathrm{ch}_-^x = \cosh_-(x). \tag{A.8}$$

Integral kernels

In order to solve for $\mathbf{P}_a^{(1)}$ in section 5.3.1 we introduce integral operators H and K with kernels

$$H(u,v) = -\frac{1}{4\pi i}\frac{\sqrt{u-2g}\sqrt{u+2g}}{\sqrt{v-2g}\sqrt{v+2g}}\frac{1}{u-v}dv, \tag{A.9}$$

$$K(u,v) = +\frac{1}{4\pi i}\frac{1}{u-v}dv, \tag{A.10}$$

which satisfy

$$\tilde{f}+f=h \ , \ f=H\cdot h \quad \text{and} \quad \tilde{f}-f=h \ , \ f=K\cdot h. \tag{A.11}$$

Since the purpose of H and K is to solve equations of the type A.11, H usually acts on functions h such that $\tilde{h}=h$, whereas K acts on h such that $\tilde{h}=-h$. On the corresponding classes of functions H and K can be represented by kernels which are equal up to a sign

$$H(u,v) = -\frac{1}{2\pi i}\frac{1}{x_u-x_v}dx_v\Big|_{\tilde{h}=h}, \tag{A.12}$$

$$K(u,v) = \frac{1}{2\pi i}\frac{1}{x_u-x_v}dx_v\Big|_{\tilde{h}=-h}. \tag{A.13}$$

In order to be able to deal with series in half-integer powers of x in section 5.3.3 we introduce modified kernels:

$$H^*\cdot f \equiv \frac{x+1}{\sqrt{x}}H\cdot\frac{\sqrt{x}}{x+1}f, \tag{A.14}$$

$$K^*\cdot f \equiv \frac{x+1}{\sqrt{x}}K\cdot\frac{\sqrt{x}}{x+1}f. \tag{A.15}$$

Finally, to write the solution to equations of the type (5.53), we introduce the operator Γ' and its more symmetric version Γ

$$\left(\Gamma'\cdot h\right)(u) \equiv \oint_{-2g}^{2g}\frac{dv}{4\pi i}\partial_u \log\frac{\Gamma[i(u-v)+1]}{\Gamma[-i(u-v)]}h(v), \tag{A.16}$$

$$\left(\Gamma\cdot h\right)(u) \equiv \oint_{-2g}^{2g}\frac{dv}{4\pi i}\partial_u \log\frac{\Gamma[i(u-v)+1]}{\Gamma[-i(u-v)+1]}h(v). \tag{A.17}$$

Periodized Chebyshev polynomials

Periodized Chebyshev polynomials appearing in $\mu_{ab}^{(1)}$ are defined as

$$p'_a(u) = \Sigma \cdot [x^a + 1/x^a] = 2\Sigma \cdot \left[T_a\left(\frac{u}{2g}\right)\right], \tag{A.18}$$

$$p_a(u) = p'_a(u) + \frac{1}{2}\left(x^a(u) + x^{-a}(u)\right), \tag{A.19}$$

where $T_a(u)$ are Chebyshev polynomials of the first kind. Here is the explicit form for the first five of them:

$$p'_0 = -i(u - i/2), \tag{A.20}$$

$$p'_1 = -i\frac{u(u-i)}{4g}, \tag{A.21}$$

$$p'_2 = -i\frac{(u-i/2)(-6g^2+u^2-iu)}{6g^2}, \tag{A.22}$$

$$p'_3 = -i\frac{u(u-i)\left(-6g^2+u(u-i)\right)}{8g^3}, \tag{A.23}$$

$$p'_4 = -i\frac{\left(u-\frac{i}{2}\right)\left(30g^4-20g^2u^2+20ig^2u+3u^4-6iu^3-2u^2-iu\right)}{30g^4}. \tag{A.24}$$

A.2 The slope function for odd J

Here we give details on solving QSC for odd J at leading order in the spin. First, the parity of the μ_{ab} functions is different from the even J case, which can be seen from the asymptotics (4.54). Following arguments similar to the discussion for even J in section 5.1, we obtain

$$\mu_{12} = 1,\ \mu_{13} = 0,\ \mu_{14} = 0,\ \mu_{24} = \cosh(2\pi u),\ \mu_{34} = 1. \tag{A.25}$$

Plugging these μ_{ab} into (4.46) we get a system of equations for $\mathbf{P}_a$

$$\tilde{\mathbf{P}}_1 = -\mathbf{P}_3, \tag{A.26}$$

$$\tilde{\mathbf{P}}_2 = -\mathbf{P}_4 - \mathbf{P}_1\cosh(2\pi u), \tag{A.27}$$

$$\tilde{\mathbf{P}}_3 = -\mathbf{P}_1, \tag{A.28}$$

$$\tilde{\mathbf{P}}_4 = -\mathbf{P}_2 + \mathbf{P}_3\cosh(2\pi u). \tag{A.29}$$

This system can be solved in a similar way to the even J case. The only important difference is that due to asymptotics (4.48) the $\mathbf{P}_a$ acquire an extra branch point at $u = \infty$.

Let us first rewrite the equations for $\mathbf{P}_1, \mathbf{P}_3$ as

$$\tilde{\mathbf{P}}_1 + \tilde{\mathbf{P}}_3 = -(\mathbf{P}_1 + \mathbf{P}_3) \tag{A.30}$$

$$\tilde{\mathbf{P}}_1 - \tilde{\mathbf{P}}_3 = \mathbf{P}_1 - \mathbf{P}_3. \tag{A.31}$$

This, together with the asymptotics (4.48) implies $\mathbf{P}_1 = \epsilon x^{-J/2},\ \mathbf{P}_3 = -\epsilon x^{J/2}$ where ϵ is a constant. Let us note that these $\mathbf{P}_1, \mathbf{P}_3$ contain half-integer powers of x, and the analytic continuation around the branch points at $\pm 2g$ replaces $\sqrt{x} \to 1/\sqrt{x}$. Now, taking the sum and difference of the equations for $\mathbf{P}_2,\ \mathbf{P}_4$ we get

$$\tilde{\mathbf{P}}_2 + \tilde{\mathbf{P}}_4 + \mathbf{P}_2 + \mathbf{P}_4 = -a_1 \left(x^{J/2} + x^{-J/2}\right) \cosh 2\pi u \tag{A.32}$$

$$\tilde{\mathbf{P}}_2 - \tilde{\mathbf{P}}_4 - (\mathbf{P}_2 - \mathbf{P}_4) = a_1 \left(x^{J/2} - x^{-J/2}\right) \cosh 2\pi u \tag{A.33}$$

We can split the expansion

$$\cosh 2\pi u = \sum_{k=-\infty}^{\infty} I_{2k} x^{2k} \tag{A.34}$$

into the positive and negative parts according to

$$\cosh 2\pi u = \cosh_- + \cosh_+ + I_0 \tag{A.35}$$

where

$$\cosh_+ = \sum_{k=1}^{\infty} I_{2k} x^{2k}, \qquad \cosh_- = \sum_{k=1}^{\infty} I_{2k} x^{-2k}. \tag{A.36}$$

Then we can write

$$\mathbf{P}_2 + \mathbf{P}_4 = -a_1 (x^{J/2} + x^{-J/2}) \cosh_- - a_1 I_0 x^{-J/2} + Q, \tag{A.37}$$

$$\mathbf{P}_2 - \mathbf{P}_4 = -a_1 (x^{J/2} - x^{-J/2}) \cosh_- + a_1 I_0 x^{-J/2} + P, \tag{A.38}$$

where Q and P are some polynomials in $\sqrt{x}, 1/\sqrt{x}$ satisfying

$$\tilde{Q} = -Q,\ \tilde{P} = P. \tag{A.39}$$

We get

$$\mathbf{P}_2 = -a_1 x^{J/2} \cosh_- + \frac{Q+P}{2}, \tag{A.40}$$

$$\mathbf{P}_4 = a_1 x^{-J/2} \cosh_- - a_1 I_0 x^{-J/2} + \frac{Q-P}{2}. \tag{A.41}$$

Now imposing the correct asymptotics of $\mathbf{P}_2$ we find

$$\frac{P+Q}{2} = a_1 x^{J/2} \sum_{k=1}^{\frac{J-1}{2}} I_{2k} x^{-2k} \tag{A.42}$$

Due to (A.39) this relation fixes Q and P completely, and we obtain the solution given in section 2.1,

$$\mu_{12} = 1,\ \mu_{13} = 0,\ \mu_{14} = 0,\ \mu_{24} = \cosh(2\pi u),\ \mu_{34} = 1, \tag{A.43}$$

$$\mathbf{P}_1 = a_1 x^{-J/2}, \tag{A.44}$$

$$\mathbf{P}_2 = -a_1 x^{J/2} \sum_{k=-\infty}^{-\frac{J+1}{2}} I_{2k} x^{2k}, \tag{A.45}$$

$$\mathbf{P}_3 = -a_1 x^{J/2}, \tag{A.46}$$

$$\mathbf{P}_4 = a_1 x^{-J/2} \cosh_- -a_1 x^{-J/2} \sum_{k=1}^{\frac{J-1}{2}} I_{2k} x^{2k} - a_1 I_0 x^{-J/2}. \tag{A.47}$$

Notice that the branch point at infinity is absent from the product of any two $\mathbf{P}$'s, as it should be [7], [8]. One can check that this solution gives again the correct result (5.36) for the slope function.

A.3 NLO solution of QSC: details

In this appendix we will provide more details on the solution of QSC and calculation of curvature function for $J = 2, 3, 4$ which was presented in the main text in section 5.3.

NLO corrections to μ_{ab} for $J = 2$

Here we present some details of calculation of NLO corrections to μ_{ab} for $J = 2$ omitted in the main text. As described in section 5.3.1, $\mu_{ab}^{(1)}$ are found as solutions of (5.53) with appropriate asymptotics. The general solution of this equation consists of a general solution of the corresponding homogeneous equation (which can be reduced to one-parametric form (5.75)) and a particular solution of the inhomogeneous one. The latter can be taken to be

$$\mu_{ab}^{disc} = \Sigma \cdot \left(\mathbf{P}_a^{(1)} \tilde{\mathbf{P}}_b^{(1)} - \mathbf{P}_b^{(1)} \tilde{\mathbf{P}}_a^{(1)} \right). \tag{A.48}$$

One can get rid of the operation Σ, expressing μ_{ab}^{disc} in terms of Γ' and p'_a. This procedure is based on two facts: the definition (5.59) of p'_a and the statement that on functions decaying at infinity Σ coincides with Γ' defined by (5.57). After a straightforward but

long calculation we find

$$\mu_{31}^{disc} = \epsilon^2 \Sigma \left(\frac{1}{x^2} - x^2\right) = -\epsilon^2 \quad \left(\Gamma \cdot x^2 + p_2\right),$$
$$\mu_{41}^{disc} = \epsilon^2 \left[-2I_1 p_1 - 4I_1 \Gamma \cdot x + \sinh(2\pi u)\left(\Gamma \cdot x^2 + p_0\right) + \Gamma \cdot \sinh_- \left(x - \frac{1}{x}\right)^2\right],$$
$$\mu_{43}^{disc} = -2\epsilon^2 \left[-2I_1 p_1 - 4I_1 \Gamma \cdot x + \sinh(2\pi u)(p_2 - p_0) + \Gamma \cdot \sinh_- \left(x - \frac{1}{x}\right)^2\right],$$
$$\mu_{21}^{disc} = \epsilon^2 \left[2I_1 \Gamma \cdot x - \sinh(2\pi u)\ \Gamma \cdot x^2 - \Gamma \cdot \sinh_- \left(x^2 + \frac{1}{x^2}\right)\right],$$
$$\mu_{24}^{disc} = \epsilon^2 \left[2I_1 \Gamma \cdot \sinh_- \left(x + \frac{1}{x}\right) + I_1^2 p_0 + \right.$$
$$\left. + \sinh(2\pi u)\Gamma \cdot \sinh_- \left(x^2 - \frac{1}{x^2}\right) - \Gamma \cdot \sinh_-^2 \left(x^2 - \frac{1}{x^2}\right)\right].$$

Here we write Γ and p_a instead of Γ' and p'_a taking into account the discussion between equations (5.80) - (5.85).

NLO solution of QSC at $J = 3$

In this appendix we present some intermediate formulas for the calculation of curvature function for $J = 3$ in section 5.3.3 omitted in the main text.

- The particular solution of the inhomogeneous equation (5.53) which we construct as $\mu_{31}^{disc} = \Sigma \cdot \left(\mathbf{P}_a^{(1)} \tilde{\mathbf{P}}_b^{(1)} - \mathbf{P}_b^{(1)} \tilde{\mathbf{P}}_a^{(1)}\right)$ can be written using the operation Γ and p_a defined by (5.85) and (5.83)[54]

$$\mu_{31}^{disc} = \Sigma \cdot (\mathbf{P}_3 \tilde{\mathbf{P}}_1 - \mathbf{P}_1 \tilde{\mathbf{P}}_3) = -2\epsilon^2 \left[\Gamma x^3 + p_3\right],$$
$$\mu_{41}^{disc} = -\epsilon^2 \left[2p_2 I_2 + 2I_2 \Gamma x^2 + 2\Gamma \cdot \cosh_- + (I_0 - \cosh(2\pi u))p_0\right],$$
$$\mu_{34}^{disc} = \epsilon^2 \left[2I_2 \Gamma x + I_0 \Gamma x^3 - \Gamma \cdot (x^3 + x^{-3}) \cosh_- + \cosh(2\pi u)(2p_3 + \Gamma x^3)\right],$$
$$\mu_{21}^{disc} = \epsilon^2 \left[2I_2 \Gamma x + (I_0 - \cosh(2\pi u))\Gamma x^3 - \Gamma \left((x^3 + x^{-3}) \cosh(2\pi u)\right)\right],$$
$$\mu_{24}^{disc} = -2\epsilon^2 \left[-\frac{1}{2}\Gamma \cdot \cosh_-^2 \left(x^3 - x^{-3}\right) + \left(\frac{\cosh(2\pi u)}{2} - I_0\right) \Gamma \cdot \frac{\cosh_-}{x^3}\right.$$
$$-I_2 \Gamma \cdot \left(x + \frac{1}{x}\right) \cosh_- - \frac{1}{2} \cosh(2\pi u) \Gamma \cdot x^3 \cosh_- +$$
$$\left. + \frac{I_0}{2} \left(I_0 - \cosh(2\pi u)\right) \Gamma \cdot x^3 + \frac{I_1 I_2}{2\pi g} \Gamma x - I_2^2 p_1\right].$$

- The zero mode of the system (5.101)-(5.104), which we added to the solution in

[54] Alternatively one can use p'_a and Γ' instead of p_a and Γ- see the discussion between the equations (5.80) - (5.85)

equations (5.107)-(5.110) to ensure correct asymptotics, is

$$\begin{aligned}
\mathbf{P}_1^{\rm zm} &= L_1 x^{-1/2} + L_3 x^{1/2}, \qquad (A.49)\\
\mathbf{P}_2^{\rm zm} &= -L_1 x^{1/2}{\rm ch}_- + L_2 x^{-1/2} - L_3 x^{-1/2}\left({\rm ch}_- + \frac{1}{2}I_0\right) + L_4\left(x^{1/2} - x^{-1/2}\right),\\
\mathbf{P}_3^{\rm zm} &= -L_1 x^{1/2} - L_3 x^{1/2},\\
\mathbf{P}_4^{\rm zm} &= -L_1\left(I_0 x^{-1/2} + x^{-1/2}\cosh_-\right) - L_2 x^{1/2} + L_4(x^{1/2} - x^{-1/2})\\
&- L_3 x^{1/2}\left({\rm ch}_- + \frac{1}{2}I_0\right).
\end{aligned}$$

NLO solution of QSC at $J = 4$

Solution of QSC at NLO for $J = 4$ is completely analogous to the case of $J = 2$. The starting point is the LO solution (5.20)-(5.23). As described in section A.3, from LO $\mathbf{P}_a$ we can find μ_{ab} at NLO. Its discontinuous part is

$$\mu_{31}^{disc} = -\epsilon^2 \left(\Gamma\cdot x^4 + p_4\right), \qquad (A.50)$$

$$\mu_{41}^{disc} = \frac{1}{2}\epsilon^2\left(\sinh(2\pi u)\left(p_0 + \Gamma\cdot x^4\right) + 2\left(I_1 p_1 + I_3 p_3\right) + \right. \qquad (A.51)$$

$$\left. +\Gamma\cdot\sinh_-\left(x^2 - \frac{1}{x^2}\right)^2 - 2\left(I_1 + I_3\right)\left(\Gamma\cdot x^3 + \Gamma\cdot x\right)\right), \qquad (A.52)$$

$$\mu_{43}^{disc} = \epsilon^2\left(\left(p_4 - p_0\right)\sinh(2\pi u) + 2\left(I_1 p_1 + I_3 p_3\right) - \right. \qquad (A.53)$$

$$\left. -\Gamma\cdot\sinh_-\left(x^2 - \frac{1}{x^2}\right)^2 + 2\left(I_1 + I_3\right)\left(\Gamma\cdot x^3 + \Gamma\cdot x\right)\right), \qquad (A.54)$$

$$\mu_{21}^{disc} = \epsilon^2\left(-\frac{1}{2}\sinh(2\pi u)\Gamma\cdot x^4 + I_1 p_3 + I_3 p_1 - \right. \qquad (A.55)$$

$$\left. -\frac{1}{2}\Gamma\cdot\sinh_-\left(x^4 + \frac{1}{x^4}\right) + I_1\Gamma\cdot x^3 + I_3\Gamma\cdot x\right), \qquad (A.56)$$

$$\mu_{24}^{disc} = \epsilon^2\left(\frac{1}{2}\sinh(2\pi u)\Gamma\cdot\sinh_-\left(x^4 - \frac{1}{x^4}\right) + I_3^2 p_2 + I_1 I_3 p_0 - \right. \qquad (A.57)$$

$$-\frac{1}{2}\Gamma\cdot\sinh_-^2\left(x^4 - \frac{1}{x^4}\right) + I_1\Gamma\cdot\sinh_-\left(x^3 + \frac{1}{x^3}\right) + \qquad (A.58)$$

$$\left. +I_3\Gamma\cdot\sinh_-\left(x + \frac{1}{x}\right) + \left(I_3^2 - I_1^2\right)\Gamma\cdot x^2\right), \qquad (A.59)$$

and as discussed for $J = 2$ the zero mode can be brought to the form

$$\pi_{12} = 0,\ \pi_{13} = 0,\ \pi_{14} = 0, \qquad (A.60)$$

$$\pi_{24} = c_{1,24}\cosh 2\pi u,\ \pi_{34} = 0. \qquad (A.61)$$

After that, we calculate r_a by formula (5.80) and solve the expanded to NLO QSC for $\mathbf{P}_a^{(1)}$ as

$$\mathbf{P}_3^{(1)} = H \cdot r_3, \tag{A.62}$$

$$\mathbf{P}_1^{(1)} = \frac{1}{2}\mathbf{P}_3^{(1)} + K \cdot \left(r_1 - \frac{1}{2}r_3\right), \tag{A.63}$$

$$\mathbf{P}_4^{(1)} = K \cdot \left[(H \cdot r_3)\sinh(2\pi u) + r_4 - \frac{1}{2}r_3 \sinh(2\pi u)\right] - C(x + 1/x), \tag{A.64}$$

$$\mathbf{P}_2^{(1)} = H \cdot \left[-\mathbf{P}_4^{(1)} - \mathbf{P}_1^{(1)}\sinh(2\pi u) + r_2\right] + C/x, \tag{A.65}$$

where C is a constant which is fixed by requiring correct asymptotics of $\mathbf{P}_2$. Finally we find leading coefficients A_a of $\mathbf{P}_a^{(1)}$ and use expanded up to $\mathcal{O}(S^2)$ formulas (4.50), (4.51) in the same way as in section 5.3.2 to obtain the result (A.66).

Result for $J = 4$

The final result for the curvature function at $J = 4$ reads

$$\begin{aligned}
\gamma^{(2)}_{J=4} = \oint \frac{du_x}{2\pi i} \oint \frac{du_y}{2\pi i} \frac{1}{ig^2(I_3 - I_5)^3} \Bigg[& \\
& \frac{2\left(\mathrm{sh}_-^x\right)^2 y^4 \left(I_3\left(x^{10}+1\right) - I_5 x^2\left(x^6+1\right)\right)}{x^4\left(x^2-1\right)} - \frac{2\left(\mathrm{sh}_-^y\right)^2 x^4\left(y^8-1\right)\left(I_3 x^2 - I_5\right)}{\left(x^2-1\right)y^4} + \\
& + \frac{4\mathrm{sh}_-^x \mathrm{sh}_-^y \left(x^4y^4-1\right)\left(I_3 + I_3 x^6 y^4 - I_5 x^2\left(x^2y^4+1\right)\right)}{x^4\left(x^2-1\right)y^4} \\
& + \mathrm{sh}_-^y \Big(\left(y^4 + y^{-4}\right)x^{-1}\left(\left(I_1 I_5 - I_3^2\right)\left(3x^4+1\right) - 2I_1 I_3 x^6\right) + \\
& + \frac{2I_3 x^2\left(I_5\left(x^2+1\right)x^2 + I_1\left(1-x^2\right)\right) - I_1 I_5\left(x^2-1\right)^2 + I_3^2\left(-2x^6+x^4+1\right)}{x(x^2-1)} + \\
& + 2\left(y^3 + y^{-3}\right)\frac{I_1 I_3 x^6 - I_1 I_5 x^4 - I_3^2\left(x^2-1\right)}{x^2-1} - \\
& - 2I_3\left(y + y^{-1}\right)\frac{I_1\left(x^2-1\right) - I_3\left(x^6 - x^2 + 1\right) + I_5\left(x^4 - x^2 + 1\right)}{x^2-1}\Bigg) + \\
& + \frac{4x^6y^2 I_3\left(I_3^2 - I_1^2\right)}{x^2-1} + \frac{4xyI_1\left(I_3y^2 + I_1\right)\left(I_3 + I_5\right)}{x^2-1} + \\
& \frac{2y^4\left(I_1 + I_3\right)\left(I_1 I_5 - I_3^2\right)}{x^2-1} - \frac{2y\left(y^2+1\right)\left(I_1 + I_3\right)\left(I_1 I_5 - I_3^2\right)}{x\left(x^2-1\right)} - \\
& - \frac{2x^3 y\left(I_1 + I_3\right)\left(I_1\left(2I_3 + \left(3\,y^2+1\right)I_5\right) - I_3\left(2I_5 y^2 + \left(y^2+3\right)I_3\right)\right)}{x^2-1} \\
& + \frac{2x^2y^4\left(-I_3^3 - I_1\left(3I_3 + I_5\right)I_3 + I_1^2 I_5\right)}{x^2-1} + \frac{2x^4 y\left(I_1^2\left(2yI_5 - 2y^3 I_3\right) - 2y\left(y^2+1\right)I_3^2 I_5\right)}{x^2-1} + \\
& + \frac{4x^5 y I_3\left(2I_1^2 y^2 + I_3\left(I_5 - I_3\right)y^2 + I_1\left(I_3 + I_5\right)\right)}{x^2-1}\Bigg] \frac{1}{4\pi i}\partial_u \log\frac{\Gamma(iu_x - iu_y + 1)}{\Gamma(1 - iu_x + iu_y)}
\end{aligned} \tag{A.66}$$

where, similarly to $J = 2, 3$, the integrals go around the branch cut between $-2g$ and $2g$.

A.4 Weak coupling expansion – details

First, we give the expansion of our results for the slope-to-slope functions $\gamma_J^{(2)}$ to 10 loops. We start with $J = 2$:

$$
\begin{aligned}
\gamma^{(2)}_{J=2} &= -8g^2\zeta_3 + g^4\left(140\zeta_5 - \frac{32\pi^2\zeta_3}{3}\right) + g^6\left(200\pi^2\zeta_5 - 2016\zeta_7\right) \\
&+ g^8\left(-\frac{16\pi^6\zeta_3}{45} - \frac{88\pi^4\zeta_5}{9} - \frac{9296\pi^2\zeta_7}{3} + 27720\zeta_9\right) \\
&+ g^{10}\left(\frac{208\pi^8\zeta_3}{405} + \frac{160\pi^6\zeta_5}{27} + 144\pi^4\zeta_7 + 45440\pi^2\zeta_9 - 377520\zeta_{11}\right) \\
&+ g^{12}\Big(-\frac{7904\pi^{10}\zeta_3}{14175} - \frac{17296\pi^8\zeta_5}{4725} - \frac{128\pi^6\zeta_7}{15} - \frac{6312\pi^4\zeta_9}{5} \\
&\qquad -653400\pi^2\zeta_{11} + 5153148\zeta_{13}\Big) \\
&+ g^{14}\Big(\frac{1504\pi^{12}\zeta_3}{2835} + \frac{106576\pi^{10}\zeta_5}{42525} - \frac{18992\pi^8\zeta_7}{405} - \frac{16976\pi^6\zeta_9}{15} \\
&\qquad + \frac{25696\pi^4\zeta_{11}}{9} + \frac{28003976\pi^2\zeta_{13}}{3} - 70790720\zeta_{15}\Big) \\
&+ g^{16}\Big(-\frac{178112\pi^{14}\zeta_3}{382725} - \frac{239488\pi^{12}\zeta_5}{127575} + \frac{2604416\pi^{10}\zeta_7}{42525} + \frac{8871152\pi^8\zeta_9}{4725} \\
&\qquad + \frac{30157072\pi^6\zeta_{11}}{945} + \frac{8224216\pi^4\zeta_{13}}{45} - 133253120\pi^2\zeta_{15} \\
&\qquad +979945824\zeta_{17}\Big) \\
&+ g^{18}\Big(\frac{147712\pi^{16}\zeta_3}{382725} + \frac{940672\pi^{14}\zeta_5}{637875} - \frac{490528\pi^{12}\zeta_7}{8505} - \frac{358016\pi^{10}\zeta_9}{189} \\
&\qquad - \frac{37441312\pi^8\zeta_{11}}{945} - \frac{9616256\pi^6\zeta_{13}}{15} - \frac{16988608\pi^4\zeta_{15}}{3} \\
&\qquad +1905790848\pi^2\zeta_{17} - 13671272160\zeta_{19}\Big) \\
&+ g^{20}\Big(-\frac{135748672\pi^{18}\zeta_3}{442047375} - \frac{103683872\pi^{16}\zeta_5}{88409475} + \frac{1408423616\pi^{14}\zeta_7}{29469825} \\
&\qquad + \frac{2288692288\pi^{12}\zeta_9}{1403325} + \frac{34713664\pi^{10}\zeta_{11}}{945} + \frac{73329568\pi^8\zeta_{13}}{105} \\
&\qquad + \frac{305679296\pi^6\zeta_{15}}{27} + 121666688\pi^4\zeta_{17} - 27342544320\pi^2\zeta_{19} \\
&\qquad +192157325360\zeta_{21}\Big)
\end{aligned}
\tag{A.67}
$$

Next, for $J = 3$,

$$\begin{aligned}
\gamma^{(2)}_{J=3} &= -2g^2\zeta_3 + g^4\left(12\zeta_5 - \frac{4\pi^2\zeta_3}{3}\right) + g^6\left(\frac{2\pi^4\zeta_3}{45} + 8\pi^2\zeta_5 - 28\zeta_7\right) \\
&+ g^8\left(-\frac{4\pi^6\zeta_3}{45} - \frac{4\pi^4\zeta_5}{15} - 528\zeta_9\right) \\
&+ g^{10}\left(\frac{934\pi^8\zeta_3}{14175} + \frac{8\pi^6\zeta_5}{9} - \frac{82\pi^4\zeta_7}{9} - 900\pi^2\zeta_9 + 12870\zeta_{11}\right) \\
&+ g^{12}\left(-\frac{572\pi^{10}\zeta_3}{14175} - \frac{104\pi^8\zeta_5}{175} - \frac{256\pi^6\zeta_7}{45} + \frac{2476\pi^4\zeta_9}{9}\right. \\
&\qquad \left. + \frac{57860\pi^2\zeta_{11}}{3} - 208208\zeta_{13}\right) \\
&+ g^{14}\left(\frac{2878\pi^{12}\zeta_3}{127575} + \frac{404\pi^{10}\zeta_5}{1215} + \frac{326\pi^8\zeta_7}{75} + \frac{3352\pi^6\zeta_9}{135}\right. \\
&\qquad \left. - \frac{80806\pi^4\zeta_{11}}{15} - 316316\pi^2\zeta_{13} + 2994992\zeta_{15}\right) \\
&+ g^{16}\left(-\frac{159604\pi^{14}\zeta_3}{13395375} - \frac{257204\pi^{12}\zeta_5}{1488375} - \frac{14836\pi^{10}\zeta_7}{6075} - \frac{71552\pi^8\zeta_9}{2025}\right. \\
&\qquad \left. + \frac{4948\pi^6\zeta_{11}}{189} + \frac{4163068\pi^4\zeta_{13}}{45} + \frac{14129024\pi^2\zeta_{15}}{3} - 41116608\zeta_{17}\right) \\
&+ g^{18}\left(\frac{494954\pi^{16}\zeta_3}{81860625} + \frac{156368\pi^{14}\zeta_5}{1819125} + \frac{6796474\pi^{12}\zeta_7}{5457375} + \frac{332\pi^{10}\zeta_9}{15}\right. \\
&\qquad + \frac{1745318\pi^8\zeta_{11}}{4725} - \frac{868088\pi^6\zeta_{13}}{315} - \frac{22594208\pi^4\zeta_{15}}{15} \\
&\qquad \left. -67084992\pi^2\zeta_{17} + 553361016\zeta_{19}\right) \\
&+ g^{20}\left(-\frac{940132\pi^{18}\zeta_3}{315748125} - \frac{244456\pi^{16}\zeta_5}{5893965} - \frac{29637008\pi^{14}\zeta_7}{49116375} - \frac{11808196\pi^{12}\zeta_9}{1002375}\right. \\
&\qquad - \frac{2265364\pi^{10}\zeta_{11}}{8505} - \frac{68767984\pi^8\zeta_{13}}{14175} + \frac{480208\pi^6\zeta_{15}}{9} \\
&\qquad \left. + \frac{71785288\pi^4\zeta_{17}}{3} + 934787840\pi^2\zeta_{19} - 7390666360\zeta_{21}\right)
\end{aligned} \tag{A.68}$$

Finally, for $J = 4$,

$$
\begin{aligned}
\gamma^{(2)}_{J=4} &= g^2\left(-\frac{14\zeta_3}{5}+\frac{48\zeta_5}{\pi^2}-\frac{252\zeta_7}{\pi^4}\right) \\
&+ g^4\left(-\frac{22\pi^2\zeta_3}{25}+\frac{474\zeta_5}{5}-\frac{8568\zeta_7}{5\pi^2}+\frac{8316\zeta_9}{\pi^4}\right) \\
&+ g^6\left(\frac{32\pi^4\zeta_3}{875}+\frac{3656\pi^2\zeta_5}{175}-\frac{56568\zeta_7}{25}+\frac{196128\zeta_9}{5\pi^2}-\frac{185328\zeta_{11}}{\pi^4}\right) \\
&+ g^8\Big(-\frac{4\pi^6\zeta_3}{175}-\frac{68\pi^4\zeta_5}{75}-\frac{55312\pi^2\zeta_7}{125}+\frac{1113396\zeta_9}{25}-\frac{3763188\zeta_{11}}{5\pi^2} \\
&\qquad +\frac{3513510\zeta_{13}}{\pi^4}\Big) \\
&+ g^{10}\Big(\frac{176\pi^8\zeta_3}{16875}+\frac{2488\pi^6\zeta_5}{7875}+\frac{2448\pi^4\zeta_7}{125}+\frac{209532\pi^2\zeta_9}{25}-\frac{3969878\zeta_{11}}{5} \\
&\qquad +\frac{13213200\zeta_{13}}{\pi^2}-\frac{61261200\zeta_{15}}{\pi^4}\Big) \\
&+ g^{12}\Big(-\frac{88072\pi^{10}\zeta_3}{20671875}-\frac{449816\pi^8\zeta_5}{4134375}-\frac{327212\pi^6\zeta_7}{65625}-\frac{338536\pi^4\zeta_9}{875} \\
&\qquad -\frac{129520798\pi^2\zeta_{11}}{875}+\frac{66969474\zeta_{13}}{5}-\frac{220540320\zeta_{15}}{\pi^2} \\
&\qquad +\frac{1017636048\zeta_{17}}{\pi^4}\Big) \\
&+ g^{14}\Big(\frac{795136\pi^{12}\zeta_3}{487265625}+\frac{522784\pi^{10}\zeta_5}{13921875}+\frac{4021288\pi^8\zeta_7}{2953125}+\frac{1869152\pi^6\zeta_9}{21875} \\
&\qquad +\frac{18573952\pi^4\zeta_{11}}{2625}+\frac{62633272\pi^2\zeta_{13}}{25}-\frac{1092799344\zeta_{15}}{5} \\
&\qquad +\frac{17844607872\zeta_{17}}{5\pi^2}-\frac{16405526592\zeta_{19}}{\pi^4}\Big) \\
&+ g^{16}\Big(-\frac{30581888\pi^{14}\zeta_3}{51162890625}-\frac{43988768\pi^{12}\zeta_5}{3410859375}-\frac{446380184\pi^{10}\zeta_7}{1136953125} \\
&\qquad -\frac{20108936\pi^8\zeta_9}{984375}-\frac{31755036\pi^6\zeta_{11}}{21875}-\frac{321449336\pi^4\zeta_{13}}{2625} \\
&\qquad -\frac{1031925232\pi^2\zeta_{15}}{25}+\frac{87296960712\zeta_{17}}{25}-\frac{283092985656\zeta_{19}}{5\pi^2} \\
&\qquad +\frac{259412389236\zeta_{21}}{\pi^4}\Big) \\
&+ g^{18}\Big(\frac{6706432\pi^{16}\zeta_3}{31672265625}+\frac{816838192\pi^{14}\zeta_5}{186232921875}+\frac{2004636572\pi^{12}\zeta_7}{17054296875} \\
&\qquad +\frac{1950592976\pi^{10}\zeta_9}{378984375}+\frac{2220222512\pi^8\zeta_{11}}{6890625}+\frac{20963856\pi^6\zeta_{13}}{875} \\
&\qquad +\frac{254959316\pi^4\zeta_{15}}{125}+\frac{584553371616\pi^2\zeta_{17}}{875} \\
&\qquad -\frac{1375388084412\zeta_{19}}{25}+\frac{4432313039616\zeta_{21}}{5\pi^2}-\frac{4049650420200\zeta_{23}}{\pi^4}\Big)
\end{aligned}
\tag{A.69}
$$

$$
\begin{aligned}
&+ \quad g^{20}\Big(-\frac{15308976272\pi^{18}\zeta_3}{209512037109375} - \frac{1764947984\pi^{16}\zeta_5}{1197211640625} - \frac{18667123736\pi^{14}\zeta_7}{517313671875} \\
&\quad -\frac{538293689008\pi^{12}\zeta_9}{399070546875} - \frac{657466372\pi^{10}\zeta_{11}}{8859375} - \frac{119709052\pi^8\zeta_{13}}{23625} \\
&\quad -\frac{9095498848\pi^6\zeta_{15}}{23625} - \frac{260407748416\pi^4\zeta_{17}}{7875} - \frac{1869110789976\pi^2\zeta_{19}}{175} \\
&\quad +\frac{4293062840352\zeta_{21}}{5} - \frac{13755955395600\zeta_{23}}{\pi^2} + \frac{62673161265000\zeta_{25}}{\pi^4}\Big)
\end{aligned}
$$

For future reference we have also computed[55] the weak coupling expansion of the anomalous dimensions at order S^3, using the known predictions from ABA which are available for any spin at $J = 2$ and $J = 3$. For $J = 2$ we have computed the expansion to three loops[56]:

$$
\begin{aligned}
\gamma^{(3)}_{J=2} &= g^2\frac{4}{45}\pi^4 + g^4\left(40\zeta_3^2 - \frac{28\pi^6}{405}\right) \\
&+ g^6\left(\frac{192}{5}\zeta_{5,3} - \frac{6992\zeta_3\zeta_5}{5} + \frac{280\pi^2\zeta_3^2}{3} + \frac{6962\pi^8}{212625}\right) + \mathcal{O}(g^8)
\end{aligned}
\tag{A.70}
$$

Compared to the S^2 part, a new feature is the appearance of multiple zeta values – here we have $\zeta_{5,3}$, which is defined by

$$
\zeta_{a_1,a_2,\ldots,a_k} = \sum_{0<n_1<n_2<\ldots<n_k<\infty} \frac{1}{n_1^{a_1} n_2^{a_2} \ldots n_k^{a_k}} \tag{A.71}
$$

and cannot be reduced to simple zeta values ζ_n.

For $J = 3$ we have obtained the expansion to four loops:

$$
\begin{aligned}
\gamma^{(3)}_{J=3} &= \frac{1}{90}\pi^4 g^2 + g^4\left(4\zeta_3^2 + \frac{\pi^6}{1890}\right) + g^6\left(4\zeta_{5,3} + 4\pi^2\zeta_3^2 - 72\zeta_3\zeta_5 - \frac{2\pi^8}{675}\right) \\
&+ g^8\left(-112\zeta_{2,8} + \frac{20}{3}\pi^2\zeta_{5,3} + 728\zeta_3\zeta_7 + 448\zeta_5^2 - \frac{224}{3}\pi^2\zeta_3\zeta_5\right. \\
&\left. + \frac{4\pi^4\zeta_3^2}{5} - \frac{41\pi^{10}}{133650}\right) + \mathcal{O}(g^{10})
\end{aligned}
\tag{A.72}
$$

A.5 Higher mode numbers

Slope function for generic filling fractions and mode numbers

Let us extend the discussion of section 5.1 by considering the state corresponding to a solution of the asymptotic Bethe equations with arbitrary mode numbers and filling

[55] As described in the main text (see section 6.4), in the calculations we used several Mathematica packages for dealing with harmonic sums.

[56] The anomalous dimension is written as $\gamma = \gamma^{(1)}S + \gamma^{(2)}S^2 + \gamma^{(3)}S^3 + \ldots$

fractions[57]. We expect that in QSC this should correspond to[58]

$$\mu_{24} = \sum_{n=-\infty}^{\infty} C_n e^{2\pi n u}. \tag{A.73}$$

As an example, for the ground state twist operator we have $\mu_{24} = \sinh(2\pi u)$, which is reproduced by choosing $C_{-1} = -1/2, C_1 = 1/2$ and all other C's set to 0.

It is straightforward to solve the QSC equations in the same way as in section 5.1, and we find the energy

$$\gamma = \frac{\sqrt{\lambda}}{J} \frac{\sum_n C_n I_{J+1}(n\sqrt{\lambda})}{\sum_n C_n I_J(n\sqrt{\lambda})/n} S, \tag{A.74}$$

which can also be written in a more familiar form as

$$\gamma = \sum_n \alpha_n \frac{n\sqrt{\lambda}}{J} \frac{I_{J+1}(n\sqrt{\lambda})}{I_J(n\sqrt{\lambda})} S, \tag{A.75}$$

where

$$\alpha_n = \frac{C_n I_J(n\sqrt{\lambda})/n}{\sum_m C_m I_J(m\sqrt{\lambda})/m} \tag{A.76}$$

are the filling fractions.

The coefficients C_n are additionally constrained by

$$\sum_n C_n I_J(n\sqrt{\lambda}) = 0, \tag{A.77}$$

which ensures that the $\mathbf{P}_a$ functions have correct asymptotics. This constraint implies a relation between the filling fractions,

$$\sum_n n\, \alpha_n = 0, \tag{A.78}$$

which is also familiar from the asymptotic Bethe ansatz.

Curvature function and higher mode numbers

In the main text we discussed the NLO solutions to QSC which are based on the leading order solutions (5.20)-(5.23) or (5.25)-(5.28). One of the assumptions for constructing the leading order solution was to allow μ_{ab} to have only $e^{\pm 2\pi u}$ in asymptotics at infinity (we recall that this led to all μ's being constant except μ_{24} which is equal to $\sinh(2\pi u)$ or $\cosh(2\pi u)$), while in principle requiring μ_{ab} to be periodic one could also allow to have $e^{2n\pi u}$ with any integer n. Thus a natural generalization of the leading order solution is to consider $\mu_{24} = \sinh(2\pi n u)$ or $\mu_{24} = \cosh(2\pi n u)$, where n is an arbitrary integer. As

[57] For simplicity we also consider even J here.

[58] We no longer expect μ_{24} to be either even or odd, since in the Bethe ansatz description of the state with generic mode numbers and filling fractions the Bethe roots are not distributed symmetrically.

discussed above (see the end of section 5.1 and appendix A.5), we believe that at the leading order in S such solutions correspond to states with mode numbers equal to n, and they reproduce the slope function for this case.

Proceeding to order S^2, the calculation of the curvature function $\gamma^{(2)}(g)$ with $\mu_{24} = \sinh(2\pi n u)$ or $\mu_{24} = \cosh(2\pi n u)$ can be done following the same steps as for $n = 1$. The final results for $J = 2, 3$ and 4 are given by exactly the same formulas as for $n = 1$ ((5.95), (5.112) and (A.66) respectively) — the only difference is that now one should set in those expressions

$$I_k = I_k(4\pi n g), \tag{A.79}$$

$$\mathrm{sh}^x_- = [\sinh(2\pi n u_x)]_- , \tag{A.80}$$

$$\mathrm{sh}^y_- = [\sinh(2\pi n u_y)]_- , \tag{A.81}$$

$$\mathrm{ch}^x_- = [\cosh(2\pi n u_x)]_- , \tag{A.82}$$

$$\mathrm{ch}^y_- = [\cosh(2\pi n u_y)]_- . \tag{A.83}$$

It would be natural to assume that this solution of QSC describes anomalous dimensions for states with mode number n at order S^2. However we found some peculiarities in the strong coupling expansion of the result. The strong coupling data available for comparison in the literature for states with $n > 1$ also relies on some conjectures (see [115], [147]), so the interpretation of this solution is not fully clear to us.

The weak coupling expansion for this case turns out to be related in a simple way to the $n = 1$ case. One should just replace $\pi \to n\pi$ in the expansions for $n = 1$ which were given in (A.67), (A.68), (A.69). For example,

$$\gamma^{(2)}_{J=2} = -8g^2\zeta_3 + g^4\left(140\zeta_5 - \frac{32n^2\pi^2\zeta_3}{3}\right) + g^6\left(200n^2\pi^2\zeta_5 - 2016\zeta_7\right) + \dots$$

It would be interesting to compare these weak coupling predictions to results obtained from the asymptotic Bethe ansatz (or by other means) as it was done for $n = 1$ in section 5.4.

Let us now discuss the strong coupling expansion. According to Basso's conjecture [115] (see also [147]), the structure of the expansion may be obtained from

$$\Delta^2 = J^2 + S\left(A_1\sqrt{\mu} + A_2 + \dots\right) + S^2\left(B_1 + \frac{B_2}{\sqrt{\mu}} + \dots\right) + S^3\left(\frac{C_1}{\mu^{1/2}} + \frac{C_2}{\mu^{3/2}} + \dots\right) + \mathcal{O}(S^4) ,$$

where $\mu = n^2\lambda$. This gives

$$\begin{aligned}\Delta &= J + \frac{S}{2J}\left(A_1 n\sqrt{\lambda} + A_2 + \frac{A_3}{n\sqrt{\lambda}} + \dots\right) \\ &+ S^2\left(-\frac{A_1^2}{8J^3}\, n^2\lambda - \frac{A_1 A_2}{4J^3}\, n\sqrt{\lambda} + \left[\frac{B_1}{2J} - \frac{A_2^2 + 2A_1A_3}{8J^3}\right]\right. \\ &\left. + \left[\frac{B_2}{2J} - \frac{A_2A_3 + A_1A_4}{4J^3}\right]\frac{1}{n\sqrt{\lambda}} + \dots\right) + \mathcal{O}(S^3)\,.\end{aligned}$$

where A_i are known from Basso's slope function. Substituting them, we find

$$\gamma_J^{(2)}(g) = -\frac{8\pi^2 g^2 n^2}{J^3} + \frac{2\pi g n}{J^3} + \frac{B_1 - 1}{2J} + \frac{8B_2J^2 - 4J^2 + 1}{64\pi g J^3 n} + \dots \tag{A.84}$$

However, already in [147] some inconsistencies were found if one assumes this structure for $n > 1$. Let us extend that analysis by comparing the prediction (A.84) to our results from QSC. To compute the expansion of our results, similarly to the $n = 1$ case, we evaluated $\gamma_J^{(2)}(g)$ numerically for many values of g, and then fitted the result by powers of g. As for $n = 1$ we found with high precision (about $\pm 10^{-16}$) that the first several coefficients involve only rational numbers and powers of π. Our results for $n = 2, 3$ and $J = 2, 3, 4$ are summarized below:

$$\gamma^{(2)}_{J=2,n=2}(g) = -4\pi^2 g^2 + \frac{\pi g}{2} + \frac{17}{8} - \frac{0.29584877037648771(2)}{g} + \dots \tag{A.85}$$

$$\gamma^{(2)}_{J=3,n=2}(g) = -\frac{32}{27}\pi^2 g^2 + \frac{4\pi g}{27} + \frac{17}{12} - \frac{0.2928304112866493(9)}{g} + \dots \tag{A.86}$$

$$\gamma^{(2)}_{J=4,n=2}(g) = -\frac{1}{2}\pi^2 g^2 + \frac{\pi g}{16} + \frac{17}{16} - \frac{0.3199099366154 48(9)}{g} + \dots \tag{A.87}$$

$$\gamma^{(2)}_{J=2,n=3}(g) = -9\pi^2 g^2 + \frac{3\pi g}{4} + \frac{23}{4} - \frac{0.8137483(9)}{g} + \dots \tag{A.88}$$

$$\gamma^{(2)}_{J=3,n=3}(g) = -\frac{8}{3}\pi^2 g^2 + \frac{2\pi g}{9} + \frac{23}{6} - \frac{0.892016609(2)}{g} + \dots \tag{A.89}$$

$$\gamma^{(2)}_{J=4,n=3}(g) = -\frac{9}{8}\pi^2 g^2 + \frac{3\pi g}{32} + \frac{23}{8} - \frac{1.035945580(6)}{g} + \dots \tag{A.90}$$

Here in the coefficient of $\frac{1}{g}$ the digit in brackets is the last known one within our precision[59].

Comparing to (A.84) we find full agreement in the first two terms (of order g^2 and of order g). The next term in (A.84) (of order g^0) is determined by B_1, which in [147] was found to be

$$B_1 = \frac{3}{2} \tag{A.91}$$

for all n, J, based on consistency with the classical energy. However, comparing our results with (A.84) we find a different value:

$$\begin{aligned} B_1 &= \frac{19}{2} \quad \text{for} \quad n = 2\,, \\ B_1 &= 23 \quad \text{for} \quad n = 3\,. \end{aligned} \tag{A.92}$$

[59] We did not seek to achieve high precision in this coefficient for $n = 3$.

For both $n = 2$ and $n = 3$ this prediction for B_1 is independent of J.

The next term is of order $\frac{1}{g}$ and is determined by B_2, which in [147] was fixed to

$$B_2 = \begin{cases} -3\,\zeta_3 + \frac{3}{8} & , \ n = 1 \\ -24\,\zeta_3 - \frac{13}{8} & , \ n = 2 \\ -81\,\zeta_3 - \frac{24}{8} & , \ n = 3 \end{cases} . \tag{A.93}$$

However, this does not agree with our numerical predictions for $n = 2$ and 3. Furthermore, for $n = 2$ we extracted the coefficient of $\frac{1}{g}$ with high precision (about 10^{-17}, see (A.85)) but were unable to fit it as a combination of simple zeta values using the EZ-Face calculator [145].

Thus our results appear to disagree with the values of B_1 and B_2 obtained in [147]. There might be two reasons for this disagreement. First, it is not clear if the solution of QSC we choose for $n > 1$ is the correct one: we have conjectured that introducing n is taken into account by replacing $\sinh(2\pi u)$ with $\sinh(2\pi n u)$, but this conjecture should be further verified against independent data. The second reason is that the ansatz for the structure of anomalous dimensions at strong coupling may need to be modified when $n > 1$ (as already suspected in [147]). At this point we do not yet know which scenario is realized and hope to clarify this issue in future.

B Appendices to chapter 6

B.1 Notation and conventions

This appendix contains some notation used throughout chapter 6, in particular a glossary of integration kernels.

We denote

$$I_{m,n} \equiv \delta_{m+1,n} + \delta_{m-1,n}. \tag{B.1}$$

and

$$T = e^{i\theta},\ c_a = e^{2iG(ia/2)},\ y_a = x(ia/2), \tag{B.2}$$

where G is the resolvent from (6.29).

We denote by $*$ the convolution over the full real axis from $-\infty$ to ∞, and by $\hat{*}$ the convolution over the range $-2g < u < 2g$.

Our definitions of the kernels coincide with the ones used in [95] and [91], and we summarize them below:

$$\mathbf{s}(u,v) = \frac{1}{2\cosh(\pi(u-v))}, \tag{B.3}$$

$$K_a(u,v) = \frac{2a}{\pi(a^2+4(u-v)^2)}, \tag{B.4}$$

$$\hat{K}_a(u) = \hat{K}_{y,a}(u,0) = \sqrt{\frac{4g^2-u^2}{4g^2+a^2/4}}K_a(u),\ \tilde{K}_a(u) = \sqrt{\frac{4g^2+a^2/4}{4g^2-u^2}}K_a(u), \tag{B.5}$$

$$K_{n,m}(u,v) = \sum_{j=-\frac{n-1}{2}}^{\frac{n-1}{2}} \sum_{k=-\frac{m-1}{2}}^{\frac{m-1}{2}} K_{2j+2k+2}(u,v), \tag{B.6}$$

$$K(u,v) = \frac{1}{2\pi i}\sqrt{\frac{4g^2-u^2}{4g^2-v^2}}\frac{1}{v-u}, \tag{B.7}$$

$$\log F_a(a,g) = \tilde{K}_a \hat{*} \log\frac{\sinh(2\pi u)}{2\pi u}\bigg|_{u=0}. \tag{B.8}$$

$$r(u,v) = \frac{x(u)-x(v)}{\sqrt{x(v)}},\ b(u,v) = \frac{1/x(u)-x(v)}{\sqrt{x(v)}}, \tag{B.9}$$

$$\mathcal{R}^{(ab)}_{nm} = \sum_{j=-\frac{n-1}{2}}^{\frac{n-1}{2}} \sum_{k=-\frac{m-1}{2}}^{\frac{m-1}{2}} \frac{1}{2\pi i}\frac{d}{dv}\log\frac{r(u+ia/2+ij, v-ib/2+ik)}{r(u-ia/2+ij, v+ib/2+ik)}, \tag{B.10}$$

$$\mathcal{B}^{(ab)}_{nm} = \sum_{j=-\frac{n-1}{2}}^{\frac{n-1}{2}} \sum_{k=-\frac{m-1}{2}}^{\frac{m-1}{2}} \frac{1}{2\pi i}\frac{d}{dv}\log\frac{b(u+ia/2+ij, v-ib/2+ik)}{b(u-ia/2+ij, v+ib/2+ik)}, \tag{B.11}$$

Given the definitions above one can prove the following identities (see [95]):

$$\mathcal{R}^{(10)}_{a1}(u,v) + \mathcal{B}^{(10)}_{a1}(u,v) = K_a(u,v), \tag{B.12}$$

$$\mathcal{R}^{(10)}_{a1}(u,v) - \mathcal{B}^{(10)}_{a1}(u,v) = K(u+ia/2,v) - K(u-ia/2,v), \tag{B.13}$$

$$\mathcal{R}^{(01)}_{1a}(u,v) + \mathcal{B}^{(01)}_{1a}(u,v) = K_a(u,v), \tag{B.14}$$

$$\mathcal{R}^{(01)}_{1a}(u,v) - \mathcal{B}^{(01)}_{1a}(u,v) = \hat{K}_{y,a}(u,v) = K(u,v-ia/2) - K(u,v+ia/2), \tag{B.15}$$

$$\mathcal{R}^{(01)}_{2n} = \frac{1}{2}\left(\hat{K}^+_n - \hat{K}^-_n + K^+_n + K^-_n\right) \tag{B.16}$$

$$\tilde{K}_{ab} = \mathcal{R}^{(10)}_{ab} + \mathcal{B}^{(10)}_{ab-2} = \tag{B.17}$$
$$= \frac{1}{2}\left(\tilde{K}_a^{[b-1]} - \tilde{K}_a^{[-b+1]} + K_a^{[b-1]} + K_a^{[-b+1]}\right) + \sum_{r=1}^{a} K_{b-a-3+2r}$$
$$\hat{K}_{ba} = \mathcal{R}^{(01)}_{ba} + \mathcal{B}^{(01)}_{b-2,a} = \tag{B.18}$$
$$= \frac{1}{2}\left(\hat{K}_a^{[b-1]} - \hat{K}_a^{[-b+1]} + K_a^{[b-1]} + K_a^{[-b+1]}\right) + \sum_{r=1}^{a} K_{b-a-3+2r}$$

B.2 Bremsstrahlung TBA in the near-BPS limit

Here we give more details concerning the derivation of the simplified Bremsstrahlung TBA system from the cusp TBA equations of [95, 155].

Asymptotic solutions

As it was mentioned in section 6.2.1, the main difference between the spectral TBA and the cusp TBA is the asymptotic large L solution. In order to obtain the asymptotic solution in our limit we expand in small ϵ the asymptotic solution given in [95] (denoting the asymptotic Y-functions by bold font as in [95])

$$\mathbf{Y}_{1,1} = 1/\mathbf{Y}_{2,2} = -\frac{\cos\theta}{\cos\phi} \approx -1 - \epsilon, \tag{B.19}$$
$$\mathbf{Y}_{a,1} = \frac{\sin^2\phi}{\sin(a+1)\phi\sin(a-1)\phi} \approx A_a - \frac{\epsilon}{\tan\phi_0}B_a, \tag{B.20}$$
$$1/\mathbf{Y}_{1,s} = \frac{\sin^2\theta}{\sin(s+1)\theta\sin(s-1)\theta} \approx A_s + \frac{\epsilon}{\tan\phi_0}B_s, \tag{B.21}$$

with A_a and B_a given by

$$A_a = \frac{\sin^2\phi_0}{\sin(1+a)\phi_0\sin(a-1)\phi_0}, \tag{B.22}$$
$$B_a = \frac{4\sin\phi_0\sin a\phi_0(a\cos a\phi_0\sin\phi_0 - \cos\phi_0\sin a\phi_0)}{(\cos 2\phi_0 - \cos 2a\phi_0)^2}. \tag{B.23}$$

Thus for the asymptotic solution the leading orders of the Y-functions (as defined in (6.9)) read

$$\mathbf{\Phi} = \mathbf{\Psi} = \frac{1}{2}, \tag{B.24}$$
$$\mathcal{Y}_{\mathbf{a}} = A_a, \tag{B.25}$$
$$\mathcal{X}_{\mathbf{a}} = \frac{B_a\cot\phi_0}{A_a}, \tag{B.26}$$

and we also have

$$\mathbf{Y}_{a,0} \approx \frac{((\phi-\theta)\sin a\phi_0)^2}{u^2}a^2\left(F(a,g)\frac{z_0^{[-a]}}{z_0^{[+a]}}\right)^2, \ u\to 0. \tag{B.27}$$

Derivation of Bremsstrahlung TBA

First, plugging into the cusp TBA equations of [95] our expansion (6.9) of the Y-functions and using the asymptotic solutions derived in the previous section we obtain

$$\begin{aligned}
\Psi - \frac{1}{2} &= K_{m-1} * \left(\mathcal{X}_m \frac{\mathcal{Y}_m}{1+\mathcal{Y}_m} - \frac{B_m \cot\phi_0}{1+A_m} \right) - \pi \mathbb{C}_a \mathcal{R}^{(01)}_{1a}(u,0), \\
\Phi - \frac{1}{2} &= K_{m-1} * \left(\mathcal{X}_m \frac{\mathcal{Y}_m}{1+\mathcal{Y}_m} - \frac{B_m \cot\phi_0}{1+A_m} \right) - \pi \mathbb{C}_a \mathcal{B}^{(01)}_{1a}(u,0), \\
\log \frac{\mathcal{Y}_m}{A_m} &= -K_{m-1,n-1} * \log \frac{1+\mathcal{Y}_n}{1+A_n} - K_{m-1} \hat{*} \log \frac{\Psi}{\Phi}, \\
\mathcal{X}_m - \frac{B_m \cot\phi_0}{A_m} &= -K_{m-1,n-1} * \left(\frac{\mathcal{Y}_n}{1+\mathcal{Y}_n} \mathcal{X}_n - \frac{B_n \cot\phi_0}{1+A_n} \right) + \pi \mathbb{C}_n \left[\mathcal{R}^{(01)}_{mn} + \mathcal{B}^{(01)}_{m-2,n} \right](u,0), \\
\Delta_a &= [\mathcal{R}^{10}_{ab} + \mathcal{B}^{10}_{a,b-2}] \hat{*} \log \frac{1+\mathcal{Y}_b}{1+A_b} + \mathcal{R}^{10}_{a1} \hat{*} \log \left(\frac{\Psi}{1/2} \right) - \mathcal{B}^{10}_{a1} \hat{*} \log \left(\frac{\Phi}{1/2} \right), \\
\mathbb{C}_a &= (-1)^{a+1} a \frac{\sin a\phi_0}{\tan \phi_0} \left(\sqrt{1 + \frac{a^2}{16 g^2}} - \frac{a}{4g} \right)^{2+2L} F(a,g) e^{\Delta_a}.
\end{aligned}$$

Using the strategy described for the small angles case in appendix F of [95] we can simplify these equations and get

$$\begin{aligned}
&\Psi - \Phi = \pi \mathbb{C}_a \left[\mathcal{B}^{(01)}_{1a} - \mathcal{R}^{(01)}_{1a} \right](u,0), \\
&\Psi + \Phi = \left(\frac{B_2 \cot\phi_0}{A_2(1+A_2)} + 1 \right) - 2\mathbf{s} * \frac{\mathcal{X}_2}{1+\mathcal{Y}_2} + 2\pi \mathbb{C}_n \mathbf{s} * \mathcal{R}^{(01)}_{2n} - \pi \mathbb{C}_a \left[\mathcal{R}^{(01)}_{1a} + \mathcal{B}^{(01)}_{1a} \right](u,0), \\
&\log \frac{\mathcal{Y}_m}{A_m} = \mathbf{s} * I_{m,n} \log \left(\frac{\mathcal{Y}_n}{1+\mathcal{Y}_n} \frac{1+A_n}{A_n} \right) + \delta_{m,2} \mathbf{s} \hat{*} \log \frac{\Phi}{\Psi}, \\
&\mathcal{X}_m = \frac{B_m \cot\phi_0}{A_m} + \mathbf{s} * I_{m,n} \left(\frac{\mathcal{X}_n}{1+\mathcal{Y}_n} - \frac{B_n \cot\phi_0}{(1+A_n)A_n} \right) + \pi \mathbb{C}_m \mathbf{s} + \delta_{m,2} \mathbf{s} \hat{*} (\Phi - \Psi).
\end{aligned}$$

Finally, substituting the explicit form of A_n, B_n we can simplify the equations even further. Using that

$$\frac{B_2 \cot\phi_0}{A_2(1+A_2)} = -1, \tag{B.28}$$

$$\frac{B_m \cot\phi_0}{A_m} - \frac{1}{2} I_{m,n} \frac{B_n/A_n \cot\phi_0}{1+A_n} = 0, \tag{B.29}$$

and

$$\frac{1}{2} \log \frac{1+A_{m+1}}{A_{m+1}} \frac{1+A_{m-1}}{A_{m-1}} + \log A_m = 0. \tag{B.30}$$

we obtain the final form of the equations as written in section 6.2.1.

B.3 Derivation of FiNLIE: details

In this appendix we extend section 6.2.2 by explaining in more detail reduction of the Bremsstrahlung TBA equation (6.11)-(6.15) to a set of three equations (6.35)-(6.37) for the quantities $\eta(u), \rho(u), \mathbb{C}_a$ called FiNLIE.

$\Psi \pm \Phi$ equations

The left hand sides of the first two Bremsstrahlung TBA equations are $\Psi \pm \Phi$. Let us express this combination in terms of ρ and η. Using the definition (6.33) of η and the explicit form (6.31) of $\mathcal{T}_m$ we get

$$\Psi - \Phi = \frac{\mathcal{T}_1^{-+}\mathcal{T}_1^{+-} - \mathcal{T}_1^{--}\mathcal{T}_1^{++}}{\mathcal{T}_2}\eta = \frac{\sin\rho\theta}{\sin\theta}\eta \tag{B.31}$$

and

$$\Psi + \Phi = \frac{\mathcal{T}_1^{+-}\mathcal{T}_1^{-+} + \mathcal{T}_1^{--}\mathcal{T}_1^{++}}{\mathcal{T}_2}\eta = \frac{\cos\rho\theta\cos(2-G^+ + G^-)\theta - \cos(2G - G^+ - G^-)\theta}{\sin\theta\sin(2-G^+ + G^-)\theta}\eta. \tag{B.32}$$

Comparing this with the first two equations of Bremsstrahlung TBA (equations (6.11) and (6.12)) give the first two FiNLIE equations (6.35) and (6.36).

Equation for Δ_a

Here we discuss the reduction of the equation (6.14) for Δ_a to the third FiNLIE equation (6.37). Using identities for kernels (6.14) can be written as

$$\Delta_a = \frac{1}{2}K_a \hat{*} \log\frac{\Psi}{\Phi} + \frac{1}{2}\tilde{K}_a \hat{*} \log\left(\frac{\Psi\Phi}{1/4}\right) + \sum_{b=2}^{\infty}\tilde{K}_{ab} * \log\left(\frac{1+\mathcal{Y}_a}{1+A_a}\right). \tag{B.33}$$

Let us introduce a notation for the asymptotic large u values of $\mathcal{T}_a$:

$$\psi_a = \frac{\sin a\phi_0}{\sin\phi_0}. \tag{B.34}$$

We can transform equation (B.33) performing the same manipulations as in section 3.3 of [91]. The only difference is that we are using $\mathcal{T}_a$ divided by their asymptotic values ψ_a in order to ensure validity of manipulations with infinite sums below. We express Y-functions through T-functions and split the infinite sums as follows:

$$\sum_{b=2}^{\infty}\tilde{K}_{ab} * \log\left(\frac{1+\mathcal{Y}_b}{1+A_b}\right) = \sum_{b=2}^{\infty}\tilde{K}_{ab} * \left[\log\frac{\mathcal{T}_b^+}{\psi_b^+} + \log\frac{\mathcal{T}_b^-}{\psi_b^-} - \log\frac{\mathcal{T}_{b+1}}{\psi_{b+1}} - \log\frac{\mathcal{T}_{b-1}}{\psi_{b-1}}\right] =$$
$$= \sum_{b=2}^{\infty}\left[\tilde{K}_{ab}^+ + \tilde{K}_{ab}^- - \tilde{K}_{a,b-1} - \tilde{K}_{a,b+1}\right] * \log\frac{\mathcal{T}_b}{\psi_b} + \tilde{K}_{a,1} * \log\frac{\mathcal{T}_2}{\psi_2} - \tilde{K}_{a,2} * \log\frac{\mathcal{T}_1}{\psi_1}. \tag{B.35}$$

We have checked numerically that this last shifting of indices in the infinite sums is valid, i.e.

$$\lim_{B\to\infty} \tilde{K}_{aB+1} * \log\frac{\mathcal{T}_B}{\psi_B} - \tilde{K}_{aB} * \log\frac{\mathcal{T}_{B+1}}{\psi_{B+1}} = 0. \tag{B.36}$$

The expression in square brackets in (B.35) is zero almost everywhere, as one can see from the equation (46) of [91]. Taking into account that $\tilde{K}_{a,1} = 0$ one gets

$$\Delta_a = \frac{1}{2}\tilde{K}_a \hat{*} \log\frac{\Psi\Phi\mathcal{T}_2^2}{\mathcal{T}_1^{+-}\mathcal{T}_1^{++}\mathcal{T}_1^{--}\mathcal{T}_1^{-+}} - \tilde{K}_a \hat{*} \log\frac{\psi_2}{\psi_1^+\psi_1^-} + \log\frac{2\mathcal{T}_a}{\psi_a}. \tag{B.37}$$

Recalling the definition of η (the second equality is due to (6.32))

$$\eta \equiv \frac{\Psi\mathcal{T}_2}{\mathcal{T}_1^{-+}\mathcal{T}_1^{+-}} = \frac{\Phi\mathcal{T}_2}{\mathcal{T}_1^{--}\mathcal{T}_1^{++}} \tag{B.38}$$

we find

$$\Delta_a = \tilde{K}_a \hat{*} \log\eta - \tilde{K}_a \hat{*} \log\frac{\psi_2}{\psi_1^+\psi_1^-} + \log\frac{2\mathcal{T}_a}{\psi_a} \tag{B.39}$$

Substituting the explicit form of ψ_a and taking into account that $\tilde{K}_a \hat{*} 1 = 1$ we finally obtain

$$\Delta_a = \tilde{K}_a \hat{*} \log\eta + \log\frac{\mathcal{T}_a}{\sin a\phi_0 \cot\phi_0}\bigg|_{u=0} \tag{B.40}$$

thus giving equation (6.34) presented in the main text.

Fixing the residues b_a

The residues b_a of $\mathcal{G}(u)$ at $ia/2$ satisfy a recursion relation which we derive in this section by comparing poles on both sides of (6.13). This recursion relation is used to find the residues of η and obtain a relation between $G(ia/a)$ and $\rho(ia/2)$ which is described in section 6.2.3 and in more details in appendix B.4.

By construction, the only poles in $1/Y_{1,m}(u)$ can originate from the poles of the resolvent at $u = ia/2,\ a \in \mathbb{Z}$. Consistently with this the equation (6.13) tells the residue at $u = 0$ should cancel and the residue at $u = i/2$ should obey

$$\log Y_{1,m} \approx -\epsilon\frac{\mathbb{C}_m}{2i(u - i/2)}. \tag{B.41}$$

Expressing $Y_{1,m}$ through T-functions which are written in terms of the resolvent (see (6.19), (6.23)), and expanding at $u = i/2$, we obtain the recursion relation for b_a which was given in (6.38):

$$q_a b_{a-2} - (q_a + p_a)b_a + p_a b_{a+2} = \mathbb{C}_a, \tag{B.42}$$

where explicitly

$$q_a = i\frac{4T^2 c_{a-2}\log T(T^{2a}-c_a^2)}{(T^2c_{a-2}-c_a)(T^{2a}-T^2c_{a-2}c_a)}, \tag{B.43}$$

$$p_a = i\frac{4T^2 c_{a+2}\log T(T^{2a}-c_a^2)}{(T^2c_a-c_{a+2})(T^{2a+2}-T^2c_ac_{a+2})}, \tag{B.44}$$

$$T = e^{i\theta}, \tag{B.45}$$

$$c_a = e^{2iG(ia/2)}. \tag{B.46}$$

B.4 Fixing the residues of η: details

In this appendix we find the residues of η at $ia/2$ from the second FiNLIE equation (6.36). These residues are then used in section 6.2.3 to derive the relation (6.58).

To use (6.36) let us first of all get rid of the convolution in the right hand side by using the following property of $\mathbf{s}$: for any function f analytical in the strip $|\mathrm{Im}\ u| < 1/2$ but having poles at $u = \pm i/2$ with residues $\mp i\mathbb{C}/2$

$$f = \mathbf{s} * g + \pi\mathbb{C}\mathbf{s}(u) \ \Leftrightarrow\ f^+(u-i0) + f^-(u+i0) = g(u). \tag{B.47}$$

Thus equation (6.36) takes the form

$$\left(\frac{\cos\rho\theta\cos(2-G^+ + G^-)\theta - \cos(2G - G^+ - G^-)\theta}{\sin\theta\sin(2-G^+ + G^-)\theta}\eta\right)^{+-} + c.c = \\ = -2\frac{\mathcal{X}_2}{1+\mathcal{Y}_2} + \pi(\hat{K}_a^+ - \hat{K}_a^-)\mathbb{C}_a. \tag{B.48}$$

Consider the residue at $ia/2$ of both sides of (B.48). The terms that appear after expanding the right hand side are proportional either to $\eta\sin\theta\rho$, or to $\eta\cos\theta\rho$. We know the residues of the first type of terms from the first FiNLIE equation (6.35):

$$\operatorname*{Res}_{u=ia/2}(\eta\sin\theta\rho) = -\frac{\pi\mathbb{C}_a}{2\pi i}\sin\theta. \tag{B.49}$$

To deal with the terms proportional to $\eta\cos\theta\rho$ let us introduce the notation

$$\operatorname*{Res}_{u=ia/2}(\eta\cos\theta\rho) = \frac{e_a}{2\pi i}. \tag{B.50}$$

In the right hand side of (B.48) residues of $\mathcal{X}_a$ are expressed in terms of coefficients b_a whose explicit value we do not know. However, a nice cancellation helps us to proceed. The residue at $ia/2$ of the $\mathcal{X}_m/(1+\mathcal{Y}_m)$ term has the form $k_1b_{a-3}+k_2b_{a-1}+k_3b_{a+1}+k_4b_{a+3}$, where k_i are some clumsy coefficients. Nevertheless when we use the recursion relation (6.38) to exclude b_{a-3} and b_{a+3} we see that b_{a-1} and b_{a+1} also cancel out! Thus we get an equation completely in terms of e_a and $\mathbb{C}_a$:

$$-\frac{T(T^2c_{a-1}-c_{a+1})}{\pi(T^2-1)}\left(\frac{e_{a-1}(T^2c_{a-3}-c_{a-1})}{c_{a-1}(T^4c_{a-3}-c_{a+1})}+\frac{e_{a+1}(T^2c_{a+1}-c_{a+3})}{c_{a+1}(T^4c_{a-1}-c_{a+3})}\right)+$$
$$+\frac{\mathbb{C}_{a+1}(c_{a+1}-T^2c_{a-1})(c_{a+1}^2+T^{2a+2})(T^2c_{a+1}-c_{a+3})}{2c_{a+1}(T^{2a+2}-c_{a+1}^2)(T^4c_{a-1}-c_{a+3})}+$$
$$+\frac{\mathbb{C}_{a-1}(c_{a-1}-T^2c_{a-3})(c_{a-1}^2+T^{2a-2})(T^2c_{a-1}-c_{a-3})}{2c_{a-1}(T^{2a-2}-c_{a-1}^2)(T^4c_{a-3}-c_{a+1})}=0. \quad \text{(B.51)}$$

One can see that this equation is solved by

$$e_a=\frac{\pi(T^2-1)}{2T}\mathbb{C}_a\frac{c_a^2+T^{2a}}{c_a^2-T^{2a}}. \quad \text{(B.52)}$$

By the same argument as in [91] the initial conditions will help us to exclude other solutions. From (6.35) one can see that $e_0=0$ (as $\rho(0)\neq 0$ in general), and $\mathbb{C}_0$ can be set to zero because the sum starts at $a=1$. Thus from (B.51) it follows that (B.52) holds for all even a. In order to fix e_a at odd a we look at the residue of the second FiNLIE equation (6.36) at $u=i/2$. The only source of singularities in the right hand side are the terms with delta-function. Hence

$$e_1=\frac{\pi(T^2-1)}{2T}\mathbb{C}_a\frac{c_1^2+T^2}{c_1^2-T^2}. \quad \text{(B.53)}$$

This agrees with (B.52), so our solution holds for all a.

B.5 Strong coupling expansion

Here we discuss the strong coupling expansion of the cusp anomalous dimension. In order to recover for $\theta=0$ the expansion given in [91] (appendix F) it is convenient to introduce the "Bremsstrahlung function" $B_L(g)$ related to the cusp anomalous dimension as

$$\Gamma_L(g)=-2(\phi-\theta)\tan\theta B_L(g), \quad \text{(B.54)}$$

It is straightforward to expand our result at strong coupling for fixed values of L, and we find, e.g.,

$$\begin{aligned}\frac{1}{\theta\cot\theta}B_{L=0} &= \frac{g}{\sqrt{\pi^2-\theta^2}}-\frac{3}{8\left(\pi^2-\theta^2\right)}+\frac{3}{128g\left(\pi^2-\theta^2\right)^{3/2}}+\frac{3}{512g^2\left(\pi^2-\theta^2\right)^2}\\ &+ \frac{63}{32768g^3\left(\pi^2-\theta^2\right)^{5/2}}+\mathcal{O}\left(1/g^4\right)\ , \qquad \text{(B.55)}\\ \frac{1}{\theta\cot\theta}B_{L=1} &= \frac{g}{\sqrt{\pi^2-\theta^2}}-\frac{9}{8\left(\pi^2-\theta^2\right)}+\frac{3\left(13\pi^2-4\theta^2\right)}{128\pi^2g\left(\pi^2-\theta^2\right)^{3/2}}\\ &+ \frac{3\left(-6\theta^4+12\pi^2\theta^2+13\pi^4\right)}{512\pi^4g^2\left(\pi^2-\theta^2\right)^2}\\ &+ \frac{9\left(-48\theta^6+64\pi^2\theta^4+136\pi^4\theta^2+31\pi^6\right)}{32768\pi^6g^3\left(\pi^2-\theta^2\right)^{5/2}}+\mathcal{O}\left(1/g^4\right) \qquad \text{(B.56)}\end{aligned}$$

We have computed such expansions for $L=0,1,\ldots,4$ and when $\theta=0$ they reproduce the results in (195) of [91]. As in [91] we observed that the coefficients are polynomial in L, so we can now extrapolate to arbitrary L which gives

$$\begin{aligned}\frac{1}{\theta\cot\theta}B_L &= \frac{g}{\sqrt{\pi^2-\theta^2}}-\frac{6L+3}{8\left(\pi^2-\theta^2\right)}+\frac{3\left(\left(6L^2+6L+1\right)\pi^2-2\theta^2(L+1)L\right)}{128g\pi^2\left(\pi^2-\theta^2\right)^{3/2}}\\ &+ \frac{f_1}{512g^2\pi^4\left(\pi^2-\theta^2\right)^2}-\frac{f_2}{32768\pi^6g^3\left(\pi^2-\theta^2\right)^{5/2}}+\mathcal{O}\left(1/g^4\right) \qquad \text{(B.57)}\end{aligned}$$

where

$$\begin{aligned}f_1 &= -3\theta^4L\left(2L^2+3L+1\right)+6\pi^2\theta^2L\left(2L^2+3L+1\right) \qquad \text{(B.58)}\\ &\quad +\pi^4\left(10L^3+15L^2+11L+3\right)\ ,\\ f_2 &= 18\theta^6L\left(5L^3+10L^2+7L+2\right)-18\pi^2\theta^4L\left(5L^3+10L^2+11L+6\right) \qquad \text{(B.59)}\\ &\quad -6\pi^4\theta^2L\left(55L^3+110L^2+47L-8\right)+9\pi^6\left(10L^4+20L^3-22L^2-32L-7\right)\end{aligned}$$

Notice that for $\theta=0$ our expansion (B.57) reduces to that in equation (196) of [91].

We can now make a comparison with the classical string energy. Expanding (B.57) at fixed $\mathfrak{L}=L/g$ and large g, we get an expansion of the form

$$\Gamma_L(g)=gE^{cl}\left(\mathfrak{L}\right)+E^{1-loop}\left(\mathfrak{L}\right)+\frac{1}{g}E^{2-loop}\left(\mathfrak{L}\right)+\ldots\ . \qquad \text{(B.60)}$$

The first term, gE^{cl}, is proportional to $\sqrt{\lambda}$ and is expected to reproduce the energy of the

classical string configuration. Indeed, we found

$$\begin{aligned}\frac{g}{2(\phi-\theta)\theta}E^{cl} &= \left(-\frac{g}{\pi}+\frac{3L}{4\pi^2}-\frac{9L^2}{64g\pi^3}-\frac{5L^3}{256g^2\pi^4}+\frac{45L^4}{16384g^3\pi^5}\right) \\ &+ \theta^2\left(-\frac{g}{2\pi^3}+\frac{3L}{4\pi^4}-\frac{21L^2}{128g\pi^5}-\frac{L^3}{16g^2\pi^6}-\frac{105L^4}{32768g^3\pi^7}\right) \\ &+ \theta^4\left(-\frac{3g}{8\pi^5}+\frac{3L}{4\pi^6}-\frac{99L^2}{512g\pi^7}-\frac{3L^3}{32g^2\pi^8}-\frac{2085L^4}{131072g^3\pi^9}\right) \\ &+ \theta^6\left(-\frac{5g}{16\pi^7}+\frac{3L}{4\pi^8}-\frac{225L^2}{1024g\pi^9}-\frac{L^3}{8g^2\pi^{10}}-\frac{7905L^4}{262144g^3\pi^{11}}\right) \\ &+ \theta^8\left(-\frac{35g}{128\pi^9}+\frac{3L}{4\pi^{10}}-\frac{1995L^2}{8192g\pi^{11}}-\frac{5L^3}{32g^2\pi^{12}}-\frac{97425L^4}{2097152g^3\pi^{13}}\right).\end{aligned} \tag{B.61}$$

and all coefficients here match perfectly the expansion of the classical string energy from equation (193) of [91]! This is a deep test of our computation at $L \neq 0$ against a result which does not rely on integrability.

B.6 Identities for $\mathcal{M}_N$

In this appendix we describe the determinant identities which, in particular, allow us to switch between different representations (6.90), (6.91), (6.93) of the final result. Though not all of those identities have been used, we decided to present all that we have found for future reference. Some of them we have not proven analytically, but checked numerically for all $N < 30$.

Recall that $\mathcal{M}_N$ is an $N+1 \times N+1$ matrix given by (6.82) and $\mathcal{M}_N^{(a,b)}$ is a matrix obtained from $\mathcal{M}_N$ by deleting the a^{th} row and the b^{th} column. It is easy to see that $\mathcal{M}_N^{(1,1)} = \mathcal{M}_{N-1}$.

Determinants with a row/column removed

Using (B.68) and the fact that $\det \mathcal{M}_N^{(a,b)}$ is proportional to $\left(\mathcal{M}^{-1}\right)_{ba}$ it is possible to show that

$$\det \mathcal{M}_N^{(a,b)} = \det \mathcal{M}_N^{(N+2-b,N+2-a)}, \;\; 1 \leq a,b \leq N+1. \tag{B.62}$$

For any even N

$$\det \mathcal{M}_N^{(1,2)} = -\det \mathcal{M}_N^{(2,1)}, \tag{B.63}$$

$$\det \mathcal{M}_N^{(a,1)} = (-1)^{a+N/2+1} \det \mathcal{M}_N^{(N+2-a,1)}, \;\; 1 \leq a \leq N+1. \tag{B.64}$$

For any odd N

$$\det \mathcal{M}_N^{(N+1,1)} = 0, \tag{B.65}$$

$$\det \mathcal{M}_N^{(a,1)} = (-1)^{a+(N+1)/2} \det \mathcal{M}_N^{(N-a+1,1)}, \;\; 1 \le a \le N \tag{B.66}$$

Derivative of a determinant

For any integer N

$$\frac{1}{2g}\partial_\theta \det \mathcal{M}_{N-1} = \det \mathcal{M}_N^{(2,1)} - \det \mathcal{M}_N^{(1,2)}. \tag{B.67}$$

Deformed Bessel functions.

The "deformed" Bessel functions I_n^θ defined by (6.75) satisfy

$$I_n^\theta = (-1)^{n+1} I_{-n}^\theta, \qquad I_0^\theta = 0. \tag{B.68}$$

In addition,

$$\partial_\theta I_n^\theta = 2g\left(I_{n-1}^\theta - I_{n+1}^\theta\right). \tag{B.69}$$

The first identity is obvious from the definition and the second one is easy to see from the generating function representation (6.74).

C Appendix to chapter 7: Elliptic Identities

This appendix contains some identities for elliptic functions which we use in chapter 7.

For real z

$$\frac{\mathbb{E}(z)}{\sqrt{1-z}} = \begin{cases} i\mathbb{E}\left(\frac{z}{z-1}\right), \; z<1, \\ \mathbb{E}\left(\frac{z}{z-1}\right) + 2i\left[\mathbb{K}\left(\frac{1}{1-z}\right) - \mathbb{E}\left(\frac{1}{1-z}\right)\right], \; z>1. \end{cases} \tag{C.1}$$

$$\sqrt{1-z}\mathbb{K}(z) = \begin{cases} \mathbb{K}\left(\frac{z}{z-1}\right), \; z<1, \\ \mathbb{K}\left(\frac{z}{z-1}\right) + 2i\mathbb{K}\left(\frac{1}{1-z}\right), \; z>1. \end{cases} \tag{C.2}$$

The following two-parametric identity holds for $r > 0,\ 0 < \psi < \pi/2$:

$$\begin{aligned}
\pi = {} & \frac{4r^2}{r^2+1}\, e^{i\psi}\, \mathbb{K}(\sin^2(q)) \\
& + \frac{4r}{r^2-1} \tan q\, \cos\psi \left[\mathbb{K}\left(-\tan^2(q)\right) - \frac{r^2+1}{4r^2} \Pi\left(\frac{(r^2-1)^2}{4r^2} \tan^2(q) \middle| -\tan^2(q) \right) \right] \\
& + 4i \left[\mathbb{E}\left(\sin^2(q)\right) \mathbb{F}\left(\sin^{-1}\left(\sqrt{\frac{r^2+1}{2}} \sqrt{1 - i\cot\psi} \right) \middle| \sin^2(q) \right) \right. \\
& \left. - \mathbb{K}\left(\sin^2(q)\right) \mathbb{E}\left(\sin^{-1}\left(\sqrt{\frac{r^2+1}{2}} \sqrt{1 - i\cot\psi} \right) \middle| \sin^2(q) \right) \right], \\
& \text{where} \sin^2(q) = \frac{4r^2 \sin^2\psi}{(r^2+1)^2}.
\end{aligned} \tag{C.3}$$

References

[1] J. M. Maldacena, "The large N limit of superconformal field theories and supergravity", Adv. Theor. Math. Phys. **2** 231 (1998) [arXiv:hep-th/9711200]. • S. S. Gubser, I. R. Klebanov and A. M. Polyakov, "Gauge theory correlators from non-critical string theory," Phys. Lett. B **428** (1998) 105, [hep-th/9802109]. • E. Witten, "Anti-de Sitter space and holography," Adv. Theor. Math. Phys. **2** (1998) 253, [hep-th/9802150].

[2] C. N. Yang, C. P. Yang, "Thermodynamics of a one-dimensional system of bosons with repulsive delta-function interaction," J. Math. Phys. 10, 1115 (1969).

[3] W. E. Thirring, "A Soluble relativistic field theory?," Annals Phys. **3** (1958) 91.

[4] S. R. Coleman, "The Quantum Sine-Gordon Equation as the Massive Thirring Model," Phys. Rev. D **11** (1975) 2088.

[5] A. B. Zamolodchikov and A. B. Zamolodchikov, "Factorized s Matrices in Two-Dimensions as the Exact Solutions of Certain Relativistic Quantum Field Models," Annals Phys. **120** (1979) 253.

[6] E. Abdalla, M. C. B. Abdalla, and K. D. Rothe. Nonperturbative methods in two-dimensional quantum field theory - 1991. World Scientific. Singapore.

[7] N. Gromov, V. Kazakov, S. Leurent and D. Volin, "Quantum Spectral Curve for Planar $\mathcal{N}$ = Super-Yang-Mills Theory," Phys. Rev. Lett. **112**, no. 1, 011602 (2014) [arXiv:1305.1939 [hep-th]].

[8] N. Gromov, V. Kazakov, S. Leurent and D. Volin, "Quantum spectral curve for arbitrary state/operator in AdS_5/CFT_4," JHEP **1509** (2015) 187 [arXiv:1405.4857 [hep-th]].

[9] N. Gromov, F. Levkovich-Maslyuk, G. Sizov and S. Valatka, "Quantum Spectral Curve at Work: From Small Spin to Strong Coupling in N=4 SYM," JHEP **1407**, 156 (2014) arXiv:1402.0871 [hep-th].

[10] N. Gromov, F. Levkovich-Maslyuk and G. Sizov, "Analytic Solution of Bremsstrahlung TBA II: Turning on the Sphere Angle," JHEP **1310**, 036 (2013) [arXiv:1305.1944 [hep-th]].

[11] G. Sizov and S. Valatka, "Algebraic Curve for a Cusped Wilson Line," JHEP **1405**, 149 (2014) [arXiv:1306.2527 [hep-th]].

[12] N. Gromov, F. Levkovich-Maslyuk and G. Sizov, "Quantum Spectral Curve and the Numerical Solution of the Spectral Problem in AdS5/CFT4," arXiv:1504.06640 [hep-th].

[13] N. Gromov, F. Levkovich-Maslyuk and G. Sizov, "NNLO BFKL Pomeron eigenvalue in N=4 SYM,", submitted to PRL arXiv:1507.04010 [hep-th].

[14] N. Gromov and G. Sizov, "Exact Slope and Interpolating Functions in N=6 Supersymmetric Chern-Simons Theory," Phys. Rev. Lett. **113** (2014) 12, 121601 [arXiv:1403.1894 [hep-th]].

[15] N. Gromov, G. Sizov, in preparation

[16] M. K. Benna and I. R. Klebanov, "Gauge-String Dualities and Some Applications," arXiv:0803.1315 [hep-th].

[17] S. Kovacs, "N=4 supersymmetric Yang-Mills theory and the AdS / SCFT correspondence," hep-th/9908171.

[18] O. Aharony, S. S. Gubser, J. M. Maldacena, H. Ooguri and Y. Oz, "Large N field theories, string theory and gravity," Phys. Rept. **323** (2000) 183 [hep-th/9905111].

[19] E. D'Hoker and D. Z. Freedman, "Supersymmetric gauge theories and the AdS / CFT correspondence," hep-th/0201253.

[20] J. M. Maldacena, "TASI 2003 lectures on AdS / CFT," hep-th/0309246.

[21] H. Nastase, "Introduction to AdS-CFT," arXiv:0712.0689 [hep-th].

[22] J. Polchinski, "Introduction to Gauge/Gravity Duality," arXiv:1010.6134 [hep-th].

[23] G. T. Horowitz and J. Polchinski, "Gauge/gravity duality," In *Oriti, D. (ed.): Approaches to quantum gravity* 169-186 [gr-qc/0602037].

[24] G. 't Hooft, "Dimensional reduction in quantum gravity," Salamfest 1993:0284-296 [gr-qc/9310026].

[25] L. Susskind, "The World as a hologram," J. Math. Phys. **36**, 6377 (1995) [hep-th/9409089].

[26] A. M. Polyakov "Gauge Fields and Strings ", CRC Press, 1987

[27] D. Volin, "Quantum integrability and functional equations: Applications to the spectral problem of AdS/CFT and two-dimensional sigma models," J. Phys. A **44** (2011) 124003 [arXiv:1003.4725 [hep-th]].

[28] J. Polchinski, "Scale and Conformal Invariance in Quantum Field Theory," Nucl. Phys. B **303** (1988) 226.

[29] A. Dymarsky, K. Farnsworth, Z. Komargodski, M. A. Luty and V. Prilepina, "Scale Invariance, Conformality, and Generalized Free Fields," arXiv:1402.6322 [hep-th].

[30] M. A. Luty, J. Polchinski and R. Rattazzi, "The a-theorem and the Asymptotics of 4D Quantum Field Theory," JHEP **1301** (2013) 152 [arXiv:1204.5221 [hep-th]].

[31] D. J. Gross and F. Wilczek, "Asymptotically Free Gauge Theories. 1," Phys. Rev. **D8**, 3633 (1973).

[32] D. J. Gross and F. Wilczek, "Asymptotically Free Gauge Theories. 1," Phys. Rev. D **8** (1973) 3633.

[33] J. A. Minahan, "Review of AdS/CFT Integrability, Chapter I.1: Spin Chains in N=4 Super Yang-Mills," Lett. Math. Phys. **99**, 33 (2012) [arXiv:1012.3983 [hep-th]].

[34] M. T. Grisaru, M. Rocek and W. Siegel, "Zero Three Loop beta Function in N=4 Superyang-Mills Theory," Phys. Rev. Lett. **45** (1980) 1063.

[35] S. Mandelstam, "Light Cone Superspace and the Ultraviolet Finiteness of the N=4 Model," Nucl. Phys. B **213** (1983) 149.

[36] L. Brink, O. Lindgren and B. E. W. Nilsson, "The Ultraviolet Finiteness of the N=4 Yang-Mills Theory," Phys. Lett. B **123** (1983) 323.

[37] A. A. Tseytlin, "Review of AdS/CFT Integrability, Chapter II.1: Classical AdS5xS5 string solutions," Lett. Math. Phys. **99**, 103 (2012) [arXiv:1012.3986 [hep-th]].

[38] N. Beisert, V. A. Kazakov, K. Sakai and K. Zarembo, "The Algebraic curve of classical superstrings on AdS(5) x S**5," Commun. Math. Phys. **263**, 659 (2006) [hep-th/0502226].

[39] N. Gromov and P. Vieira, "The AdS(5) x S**5 superstring quantum spectrum from the algebraic curve," Nucl. Phys. B **789** (2008) 175 [hep-th/0703191 [HEP-TH]].

[40] J. M. Maldacena, "The Large N limit of superconformal field theories and supergravity," Adv. Theor. Math. Phys. **2**, 231 (1998) [hep-th/9711200].

[41] D. J. Gross, Nucl. Phys. B **400** (1993) 161 doi:10.1016/0550-3213(93)90402-B [hep-th/9212149].

[42] D. J. Gross and W. Taylor, Nucl. Phys. B **400** (1993) 181 doi:10.1016/0550-3213(93)90403-C [hep-th/9301068].

[43] J. A. Minahan, Phys. Rev. D **47** (1993) 3430 doi:10.1103/PhysRevD.47.3430 [hep-th/9301003].

[44] E. Witten, "Anti-de Sitter space and holography," Adv. Theor. Math. Phys. **2** (1998) 253 [hep-th/9802150].

[45] S. S. Gubser, I. R. Klebanov and A. M. Polyakov, "Gauge theory correlators from noncritical string theory," Phys. Lett. B **428**, 105 (1998) [hep-th/9802109].

[46] D. E. Berenstein, J. M. Maldacena and H. S. Nastase, "Strings in flat space and pp waves from N=4 superYang-Mills," JHEP **0204**, 013 (2002) [hep-th/0202021].

[47] S. S. Gubser, I. R. Klebanov and A. M. Polyakov, "A Semiclassical limit of the gauge / string correspondence," Nucl. Phys. B **636**, 99 (2002) [hep-th/0204051].

[48] A. A. Tseytlin, "Semiclassical strings and AdS/CFT," hep-th/0409296.

[49] O. Aharony, O. Bergman, D. L. Jafferis and J. Maldacena, "N=6 superconformal Chern-Simons-matter theories, M2-branes and their gravity duals," JHEP **0810**, 091 (2008) [arXiv:0806.1218 [hep-th]].

[50] O. Aharony, O. Bergman and D. L. Jafferis, "Fractional M2-branes," JHEP **0811** (2008) 043 [arXiv:0807.4924 [hep-th]].

[51] A. Giveon, D. Kutasov and N. Seiberg, "Comments on string theory on AdS(3)," Adv. Theor. Math. Phys. **2** (1998) 733 [hep-th/9806194].

[52] S. Elitzur, O. Feinerman, A. Giveon and D. Tsabar, "String theory on AdS(3) x S**3 x S**3 x S**1," Phys. Lett. B **449** (1999) 180 [hep-th/9811245].

[53] A. Babichenko, B. Stefanski, Jr. and K. Zarembo, "Integrability and the AdS(3)/CFT(2) correspondence," JHEP **1003** (2010) 058 [arXiv:0912.1723 [hep-th]].

[54] G. 't Hooft, "A planar diagram theory for strong interactions," Nucl. Phys. B72. 461-473 (1974).

[55] H. Y. Chen, N. Dorey and K. Okamura, "Dyonic giant magnons," JHEP **0609** (2006) 024 [hep-th/0605155].

[56] S. Frolov and A. A. Tseytlin, "Semiclassical quantization of rotating superstring in AdS(5) x S**5," JHEP **0206**, 007 (2002) [hep-th/0204226].

[57] G. P. Korchemsky, "Asymptotics of the Altarelli-Parisi-Lipatov Evolution Kernels of Parton Distributions," Mod. Phys. Lett. A **4** (1989) 1257.

[58] G. P. Korchemsky and G. Marchesini, "Structure function for large x and renormalization of Wilson loop," Nucl. Phys. B **406** (1993) 225 [hep-ph/9210281].

[59] S. Frolov and A. A. Tseytlin, "Multispin string solutions in AdS(5) x S**5," Nucl. Phys. B **668**, 77 (2003) [hep-th/0304255].

[60] S. Frolov and A. A. Tseytlin, "Quantizing three spin string solution in AdS(5) x S**5," JHEP **0307**, 016 (2003) [hep-th/0306130].

[61] L. F. Alday and J. M. Maldacena, "Gluon scattering amplitudes at strong coupling," JHEP **0706** (2007) 064 [arXiv:0705.0303 [hep-th]].

[62] L. F. Alday, "Review of AdS/CFT Integrability, Chapter V.3: Scattering Amplitudes at Strong Coupling," Lett. Math. Phys. **99**, 507 (2012) [arXiv:1012.4003 [hep-th]].

[63] N. Beisert *et al.*, "Review of AdS/CFT Integrability: An Overview," Lett. Math. Phys. **99** (2012) 3 [arXiv:1012.3982 [hep-th]].

[64] L. D. Faddeev and G. P. Korchemsky, "High-energy QCD as a completely integrable model," Phys. Lett. B **342** (1995) 311 [hep-th/9404173].

[65] L. N. Lipatov, "High-energy asymptotics of multicolor QCD and exactly solvable lattice models," hep-th/9311037.

[66] A. V. Belitsky, "Integrability and WKB solution of twist - three evolution equations," Nucl. Phys. B **558** (1999) 259 [hep-ph/9903512].

[67] A. V. Belitsky, "Renormalization of twist - three operators and integrable lattice models," Nucl. Phys. B **574** (2000) 407 [hep-ph/9907420].

[68] S. E. Derkachov, G. P. Korchemsky and A. N. Manashov, "Evolution equations for quark gluon distributions in multicolor QCD and open spin chains," Nucl. Phys. B **566** (2000) 203 [hep-ph/9909539].

[69] V. M. Braun, S. E. Derkachov and A. N. Manashov, "Integrability of three particle evolution equations in QCD," Phys. Rev. Lett. **81** (1998) 2020 [hep-ph/9805225].

[70] C. Sieg and A. Torrielli, "Wrapping interactions and the genus expansion of the 2-point function of composite operators," Nucl. Phys. B **723** (2005) 3 [hep-th/0505071].
• J. Ambjorn, R. A. Janik and C. Kristjansen, "Wrapping interactions and a new source of corrections to the spin-chain/string duality," Nucl. Phys. B **736** (2006) 288 [hep-th/0510171].

[71] N. Beisert, C. Kristjansen and M. Staudacher, "The Dilatation operator of conformal N=4 superYang-Mills theory," Nucl. Phys. B **664**, 131 (2003) [hep-th/0303060].

[72] N. Beisert, "The complete one loop dilatation operator of N=4 superYang-Mills theory," Nucl. Phys. B **676**, 3 (2004) [hep-th/0307015].

[73] N. Beisert, "The su(2—3) dynamic spin chain," Nucl. Phys. B **682** (2004) 487 [hep-th/0310252].

[74] J. A. Minahan and K. Zarembo, "The Bethe ansatz for N=4 superYang-Mills," JHEP **0303** (2003) 013 [hep-th/0212208].

[75] H. Bethe, "On the theory of metals. 1. Eigenvalues and eigenfunctions for the linear atomic chain," Z. Phys. 71 205-226 (1931).

[76] L. D. Faddeev, "How algebraic Bethe ansatz works for integrable model," hep-th/9605187.

[77] N. Beisert, V. Dippel and M. Staudacher, "A Novel long range spin chain and planar N=4 super Yang-Mills," JHEP **0407**, 075 (2004) [hep-th/0405001].

[78] N. Beisert, "The SU(2—2) dynamic S-matrix," Adv. Theor. Math. Phys. **12** (2008) 945 [hep-th/0511082].

[79] N. Beisert and M. Staudacher, "Long-range psu(2,2—4) Bethe Ansatze for gauge theory and strings," Nucl. Phys. B **727**, 1 (2005) [hep-th/0504190].

[80] R. A. Janik, "The AdS(5) x S**5 superstring worldsheet S-matrix and crossing symmetry," Phys. Rev. D **73**, 086006 (2006) [hep-th/0603038].

[81] A. V. Kotikov, L. N. Lipatov, A. Rej, M. Staudacher and V. N. Velizhanin, "Dressing and wrapping," J. Stat. Mech. **0710** (2007) P10003 [arXiv:0704.3586 [hep-th]].

[82] M. Lüscher, "Volume dependence of the energy spectrum in massive quantum field theories," Communications in Mathematical Physics, Volume 105, Issue 2, pp 153-188 (1986).

[83] Z. Bajnok and R. A. Janik, "Four-loop perturbative Konishi from strings and finite size effects for multiparticle states," Nucl. Phys. B **807**, 625 (2009) [arXiv:0807.0399 [hep-th]].

[84] Z. Bajnok, R. A. Janik and T. Lukowski, "Four loop twist two, BFKL, wrapping and strings," Nucl. Phys. B **816** (2009) 376 [arXiv:0811.4448 [hep-th]].

[85] D. Astolfi, V. Forini, G. Grignani and G. W. Semenoff, "Gauge invariant finite size spectrum of the giant magnon," Phys. Lett. B **651** (2007) 329 [hep-th/0702043 [HEP-TH]].

[86] G. Arutyunov, S. Frolov and M. Zamaklar, "Finite-size Effects from Giant Magnons," Nucl. Phys. B **778** (2007) 1 [hep-th/0606126].

[87] R. A. Janik, "Review of AdS/CFT Integrability, Chapter III.5: Lúscher Corrections," Lett. Math. Phys. **99** (2012) 277 [arXiv:1012.3994 [hep-th]].

[88] D. Bombardelli, D. Fioravanti and R. Tateo, "Thermodynamic Bethe Ansatz for planar AdS/CFT: A Proposal," J. Phys. A **42** (2009) 375401 [arXiv:0902.3930 [hep-th]].

[89] N. Gromov, V. Kazakov, A. Kozak and P. Vieira, "Exact Spectrum of Anomalous Dimensions of Planar N = 4 Supersymmetric Yang-Mills Theory: TBA and excited states," Lett. Math. Phys. **91** (2010) 265 [arXiv:0902.4458 [hep-th]].

[90] G. Arutyunov and S. Frolov, "Thermodynamic Bethe Ansatz for the AdS(5) x S(5) Mirror Model," JHEP **0905** (2009) 068 [arXiv:0903.0141 [hep-th]].

[91] N. Gromov and A. Sever, "Analytic Solution of Bremsstrahlung TBA," JHEP **1211** (2012) 075 [arXiv:1207.5489 [hep-th]].

[92] A. Hegedus, "Discrete Hirota dynamics for AdS/CFT," Nucl. Phys. B **825** (2010) 341 [arXiv:0906.2546 [hep-th]].

[93] N. Gromov, V. Kazakov, S. Leurent and Z. Tsuboi, "Wronskian Solution for AdS/CFT Y-system," JHEP **1101**, 155 (2011) [arXiv:1010.2720 [hep-th]].

[94] N. Gromov, V. Kazakov, S. Leurent and D. Volin, "Solving the AdS/CFT Y-system," JHEP **1207**, 023 (2012) [arXiv:1110.0562 [hep-th]].

[95] D. Correa, J. Maldacena and A. Sever, "The quark anti-quark potential and the cusp anomalous dimension from a TBA equation," JHEP **1208**, 134 (2012) [arXiv:1203.1913 [hep-th]].

[96] D. Bombardelli, D. Fioravanti and R. Tateo, "TBA and Y-system for planar AdS(4)/CFT(3)," Nucl. Phys. B **834**, 543 (2010) [arXiv:0912.4715 [hep-th]].

[97] N. Gromov and F. Levkovich-Maslyuk, "Y-system, TBA and Quasi-Classical strings in AdS(4) x CP3," JHEP **1006**, 088 (2010) [arXiv:0912.4911 [hep-th]].

[98] V. A. Kazakov, A. Marshakov, J. A. Minahan and K. Zarembo, "Classical/quantum integrability in AdS/CFT," JHEP **0405**, 024 (2004) [hep-th/0402207].

[99] S. Schafer-Nameki, "Review of AdS/CFT Integrability, Chapter II.4: The Spectral Curve," Lett. Math. Phys. **99** (2012) 169 [arXiv:1012.3989 [hep-th]].

[100] R. A. Janik and P. Laskos-Grabowski, "Surprises in the AdS algebraic curve constructions: Wilson loops and correlation functions," Nucl. Phys. B **861**, 361 (2012) [arXiv:1203.4246 [hep-th]].

[101] A. Dekel, "Wilson Loops and Minimal Surfaces Beyond the Wavy Approximation," JHEP **1503** (2015) 085 [arXiv:1501.04202 [hep-th]].

[102] A. Dekel, "Algebraic Curves for Factorized String Solutions," JHEP **1304** (2013) 119 [arXiv:1302.0555 [hep-th]].

[103] M. Cooke and N. Drukker, "From algebraic curve to minimal surface and back," JHEP **1502** (2015) 090 [arXiv:1410.5436 [hep-th]].

[104] A. Cagnazzo, "Integrability and Wilson loops: the wavy line contour," arXiv:1312.6891 [hep-th].

[105] I. Krichever, O. Lipan, P. Wiegmann and A. Zabrodin, "Quantum integrable systems and elliptic solutions of classical discrete nonlinear equations," Commun. Math. Phys. **188** (1997) 267 [hep-th/9604080].

[106] Z. Tsuboi, Nucl. Phys. B **826** (2010) 399 doi:10.1016/j.nuclphysb.2009.08.009 [arXiv:0906.2039 [math-ph]].

[107] Z. Tsuboi, "Wronskian solutions of the T, Q and Y-systems related to infinite dimensional unitarizable modules of the general linear superalgebra gl(M—N)," Nucl. Phys. B **870** (2013) 92 [arXiv:1109.5524 [hep-th]].

[108] N. Gromov, V. Kazakov and Z. Tsuboi, JHEP **1007** (2010) 097 doi:10.1007/JHEP07(2010)097 [arXiv:1002.3981 [hep-th]].

[109] V. Kazakov, S. Leurent and D. Volin, "T-system on T-hook: Grassmannian Solution and Twisted Quantum Spectral Curve," arXiv:1510.02100 [hep-th].

[110] M. Alfimov, N. Gromov and V. Kazakov, "QCD Pomeron from AdS/CFT Quantum Spectral Curve," arXiv:1408.2530 [hep-th].

[111] N. Beisert, B. Eden and M. Staudacher, "Transcendentality and Crossing," J. Stat. Mech. **0701**, P01021 (2007) [hep-th/0610251].

[112] N. Gromov and P. Vieira, "Complete 1-loop test of AdS/CFT," JHEP **0804** (2008) 046 [arXiv:0709.3487 [hep-th]].

[113] G. P. Pronko and Y. G. Stroganov, "Bethe equations 'on the wrong side of equator'," J. Phys. A **32** (1999) 2333 [hep-th/9808153].

[114] N. Beisert, R. Hernandez and E. Lopez, "A Crossing-symmetric phase for AdS(5) x S**5 strings," JHEP **0611**, 070 (2006) [hep-th/0609044].

[115] B. Basso, "An exact slope for AdS/CFT," arXiv:1109.3154 [hep-th].

[116] B. Basso, "Scaling dimensions at small spin in N=4 SYM theory," arXiv:1205.0054 [hep-th].

[117] N. Gromov, "On the Derivation of the Exact Slope Function," JHEP **1302**, 055 (2013) [arXiv:1205.0018 [hep-th]].

[118] M. Beccaria and A. A. Tseytlin, "More about 'short' spinning quantum strings," JHEP **1207** (2012) 089 [arXiv:1205.3656 [hep-th]].

[119] M. Beccaria, S. Giombi, G. Macorini, R. Roiban and A. A. Tseytlin, "'Short' spinning strings and structure of quantum $AdS_5 \times S^5$ spectrum," Phys. Rev. D **86** (2012) 066006 [arXiv:1203.5710 [hep-th]].

[120] M. Beccaria, C. Ratti and A. A. Tseytlin, "Leading quantum correction to energy of 'short' spiky strings," J. Phys. A **45** (2012) 155401 [arXiv:1201.5033 [hep-th]].

[121] A. Tirziu and A. A. Tseytlin, "Quantum corrections to energy of short spinning string in AdS(5)," Phys. Rev. D **78** (2008) 066002 [arXiv:0806.4758 [hep-th]].

[122] M. Kruczenski and A. A. Tseytlin, Nucl. Phys. B **875** (2013) 213 [arXiv:1212.4886 [hep-th]].

[123] S. E. Derkachov, G. P. Korchemsky, J. Kotanski and A. N. Manashov, "Noncompact Heisenberg spin magnets from high-energy QCD. 2. Quantization conditions and energy spectrum," Nucl. Phys. B **645**, 237 (2002) [hep-th/0204124].

[124] R. A. Janik, "Twist-two operators and the BFKL regime - nonstandard solutions of the Baxter equation," JHEP **1311**, 153 (2013) [arXiv:1309.2844 [hep-th]].

[125] N. Gromov, V. Kazakov, unpublished (2013)

[126] A. V. Kotikov and L. N. Lipatov, "DGLAP and BFKL evolution equations in the N=4 supersymmetric gauge theory," hep-ph/0112346.

[127] A. V. Kotikov, L. N. Lipatov and V. N. Velizhanin, "Anomalous dimensions of Wilson operators in N=4 SYM theory," Phys. Lett. B **557** (2003) 114 [hep-ph/0301021].

[128] A. V. Kotikov, L. N. Lipatov, A. I. Onishchenko and V. N. Velizhanin, "Three loop universal anomalous dimension of the Wilson operators in N=4 SUSY Yang-Mills model," Phys. Lett. B **595** (2004) 521 [Erratum-ibid. B **632** (2006) 754] [hep-th/0404092].

[129] S. Moch, J. A. M. Vermaseren and A. Vogt, "The Three loop splitting functions in QCD: The Nonsinglet case," Nucl. Phys. B **688** (2004) 101 [hep-ph/0403192].

[130] M. Staudacher, "The Factorized S-matrix of CFT/AdS," JHEP **0505** (2005) 054 [hep-th/0412188].

[131] T. Lukowski, A. Rej and V. N. Velizhanin, "Five-Loop Anomalous Dimension of Twist-Two Operators," Nucl. Phys. B **831** (2010) 105 [arXiv:0912.1624 [hep-th]].

[132] V. N. Velizhanin, JHEP **1406** (2014) 108 [arXiv:1311.6953 [hep-th]].

[133] L. Freyhult, "Review of AdS/CFT Integrability, Chapter III.4: Twist States and the cusp Anomalous Dimension," Lett. Math. Phys. **99** (2012) 255 [arXiv:1012.3993 [hep-th]].

[134] D. Maitre, "HPL, a mathematica implementation of the harmonic polylogarithms," Comput. Phys. Commun. **174** (2006) 222 [hep-ph/0507152]. • D. Maitre, "Extension of HPL to complex arguments," Comput. Phys. Commun. **183** (2012) 846 [hep-ph/0703052 [HEP-PH]].

[135] S. Leurent, D. Volin, Mathematica packages for working with zeta functions and FiNLIE-based weak coupling expansion. (http://people.kth.se/~dmytrov/konishi8.zip)

[136] S. Leurent and D. Volin, "Multiple zeta functions and double wrapping in planar $N = 4$ SYM," Nucl. Phys. B **875** (2013) 757 [arXiv:1302.1135 [hep-th]].

[137] J. Ablinger. A Computer Algebra Toolbox for Harmonic Sums Related to Particle Physics. Johannes Kepler University. Diploma Thesis. February 2009. arXiv:1011.1176 [math-ph]. • J. Ablinger. Computer Algebra Algorithms for Special Functions in Particle Physics. Johannes Kepler University. PhD Thesis. April 2012. • J. Ablinger, J. Blümlein and C. Schneider. Analytic and Algorithmic Aspects of Generalized Harmonic Sums and Polylogarithms. arXiv:1212.xxxx [math-ph]. • J. Ablinger, J. Blümlein and C. Schneider, "Harmonic Sums and Polylogarithms Generated by Cyclotomic Polynomials," J. Math. Phys. **52** (2011) 102301 [arXiv:1105.6063 [math-ph]]. • J. Blümlein. Structural Relations of Harmonic Sums and Mellin Transforms up to Weight w = 5. Comput. Phys. Commun. 180 (2009) 2218. [arXiv:0901.3106 [hep-ph]]. • E. Remiddi and J. A. M. Vermaseren. Harmonic polylogarithms. Int. J. Mod. Phys. A 15 (2000) 725. [hep-ph/9905237]. • J. A. M. Vermaseren. Harmonic sums, Mellin transforms and integrals. Int. J. Mod. Phys. A 14 (1999) 2037. [hep-ph/9806280].

[138] M. Beccaria, "Anomalous dimensions at twist-3 in the sl(2) sector of N=4 SYM," JHEP **0706** (2007) 044 [arXiv:0704.3570 [hep-th]].

[139] M. Beccaria, V. Forini, T. Lukowski and S. Zieme, "Twist-three at five loops, Bethe Ansatz and wrapping," JHEP **0903** (2009) 129 [arXiv:0901.4864 [hep-th]].

[140] V. N. Velizhanin, "Six-Loop Anomalous Dimension of Twist-Three Operators in N=4 SYM," JHEP **1011** (2010) 129 [arXiv:1003.4717 [hep-th]].

[141] M. Beccaria and F. Catino, "Sum rules for higher twist sl(2) operators in N=4 SYM," JHEP **0806** (2008) 103 [arXiv:0804.3711 [hep-th]].

[142] A. V. Belitsky, G. P. Korchemsky and R. S. Pasechnik, "Fine structure of anomalous dimensions in N=4 super Yang-Mills theory," Nucl. Phys. B **809** (2009) 244 [arXiv:0806.3657 [hep-ph]].

[143] N. Dorey, D. M. Hofman and J. M. Maldacena, "On the Singularities of the Magnon S-matrix," Phys. Rev. D **76** (2007) 025011 [hep-th/0703104 [HEP-TH]].

[144] P. Vieira and D. Volin, "Review of AdS/CFT Integrability, Chapter III.3: The Dressing factor," Lett. Math. Phys. **99** (2012) 231 [arXiv:1012.3992 [hep-th]].

[145] http://www.cecm.sfu.ca/projects/EZFace/index.html

[146] L. N. Lipatov, "Reggeization of the vector meson and the vacuum singularity in nonabelian gauge theories," Sov. J. Nucl. Phys. **23** (1976) 338 [Yad. Fiz. **23** (1976) 642]. • E. A. Kuraev, L. N. Lipatov and V. S. Fadin, "The Pomeranchuk singularity in nonabelian gauge theories," Sov. Phys. JETP **45** (1977) 199 [Zh. Eksp. Teor. Fiz. **72** (1977) 377]. • I. I. Balitsky and L. N. Lipatov, "The Pomeranchuk singularity in Quantum Chromodynamics,
Sov. J. Nucl. Phys. **28** (1978) 822 [Yad. Fiz. **28** (1978) 1597].

[147] N. Gromov and S. Valatka, "Deeper Look into Short Strings," JHEP **1203** (2012) 058 [arXiv:1109.6305 [hep-th]].

[148] N. Gromov, D. Serban, I. Shenderovich and D. Volin, "Quantum folded string and integrability: From finite size effects to Konishi dimension," JHEP **1108**, 046 (2011) [arXiv:1102.1040 [hep-th]].

[149] S. Frolov, "Konishi operator at intermediate coupling," J. Phys. A **44** (2011) 065401 [arXiv:1006.5032 [hep-th]].

[150] A. M. Polyakov, "Gauge Fields as Rings of Glue," Nucl. Phys. B **164**, 171 (1980).

[151] D. Correa, J. Henn, J. Maldacena and A. Sever, "An exact formula for the radiation of a moving quark in N=4 super Yang Mills," JHEP **1206** (2012) 048 [arXiv:1202.4455 [hep-th]].

[152] B. Fiol, B. Garolera and A. Lewkowycz, "Exact results for static and radiative fields of a quark in N=4 super Yang-Mills," JHEP **1205** (2012) 093 [arXiv:1202.5292 [hep-th]].

[153] B. Fiol, B. Garolera and G. Torrents, "Exact momentum fluctuations of an accelerated quark in N=4 super Yang-Mills," JHEP **1306** (2013) 011 [arXiv:1302.6991 [hep-th]].

[154] N. Drukker, D. J. Gross and H. Ooguri, "Wilson loops and minimal surfaces," Phys. Rev. D **60**, 125006 (1999) [hep-th/9904191].

[155] N. Drukker, "Integrable Wilson loops," JHEP **1310** (2013) 135 [arXiv:1203.1617 [hep-th]].

[156] N. Gromov, V. Kazakov and P. Vieira, "Exact Spectrum of Planar $\mathcal{N} = 4$ Supersymmetric Yang-Mills Theory: Konishi Dimension at Any Coupling," Phys. Rev. Lett. **104**, 211601 (2010) [arXiv:0906.4240 [hep-th]].

[157] S. Frolov, "Scaling dimensions from the mirror TBA," J. Phys. A **45** (2012) 305402 [arXiv:1201.2317 [hep-th]].

[158] G. Arutyunov, S. Frolov and A. Sfondrini, "Exceptional Operators in N=4 super Yang-Mills," JHEP **1209** (2012) 006 [arXiv:1205.6660 [hep-th]].

[159] K. Zarembo, "Supersymmetric Wilson loops," Nucl. Phys. B **643**, 157 (2002) [hep-th/0205160].

[160] N. Drukker and S. Kawamoto, "Small deformations of supersymmetric Wilson loops and open spin-chains," JHEP **0607** (2006) 024 [hep-th/0604124].

[161] J. K. Erickson, G. W. Semenoff and K. Zarembo, "Wilson loops in N=4 supersymmetric Yang-Mills theory," Nucl. Phys. B **582**, 155 (2000) [hep-th/0003055]. • N. Drukker and D. J. Gross, "An Exact prediction of N=4 SUSYM theory for string theory," J. Math. Phys. **42**, 2896 (2001) [hep-th/0010274]. • N. Drukker, "1/4 BPS circular loops, unstable world-sheet instantons and the matrix model," JHEP **0609**, 004 (2006) [hep-th/0605151]. • N. Drukker, S. Giombi, R. Ricci and D. Trancanelli, "On the D3-brane description of some 1/4 BPS Wilson loops," JHEP **0704**, 008 (2007) [hep-th/0612168]. • N. Drukker, S. Giombi, R. Ricci and D. Trancanelli, "More supersymmetric Wilson loops," Phys. Rev. D **76**, 107703 (2007) [arXiv:0704.2237 [hep-th]]. • N. Drukker, S. Giombi, R. Ricci and D. Trancanelli, "Wilson loops: From four-dimensional SYM to two-dimensional YM," Phys. Rev. D **77**, 047901 (2008) [arXiv:0707.2699 [hep-th]]. • S. Giombi, V. Pestun and R. Ricci, "Notes on supersymmetric Wilson loops on a two-sphere," JHEP **1007**, 088 (2010) [arXiv:0905.0665

[hep-th]]. • S. Giombi and V. Pestun, "Correlators of local operators and 1/8 BPS Wilson loops on S**2 from 2d YM and matrix models," JHEP **1010**, 033 (2010) [arXiv:0906.1572 [hep-th]].

[162] V. Pestun, Commun. Math. Phys. **313** (2012) 71 [arXiv:0712.2824 [hep-th]]. • V. Pestun, JHEP **1212** (2012) 067 [arXiv:0906.0638 [hep-th]].

[163] V. Kazakov and N. Gromov, "Talk at IGST-2010, Nordita, Stockholm", http://agenda.albanova.se/contributionDisplay.py?contribId=258&confId=1561 .

[164] R. Suzuki, "Hybrid NLIE for the Mirror AdS5 x S5," J. Phys. A **44** (2011) 235401 [arXiv:1101.5165 [hep-th]].

[165] J. Balog and A. Hegedus, "Hybrid-NLIE for the AdS/CFT spectral problem," JHEP **1208** (2012) 022 [arXiv:1202.3244 [hep-th]].

[166] N. Gromov and F. Levkovich-Maslyuk, "Quantum Spectral Curve for a Cusped Wilson Line in N=4 SYM," arXiv:1510.02098 [hep-th].

[167] S. Leurent, D. Serban and D. Volin, "Six-loop Konishi anomalous dimension from the Y-system," Phys. Rev. Lett. **109** (2012) 241601 [arXiv:1209.0749 [hep-th]].

[168] Z. Bajnok, A. Hegedus, R. A. Janik and T. Lukowski, "Five loop Konishi from AdS/CFT," Nucl. Phys. B **827**, 426 (2010) [arXiv:0906.4062 [hep-th]].

[169] Z. Bajnok and R. A. Janik, "Six and seven loop Konishi from Luscher corrections," JHEP **1211** (2012) 002 [arXiv:1209.0791 [hep-th]].

[170] K. Zoubos, "Review of AdS/CFT Integrability, Chapter IV.2: Deformations, Orbifolds and Open Boundaries," Lett. Math. Phys. **99** (2012) 375 [arXiv:1012.3998 [hep-th]]. • N. Gromov and F. Levkovich-Maslyuk, "Y-system and β-deformed N=4 Super-Yang-Mills," J. Phys. A **44** (2011) 015402 [arXiv:1006.5438 [hep-th]]. • C. Ahn, Z. Bajnok, D. Bombardelli and R. I. Nepomechie, "TBA, NLO Luscher correction, and double wrapping in twisted AdS/CFT," JHEP **1112** (2011) 059 [arXiv:1108.4914 [hep-th]]. • M. de Leeuw and S. J. van Tongeren, "The spectral problem for strings on twisted AdS5 x S5," Nucl. Phys. B **860** (2012) 339 [arXiv:1201.1451 [hep-th]]. • G. Arutyunov, M. de Leeuw and S. J. van Tongeren, "The Quantum Deformed Mirror TBA I," JHEP **1210** (2012) 090 [arXiv:1208.3478 [hep-th]]. • G. Arutyunov, M. de Leeuw and S. J. van Tongeren, "The Quantum Deformed Mirror TBA II," JHEP [JHEP **1302** (2013) 012] [arXiv:1210.8185 [hep-th]]. •

[171] R. R. Metsaev and A. A. Tseytlin, "Type IIB superstring action in AdS(5) x S**5 background," Nucl. Phys. B **533**, 109 (1998) [hep-th/9805028].

[172] I. Bena, J. Polchinski and R. Roiban, "Hidden symmetries of the AdS(5) x S**5 superstring," Phys. Rev. D **69**, 046002 (2004) [hep-th/0305116].

[173] M. Beccaria and G. Macorini, "On a discrete symmetry of the Bremsstrahlung function in N=4 SYM," arXiv:1305.4839 [hep-th].

[174] R. Kallosh, J. Rahmfeld and A. Rajaraman, "Near horizon superspace," JHEP **9809** (1998) 002 [hep-th/9805217].

[175] N. Berkovits, M. Bershadsky, T. Hauer, S. Zhukov and B. Zwiebach, "Superstring theory on AdS(2) x S**2 as a coset supermanifold," Nucl. Phys. B **567**, 61 (2000) [hep-th/9907200].

[176] R. Roiban and W. Siegel, "Superstrings on AdS(5) x S**5 supertwistor space," JHEP **0011** (2000) 024 [hep-th/0010104].

[177] N. Gromov, S. Schafer-Nameki and P. Vieira, "Efficient precision quantization in AdS/CFT," JHEP **0812**, 013 (2008) [arXiv:0807.4752 [hep-th]].

[178] N. Beisert, J. A. Minahan, M. Staudacher and K. Zarembo, "Stringing spins and spinning strings," JHEP **0309** (2003) 010 [hep-th/0306139].

[179] R. Roiban and A. A. Tseytlin, "Quantum strings in AdS(5) x S**5: Strong-coupling corrections to dimension of Konishi operator," JHEP **0911**, 013 (2009) [arXiv:0906.4294 [hep-th]].

[180] S. Schafer-Nameki, "The Algebraic curve of 1-loop planar N=4 SYM," Nucl. Phys. B **714** (2005) 3 [hep-th/0412254].

[181] T. Bargheer, N. Beisert and N. Gromov, "Quantum Stability for the Heisenberg Ferromagnet," New J. Phys. **10** (2008) 103023 [arXiv:0804.0324 [hep-th]].

[182] N. Drukker and V. Forini, "Generalized quark-antiquark potential at weak and strong coupling," JHEP **1106** (2011) 131 [arXiv:1105.5144 [hep-th]].

[183] R. Roiban and A. A. Tseytlin, "Semiclassical string computation of strong-coupling corrections to dimensions of operators in Konishi multiplet," Nucl. Phys. B **848**, 251 (2011) [arXiv:1102.1209 [hep-th]].

[184] B. C. Vallilo and L. Mazzucato, "The Konishi multiplet at strong coupling," JHEP **1112**, 029 (2011) [arXiv:1102.1219 [hep-th]].

[185] S. Frolov, M. Heinze, G. Jorjadze and J. Plefka, "Static Gauge and Energy Spectrum of Single-mode Strings in $AdS_5 x S^5$," arXiv:1310.5052 [hep-th].

[186] K. Zoubos, "Review of AdS/CFT Integrability, Chapter IV.2: Deformations, Orbifolds and Open Boundaries," Lett. Math. Phys. **99** (2012) 375 [arXiv:1012.3998 [hep-th]].

[187] A. V. Kotikov and L. N. Lipatov, "DGLAP and BFKL equations in the N=4 supersymmetric gauge theory," Nucl. Phys. B **661**, 19 (2003) [Erratum-ibid. B **685**, 405 (2004)] [hep-ph/0208220].

[188] R. C. Brower, J. Polchinski, M. J. Strassler and C. -ITan, "The Pomeron and gauge/string duality," JHEP **0712**, 005 (2007) [hep-th/0603115].

[189] M. S. Costa, V. Goncalves and J. Penedones, "Conformal Regge theory," JHEP **1212**, 091 (2012) [arXiv:1209.4355 [hep-th]].

[190] A. V. Kotikov and L. N. Lipatov, "Pomeron in the N=4 supersymmetric gauge model at strong couplings," Nucl. Phys. B **874**, 889 (2013) [arXiv:1301.0882 [hep-th]].

[191] R. C. Brower, M. Costa, M. Djuric, T. Raben and C. -ITan, "Conformal Pomeron and Odderon in Strong Coupling," arXiv:1312.1419 [hep-ph].

[192] T. Jaroszewicz, "Gluonic Regge Singularities and Anomalous Dimensions in QCD," Phys. Lett. B **116** (1982) 291.

[193] L. N. Lipatov, "The Bare Pomeron in Quantum Chromodynamics," Sov. Phys. JETP **63**, 904 (1986) [Zh. Eksp. Teor. Fiz. **90**, 1536 (1986)].

[194] A. Cavagli, D. Fioravanti, N. Gromov and R. Tateo, "The Quantum Spectral Curve of the ABJM theory," Phys. Rev. Lett. **113**, 021601 (2014) [arXiv:1403.1859 [hep-th]].

[195] C. R. Schmidt, "Review of BFKL," hep-ph/0106181.

[196] V. S. Fadin and L. N. Lipatov, "BFKL pomeron in the next-to-leading approximation," Phys. Lett. B **429** (1998) 127 [hep-ph/9802290].

[197] M. Ciafaloni and G. Camici, "Energy scale(s) and next-to-leading BFKL equation," Phys. Lett. B **430** (1998) 349 [hep-ph/9803389].

[198] A. V. Kotikov and L. N. Lipatov, "NLO corrections to the BFKL equation in QCD and in supersymmetric gauge theories," Nucl. Phys. B **582** (2000) 19 [hep-ph/0004008].

[199] C. Marboe and D. Volin, "Quantum spectral curve as a tool for a perturbative quantum field theory," arXiv:1411.4758 [hep-th].

[200] C. Marboe, V. Velizhanin and D. Volin, "Six-loop anomalous dimension of twist-two operators in planar N=4 SYM theory," arXiv:1412.4762 [hep-th].

[201] L. Cornalba, "Eikonal methods in AdS/CFT: Regge theory and multi-reggeon exchange," arXiv:0710.5480 [hep-th].

[202] T. Klose, "Review of AdS/CFT Integrability, Chapter IV.3: N=6 Chern-Simons and Strings on AdS4xCP3," Lett. Math. Phys. **99**, 401 (2012) [arXiv:1012.3999 [hep-th]].

[203] M. Benna, I. Klebanov, T. Klose and M. Smedback, "Superconformal Chern-Simons Theories and AdS(4)/CFT(3) Correspondence," JHEP **0809** (2008) 072 [arXiv:0806.1519 [hep-th]].

[204] J. A. Minahan and K. Zarembo, "The Bethe ansatz for superconformal Chern-Simons," JHEP **0809**, 040 (2008) [arXiv:0806.3951 [hep-th]].

[205] D. Bak and S. J. Rey, "Integrable Spin Chain in Superconformal Chern-Simons Theory," JHEP **0810** (2008) 053 [arXiv:0807.2063 [hep-th]].

[206] J. A. Minahan, W. Schulgin and K. Zarembo, "Two loop integrability for Chern-Simons theories with N=6 supersymmetry," JHEP **0903** (2009) 057 [arXiv:0901.1142 [hep-th]].

[207] B. I. Zwiebel, "Two-loop Integrability of Planar N=6 Superconformal Chern-Simons Theory," J. Phys. A **42** (2009) 495402 [arXiv:0901.0411 [hep-th]].

[208] N. Gromov and P. Vieira, "The all loop AdS4/CFT3 Bethe ansatz," JHEP **0901** (2009) 016 [arXiv:0807.0777 [hep-th]].

[209] D. Berenstein and D. Trancanelli, "S-duality and the giant magnon dispersion relation," Eur. Phys. J. C **74** (2014) 2925 [arXiv:0904.0444 [hep-th]].

[210] B. Stefański, jr, "Green-Schwarz action for Type IIA strings on AdS(4) x CP**3," Nucl. Phys. B **808**, 80 (2009) [arXiv:0806.4948 [hep-th]].

[211] G. Arutyunov and S. Frolov, "Superstrings on AdS(4) x CP**3 as a Coset Sigma-model," JHEP **0809**, 129 (2008) [arXiv:0806.4940 [hep-th]].

[212] N. Gromov and P. Vieira, "The AdS(4) / CFT(3) algebraic curve," JHEP **0902** (2009) 040 [arXiv:0807.0437 [hep-th]].

[213] N. Gromov, V. Kazakov and P. Vieira, "Exact Spectrum of Anomalous Dimensions of Planar N=4 Supersymmetric Yang-Mills Theory," Phys. Rev. Lett. **103** (2009) 131601 [arXiv:0901.3753 [hep-th]].

[214] M. Beccaria and G. Macorini, *QCD properties of twist operators in the N=6 Chern-Simons theory*, *JHEP* **0906** (2009) 008, [arXiv:0904.2463].

[215] M. Beccaria, G. Macorini, C. Ratti and S. Valatka, "Semiclassical folded string in AdS_5XS^5," JHEP **1205**, 030 (2012) [Erratum-ibid. **1205**, 137 (2012)] [arXiv:1203.3852 [hep-th]].

[216] M. Beccaria, G. Macorini, C. Ratti and S. Valatka, "Semiclassical energy of the $AdS_4 \times \mathbb{CP}^3$ folded string," J. Phys. Conf. Ser. **411**, 012006 (2013) [arXiv:1209.3205 [hep-th]].

[217] M. Beccaria and G. Macorini, *The Virtual scaling function of twist operators in the N=6 Chern-Simons theory*, *JHEP* **0909** (2009) 017, [arXiv:0905.1030].

[218] M. Marino and P. Putrov, "Exact Results in ABJM Theory from Topological Strings," JHEP **1006**, 011 (2010) [arXiv:0912.3074 [hep-th]].

[219] N. Drukker, M. Marino and P. Putrov, "Nonperturbative aspects of ABJM theory," JHEP **1111** (2011) 141 [arXiv:1103.4844 [hep-th]].

[220] N. Drukker, M. Marino and P. Putrov, "From weak to strong coupling in ABJM theory," Commun. Math. Phys. **306** (2011) 511 [arXiv:1007.3837 [hep-th]].

[221] V. Pestun, "Localization of gauge theory on a four-sphere and supersymmetric Wilson loops," Commun. Math. Phys. **313** (2012) 71 [arXiv:0712.2824 [hep-th]].

[222] A. Kapustin, B. Willett and I. Yaakov, "Exact Results for Wilson Loops in Superconformal Chern-Simons Theories with Matter," JHEP **1003** (2010) 089 [arXiv:0909.4559 [hep-th]].

[223] J. A. Minahan, O. Ohlsson Sax and C. Sieg, "Magnon dispersion to four loops in the ABJM and ABJ models," J. Phys. A **43**, 275402 (2010) [arXiv:0908.2463 [hep-th]].

[224] M. Leoni, A. Mauri, J. A. Minahan, O. Ohlsson Sax, A. Santambrogio, C. Sieg and G. Tartaglino-Mazzucchelli, "Superspace calculation of the four-loop spectrum in N=6 supersymmetric Chern-Simons theories," JHEP **1012**, 074 (2010) [arXiv:1010.1756 [hep-th]].

[225] T. McLoughlin, R. Roiban, and A. A. Tseytlin, *Quantum spinning strings in AdS(4) x CP**3: Testing the Bethe Ansatz proposal*, *JHEP* **0811** (2008) 069, [arXiv:0809.4038].

[226] M. C. Abbott, I. Aniceto, and D. Bombardelli, *Quantum Strings and the AdS_4/CFT_3 Interpolating Function*, *JHEP* **1012** (2010) 040, [arXiv:1006.2174].

[227] C. Lopez-Arcos and H. Nastase, "Eliminating ambiguities for quantum corrections to strings moving in $AdS_4 \times \mathbb{CP}^3$," Int. J. Mod. Phys. A **28** (2013) 1350058 [arXiv:1203.4777 [hep-th]].

[228] O. Bergman and S. Hirano, "Anomalous radius shift in AdS(4)/CFT(3)," JHEP **0907** (2009) 016 [arXiv:0902.1743 [hep-th]].

[229] A. Lewkowycz and J. Maldacena, "Exact results for the entanglement entropy and the energy radiated by a quark," JHEP **1405** (2014) 025 [arXiv:1312.5682 [hep-th]].

[230] C. A. Agon, A. Guijosa and J. F. Pedraza, "Radiation and a dynamical UV/IR connection in AdS/CFT," arXiv:1402.5961 [hep-th].

[231] V. Forini, V. G. M. Puletti and O. Ohlsson Sax, "The generalized cusp in AdS_4 x CP^3 and more one-loop results from semiclassical strings," J. Phys. A **46** (2013) 115402 [arXiv:1204.3302 [hep-th]].

[232] M. S. Bianchi, L. Griguolo, M. Leoni, S. Penati and D. Seminara, "BPS Wilson loops and Bremsstrahlung function in ABJ(M): a two loop analysis," JHEP **1406** (2014) 123 [arXiv:1402.4128 [hep-th]].

[233] L. Bianchi, M. S. Bianchi, A. Bres, V. Forini and E. Vescovi, "Two-loop cusp anomaly in ABJM at strong coupling," JHEP **1410** (2014) 13 [arXiv:1407.4788 [hep-th]].

[234] M. Beccaria, F. Levkovich-Maslyuk, G. Macorini and A. A. Tseytlin, "Quantum corrections to spinning superstrings in $AdS_3xS^3xM^4$: determining the dressing phase," JHEP **1304** (2013) 006 [arXiv:1211.6090 [hep-th]].

[235] R. Borsato, O. Ohlsson Sax and A. Sfondrini, "A dynamic $su(1|1)^2$ S-matrix for AdS3/CFT2," JHEP **1304** (2013) 113 [arXiv:1211.5119 [hep-th]].

[236] R. Borsato, O. Ohlsson Sax and A. Sfondrini, "All-loop Bethe ansatz equations for AdS3/CFT2," JHEP **1304** (2013) 116 [arXiv:1212.0505 [hep-th]].

[237] R. Borsato, O. Ohlsson Sax, A. Sfondrini, B. Stefaski and A. Torrielli, "The all-loop integrable spin-chain for strings on $\mathrm{AdS}_3 \times S^3 \times T^4$: the massive sector," JHEP **1308** (2013) 043 [arXiv:1303.5995 [hep-th]].

[238] R. Borsato, O. Ohlsson Sax, A. Sfondrini, B. Stefanski, Jr. and A. Torrielli, "Dressing phases of AdS3/CFT2," Phys. Rev. D **88** (2013) 066004 [arXiv:1306.2512 [hep-th]].

[239] R. Borsato, O. Ohlsson Sax, A. Sfondrini and B. Stefanski, "Towards the All-Loop Worldsheet S Matrix for $AdS_3 \times S^3 \times T^4$," Phys. Rev. Lett. **113** (2014) 13, 131601 [arXiv:1403.4543 [hep-th]].

[240] T. Lloyd, O. Ohlsson Sax, A. Sfondrini and B. Stefaski, Jr., "The complete worldsheet S matrix of superstrings on $AdS_3xS^3xT^4$ with mixed three-form flux," Nucl. Phys. B **891** (2015) 570 [arXiv:1410.0866 [hep-th]].

[241] R. Borsato, O. Ohlsson Sax, A. Sfondrini and B. Stefanski, "The complete $\mathrm{AdS}_3\times$ $\mathrm{S}^3\times$ T^4 worldsheet S matrix," JHEP **1410** (2014) 66 [arXiv:1406.0453 [hep-th]].

[242] A. Sfondrini, "Towards integrability for $\mathrm{AdS}_{\mathbf{3}}/\mathrm{CFT}_{\mathbf{2}}$," J. Phys. A **48** (2015) 2, 023001 [arXiv:1406.2971 [hep-th]].

[243] R. Borsato, O. O. Sax, A. Sfondrini and B. Stefaski, "The $\mathrm{AdS}_3 \times \mathrm{S}^3 \times \mathrm{S}^3 \times \mathrm{S}^1$ worldsheet S matrix," arXiv:1506.00218 [hep-th].

[244] A. Cavagli, M. Cornagliotto, M. Mattelliano and R. Tateo, "A Riemann-Hilbert formulation for the finite temperature Hubbard model," JHEP **1506** (2015) 015 [arXiv:1501.04651 [hep-th]].

[245] Y. Jiang, S. Komatsu, I. Kostov and D. Serban, "The hexagon in the mirror: the three-point function in the SoV representation," arXiv:1506.09088 [hep-th].

[246] Y. Jiang, I. Kostov, A. Petrovskii and D. Serban, "String Bits and the Spin Vertex," Nucl. Phys. B **897** (2015) 374 [arXiv:1410.8860 [hep-th]].

[247] Y. Jiang, I. Kostov, F. Loebbert and D. Serban, "Fixing the Quantum Three-Point Function," JHEP **1404** (2014) 019 [arXiv:1401.0384 [hep-th]].

[248] O. Foda, Y. Jiang, I. Kostov and D. Serban, "A tree-level 3-point function in the su(3)-sector of planar N=4 SYM," JHEP **1310** (2013) 138 [arXiv:1302.3539 [hep-th]].

[249] B. Basso, S. Komatsu and P. Vieira, "Structure Constants and Integrable Bootstrap in Planar N=4 SYM Theory," arXiv:1505.06745 [hep-th].

[250] N. Kanning, Y. Ko and M. Staudacher, "Gramannian integrals as matrix models for non-compact Yangian invariants," Nucl. Phys. B **894** (2015) 407 [arXiv:1412.8476 [hep-th]].

[251] L. Ferro, T. Lukowski and M. Staudacher, "$\mathcal{N} = 4$ scattering amplitudes and the deformed Gramannian," Nucl. Phys. B **889** (2014) 192 [arXiv:1407.6736 [hep-th]].

[252] L. Koster, V. Mitev and M. Staudacher, "A Twistorial Approach to Integrability in $\mathcal{N} = 4$ SYM," Fortsch. Phys. **63** (2015) 2, 142 [arXiv:1410.6310 [hep-th]].

[253] N. Kanning, T. Lukowski and M. Staudacher, "A shortcut to general tree-level scattering amplitudes in $\mathcal{N} = 4$ SYM via integrability," Fortsch. Phys. **62** (2014) 556 [arXiv:1403.3382 [hep-th]].

[254] R. Frassek, N. Kanning, Y. Ko and M. Staudacher, "Bethe Ansatz for Yangian Invariants: Towards Super Yang-Mills Scattering Amplitudes," Nucl. Phys. B **883** (2014) 373 [arXiv:1312.1693 [math-ph]].

[255] L. Ferro, T. Lukowski, C. Meneghelli, J. Plefka and M. Staudacher, "Spectral Parameters for Scattering Amplitudes in N=4 Super Yang-Mills Theory," JHEP **1401** (2014) 094 [arXiv:1308.3494 [hep-th], arXiv:1308.3494].

[256] L. F. Alday, D. Gaiotto and J. Maldacena, "Thermodynamic Bubble Ansatz," JHEP **1109** (2011) 032 [arXiv:0911.4708 [hep-th]].

[257] L. F. Alday, J. Maldacena, A. Sever and P. Vieira, "Y-system for Scattering Amplitudes," J. Phys. A **43** (2010) 485401 [arXiv:1002.2459 [hep-th]].

[258] J. Maldacena and A. Zhiboedov, "Form factors at strong coupling via a Y-system," JHEP **1011** (2010) 104 [arXiv:1009.1139 [hep-th]].